



Medicinal Properties of Saudi Arabian Flora Extracts

Ahmed Reda Yonbawi Pharm.D, MSc

School of Pharmacy and Pharmaceutical Sciences, Cardiff University

Thesis submitted as a requirement for the degree of Doctor of
Philosophy (PhD)

September 2022

Plagiarism statement

This project is conducted in the School of Pharmacy Pharmacy and Pharmaceutical Sciences, Cardiff University under the supervision of Dr. Charles Heard. I certify that the research described in this work is original and that any parts of the work that I have been conducted in collaboration are clearly indicated. I also certify that I have written all the text herein and have clearly indicated by suitable citation any part of this project that has already appeared in publication.

Ahmed Reda Yonbawi

Acknowledgments

First, I would like to express my thanks to Dr. Charles Heard for his tremendous guidance and support during my project, I couldn't have completed my project without your guidance, support, encouragement, and energy, all of which were priceless to me. Prof. Les Baillie for opening his lab to me and providing me with a great support and insight. Also, I wish to thank Dr. Vildan Celiksoy who has been a tremendous assistance in every way and provided me with exceptional training. In addition, I would like to extend my sincere appreciation to Dr. Alex White for his advice and guidance on NMR and Phytochemistry.

Moreover, I would like to thank my friends Majed, Saeed, Ahmed, Abdulaziz, Jabril, Raed, Tawfiq, Khaled, Adnan, and Andy - Ph.D. students at the School of Pharmacy and Pharmaceutical Sciences, Cardiff University for their great support and for their friendship throughout these years. I would also like to thank the great team at the School of Pharmacy, especially Wendy and Dean for their support and advice.

I will always be in debt to my family. Thank you for embracing my decision to study abroad, and offering your continuous support over the years. I love you all and I am really grateful for everything you've done for me. Finally, I am grateful to King Abdulaziz University for sponsoring me to study at School of Pharmacy and Pharmaceutical Sciences, Cardiff University.

Abstract

Infectious diseases account for increasing levels of mortality around the world. When microorganisms overcome epithelia barriers and immunological bodily defensive mechanisms of the skin, they can cause soft-tissue infections (SSTIs). This project explores the medicinal properties of five plants indigenous to the western region of Saudi Arabia, with a history of folkloric use: *Aizoon canariense* L. (Aizoaceae), *Citrullus colocynthis* (L.) Schrad. (Cucurbitaceae), *Maerua crassifolia* Forssk. (Capparaceae), *Rhazya stricta* Decne. (Apocynaceae), and *Tribulus macropterus* Boiss. (Zygophyllaceae), focusing on treating SSTIs and chronic wounds. An additional aim was to identify compounds to treat infections by following a bio-guided fractionation approach.

Following a field trip, the target plants were collected and identified before undergoing methanolic extraction to yield approximately 200g of residual material. Initially, these extracts were evaluated for their effect on immortalized human skin keratinocytes (HaCaT) cell line proliferation, migration, and cytotoxicity through MTT, scratch wound, and flow cytometry. Confocal microscopy (CLSM) was utilized to confirm the morphology and viability of the cells. Antioxidant effects were determined using the acellular 1,1-Diphenyl-2-picrylhydrazyl (DPPH) method, and a cell-based method was utilized to measure a reactive oxygen species (ROS) level, namely hydrogen peroxide level (H_2O_2) in cell culture settings (ROS-Glo H_2O_2 assay). Antimicrobial properties were investigated by well diffusion, broth microdilution, and direct bio-autographic methods. The ability of medicinal plants to inhibit and eradicate bacterial biofilm was investigated by crystal violet and Live/Dead microbial viability method using CLSM. Plants that exhibited interesting antimicrobial activities were subjected to bio-guided fractionation with liquid-liquid partitioning and column chromatography to identify and isolate active compounds. The anti-inflammatory effects of plant extracts were evaluated by utilising LPS-stimulated HaCaT cells to determine effects on expression of a panel of inflammatory mediators.

Results indicated that *C. colocynthis* possesses cytotoxic activity with significant inhibition of proliferation and migration of human skin keratinocytes. On the other hand, *M. crassifolia* promoted the wound healing potential of HaCaT by stimulating the proliferation and migration. *A. canariense* and *T. macropterus* demonstrated antimicrobial activity against Gram-positive strains in planktonic and biofilm conditions. *R. stricta* demonstrated broad-spectrum antimicrobial properties in planktonic and biofilm conditions against Gram-positive and negative bacterial species associated with SSTIs. The free radical scavenging data showed that both *R. stricta* and *M. crassifolia* gave the highest capacity for scavenging the DPPH radical with an IC_{50} of 335 and 448 $\mu\text{g/mL}$, respectively. In addition, *R. stricta* showed the highest H_2O_2 scavenging activity in the cell-based antioxidant method. Bio-guided fractionating of *A. canariense* and *R. stricta* successfully isolated γ -linolenic acid and

vincadifformine; further antimicrobial investigation with broth microdilution assay revealed these two compounds' contribution to the antimicrobial activity of the whole plant extract. However, this approach failed to identify and isolate the antimicrobial compounds detected via direct bio-autographic assay in *T. macropterus*. The anti-inflammatory investigation revealed that a number of plant extracts can decrease the protein levels of several inflammatory mediators. Finally, our study supports some of the documented ethnobotanical uses.

Publications, Presentations

Publications

Yonbawi, A.R., Abdallah, H.M., Alkhilaiwi, F.A., Koshak, A.E. and Heard, C.M. 2021. Anti-proliferative, cytotoxic and antioxidant properties of the methanolic extracts of five Saudi Arabian flora with folkloric medicinal use: *Aizoon canariense*, *Citrullus colocynthis*, *Maerua crassifolia*, *Rhazya stricta* and *Tribulus macropterus*. *Plants* 10(10), pp. 1–21.

Poster Presentation

Medicinal Properties of Saudi Arabian Flora Extracts. **Yonbawi AR**, Baillie LW, Heard CM. Postgraduate research day of Pharmacy School, Cardiff School of Pharmacy and Pharmaceutical Sciences, Redwood Building, Cardiff University, Cardiff, UK (May 2019).

Oral Presentation

Medicinal Properties of Saudi Arabian Flora Extracts. **Yonbawi AR**, Baillie LW, Heard CM. Pharmacy School Postgraduate research day, Cardiff School of Pharmacy and Pharmaceutical Sciences, Redwood Building, Cardiff University, Cardiff, UK (April 2021).

Table of Contents

Chapter 1: General Introduction	1
1.1 Overview.....	2
1.2 A Brief History of Medicinal Plants.....	2
1.3 Natural Flora Indigenous to Saudi Arabia	7
1.3.1 <i>Aizoon canariense</i>	7
1.3.2 <i>Citrullus colocynthis</i>	9
1.3.3 <i>Maerua crassifolia</i>	11
1.3.4 <i>Rhazya stricta</i>	13
1.3.5 <i>Tribulus macropterus</i>	15
1.4 Human Skin	16
1.4.1 Human Skin Function	16
1.4.2 Human Skin Structure.....	17
1.4.2.1 The Epidermis.....	17
1.4.2.2 The Dermis	20
1.4.2.3 The Hypodermis (Subcutaneous Fat).....	20
1.5 Infections	21
1.5.1 Skin Microflora	21
1.5.2 Skin and Soft-Tissue Infections (SSTI).....	23
1.5.2.1 SSTI Causative Microbes.....	23
1.5.2.2 SSTI Classification	24
1.5.2.3 Management of Skin and Soft-Tissue Infections (SSTI).....	26
1.5.2.4 Inflammation Accompanying SSTI	28
1.5.2.4.1 Inflammatory Cytokines in the Skin	29
1.5.3 Antimicrobial Agents from Natural Products	31
1.5.3.1 Resistance to Current Antimicrobial Therapy.....	35
1.6 Wounds.....	38
1.6.1 Wounds Classification	39
1.6.1.1 Acute Wounds	39
1.6.1.2 Chronic Wounds	40
1.6.1.2.1 Management of Chronic Wounds.....	42
1.6.2 Wound Healing Process.....	42
1.6.2.1 Haemostasis Phase.....	43
1.6.2.2 Inflammatory Phase	44
1.6.2.3 Proliferative Phase	46
1.6.2.4 Remodeling Phase.....	51
1.6.3 Natural Products in Wound Management.....	51

1.6.3.1 Wound Dressings	52
1.6.4 Wounds Infection and Biofilm Formation	53
1.6.4.1 Management of Bacterial Biofilm Infections	56
1.7 Aims and Objectives.....	57
1.7.1 Project Aim	57
1.7.2 Project Objectives.....	57
Chapter 2: Plant Material Collection, Extraction and Fractionation	59
2.1 Introduction.....	60
2.2 Chapter Aim and Objectives.....	62
2.3 Materials	63
2.4 Methods	63
2.4.1 Plant Material Collection	63
2.4.2 Plant Extraction	65
2.4.3 Liquid-Liquid Chromatography	65
2.4.4 Thin-Layer Chromatography (TLC).....	66
2.4.5 Column Chromatography (CC).....	68
2.4.6 Nuclear Magnetic Resonance (NMR)	69
2.4.6.1 ¹ H-NMR	69
2.4.6.2 ¹³ C-NMR	70
2.4.6.3 Distortionless Enhancement by Polarisation Transfer (DEPT-135).....	71
2.4.6.4 Correlation Spectroscopy (COSY)	71
2.4.6.5 Nuclear Overhauser Effect Spectroscopy (NOESY).....	71
2.4.6.6 Heteronuclear Multiple Quantum Coherence (HMQC).....	72
2.4.6.7 Heteronuclear Multiple Bond Coherence (HMBC).....	72
2.4.7 Mass Spectroscopy (MS)	72
2.5 Results and Discussion	73
2.5.1 Plant Extractions Yields.....	73
2.5.2 Plant Extract Liquid-Liquid Partition Yield.....	74
2.5.3 Fractionation of Plant Extracts by Column Chromatography.....	75
2.5.3.1 <i>Aizoon canariense</i>	75
2.5.3.2 <i>Rhazya stricta</i>	78
2.5.3.3 <i>Tribulus macropterus</i>	79
2.5.4 Thin-Layer Chromatography (TLC).....	81
2.5.4.1 Optimise the Organic Solvent System for the Separation of Plant Extracts ...	81
2.5.4.2 Separation of Plant Extracts by Thin-Layer Chromatography	82
2.5.5 Structure Elucidation of the Isolated Compounds.....	84
2.5.5.1 Identification of RSH6 as Vincadifformine	84
2.5.5.2 Identification of ACC8 as γ -Linolenic Acid	92

2.6 Conclusion	97
Chapter 3: The Effect of Plant Extracts on Human Skin Keratinocyte Cell Proliferation and Survival.....	99
3.1 Introduction.....	100
3.2 Chapter Aim and Objectives.....	103
3.3 Materials	104
3.4 Methods	105
3.4.1 Preparation of the Stock Solution of Extracts	105
3.4.2 Culturing of HaCaT Cell Line.....	105
3.4.2.1 Cell Culture Medium Preparation.....	105
3.4.2.2 HaCaT Cell Passaging and Counting.....	106
3.4.2.3 HaCaT cell Freezing and Thawing	107
3.4.3 Cell Growth Study	108
3.4.4 MTT Assay (3-(4,5-dimethylthiazol-2-yl)-2,5-diphenyl tetrazolium bromide reduction).....	109
3.4.5 Fluorescein Diacetate and Propidium Iodide-based Fluorescence-Activated Cell Sorting (FACS) Analysis.....	110
3.4.6 Fluorescein Diacetate and Propidium Iodide-based Confocal Laser Scanning Microscopy Analysis (CLSM).....	112
3.4.7 Statistical Analysis	113
3.5 Results and Discussion	113
3.5.1 HaCaT Cell Growth.....	113
3.5.2 Evaluating the Effects of Plant Extracts on the Viability of HaCaT	115
3.5.3 Evaluating the Cytotoxic Effect of Plant Extracts on HaCaT	120
3.5.3.1 Determining Cytotoxicity Using Fluorescence-Activated Cell Sorting	120
3.5.3.2 Confocal Laser Scanning Microscopy (CLSM)	125
3.6 Conclusion	130
Chapter 4: Antioxidant and Wound Healing Properties of Plant Extracts.....	132
4.1 Introduction.....	133
4.1.1 The Role of Reactive Oxygen Species (ROS) in Wound Healing.....	135
4.2 Chapter Aim and Objectives.....	139
4.3 Materials	139
4.4 Methods	140
4.4.1 Preparation of Samples	140
4.4.2 Determination of Extracts Total Phenolic Content:	140

4.4.3 DPPH (1,1-diphenyl-2-picrylhydrazyl) Free Radical Scavenging Assay	141
4.4.3.1 Preparation of DPPH Radical	141
4.4.4 ROS-Glo H ₂ O ₂ Assay	142
4.4.5 Scratch Wound Assay	143
4.4.6 Statistical Analysis	144
4.5 Results and Discussion	144
4.5.1 Total Phenolic Content	144
4.5.2 Chemical-Based Assessment of Antioxidant Activity	145
4.5.3 Cell-Based Assessment of Antioxidant Activity	148
4.5.4 Effects of Plant Extracts on HaCaT Migration	150
4.6 Conclusion	159
Chapter 5: Antimicrobial Activities of Plant Extracts and Fractions	160
5.1 Introduction	161
5.1.1 Antibiotics Resistance in Bacterial Biofilm	164
5.2 Chapter Aim and Objectives	168
5.3 Materials	168
5.3.1 Chemicals and Culture Media	168
5.3.2 Bacterial Cultures	169
5.4 Methods	169
5.4.1 Preparation of Samples	169
5.4.2 Freezing Bacterial Strains	170
5.4.3 Bacterial Overnight Culture	170
5.4.4 Preparation of Bacterial Slope	170
5.4.5 Bacterial Counting by Miles and Misra Method	171
5.4.6 Bacteria Gram Staining	173
5.4.7 Agar Well Diffusion Assay	175
5.4.8 Broth Microdilution Assay to Determine Minimum Inhibitory and Minimum Bactericidal Concentrations	176
5.4.9 Detecting Antimicrobial Compounds Through Bio-Autographic Assay	178
5.4.10 <i>In Vitro</i> Assessment of Plant Extracts on Biofilm Formation and Biofilm Eradication	179
5.4.10.1 Evaluating the Ability of Selected Bacterial Species to Form a Reproducible Biofilm	179
5.4.10.2 Assessment of Plant Extracts Effect on Biofilm Formation and Biofilm Eradication	180
5.4.10.3 Live/Dead Imaging of Plant Extract-Treated Biofilms Using Confocal Laser Scanning Microscopy	181
5.4.11 Statistical Analysis	182

5.5 Results and Discussion	183
5.5.1 Agar Well Diffusion Assay	183
5.5.2 Broth Microdilution Assay.....	189
5.5.3 Antibacterial Bio-Autographic Assay.....	190
5.5.4 Evaluating the Ability of Tested Microorganism to Form a Reproducible Biofilm	196
5.5.5 Inhibition of Biofilm Formation and Biofilm Eradication.....	197
5.5.6 CLSM Live/Dead Microbial Viability Method to Evaluate Biofilm Eradication	204
5.6 Conclusion	209
Chapter 6: Antimicrobial Activities of Isolated Compounds	211
6.1 Introduction.....	212
6.2 Chapter Aim and Objectives.....	216
6.3 Materials	217
6.3.1 Chemicals and Culture Media	217
6.3.2 Bacterial Cultures	217
6.4 Methods	218
6.4.1 Preparation of Samples	218
6.4.2 Broth Microdilution Test to Determine Minimum Bactericidal and Minimum Inhibitory Concentrations	218
6.4.3 <i>In Vitro</i> Assessment of Isolated Compounds on Biofilm Formation and Biofilm Eradication.....	220
6.4.3.1 Assessment of Isolated Compounds on Biofilm Formation and Biofilm Eradication	220
6.4.3.2 Live/Dead Imaging of Biofilms Treated with Compounds through Confocal Laser Scanning Microscopy.....	221
6.4.4 Statistical Analysis	222
6.5 Results and Discussion	223
6.5.1 Broth Microdilution Assay.....	223
6.5.2 The Effect of Isolated Compounds on the Inhibition of Biofilm Formation and Biofilm Eradication	226
6.5.3 Evaluation of Biofilm Eradication by Live/Dead Bacterial Viability Assay.....	231
6.6 Conclusion	236
Chapter 7: Anti-inflammatory Properties of Plant Extracts.....	238
7.1 Introduction.....	239
7.2 Chapter Aim and Objectives.....	244

7.3 Materials	244
7.4 Methods	245
7.4.1 Preparation of the Stock Solution of Extracts	245
7.4.2 Cell Culture and Stimulation of Inflammatory Mediators by LPS.....	246
7.4.3 Enzyme-Linked Immunosorbent Assays (ELISAs)	246
7.4.3.1 Modulation of TNF- α , IL-1 β , IL-6, and IL-8 in HaCaT Cells	246
7.4.3.2 Modulation of COX-2 in HaCaT Cells.....	248
7.4.4 Statistical Analysis	249
7.5 Results and Discussion	250
7.5.1 Measuring the Cytokine Levels.....	250
7.5.2 COX-2 Modulation.....	258
7.6 Conclusion	262
Chapter 8: General Discussion	263
8.1 Overview.....	264
8.2 Ethnobotanical Fieldwork.....	265
8.3 <i>Aizoon canariense</i>	266
8.4 <i>Citrullus colocynthis</i>	270
8.5 <i>Maerua crassifolia</i>	272
8.6 <i>Rhazya stricta</i>	275
8.7 <i>Tribulus macropterus</i>	280
8.8 Future Prospects	282
9. References:	285

List of Figures

Figure 1 <i>A. canariense</i>	8
Figure 2 Examples of <i>A. canariense</i> isolated compounds	8
Figure 3 <i>C. colocynthis</i>	10
Figure 4 Examples of <i>C. colocynthis</i> isolated compounds.....	11
Figure 5 <i>M. crassifolia</i>	12
Figure 6 <i>R. stricta</i>	14
Figure 7 Examples of <i>R. stricta</i> isolated compounds.....	14
Figure 8 <i>T. macropterus</i>	16
Figure 9 Three layers of the skin	17
Figure 10 Epidermis cross-sectional diagram to show the five layers.....	18
Figure 11 Shows uncomplicated skin and soft tissue infections (SSTI) cases with superficial layers of the skin involvement (A) furuncles (B) abscesses	25
Figure 12 Clinical presentation of cellulitis skin and soft tissue infection (SSTI) involves deeper layer of the skin	25
Figure 13 Structures of antimicrobial agents of natural origin.....	35
Figure 14 Four different stages of the wound healing process.....	43
Figure 15 Different stages of bacterial biofilm formation	55
Figure 16 The stages of the bioassay-guided fractionation approach.....	62
Figure 17 <i>R. stricta</i> liquid-liquid partition between two immiscible liquid phases (A) hexane (B) chloroform.....	66
Figure 18 A comparison of <i>R. stricta</i> liquid-liquid partition extraction yields.....	75
Figure 19 Shows developed TLC plates spotted with <i>M. crassifolia</i> comparing two solvent systems	82
Figure 20 <i>R. stricta</i> and <i>C. colocynthis</i> TLC plates developed with 30% ethyl acetate and 70% hexane, it indicate the presence of many compounds in these two extract (A) The plate was sprayed with p-anisaldehyde and sulphuric acid reagent and heated at 110 °C for 3 min (B) UV active compounds were visualized at 254 nm UV light.....	84
Figure 21 Chemical structure of RSH6 (vincadifformine).	85
Figure 22 ¹ H-NMR spectrum of RSH6.....	85

Figure 23 ¹³ C-NMR APT spectrum for RSH6	86
Figure 24 HMQC spectrum for RSH6	87
Figure 25 HMBC ¹ H- ¹³ C NMR for RSH6	87
Figure 26 Mass spectrum of RSH6.....	88
Figure 27 Chemical structure of ACC8 (γ -linolenic acid).....	92
Figure 28 ¹ H-NMR spectrum of ACC8	93
Figure 29 ¹³ C-NMR APT spectrum of ACC8	93
Figure 30 ¹³ C-NMR DEPT-135 spectrum of ACC8.....	94
Figure 31 HMQC spectrum for ACC8.....	94
Figure 32 HMBC spectrum of ACC8	95
Figure 33 MTT reduction reaction.....	102
Figure 34 Illustration of a haemocytometer's gridded areas	107
Figure 35 HaCaT growth curve with normal culturing conditions.....	114
Figure 36 Proliferation percentage of HaCaT cells treated with (A) <i>A. canariense</i> (B) <i>C. colocynthis</i> (C) <i>M. crassifolia</i> (D) <i>R. stricta</i> (E) <i>T. macropterus</i>	116-118
Figure 37 Red dots represent population 1 (P1) cells chosen from the untreated, unstained control. (A) dot plot of FSC against SSC, and (B) dot plot of PI-H against FDA-H; non-stained cells are shown in the lower left quadrant.....	122
Figure 38 Defining the area of PI-stained cells utilising FACS analysis. (A) The PI stain will collect within the nucleus of dead cells and emit a red fluorescence, which can be seen as red spots in the upper left region. (B) Histogram for PI-H	122
Figure 39 Dot plot depicting cells stained with FD. (A) The green spots in the lower right region are FD-stained cells, and, (B) Histogram of the FDA-H.....	123
Figure 40 Percentage of PI-stained HaCaT cells treated with plant extracts in comparison to the PI control cells (fixed cells) at varying concentrations (A) <i>A. canariense</i> , (B) <i>C. colocynthis</i> , (C) <i>M. crassifolia</i> , (D) <i>R. stricta</i> , (E) <i>T. macropterus</i>	125
Figure 41 Obtained images via CLSM of dual-stained HaCaT cells using PI and FD .	126-127
Figure 42 The two overlapping functions of keratinocyte migration and proliferation are illustrated in a diagram of the skin re-epithelialization process.	134
Figure 43 Role of reactive oxygen species (ROS) in normal wound healing and diabetic chronic wounds.....	136

Figure 44 The Formation of stable alkyl hydroperoxide through a donation of electron by phenolic antioxidant natural product.....	137
Figure 45 The percentage of DPPH free radical scavenging ability over a range of concentrations of selected plant extracts.....	146
Figure 46 Inhibition of H ₂ O ₂ radicals generation by various plant extracts at different concentrations.....	148
Figure 47 The difference in H ₂ O ₂ production between <i>C. colocynthis</i> with and without cells.	149
Figure 48 EVOS images of wound area in HaCaT cells monolayer by employing scratch assay <i>in vitro</i>	151-155
Figure 49 Analysis of wound area (uncovered area) in HaCaT cells following scratch wound, treated with (A) <i>A. canariense</i> (B) <i>C. colocynthis</i> (C) <i>M. crassifolia</i> (D) <i>R. stricta</i> (E) <i>T. macropterus</i>	155-157
Figure 50 Characteristics of planktonic and biofilm bacteria.	163
Figure 51 MRSA standard curve.....	172
Figure 52 <i>P. aeruginosa</i> standard curve.....	172
Figure 53 <i>E. coli</i> standard curve.....	173
Figure 54 Obtained images under a light microscope of Gram-stained (A) <i>Staphylococcus aureus</i> , (B) MRSA, (C) <i>Staphylococcus epidermidis</i> , (D) <i>P. aeruginosa</i> , and (E) <i>E. coli</i> ..	174-175
Figure 55 The well diffusion assay used to evaluate the antimicrobial activity of <i>A. canariense</i> exhibited a partial inhibitory zone towards MRSA.	187
Figure 56 <i>R. stricta</i> hexane and chloroform extracts were examined utilising the bacterial bio-autographic method.....	191
Figure 57 The antimicrobial activity of <i>R. stricta</i> hexane fractions was determined using a bacterial bio-autographic test against <i>Staphylococcus aureus</i>	195
Figure 58 (A) After 24 h incubation in MH broth, the crystal violet staining technique was used to compare biofilm formation between the bacterial strains investigated. (B) biofilm mass of <i>P. aeruginosa</i> stained with crystal violet	197
Figure 59 Comparison of the ability of plant extracts to inhibit biofilm formation for (A) <i>A. canariense</i> (B) <i>R. stricta</i> (C) <i>T. macropterus</i>	199-200

Figure 60 Comparison of the ability of plant extracts to eradicate pre-formed biofilm for (A) <i>A. canariense</i> (B) <i>R. stricta</i> (C) <i>T. macropterus</i>	200-201
Figure 61 Effects of <i>A. canariense</i> , <i>R. stricta</i> , and <i>T. macropterus</i> on the biofilm eradication of <i>S. aureus</i> using a live/dead bacterial viability assay.....	206-207
Figure 62 Effects of <i>A. canariense</i> , <i>R. stricta</i> , and <i>T. macropterus</i> on the biofilm eradication of MRSA using a live/dead bacterial viability assay.....	208-209
Figure 63 Inhibitory effect of vincadifformine at different concentrations ($\mu\text{g/mL}$) on the growth of selected bacterial strains.....	225
Figure 64 Inhibitory effect of γ -linolenic acid at different concentrations ($\mu\text{g/mL}$) on the growth of selected bacterial strains.....	225
Figure 65 Comparison of the ability of isolated compounds to inhibit biofilm formation for (A) vincadifformine (B) γ -linolenic acid.....	228
Figure 66 Comparison of the ability of isolated compounds to eradicate pre-formed biofilm for (A) vincadifformine (B) γ -linolenic acid.....	229
Figure 67 Effects of vincadifformine and γ -linolenic acid on the biofilm eradication of <i>S. aureus</i> using a live/dead bacterial viability assay.....	233-234
Figure 68 Effects of vincadifformine and γ -linolenic acid on the biofilm eradication of MRSA using a live/dead bacterial viability assay.....	235-236
Figure 69 TNF- α levels in HaCaTs, cultured in the presence of (A) <i>A. canariense</i> (B) <i>M. crassifolia</i> (C) <i>T. macropterus</i> (D) <i>R. stricta</i> (E) <i>C. colocynthis</i>	252
Figure 70 IL-1 β levels in HaCaTs, cultured in the presence of (A) <i>A. canariense</i> (B) <i>M. crassifolia</i> (C) <i>T. macropterus</i> (D) <i>R. stricta</i> (E) <i>C. colocynthis</i>	253
Figure 71 IL-6 levels in HaCaTs, cultured in the presence of (A) <i>A. canariense</i> (B) <i>M. crassifolia</i> (C) <i>T. macropterus</i> (D) <i>R. stricta</i> (E) <i>C. colocynthis</i>	254
Figure 72 IL-8 levels in HaCaTs, cultured in the presence of (A) <i>A. canariense</i> (B) <i>M. crassifolia</i> (C) <i>T. macropterus</i> (D) <i>R. stricta</i> (E) <i>C. colocynthis</i>	255
Figure 73 COX-2 levels in HaCaTs, cultured in the presence of (A) <i>A. canariense</i> (B) <i>M. crassifolia</i> (C) <i>T. macropterus</i> (D) <i>R. stricta</i> (E) <i>C. colocynthis</i>	259

List of Tables

Table 1 Site A of collected plants.....	64
Table 2 Site B of the collected plant.....	64
Table 3 The yield following plant extraction with methanol for 72h.....	74
Table 4 <i>Aizoon canariense</i> hexane extract collected fractions by column chromatography. .	76
Table 5 <i>Aizoon canariense</i> chloroform extract collected fractions by column chromatography.	77
Table 6 <i>Rhazya stricta</i> hexane extract collected fractions by column chromatography.....	78
Table 7 <i>Tribulus macropterus</i> hexane extract collected fractions using a gradient elution system.....	79
Table 8 <i>Tribulus macropterus</i> chloroform extract collected fractions by column chromatography.....	80
Table 9 The different ratios of organic solvents are typically used in TLC separation methods	81
Table 10 R _f values of different phytochemical bands in plant extracts.....	83
Table 11 ¹ H and ¹³ C NMR data for RSH6, obtained in DMSO-d ₆ (500 MHz).....	91
Table 12 ¹ H and ¹³ C NMR data for ACC8, obtained in DMSO-d ₆ (500 MHz).	97
Table 13 The IC ₅₀ of <i>C. colocynthis</i> , <i>R. stricta</i> , <i>A. canariense</i> , <i>M. crassifolia</i> , and <i>T.</i> <i>macropterus</i> as measured by the MTT test after Five and seven days of treatment.....	120
Table 14 Total phenolic content (TPC) of five plant extracts.....	145
Table 15 IC ₅₀ values (µg/mL) of plant extracts as determined by the DPPH test.....	146
Table 16 Summary of antibacterial activities of plant extracts against <i>Staphylococcus aureus</i>	184
Table 17 Summary of antibacterial activities of plant extracts against MRSA.	184
Table 18 Summary of antibacterial activities of plant extracts against <i>Staphylococcus</i> <i>epidermidis</i>	185
Table 19 Summary of antibacterial activities of plant extracts against <i>Pseudomonas</i> <i>aeruginosa</i>	185
Table 20 Summary of antibacterial activities of plant extracts against <i>Propionibacterium acne</i>	186

Table 21 Summary of antibacterial activities of plant extracts against <i>Escherichia coli</i>	186
Table 22 Summary of MIC and MBC values of <i>Rhazya stricta</i>	189
Table 23 Summary of MIC and MBC values of positive control thymol.....	190
Table 24 Summary of Rf values of tested plant extracts.....	192
Table 25 Active <i>A. canariense</i> and <i>T. macropterus</i> fractions of hexane and chloroform extracts were determined via bacterial bio-autographic test against <i>Staphylococcus aureus</i> and MRSA	196
Table 26 Present MIC ₉₀ and MBC values of tested isolated compounds and positive controls against selected bacterial stains.	226

List of abbreviations

ABTS	2,2'-azino-bis-3-ethylbenzthiazoline-6-sulphonic acid
AMR	Antimicrobial resistance
ANOVA	One way analysis of variance
ATCC	American Type Culture Collection
CCM	Serum containing culture medium
CFU	Colony-forming units
CLSI	Clinical and Laboratory Standards Institute
CLSM	Confocal laser scanning microscopy
COX-2	Cyclooxygenase-2
°C	Degrees Celsius
DMEM	Dulbecco's Modified Eagle Medium
DMSO	Dimethyl sulfoxide
DPPH	1,1-Diphenyl-2-picrylhydrazyl
ECM	Extracellular matrix
ELISA	Enzyme-linked immunosorbent assay
FACS	Fluorescence-activated cell sorting
FBS	Fetal bovine serum
FD	Fluorescein diacetate
FC	Flash chromatography
HaCaT	Immortalized human skin keratinocytes
HDL	High-density lipoprotein
HELA	Cervix cancer cell line

HEPG2	Hepatocellular carcinoma cell line
HIV	Human immunodeficiency virus
HPLC	High performance liquid chromatography
HRMS	High resolution mass spectrometry
H ₂ O ₂	Hydrogen peroxide
IC ₅₀	Inhibitory concentration 50
IL-1	Interleukin-1
IL-6	Interleukin-6
IL-8	Interleukin-8
KSA	Kingdom of Saudi Arabia
Kg	Kilogram
LC-MS	Liquid chromatography–mass spectrometry
LDH	Lactate dehydrogenase
LDL	Low-density lipoprotein
LPS	Lipopolysaccharide
MBC	Minimum bactericidal concentration
MCF7	Breast cancer cell line
MHA	Mueller Hinton agar
MHB	Mueller Hinton broth
MIC	Minimum inhibitory concentration
MRSA	Methicillin-resistant <i>Staphylococcus aureus</i>
MRSE	Methicillin-resistant <i>Staphylococcus epidermidis</i>
MTT	Thiazolyl blue tetrazolium bromide
m/z	Mass-to-charge ratios

NADH	Nicotinamide adenine dinucleotide
NCTC	National Collection of Type Cultures
NMR	Nuclear magnetic resonance
NOD2	Nucleotide-binding oligomerization domain 2
NSAIDs	Nonsteroidal anti-inflammatory drugs
OD	Optical density
PAMP	Pathogen-associated molecule
PBS	Phosphate buffered saline
PGE2	Prostaglandin E2
PHMB	Polyhexamethylene biguanide
PI	Propidium iodide
ROS	Reactive oxygen species
Rf	Retention Factor
SD	Standard deviation
SE	Standard error
SSTI	Skin and soft-tissue infections
TLC	Thin layer chromatography
TNF	Tumour necrosis factor
TLRs	Toll-like receptors
UK	United Kingdom
USA	United States of America
UV	Ultraviolet
WHO	World Health Organization
ZOI	Zone of inhibition

Chapter 1: General Introduction

1.1 Overview

Based on folkloric use, this project explored the medicinal properties of the following five plants indigenous to the Western region of Saudi Arabia: *Aizoon canariense*, *Citrullus colocynthis*, *Maerua crassifolia*, *Rhazya stricta*, and *Tribulus macropterus*. Bioassay-guided fractionation was conducted to evaluate the antimicrobial, antibiofilm, cytotoxic, anti-proliferative, anti-inflammatory, and antioxidant activities. Furthermore, with the rapid rise of bacterial resistance to current antimicrobial agents, especially systemic ones, particular attention will be paid to the potential of discovering a new topical therapeutic antimicrobial agent against skin infections that can be used alone or as adjunctive therapy to systemic treatment to lower the risk of bacterial resistance.

1.2 A Brief History of Medicinal Plants

One of the earliest written descriptions of medicinal plant use was documented through a clay slab in Nagpur city written by Sumerians around 4000 BC. It contains twelve drug recipes for the sum of 200 plants and plant extracts, including henbane, poppy, and mandrake (Natnoo, 2014). Another ancient example of documented use of medicinal plants took place around 2500 BC, when the Chinese Emperor Shen Nung wrote a book on medicinal roots and grasses, "Pen T'Sao," (Natnoo, 2014). Then, in 1500 BC, the Egyptian Ebers Papyrus detailed many plants utilized as drugs, such as acacia, saffron, olive, opium, peppermint, and henbane. During the classical Greek period, a great advancement in the science of pharmacognosy was established by Aristotle, as he recognized more than 500 remedies from medicinal plants and was followed by the father of allopathic medicine, Hippocrates, 460 BC (Khan, 2014). In 77 AD, Dioscorides

wrote the first pharmacopeia of herbs with more than 900 medicinal plants defined with detailed descriptions of their location, morphological character, collection method, and uses.

After the decline of the Roman Empire, the Arabic world became a hub of scientific and medical advancement for several centuries. Ancient Greek and Roman works were translated into Arabic and studied by scholars. They expanded and enhanced Hippocrates's principles, and physicians began to treat patients with dietary restrictions, exercise routines, and the prescription of medicinal plants. Moreover, Rhazes (Al Razi, 846-930) and Avicenna (Ibn Sina, 980-1037) played a significant role in establishing this period as the Golden Age. The final phase of the development of Arab medicine began in the 12th century when European scholars began to study and translate Arabic texts into Latin (Saad et al., 2005; Al-Rawi and Fetters, 2012). Scientists in the fields of pharmacology and ethnopharmacology began exploring the chemical constituents of medicinal plants traditionally and experimentally employed in treating and preventing disease. Scientists like Jaber Bin Hayan explored innovative methods to extract and purify sulfuric acid, alcohol, and nitric acid. Plant extracts were prepared and administered orally, topically, and by vapour inhalation or fumigation (Saad et al., 2005). Tibb Nabawi, or traditional Arabic and Islamic medicine, is widely used in Saudi Arabia and the Middle East (Saad et al., 2005; Al-Rawi and Fetters, 2012).

Nigella sativa (L.), often known as black seed, is a popular plant used throughout the Middle East and South East Asia for hundreds of years to treat and prevent a wide range of illnesses (Al-Ghamdi, 2001). In the prophetic tradition, the black seed is highly valued for its healing abilities. Black seed is indicated for respiratory health, the body's immune support, and intestinal and stomach health. In addition, studies have indicated its antibacterial, antihypertensive, anti-inflammatory, hepatoprotective, cytotoxic, and analgesic effects

(Sharma et al., 2009). Another promising medicinal plant commonly used in the Middle East is *Ziziphus spina-christi* (L.), known locally as "Sidr. *Z. spina-christi* has been used in Chinese traditional medicine to enhance blood flow to the liver and heart and to manage irritability, anxiety, and arrhythmias. In Saudi folk medicine, the leaves of *Z. spina-christi* are applied to promote wounds healing, treat some skin illnesses and sores, cure ringworm, act as an antipyretic, and treat gonorrhea, sex disorders, and certain inflammatory disorders. Furthermore, it has been claimed that *Z. spina-christi* leaves are used as an anti-diabetic therapy in folk medicine (Abdel-Zaher et al., 2005; Tawfika et al., 2015; Rajendrasozhan et al., 2017).

Around the Sixteenth century in Europe, relieving diseases by compounding mixtures of medicinal plants was starting to develop (Petrovska, 2012), although advancement was severely hindered by paranoia concerning witchcraft. Later in the Seventeenth century, more scientific approaches were adopted; for example, the bark of the cinchona tree was introduced to treat malaria, and in the Ninetieth century, quinine was isolated from the tree and still used for the treatment of malaria (Hassan, 2015).

Aerial parts of the Foxglove plant (*Digitalis purpurea*) were introduced to the London Pharmacopoeia for its general medicinal uses; however, due to its toxicity and nonspecific medicinal use, it was removed later from the Pharmacopoeia (Wilkins et al., 1985). In the following years, English physician William Withering published: *An Account of the Foxglove*. He was the first to draw a clear link between improved cardiac edema manifested in congestive heart failure and the administration of digitalis. Over ten years, Withering conducted a trial on more than 160 patients in which he administered a powder from fresh leaves of Foxglove. Then he fully described the drug therapeutic and toxic effects, documented the plant diuretic

effect, and noticed the favorable effect on the heart pulse. The activity of this plant was attributed to the presence of cardiac glycosides. Even in the present day, digitalis continues to be prescribed as digitoxin (active constituent from *Digitalis purpurea*) and digoxin (from *Digitalis lanata*) for the management of congestive heart failure (Bessen, 1986).

A major discovery in the Nineteenth century was the isolation of morphine from *Papaver somniferum* (the opium poppy) by the German pharmacist Friedrich Serturmer (Hamilton et al., 2000), followed by the breakthrough discovery of penicillin antibiotic in 1929 by Fleming (Fleming, 1929), and the isolation of penicillin F by Florey et al. (1943). These discoveries contributed to saving countless lives and laid the ground for future work of isolation and the purification of natural products from plants, while also spawning an explosion in synthetic/semi-synthetic medicinal chemistry.

An example of a fruit that is considered to be a medicinal plant is *Punica granatum* (pomegranate), which is native to the regions between Iran and India. In Arabic cultures, pomegranate is considered the fruit of paradise, while the ancient Greeks refer to it as the fruit of the dead. This fruit has been acknowledged as a medicine since ancient history. It was first documented in the Egyptian Ebers Papyrus as a treatment of tapeworms through the infusion of the plant root in water, and traditionally pomegranate has been used for diarrhea, dysentery, prevention abortion, snakebite and to lower body temperature. Moreover, in Brazil, pomegranate is used traditionally for the treatment of throat infection and cough (Lansky et al., 2000; Baraga et al., 2005; Seeram et al., 2006; Stover, 2007). The pharmacological activities of pomegranate have been intensively investigated, and a recent study by Houston explored the activity of pomegranate rind extract (PRE) and its punicalagin one of the active constituents of PRE against Herpes simplex virus (HSV), including acyclovir-resistant HSV

and it revealed promising enhanced activity when combined with zinc salts (Houston et al., 2017).

Although medicinal chemistry and drug design are sources for the development of novel drugs, natural products are still considered important for the discovery of new drugs. This is a consequence of the molecular complexity and structural diversity of natural products (Cragg and Newman, 2013), coupled with the fact that part of the entire world's flowering system remains to be investigated as potential sources of new drugs (Li and Vederas, 2009; Dias et al., 2012). One-third of the world's plant species are found in relatively untapped regions like the Amazonian rainforests, which are believed to hold the world's largest plant diversity. There are around 30,000 species of plants present there (Silman, 2007; Pimm et al., 2014). Moreover, traditional plant healing among indigenous communities has a long and rich history. Despite the region's rich biodiversity of plant life, few medicinal compounds sourced from the area have made it to the markets (Desmarchelier, 2010). Among the plants and trees native to the iron-rich soils of the Flona de Carajasi in the Brazilian Amazon is the little tree *Pilocarpus microphyllus*, commonly known as jaborandi. Jaborandi is utilised by native communities to alleviate symptoms of the common cold and flu virus. Reports of its therapeutic use in writing first appeared in the Sixteenth century. Recently, it was discovered that jaborandi causes both perspiration and salivation. Based on these findings, the anti-glaucoma medication Timpilo (pilocarpine, an imidazole alkaloid) was developed and is currently approved by the Food and Drug Administration in the United States (Skiryicz et al., 2016).

1.3 Natural Flora Indigenous to Saudi Arabia

Saudi Arabia is one of the largest countries in the Middle East in terms of size. Consequently, It has a wide range of regions, including meadows, mountains, lava regions, valleys, and rocky deserts. The Kingdom of Saudi Arabia consists of two regions: the rain-fed zones of the Western and Southwestern highlands and the desert region of the interior (Aati et al., 2019). More than 2,250 species in 142 families make up the natural flora, providing a vast, mostly unexplored supply of plant-based drugs. However, despite this, most medicinal plants have not had their pharmacological properties properly explored (Saadabi, 2006; Yusuf et al., 2014).

1.3.1 *Aizoon canariense*

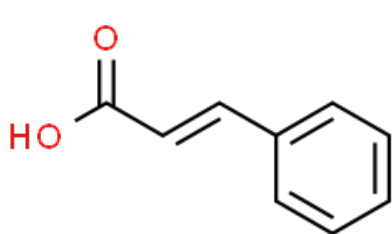
This plant belongs to the *Aizoaceae* family and is locally known as Hadag (Al-Sodany et al., 2013). Traditionally, *A. canariense* whole plant has been used to treat hepatitis and jaundice and to alleviate hypertension, flatulence, and its leaves paste applied topically to heal wounds (Hassan-Abdallah et al., 2013; Al-Laith et al., 2015; Phondani et al., 2016). Phenolics, steroids, triterpenes, coumarins, alkaloids, tannins, flavonoids, and saponins, as well as fatty acids such as protocatechuic acid and cinnamic acid, were identified in *A. canariense* in previous phytochemical analyses (Phoboo et al., 2015).

Recent pharmacological studies have demonstrated that *A. canariense* possesses antioxidant and free radical scavenging properties. Al-Laith et al. (2015) demonstrated that the IC₅₀ of *A. canariense* is 66 mg/mL for 1,1-diphenyl-2-picrylhydrazyl (DPPH) assay and 16.06 mg/mL for 2,2'-azino-bis-3-ethylbenzthiazoline-6-sulphonic acid (ABTS) assay. Another study showed that the cytotoxic activities of the extract were 21.5, 25.7 and 24.5 µg/mL against breast cancer cell line (MCF7), cervix cancer cell line (HELA) and hepatocellular carcinoma cell line

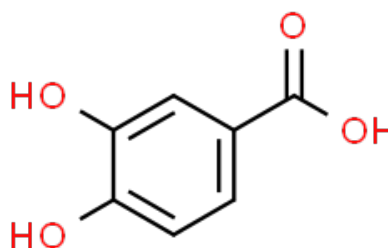
(HEPG2) (Almehdar et al., 2012). In brine shrimp toxicity studies, *A. canariense* showed cytotoxic activity with an LC₅₀ of 90.5 µg/mL (Tawaha, 2006). Figure 1 presents an image of *A. canariense*. Figure 2 presents examples of isolated compounds from *A. canariense*



Figure 1 *A. canariense* (collected previously by Dr. Hossam Afifi at King Abdulaziz University, available at https://floraofqatar.com/aizoon_canariense.htm)



Cinnamic acid



Protocatechuic acid

Figure 2 Examples of *A. canariense* isolated compounds

1.3.2 *Citrullus colocynthis*

Locally recognized as Handhal, this plant is a member of the *Cucurbitaceae* family and has been used for a variety of illnesses, including diabetes, jaundice, rheumatism, asthma, eye redness, analgesic, urinary disorders, ascites, cough, and for its wound healing ability (skin infections). In Saudi Arabia, fruits are used as antiparasitic, laxative, purgative, carminative, and for inflammatory conditions (Delazar et al., 2006; Gamal et al., 2010; Bnyan et al., 2013; Hussain et al., 2014). Previous phytochemical studies on *C. colocynthis* seeds and aerial plant parts revealed the presence of tocopherol, triterpenes, and fatty acids compounds, particularly cucurbitacin B and E, which have been effectively isolated and identified (Chawech et al., 2015; Saeed et al., 2019). Other studies revealed the presence of alkaloids, glycosides, essential oils, carbohydrates, and flavonoids (Nehdi et al., 2013; Hussain et al., 2014). Several flavonoids glycosides has been isolated from *C. colocynthis*, such as isosaponarin, isovitexin, and isoorientin 3'-O-methyl ether (Delazar et al., 2006). Four flavonoids (kaempferol, catechin, myricetin, and quercetin) and eight phenolic acids (gallic acid, chlorogenic acid, p-hydroxybenzoic acid, caffeic acid, vanillic acid, p-coumeric acid, sinapic acid, and ferulic acid) were identified in the ethanolic extracts of *C. colocynthis* fruits (Meena and Patni, 2008; Hussain et al., 2013).

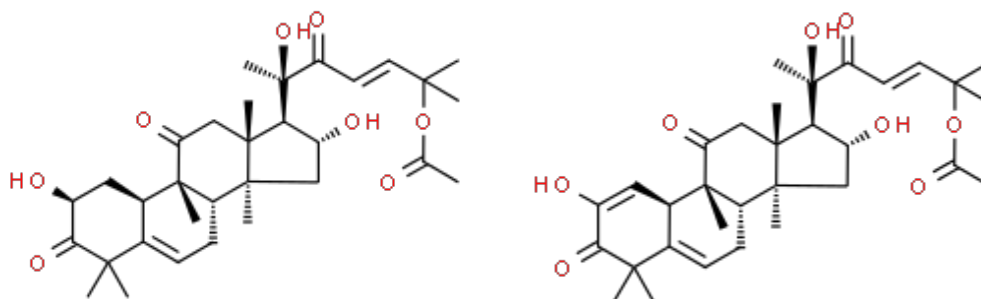
In contrast to many traditional medicines, this plant has been the focus of several clinical trials, such as the antihyperglycemic effect of the plant in a recent double-blind clinical trial for the period of two months with 50 patients diagnosed with type II diabetes. In which a significant reduction in fasting blood glucose and glycated haemoglobin (HbA1c) was observed as an indicator of blood glucose level in the previous two to three months, but no change was noticed in the cholesterol profile (Abdel-Hassan et al., 2000; Huseini et al., 2009; Al-Ghathithi et al.,

2004). The additional clinical investigation demonstrated a decrease in total cholesterol and triglyceride levels (Rahbar and Nabipour, 2010). In addition, Ali et al. (2013) reported the antimicrobial activity of *C. colocynthis* through disc diffusion assay, which indicated that the ethanolic fruit extract (500 mg/mL) has an inhibition zone of 15 mm against *Bacillus cereus*, 18 mm against *Staphylococcus aureus*, and 9 mm against *Klebsiella pneumoniae*.

In another study, Bnyan et al. (2013) found that ethanolic extracts of aerial parts inhibited *Escherichia coli* by 20 mm, *Proteus mirabilis* by 16 mm, and *Streptococcus agalactiae* by 8 mm. The IC₅₀ for the cytotoxic activity of *C. colocynthis* alcohol extracts was determined to be 17 µg/mL against the breast cancer cell line MCF-7; and 12 µg/mL against the liver cancer cell line, HepG-2 (Yin et al., 2008; Mukherjee and Patil, 2012). Evaluation of the antioxidant activity of methanolic fruit extracts revealed an 88% free radical scavenging activity in the DPPH experiment at a concentration of 2500 µg/mL (Kumar et al., 2008). Figure 3 shows an image of *C. colocynthis* obtained during the fieldwork. Figure 4 presents examples of isolated compounds from *C. colocynthis*.



Figure 3 *C. colocynthis* (obtained from the city of Al Taif in the southwestern province of Saudi Arabia, Al Sail Al-Kabeer)



Cucurbitacin B

Cucurbitacin E

Figure 4 Examples of *C. colocynthis* isolated compounds

1.3.3 *Maerua crassifolia*

This plant is a member of the *Capparaceae* family and is locally known as Sarh or Merro. Plant leaves extract is used traditionally to treat stomach ulcers, intestinal disorders, tooth pain, and for its wound healing properties. Volpato et al. (2012) reported that Sahrawi refugees in southwestern Algeria were using the plant. Burned plant leaves are used as a poultice, antiseptic for wounds, boils, and irritation. The leaves are administered as a powder or combined with water to form a poultice. A similar ethnobotanical study conducted in Tarfaya, Morocco, revealed a similar traditional use of plant leaves as poultice on wounds, and plant stem is chewed and used as a traditional toothbrush by local community members. Previous phytochemical analyses of *M. crassifolia* indicated the presence of alkaloids, phenols, tannins, steroids, terpenoids, cardiac glycosides, saponins, and flavonoids (Christian et al., 2014; Idm'hand et al., 2020).

Antimalarial, anti-inflammatory, analgesic, and antipyretic activities of *M. crassifolia* were studied by Christian et al. (2014, 2016), experimental animal models were used to evaluate

analgesic activity by injecting mice with acetic acid to induce pain and then observing the number of abdominal constrictions that were lowered compared to control. Moreover, antipyretic activity was evaluated by injecting rats with yeast or amphetamine to induce pyrexia and then measuring the rat's rectal temperature, other groups of rats were inoculated with parasite that causes malaria *Plasmodium berghei* then treated with *M. crassifolia* methanolic extract and rats blood was evaluated for the presence of the parasite. The Ckilaka et al. (2015) evaluated the antibacterial activity of methanolic *M. crassifolia* extract through disc diffusion method with concentrations of 12.5, 25, 50, 100 and 150 µg/mL on the following strains: *E. coli* (zones of inhibition: 7.7, 10, 12, 16, 20 mm), *S. aureus* (zones of inhibition: 12, 14, 15, 20, 29 mm), *S. typhi* (zones of inhibition: 10, 13, 19, 24 mm), and *B. subtilis* (zones of inhibition: 9, 12, 14, 18, 22 mm). In addition, free radical scavenging activity of 122 µg/mL was observed in a study using the DPPH assay to evaluate the antioxidant activity of *M. crassifolia* aqueous extract (Chaib et al., 2015). Figure 5 shows an image of *M. crassifolia* obtained during the fieldwork.



Figure 5 *M. crassifolia* (obtained from the city of Al Taif in the southwestern province of Saudi Arabia, Al Sail Al-Kabeer)

1.3.4 *Rhazya stricta*

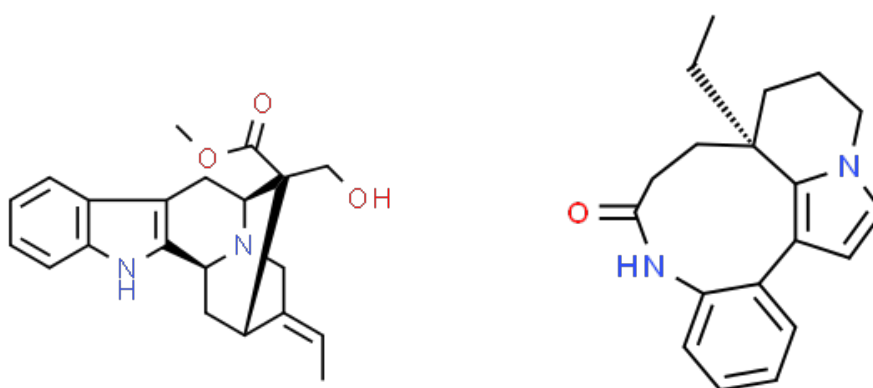
This species belongs to the *Apocynaceae* family and is commonly known as Harmal. In folkloric medicine, leaf extract is used to manage various diseases, including diabetes, sore throat, parasitic infections, inflammatory conditions, muscular discomfort, microbial infections, and arthritis. Moreover, traditional medicine uses it as a tonic and remedy for rheumatic pain, sore throat, syphilis, diabetes, ringworm, inflammatory conditions, and fever (Ali et al., 1998; Gamal et al., 2010; Baeshen et al., 2016; Bhadane et al., 2018). The presence of several chemical classes, including alkaloids, peptides, triterpenes, glycosides and flavonoids, demonstrates the diversity of the phytochemicals in *R. stricta* (Marwat et al., 2012). Several alkaloids has been reported, including akuammidine, tetrahydrosecamine, and rhazinilam (Bashir et al., 1994), 16-epi-z-isositsirikine, bhimberine, rhazidigenine-n-oxide, rhazicine, and dihydrosecodine (Obaid et al., 2017). Flavonoids has been isolated from this plant, such as rhazianoside A and B (Zaman, 1990) as well as triterpenes like 3a-hydroxy-ursane-5-ene, stigma sterol, and fatty esters such as 5, 7-dihydroxy-6, 20-dimethoxy isoflavone and oleanolic acid (Sultana and Khalid, 2010).

Anti-inflammatory research on *R. stricta* indicated that the plant extract could stimulate the production of pro-inflammatory mediators in mice. It relaxes the intestinal muscles of rats due to its antispasmodic and antipyretic properties; and it reduces the blood glucose level in rats (Tanira et al., 1996). The disc diffusion method was used to evaluate the antimicrobial activity of *R. stricta* aqueous extracts against *Neisseria meningitidis* at concentrations of 12 and 48 mg/mL; the results showed 9 and 19 mm zones of inhibition, respectively. Meanwhile, antifungal studies of the methanolic extract at 100 mg/mL showed that it inhibited the growth of *Trichophyton longifusus*, *Candida albicans* and *Fusarium solani* (Khan and Khan, 2007;

Abadi et al., 2011). Figure 6 shows an image of *R. stricta* obtained during the fieldwork. Figure 7 presents examples of isolated compounds from *R. stricta*.



Figure 6 *R. stricta* (obtained from the city of Al Taif in the southwestern province of Saudi Arabia, Al-Shafa mountains)



Akuammidine

Rhazinilam

Figure 7 Examples of *R. stricta* isolated compounds

1.3.5 *Tribulus macropterus*

This plant is a member of the *Zygophyllaceae* family, popularly known as ‘Zahr’, and is traditionally used to treat cardiovascular disorders and sexual dysfunction. Alkaloids, tannins, flavonoids, saponins, and cardiac glycosides were observed in *T. macropterus* constituents, according to a study (Ksiksi et al., 2017). In rats injected with streptozotocin, an agent that induces hypoinsulinemia and hyperglycemia by damaging pancreatic cells, the antihyperglycemic activity of a methanolic extract of a plant was studied. In this trial, the level of blood glucose was lowered by 18% during the third week and by 30% during the fourth week. In a related study, the antihyperlipidemic effect of the plant was investigated. Although the high-density lipoprotein (HDL) was down by 30%, diabetic rats exhibited a significant decline in triglyceride, low-density lipoprotein (LDL), and total cholesterol (Ezzat et al., 2014). Antioxidant activity as measured by DPPH assay and free radical scavenging activity of 42.7% at 1 mg/mL concentration (Ksiksi et al., 2017). In a previous report, the IC₅₀ for *T. macropterus* cytotoxic activity against the cancer cell line HepG2 was 2.9 µg/mL (Abdel-Hameed et al., 2007). Figure 8 shows an image of *T. macropterus*.



Figure 8 *T. macropterus* (collected previously by Dr. Hossam Afifi at King Abdulaziz University, available at https://floraofqatar.com/tribulus_macropterus.htm)

1.4 Human Skin

1.4.1 Human Skin Function

The skin is the largest organ in the human body, covering a surface area of around two square metres and representing approximately 15% of the body's total weight. One of the main functions of the skin is acting as a physical and chemical barrier to protect the body. It is one of the body initial lines of defence against pathogenic microorganisms. Other skin functions include; regulating body's temperature, contributing to the production of vitamin D, and serving as a sensory organ (Nizet et al., 2001; Schröder and Harder, 2006).

1.4.2 Human Skin Structure

The skin consists of three layers (Figure 9):

- The epidermis, the outer layer, consists mainly of keratinocyte cells, dendritic cells, and other cells such as melanocytes, Merkel, and Langerhans cells.
- The dermis contains nerve endings and several cells (mast cells, dermal dendrocytes, fibroblasts).
- The hypodermis (Subcutaneous fat): the last layer of the skin.

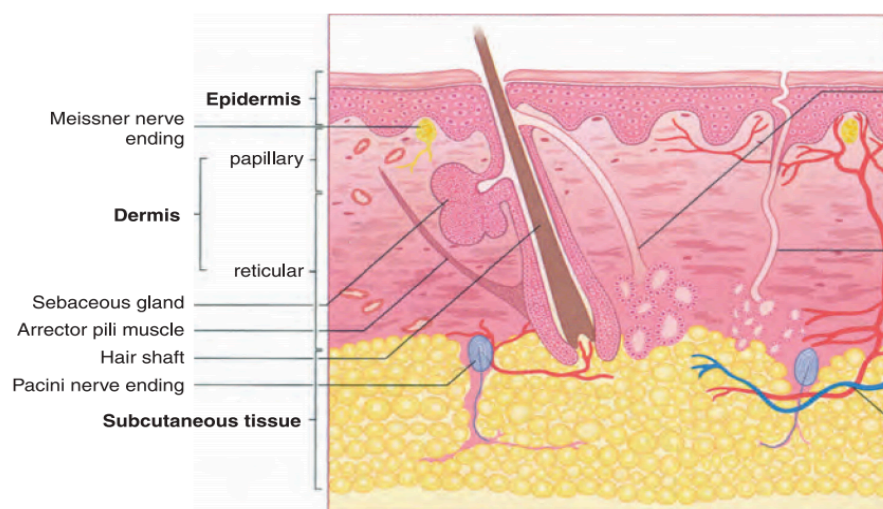


Figure 9 Three layers of the skin (James et al., 2011)

1.4.2.1 The Epidermis

Its primary function is to protect and waterproof the organs underneath it. Moreover, it has a thick and avascular structure. Its thickness varies from 5 to 50 μm on the scrotum and eyelids to 600 to 900 μm on the soles of the feet, and it covers the vast majority of the body's surface. Composed primarily of keratinocyte cells, dendritic cells, and other cells such as

melanocytes, Merkel, and Langerhans cells. The epidermis is divided into five layers based on the position and morphology of keratinocytes (Figure 10):

- *Stratum basale*, (basal layer).
- *Stratum spinosum* (squamous cell layer).
- *Stratum granulosum* (granular cell layer).
- *Stratum lucidum*
- *Stratum corneum* (corny cell layer).

The deepest layer, *Stratum basale*, contains keratinocyte stem cells linked with melanocytes, Langerhans cells, and Merkel cells. This basal layer serves a crucial role in sensory perception, is sparsely dispersed throughout adult skin, but is more prevalent in the fingers (Cracowski and Roustit, 2020). The continuous renewal of the epidermal layer leads to the formation of structures such as nails and sweat glands.

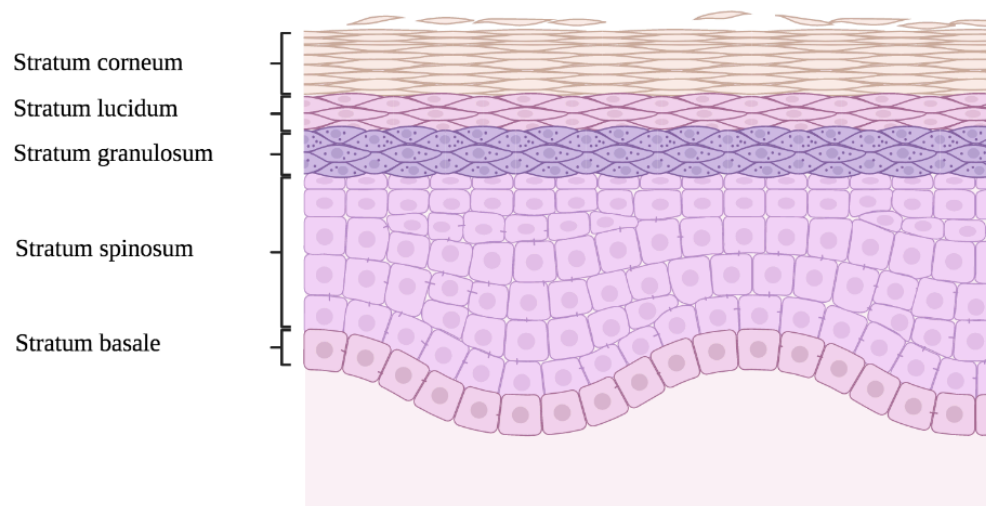


Figure 10 Epidermis cross-sectional diagram to show the five layers (created using BioRender.com)

The basal cells of the epidermis proliferate in cycles to renew the epidermis' outer layer. As cells migrate to the skin's surface, the epidermis is a dynamic tissue in which cells are

constantly in unsynchronized motion, passing not only one another but also melanocytes and Langerhans cells. As the cells migrate from the basal layer to the skin's surface, they undergo keratinization. The keratinocyte first undergoes a synthetic phase and then a degradative phase. Most mitotically active epidermal cells that give birth to the outer epidermal layers are located in the basal layer. However, not all basal cells are capable of division; it takes a basal cell at least 14 days to migrate from the basal layer to the *Stratum corneum* (SC) and another 14 days to go through the cornified layer to the epidermis' outermost layer (Kolarsick et al., 2011). *Stratum corneum* corneocytes give mechanical protection to the epidermis and a barrier against water loss and foreign material penetration. The protein-rich and lipid-deficient corneocytes are surrounded by a continuous extracellular lipid matrix. During terminal differentiation, cells in SC lose their nuclei and are technically considered to be dead (Kolarsick et al., 2011).

Melanocytes are dendritic pigment-producing cells generated from the neural crest and limited to the basal layer of the skin. Melanocytes are in charge of producing the pigment melanin and transferring it to keratinocytes (Tobin and Paus, 2001; Plonka et al., 2009). Merkel cells are clear oval-shaped cells located in the epidermis basal cell layer scattered through the dermal-epidermal junction. Distributed in both skin and mucosal tissues, with palms, finger pads, feet, and the plantar surface of the toes having the highest number. They are significantly more prevalent in the oral mucosa and more common on sun-exposed skin than on covered skin. The exact function of these cells is still unclear. However, they appear to have a role in neural development and touch sensation (Abraham and Mathew, 2019).

Langerhans cells not only play an essential role in immune surveillance and homeostasis but also affect disease by establishing tolerance or triggering inflammation. Their ability to self-renew inside the epidermis, as well as travel to lymph nodes in order to deliver antigens, is

unique. The exact function of LCs in immunological responses has not been clearly revealed (Egbuniwe et al., 2015; Deckers et al., 2018).

1.4.2.2 The Dermis

The epidermis and dermis are connected by the dermal-epidermal junction, which is a zone of permeable basement membrane that allows the interchange of cells and fluid and holds the two layers intact (James et al., 2011). The dermis is a network of fibrous, filamentous, and amorphous connective tissue with a nerve and vascular network that permits fibroblasts, macrophages, and mast cells to penetrate in response to foreign body stimulation. Lymphocytes, plasma cells, and several other leukocytes can also enter the dermis as a result of numerous stimuli. Skin elasticity, pliability, and tensile strength are provided by the dermis. The dermis and the epidermis work together to repair and reconstruct the skin as wounds are healed, and the dermis binds water, regulates temperature, and includes sense receptors (Tobin and Paus, 2001; Plonka et al., 2009).

The dermis is composed mostly of collagen, a family of proteins including at least 15 genetically distinct types. Tendons, ligaments, bone lining, and the dermis all contain collagen, an essential structural protein for the whole body. Collagen is the principal stress-resistant component of the skin. In contrast, elastic fibers help to preserve elasticity but have a negligible impact on the skin's resistance to deformation and tearing (James et al., 2011).

1.4.2.3 The Hypodermis (Subcutaneous Fat)

The subcutaneous layer of skin is composed primarily of adipocytes, whose principal role is to store energy and produce heat in response to hypothermia. Recent research has highlighted the

essential involvement of adipocytes as a source of antimicrobial peptides in barrier immunity. Dermal fibroblasts can develop into adipocytes and generate the antimicrobial peptide cathelicidin in response to infections, such as those caused by *S. aureus* (Chen et al., 2019).

1.5 Infections

When the skin barrier is compromised by the presence of a wound, it can lead to serious consequences. If microorganisms, such as bacteria, fungi, viruses, or parasites, enter the body directly or indirectly, these can produce a variety of symptoms, such as fever, fatigue, diarrhea, coughing, and muscle aches, and lead to life-threatening sepsis (Felgueiras, 2021).

1.5.1 Skin Microflora

A small number of microorganisms usually colonise the outer surface of adult skin. These are frequently identified when skin is analysed and form a population known as the normal flora, or indigenous microbiota. The indigenous microflora is largely consistent in terms of composition and quantity in any particular area and throughout an individual's lifespan (Mackowiak, 1982; Percival et al., 2012). The indigenous skin microflora differs by the anatomical site in terms of density and composition, and it has been noted that moist places like the axillae, groin and the space between the toes have a higher density of microorganisms. Moreover, in other dry areas, low moisture content and a neutral or slightly acidic pH facilitates the adherence of certain bacteria to the skin surface, while preventing others (Altöparlak et al., 2004).

In addition to the native microflora, the skin offers a suitable habitat for additional microorganisms that rest freely on its surface. These microorganisms are not permanent skin

inhabitants; they are transient microflora. The function that transient microorganisms play in infection and colonisation resistance of the skin surface is mainly unclear. However, it is highly possible that they impact the infection life cycle. The skin microflora supports defensive and immunological responses, prevents opportunistic or pathogenic organisms from colonising and infecting the skin, and supports tissue repair and barrier functions. Through the process of colonisation resistance, indigenous microbiota defends the skin against invading, pathogenic, or opportunistic bacteria. Direct destruction of other microorganisms is one method through which bacteria might remove competition. The entire nature of these interactions is unclear, although those involving coagulase-negative *Staphylococcus* species inhibiting its related but pathogenic, *S. aureus*, have attracted the most attention. Across the skin microflora, coagulase-negative *Staphylococcus* species are abundant, and *S. aureus*, which is coagulase positive and capable of coagulating blood, is distinguishable from these Gram-positive strains (Percival et al., 2012; Sanford and Gallo, 2013; O'Sullivan et al., 2019).

S. haemolyticus, *S. hominis*, *S. capitis*, *S. caprae*, *S. lugdunensis* and *S. epidermidis* are the most common coagulase-negative *Staphylococcus* species found on human skin (O'Sullivan et al., 2019). Another common bacterial species found in the skin microflora of healthy adults is *Cutibacterium acnes*. *C. acnes* appear in the human skin microflora as the sebaceous gland matures and produces sebum. In its position as a commensal skin microbe, *C. acnes* releases propionic acid, which aids in maintaining the acidic pH of healthy skin and preventing further colonisation by pathogenic microorganisms (Youn et al., 2013). However, *C. acnes* can cause an inflammatory skin condition known as Acne vulgaris. Consequently, *C. acnes* has the potential to cause inflammation and tissue damage both directly and indirectly (Fitz-Gibbon et al., 2013).

1.5.2 Skin and Soft-Tissue Infections (SSTI)

When a microorganism penetrates the barrier function of the skin layers or the underlying soft tissues and overcomes the immune response, SSTI could occur. SSTI impacts between 7-10% of hospitalised patients, and they are highly common in the emergency care setting (Ki and Rotstein, 2008). Physical and chemical changes to the skin, such as wounds, burns, scratches, bites, and ulcers, along with the bacteria virulence factors, can facilitate the entrance of the bacteria, which may result in an infection in the site, subsequently triggering the host immune response. Other risk factors for SSTI include; changes to the skin pH or temperature, diabetes mellitus, inflammatory skin conditions, immunocompromised people, and poor skin hygiene. Among risk factors, smoking has been reported to increase the risk of surgical-site infections among patients undergoing elective plastic surgery (Kaye et al., 2019).

1.5.2.1 SSTI Causative Microbes

SSTI causative agents tend to be bacteria colonizing skin flora; Gram-positive bacteria usually colonise the upper section of the skin, such as *Staphylococcus aureus*, *Streptococcus pyogenes*, *Staphylococcus epidermidis* and *Corynebacterium* species, the former two causative agents account for most of the SSTI, on the other hand, Gram-positive and Gram-negative bacteria usually colonized the lower section of the skin can cause SSTI, examples of these colonizing bacteria include *Enterococcus* and *Enterobacteriaceae* species and surgical site skin infections (SSIs) of the abdominal wall or infections of soft tissue in the anal and perineal area are more likely to be caused by Gram-negative and anaerobic bacteria (Esposito et al., 2017).

Methicillin-resistant *S. aureus* (MRSA) is a global health problem and a frequent pathogen of SSTIs in both community and healthcare settings. A previous report investigated the frequency

of MRSA among patients with SSTIs in the emergency department. 18% of the 137 participants in the study were homeless, 28% injected illegal substances, 63% presented with a deep or superficial abscess, and 26% required hospitalisation for the infection. 51% of infection-site cultures included MRSA. 75% (89) of the 119 *S. aureus* isolates (from the infection site) were MRSA (Frazee et al., 2005). Moreover, recently more cases of methicillin-resistant *S. aureus* (MRSA) infection have been identified, and this calls for the utilization of effective new antimicrobial agents (Ki and Rotstein, 2008).

1.5.2.2 SSTI Classification

Classification of SSTI varies depending on the severity of the infection to simple, uncomplicated cases and necrotizing and non-necrotizing complicated cases that involve a deeper layer of the skin (Ramakrishnan et al., 2015). Another way of classifying SSTI depends on the skin layers involved, infection of the epidermal layer (carbuncles, folliculitis, furuncles, impetigo, ecthyma, abscesses) (Figures 11 A and B), and in general, erysipelas refers to the involvement of superficial layers of the skin and cellulitis refers to the involvement of dermal and subcutaneous fat layers of the skin which may lead to fasciitis or myositis (Ki and Rotstein, 2008; Hayeri et al., 2016).

Cellulitis is an acute infection of the dermis and subcutaneous tissue that often affects the legs and is frequently associated with acute or chronic skin damage. It is a common reason for outpatient medical visits and hospitalisations (Figure 12). Up to 47% of individuals with cellulitis will experience a recurrence within three years. Penicillin prophylaxis is beneficial for avoiding cellulitis recurrence (Kaye et al., 2019). Patients presenting with the signs and symptoms of systemic toxicity, such as hypothermia, fever, tachycardia (heart rate more than

100 beats/min), and hypotension (systolic blood pressure 90 or 20 mmHg below baseline), are classified as complicated SSTI cases and are likely to require hospitalisation to stabilise their clinical status and avoid illness progression (Dryden, 2010).



Figure 11 Shows uncomplicated skin and soft tissue infections (SSTI) cases with superficial layers of the skin involvement (A) furuncles (B) abscesses (adapted from Ramakrishnan et al., 2015)



Figure 12 Clinical presentation of cellulitis skin and soft tissue infection (SSTI) involves deeper layer of the skin (adapted from Raff and Kroshinsky, 2016)

Depending on the severity of SSTI, symptoms can be manifested as skin redness, edema, warmth, pain to loss of a leg or arm function. These symptoms arise from the causative agent itself and from the host inflammatory response, which begins by increasing the blood flow to the site of infection by inducing some alteration to the vascular tone, followed by the release of leukocytes producing cytokines, phagocytes, and several plasma proteins subsequently, those cells will reach the site of infection and renders the microorganisms inactive. However, in certain cases, such as diabetic patients with peripheral neuropathy (a common complication of diabetes), when they develop foot ulcer infection, the inflammatory response persists, resulting in irreversible tissue damage, as there is a connection between wound healing and the nervous system (Pradhan et al., 2009), and the management of this cases usually require strict control of blood glucose level, debridement procedure (surgical removal of necrotic and hyperkeratotic tissue), and targeted antibiotics treatment (Kanitakis, 2002; Lim et al., 2017).

1.5.2.3 Management of Skin and Soft-Tissue Infections (SSTI)

Treatment of SSTI varies depending on the severity, infection site, comorbidities (HIV, diabetes mellitus), depth, and the involvement of skin layers. Due to the long duration (2 to 3 days) required for the proper identification of causative microorganisms through culture methods. SSTI treatment is usually started with empirical antibiotic therapy. To prevent the development of antimicrobial resistance, a topical antiseptic, such as 1% hydrogen peroxide cream, should be considered as an alternative to topical fusidic acid or mupirocin in uncomplicated cases of impetigo caused by MRSA in which there is a localised, non-bullous infection and the patient is clinically well. In addition, topical fusidic acid or mupirocin is the second choice in this clinical situation and only if the MRSA isolate is known to be sensitive,

and systemic antimicrobial treatment for severe impetigo with the choice of antibiotic established by susceptibility testing (Brown et al., 2021).

Cellulitis prophylaxis with penicillin is effective in preventing recurrence (Webb et al., 2020). Complicated cases with a deeper infection, such as infected burns, abscesses, diabetic foot, and deep wound infections, usually require hospitalization and the administration of systemic antibiotics plus the removal of damaged and infected tissues through a debridement procedure. Systemic therapy of complicated wound infection involves the administration of β -lactam antibiotics. Moreover, to minimize the effect of bacterial toxins, clindamycin is usually prescribed as an adjunct therapy. Several antibiotics are utilized to treat resistance cases of SSTI, which include; linezolid, vancomycin, tetracyclines, daptomycin, doxycycline, tigecycline, or trimethoprim-sulphamethoxazole (Ki and Rotstein, 2008; Tognetti et al., 2012; Brown et al., 2021). Failure to manage SSTIs may result in life-threatening complications such as endocarditis, osteomyelitis, lymphadenitis, necrotizing fasciitis, gangrene, bacteremia, or sepsis (Suaya et al., 2013).

The majority of skin and soft tissue infections are caused by *S. aureus*, with MRSA accounting for 50% of all SSTIs. Moreover, Gram-negative organisms such as *Pseudomonas aeruginosa* and vancomycin-resistant *Enterococcus* (VRE) are increasingly being isolated from chronic wounds, offering significant difficulty in managing these infections, especially given the current resistance crisis. The extensive use of topical antimicrobials for the treatment of SSTIs, such as mupirocin and fusidic acid, has been correlated to a rise in bacterial resistance, hence diminishing the potential efficiency of these medicines (McNeil et al., 2014; Williamson et al., 2014). As a result, novel therapeutic options for bacterial SSTIs are urgently needed (Bandyopadhyay, 2021).

1.5.2.4 Inflammation Accompanying SSTI

Skin serves as the first line of defense against different pathogens through many defensive mechanisms. Keratinocyte cells in the epidermal layer are equipped with a mechanism to detect microorganisms and initiate an immune response, and this immune response involves both an innate immune system with a nonspecific immune response such as the release of pro-inflammatory mediators (macrophage and neutrophil), along with antimicrobial peptides and a specific adaptive immune response through the recognition of microorganism antigen by B and T lymphocytes. Recently, it has been discovered that the innate immune system has some specificity toward one of the microorganism components called pathogen-associated molecular patterns (PAMPs) by recognizing these components through specific receptors within the keratinocytes known as pattern recognition receptors (PRRs). The recognition of PAMPs by PRRs will trigger the production of pro-inflammatory mediators, chemokines, cytokines, and antimicrobial peptides (AMPs) (Santoni et al., 2015; Amarante-Mendes et al., 2018).

The cathelicidin-derived cationic antimicrobial peptide (LL37), α -defensins, and β -defensins are the most common AMPs in human skin. LL-37 is produced, stored, and activated by keratinocytes, and it is also found in mast cells, neutrophils, NK cells, and epithelial cells. α -defensins and β -defensins are produced by neutrophils, whereas β -defensins are produced by sebocytes and sweat glands (Bernard and Gallo, 2011).

Moreover, it will promote the entrance of neutrophils from the blood circulation to the site of infection (Takeuchi and Akira, 2010). Both Toll-like receptors (TLRs) such as TLR 1, 2, 6 and nucleotide-binding oligomerization domain two receptors (NOD2) are forms of PRRs within the keratinocytes. Any disruptions in the regulation process of the inflammatory response such

as excessive stimulation will result in overwhelming inflammatory responses that can cause autoimmune diseases and inflammatory skin diseases (Krishna and Miller, 2012; Ryu et al., 2015).

Normal adult skin cells produces reactive oxygen species (ROS), which are metabolic byproducts, in addition to the basal proliferation rate. ROS and other pro-inflammatory cytokines can cause excessive inflammation, which can result in localised tissue damage. Constant exposure to oxygen, ultraviolet (UV) radiation, and high localised concentrations of superoxide radicals released by leukocytes and macrophages can cause an excessive synthesis of ROS in the skin, which can cause eczema and other forms of dermatitis (Trenam et al., 1992). Furthermore, chronic inflammation and high ROS levels may lead to skin ageing (Chung et al., 2011).

1.5.2.4.1 Inflammatory Cytokines in the Skin

Inflammatory cytokines are specialized cell-signaling molecules that mediate cutaneous inflammation and allow T cells, epidermal keratinocytes, and other immune cells to communicate with one another. After cell or tissue injury, interleukin-1 (IL-1) and other cytokines signal the immune system (Bak and Mikkelsen, 2010). Once PRRs are activated, keratinocytes release anti-infection-related cytokines, including proinflammatory cytokines (IL-1, IL-18, IL-6, TNF, and IFN), anti-inflammatory cytokines (IL-10), and chemokines (IL-8, CXCL1, CXCL2, CXCL10, CCL2, and CCL20) (Olaru and Jensen, 2010). IL-1 is a crucial inflammatory cytokine that may warn the body of imminent threats, activate gene expression, and produce inflammatory mediators in the skin. Members of the IL-1 cytokine family activate the inflammatory cascade in the skin during acute or chronic inflammatory disorders. Among

the 11 known members of the IL-1 family, IL-1 α and IL-1 β play a crucial role in inflammation, acting on practically every cell type and organ system to trigger other cytokines, chemokines, adhesion molecules, and mediators in general (Sims et al., 2005).

The IL-1 α main role is to maintain epidermal barrier function by preventing pathogenic microorganisms from entering the body. The stimulation of cytokines, mediators, and adhesion molecules by the release of IL-1 α causes skin inflammation. IL-1 α also stimulates the synthesis of inflammatory mediators, such as COX-2 and inducible nitric oxide synthase (Henderson and Goldbach-Mansky, 2010). Despite the fact that IL-1 α and IL-1 β bind to the same receptor, they are encoded by different genes and differ in a number of ways. A limited number of cells, mostly monocytes, macrophages, and dendritic cells, produce IL-1 β . IL-1 β binds to IL-1 receptors upon activation, resulting in activation of the mitogen-activated protein kinase signaling pathway, and IL-1 has broad activities at the tissue and systemic levels and is essential for processes such as antibiotic resistance, T helper 17 cell responses, and activation of the acute-phase response (Galli et al., 2011; Garlanda et al., 2013).

IL-6 pro-inflammatory cytokine is involved in innate immune function. It is also required for the production of antibodies by B cells. IL-6 is produced by keratinocytes, fibroblasts, T-lymphocytes, and endothelial cells. Furthermore, monocytes and macrophages can synthesize it in response to antigen stimulation. The production of IL-6 by keratinocytes in response to skin damage may play a crucial role in the development of adaptive immunity in atopic dermatitis (Oyoshi et al., 2009).

IL-8 is produced by keratinocytes or fibroblasts in response to proinflammatory cytokines, such as IL-1 α , IL-1 β , interferon, or tumour necrosis factor- α (TNF- α). IL-8 is a potent stimulator of

polymorphonuclear leukocyte activities, such as superoxide generation, chemotaxis, and enzyme release (Bernhard et al., 2021). ILs such as IL-6 and IL-8 are commonly employed as diagnostic and prognostic markers for infectious and other inflammatory disorders (Bernhard et al., 2021).

Keratinocytes release the proinflammatory cytokine TNF- α , an important mediator that promotes the formation of cutaneous and endothelial adhesion molecules. Mitogen-activated protein kinase is a crucial signal transduction pathway involved in cellular regulation that is induced by TNF- α (Kupper and Fuhlbrigge, 2004). TNF- α is overexpressed in psoriatic skin, which has a negative effect on the production of the epidermal proteins loricrin, filaggrin and involucrin, hence affecting the epidermal skin barrier function (Kim et al., 2011).

1.5.3 Antimicrobial Agents from Natural Products

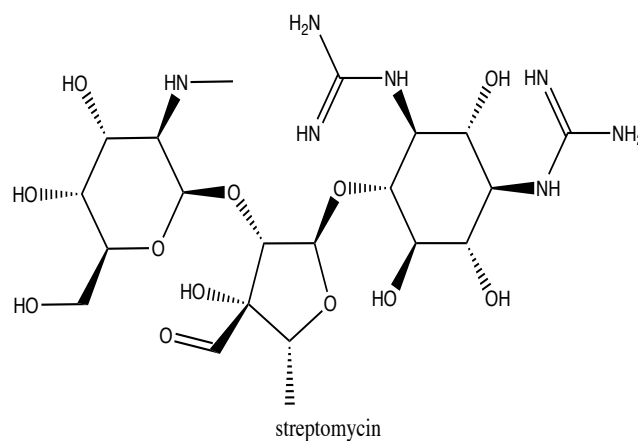
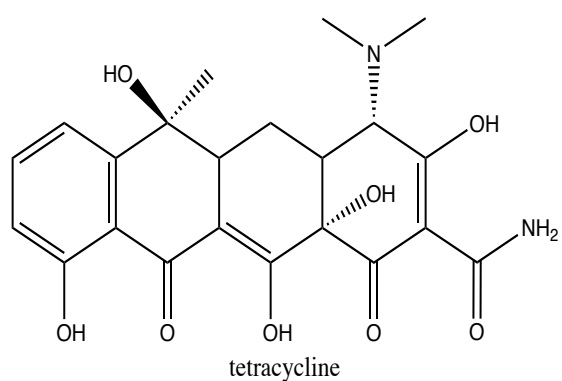
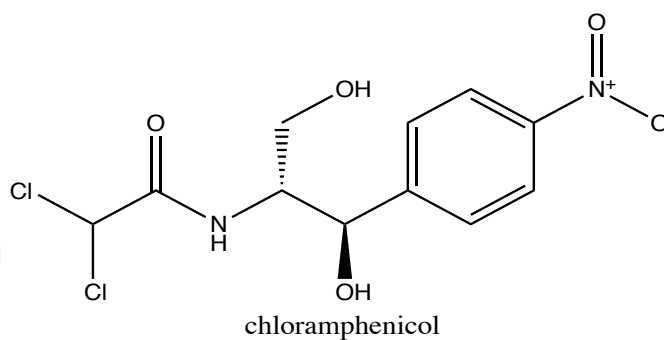
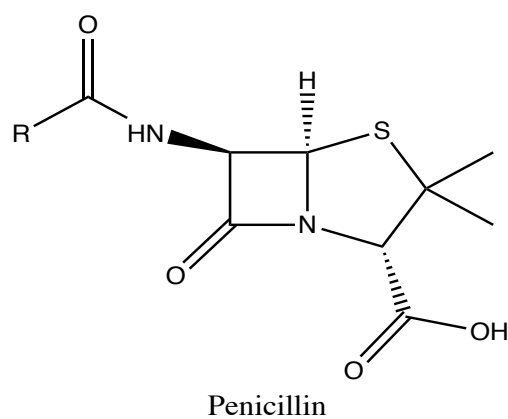
Morphine, salicylic acid, and quinine are successful examples of drugs that were successfully separated from medicinal plants. Natural products have been a valuable source of drugs treating many human diseases for many years. The golden era of antibiotics (the 1940s to 1970s) was marked by the breakthrough discovery of penicillin from *Penicillium rubens* (filamentous fungus) by Fleming in 1929, and the isolation of penicillin F by Florey et al. (1943). Later in the 1940s, it was introduced to the market and contributed to saving thousands of lives during World War II. Penicillin acts by inhibiting the formation of the bacterial peptidoglycan cell wall. Later in 1947, an antimicrobial agent, chloramphenicol which was secreted from *Streptomyces venezuelae* species, was discovered with a mechanism of action inhibiting bacterial protein synthesis. Other discovered antimicrobial agents from natural products sources include; tetracycline (inhibits protein synthesis), streptomycin (inhibits protein

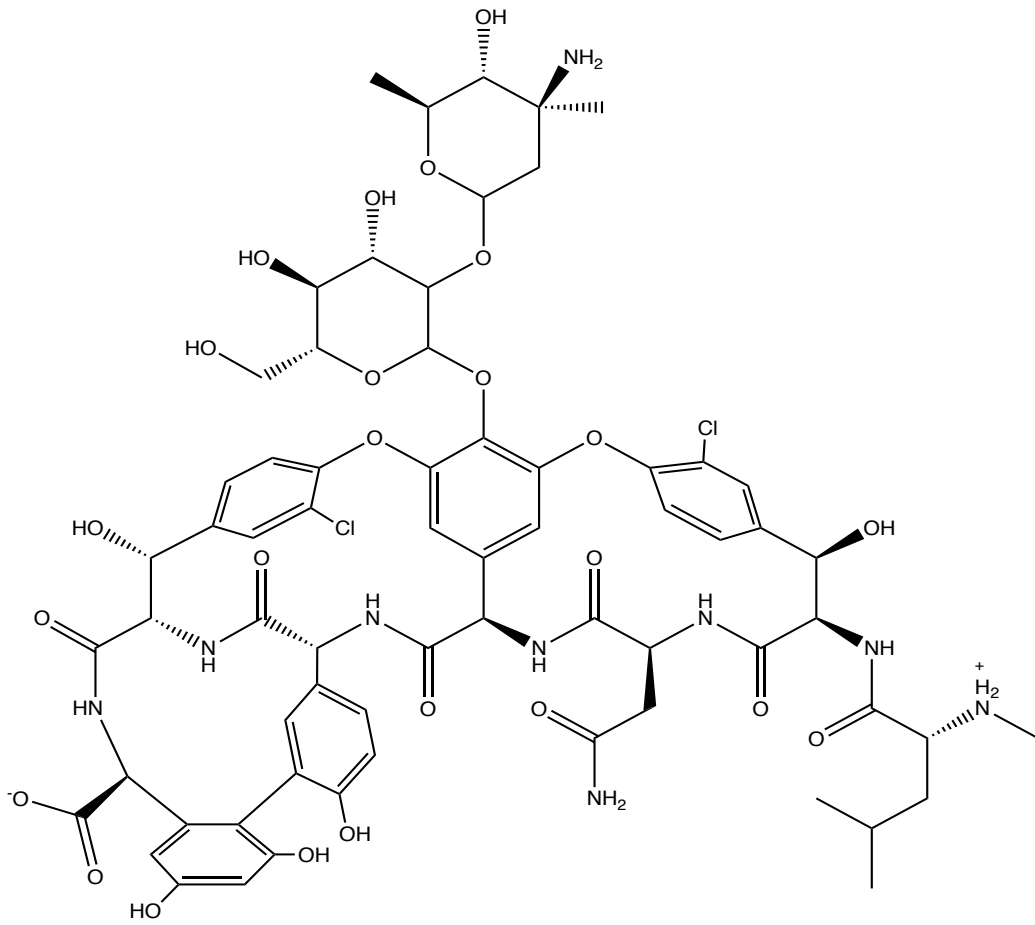
synthesis), vancomycin (inhibits cell wall synthesis), erythromycin, neomycin, kanamycin, gentamicin, and rifamycin. The structures of these antimicrobial products reveal the complexity and diversity of the natural products (Figure 13) (Singh and Barrett, 2006; Lyddiard et al., 2016). Several low molecular weight antimicrobial compounds are known to be produced by plants (secondary metabolites). However, in some cases, they have proven to be significantly weaker than antibiotics produced by bacteria and fungi. This could be due to the superior selectivity these antibiotics exhibit. Moreover, plant-driven antimicrobial compounds could be used as antiseptics, such as thymol, allicin, and tea tree oil (Carson et al., 2006; Abreu et al., 2012; Borlinghaus et al., 2014; Marchese et al., 2016).

In the 1980s, antimicrobial peptides (AMPs) or host defence peptides were discovered for the first time and have quickly gathered interest as potential new therapeutic options. AMPs are present in nearly all organisms (plants, bacteria, fungi, and mammals), and their structural and functional diversity is extraordinary. The antimicrobial activity of AMPs is broad-spectrum and potent against bacteria, fungi, and viruses. Antimicrobial peptides (AMPs) are crucial components of the innate immune system in humans, animals, and plants and serve as the first line of defence against foreign invaders (Starr et al., 2018). In addition, their antibacterial processes differ from those of conventional antibiotics. Thus, they can be used to treat different bacteria, even those that are resistant to drugs, making them a target for the development of new therapies (Fjell et al., 2012; Kościuczuk et al., 2012).

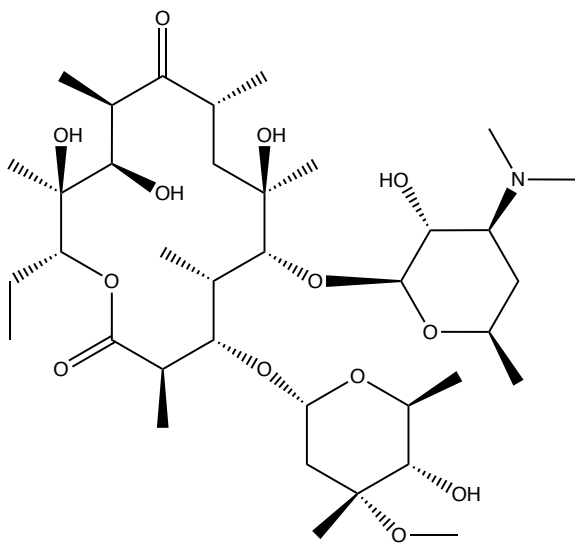
AMPs often have a greater ratio of cationic and hydrophobic amino acids, as well as cationic (positively charged) and amphiphilic (both hydrophilic and hydrophobic) properties due to the presence of many hydrophobic groups and the presence of both hydrophobic and hydrophilic areas (Mirski et al., 2018). The mechanism of action of AMPs involves interacting with

bacterial plasma membranes by neutralising the charge and then penetrating through bacterial membranes to cause bacterial death, hence decreasing the likelihood of bacterial drug resistance (Mahlapuu et al., 2016). Additionally, these AMPs show fewer or no toxic side effects and make it difficult to develop bacterial drug resistance in comparison to conventional antibiotics (Rathinakumar et al., 2009).

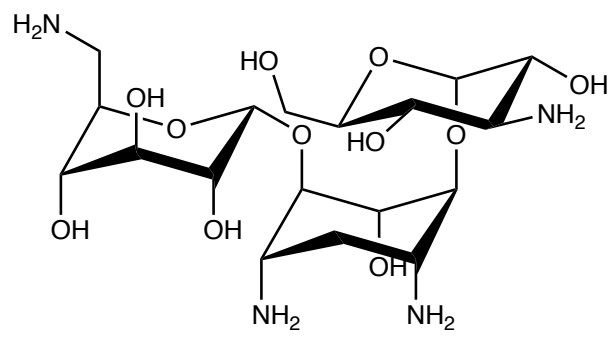




Vancomycin



erythromycin



kanamycin

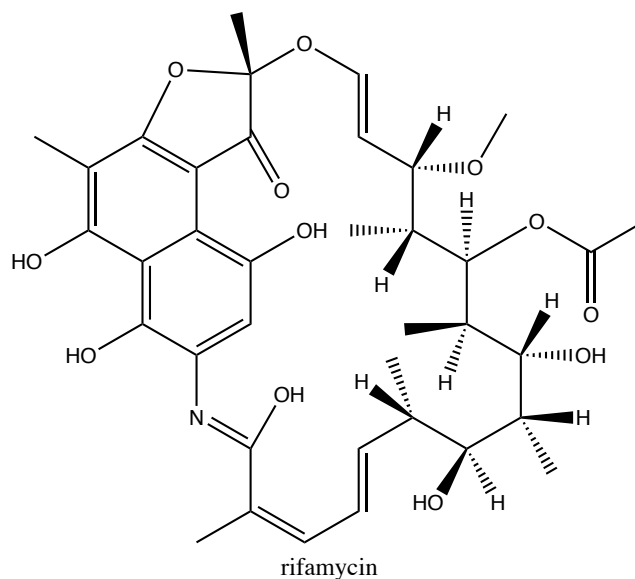


Figure 13 Structures of antimicrobial agents of natural origin (created by ChemDraw)

1.5.3.1 Resistance to Current Antimicrobial Therapy

Antimicrobial resistance (AMR) develops when microorganisms such as bacteria, viruses, fungi, and parasites are able to adapt and grow in the presence of antibiotics that once inhibited their activity (Founou et al., 2017). AMR is one of the most serious threats to human health at present. AMR already accounts for 700,000 annual fatalities. After 2050, it is predicted that 10 million fatalities will occur annually due to antimicrobial resistance, which equals the number of people that die annually from cancer in the present day (Tagliabue and Rappuoli, 2018). AMR hinders the ability of the human immune system to fight infectious microorganisms and adds to a range of complications in immunocompromised patients undergoing surgery, dialysis, chemotherapy, and joint replacement. Antimicrobial resistance will also have a significant effect on patients who already suffer from chronic diseases such as rheumatoid arthritis, asthma, and diabetes (Dadgostar, 2019).

The first cases of antibiotic resistance *S. aureus* were identified in the 1940s when infections caused by penicillin-resistant *S. aureus* were identified in hospitals. These microorganisms generate plasmid-encoded lactamase (penicillinase) that can hydrolyze the β -lactam ring of penicillin. As the antibacterial activity of penicillin is attributed to this ring, its hydrolysis turns the antibiotic inactive. Within a few years of its emergence in hospitals, this bacterial resistance strain had spread to the general population. In the 1950s and 1960s, penicillin-resistant bacteria had reached pandemic proportions in the community. Moreover, the introduction of methicillin in 1959 managed to effectively control the infection caused by *S. aureus* resistant to penicillin. However, just two years following the use of methicillin, scientists confirmed the isolation of an MRSA strain in 1961 (Chambers and DeLeo, 2009).

Today, more than 90% of *Staphylococcus aureus* isolates release penicillinase and are therefore resistant to penicillin and, in certain situations, ceftriaxone; these two antimicrobials are regarded as two of the last-resort treatments (Chambers and DeLeo, 2009).

Methicillin resistance *Staphylococcus aureus* (MRSA), one of the most well-known cases of AMR, has been associated with significant death rates worldwide each year. Furthermore, multidrug-resistant Gram-negative bacteria have made it more challenging to treat infections such as urinary tract and pneumonia. Furthermore, antibiotic resistance to tuberculosis, gonorrhoea and typhoid fever increases annually and adds considerably to the high expenditures of health care systems globally, especially in underdeveloped nations (Dadgostar, 2019). There have been reports that some bacterial infections, such as gonorrhoea, are essentially untreatable, according to a recent WHO study in which they installed a Global Gonococcal Antimicrobial Surveillance Programme (GASP) to monitor cases of gonorrhoea caused by *Neisseria gonorrhoeae* in more than 77 countries around the world, and they have identified

and verified resistance cases of gonorrhoea to cefixime and even some cases to ceftriaxone those two antimicrobial agents are considered to be the last-line treatment (Wi et al., 2017).

Bacteria can develop resistance to fluoroquinolones through three different mechanisms: 1) modification and mutation of target site genes so that fluoroquinolones wouldn't be able to bind to it; 2) production of enzymes that alter fluoroquinolones sites; 3) Efflux pump overexpression to clear antibiotics from resistance bacteria (Munita and Arias, 2016). In these cases, vancomycin can be administered to treat Gram-positive infections caused by methicillin-resistant *Staphylococci* and amikacin for Gram-negative organisms resistant to tobramycin and gentamicin (Gokhale, 2008). Keratitis is an inflammatory disease that affects the eye cornea, and it is usually caused by Gram-positive *S. aureus* or Gram-negative *P. aeruginosa*. Resistance to anti-keratitis drugs is also a growing concern; a recent retrospective survey conducted in the United Kingdom for the duration of 10 years has retrieved 162 isolates of bacterial keratitis from patients. Moreover, they have identified a widespread resistance to chloramphenicol (74%) and 8 cases of ciprofloxacin resistance (Shalchi et al., 2011).

Several factors contributed to the rise in AMR, which includes the misuse or overuse of antibiotics. Various global surveys suggest that a substantial proportion of patients genuinely believe antibacterial drugs are effective against viral illnesses such as influenza and the common cold. Moreover, in many developing nations where proper diagnostic tools are lacking, patient care is primarily dependent on the prescription of medication, notably antibiotics (Bin et al., 2017). In some countries, many antibiotics of poor quality can be purchased freely over the counter, and physicians tend to give inappropriate extended or very short courses of antibiotics, which can lead to the development of antibacterial resistance. Financial incentives play a significant role in antibiotic overprescribing (Spellberg, 2018).

Agricultural use of antibiotics is a significant contributor to antimicrobial resistance in humans. In the United States, for instance, over 80% of antibiotics manufactured are utilised in livestock feed (Bartlett et al., 2013). Antibiotic resistance might develop spontaneously through mutation and bacterial evolution. In addition, via transposons and insertion sequences, plasmids, which are small circular fragments of DNA in bacteria, may acquire a wide range of resistance genes. These plasmids may be transferred to other bacterial species, therefore spreading antibiotic resistance across the microbial species (Dadgostar, 2019). Over the years, these antimicrobial agents have been successfully utilized to eradicate microorganisms from the site of infection. However, the widespread antimicrobial resistance has imposed major attention on discovering new antimicrobial agents. Despite the importance of medicinal chemistry as a source of novel agents, natural products continue to be of great interest in the development of new agents. This is due to the molecular complexity and structural diversity of natural products (Cragg and Newman, 2013).

1.6 Wounds

A wound can be defined as a chemical, thermal, or mechanical trauma that causes a disruption to the integrity of the layers of skin or mucous membrane, and it can be a simple wound limited to the layers of the skin or a complicated one with deeper involvement of blood vessels, nerves, and muscles.

In order to maintain the functions of the skin, its integrity must be restored shortly after damage. The wound healing process involves peripheral blood mononuclear cells, resident skin cells, regulatory molecules, cytokines, extracellular matrix, chemokines, and growth factors (Dorantes and Ayala, 2019). Wounds sometimes are associated with a chronic underlying

condition such as dermatological or immunological diseases, diabetes mellitus, and venous insufficiency (Kujath and Michelsen, 2008). Infected wounds can lead to lymphangitis, cellulitis, bacteremia, systemic inflammatory response syndrome, multi-organ dysfunction syndrome, organ failure, sepsis, and mortality if not sufficiently managed by the host immune response or medication (Leaper et al., 2015).

1.6.1 Wounds Classification

Depending on the cause and the time required to heal, wounds are either acute or chronic. In most cases, the functional and anatomical integrity of an acute wound is fully restored by a coordinated and efficient healing process. Chronic wounds are incapable of achieving full functional and anatomical integrity. Both pathological processes and the nature, degree, and condition of the host and environment influence and determine the healing process. Wound healing may be affected by the patient's age, the existence of vascular, metabolic, or autoimmune disorders, and any medications currently being used (Lazarus et al., 1994; Velnar et al., 2009; Karimi et al., 2017).

1.6.1.1 Acute Wounds

Acute wounds are tissue injuries that heal within 7–10 days. They are often triggered by skin damage caused by trauma such as lacerations, abrasions, or burns. Haemostasis, inflammatory, proliferative, and remodeling are the normal phases of the wound healing process. In acute wounds, the injury site typically progresses through the usual wound healing stages, resulting in a consistent and structured arrangement of tissue repair (Dai et al., 2020). Several critical factors that can have a direct effect on wound healing include maintaining a moist wound condition and providing adequate wound care education to patients (Fonder et al., 2007).

Management of acute wounds consists of the removal of harmful debris and necrotic tissue, wound infection prevention, and closure (Dai et al., 2020).

1.6.1.2 Chronic Wounds

Chronic wounds are characterized by an abnormal healing process and can be classified into pressure ulcers, vascular ulcers (including venous and arterial ulcers), and diabetic foot ulcers. Chronic wounds are frequently noted in elderly patients with chronic diseases such as diabetes, obesity, and vascular disease (Tomic-Canic et al., 2020). All four phases of the skin wound healing process are affected by diabetes mellitus (Bagheri et al., 2020). Increased expression of pro-inflammatory cytokines, such as TNF- α , and reduced production of pro-healing mediators, such as transforming growth factor- β (TGF- β) and IL-10, are associated with diabetic ulcers (Shofler et al., 2021).

Moreover, the presence of other forms of cells, such as monocytes, macrophages, and neutrophils, for a longer duration in the late phase of inflammation is notable in the chronic wound healing process. On the other hand, the percentage of eosinophils and Langerhans cells decreases during the process (Joshi et al., 2020). Mast cells have a role in the development of chronic wounds as well. Cutaneous mast cells degranulate in diabetic ulcers, and their activity is reduced, which speeds up wound healing. Keratinocytes play an important role in the development of chronic wounds, although the exact mechanism is unknown. Certain microRNAs are known to have poor regulation in keratinocytes, causing immunological dysregulation and a delay in wound healing (Li et al., 2021).

Matrix metalloproteinase (MMP) is another factor that contributes to the slow healing of wounds (Dissemond et al., 2020). Local mediators increase the secretion of MMPs by cells

such as fibroblasts, keratinocytes, and immune cells during normal wound healing. TGF- β , vascular endothelial growth factor (VEGF), epidermal growth factor (EGF), interleukins, and interferons are only a few of the many cytokines and growth factors that play a role in wound healing (Goldberg and Diegelmann, 2020). A small amount of MMPs is necessary for appropriate epithelialization and proliferation. As a result of their dysfunction, epithelialization is impaired and is observed with wounds that are difficult to heal (Raziyeve et al., 2021).

Regardless of the underlying cause, most chronic wounds behave and progress in a similar manner. Prolonged or excessive inflammation, persistent infections, localized tissue hypoxia, the development of drug-resistant bacteria biofilms, the failure of dermal and/or epidermal cells to react to reparative stimuli, reduced angiogenesis, and excessive generation of reactive oxygen species are all common features of these wounds (Frykberg and Banks, 2015; Huang et al., 2020). Persistent inflammation in chronic wounds is caused by a dysregulation of the immune response during the wound healing process. Thus, the inflammatory phase of chronic wounds does not resolve, resulting in poor and delayed healing (Schilrreff and Alexiev, 2022).

The pro-inflammatory cytokine cascade, which includes interleukin-1 (IL-1) and tumour necrosis factor (TNF), is extended, resulting in elevated protease levels in the wound bed. Protease levels in chronic wounds rise above inhibitory levels, causing extracellular matrix (ECM) destruction and boosting proliferative and inflammatory phases. Inflammatory cells accumulated in the chronic wound site produce reactive oxygen species (ROS), injuring ECM proteins and causing premature oxidative damage (Tottoli et al., 2020).

1.6.1.2.1 Management of Chronic Wounds

Management of chronic wounds is still a challenge due to the difficulty in controlling the persistent inflammation in these wounds. The growth of bacterial biofilms on the surface and within chronic wounds is another cause of this. Once an infection is identified, it has to be treated promptly and thoroughly. This may involve a debridement process, drainage of abscesses, and antibiotic treatment. However, antibiotic resistance of bacteria frequently observed in chronic wounds might complicate management. Antimicrobial resistance among pathogens and biofilm formation by bacteria in wounds are two factors that substantially limit the efficiency of antimicrobial treatment of wound infections (Frykberg and Banks, 2015). Biofilms interact with the human immune system by stimulating neutrophils and pro-inflammatory macrophages, resulting in the buildup of inflammatory cytokines like IL-6 and TNF- α , and MMP (Wu et al., 2019). In addition, biofilms are extremely difficult to remove effectively due to the limited penetration of antimicrobial drugs into the biofilm, the fast development of antibiotic resistance by biofilm bacteria, and the presence of several microbes (Omar et al., 2017). Few targeted strategies for chronic wounds have been developed so far, with the majority relying on topical administration of growth factors, which regrettably have little clinical effectiveness. Thus, it is necessary to identify new therapeutic targets and develop more effective treatments (Sun et al., 2014; Landén et al., 2016).

1.6.2 Wound Healing Process

Wound healing is a complex process with a molecular and cellular mechanism that begins and ends in a precise sequence and in a timely manner (Guo and DiPietro, 2010). Tissue injury initiates the cascade of the healing process with the involvement of both biological and

immunological systems with different cell types participating in the cascade. This complex process has been divided into four overlapping stages to facilitate comprehension: hemostasis, inflammation, proliferation, remodeling, and scar maturation (Figure 14) (Velnar et al., 2009).

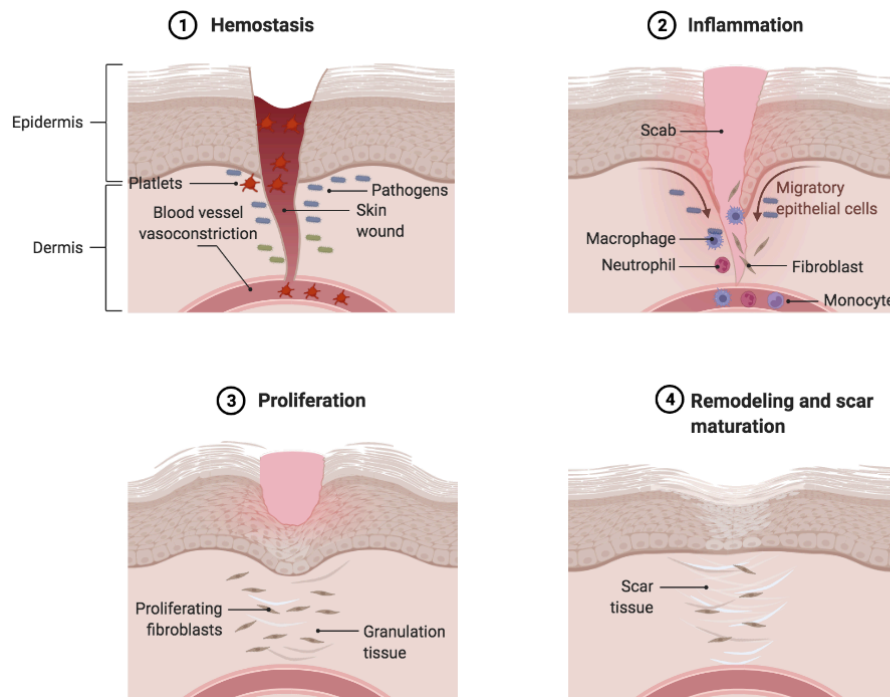


Figure 14 Four different stages of the wound healing process (created with BioRender.com)

1.6.2.1 Haemostasis Phase

It begins directly after the injury, and one of the aims of this stage is to control bleeding in the injury site by promoting blood vessel vasoconstriction. Furthermore, with the formation of fibrin clots and platelet aggregation, the formed clot provides a provisional matrix for other extracellular cells to migrate to the site for this stage and later stages (Velnar et al., 2009). Platelets located within the clot will release alpha granules that secrete multiple growth factors

such as transforming growth factor- β (TGF- β), epidermal growth factor, platelet-derived growth factor (PDGF), and insulin-like growth factor (Enoch and Leaper, 2008).

1.6.2.2 Inflammatory Phase

The aim of this stage is to promote an immune response to neutralize invading microorganisms, and it can be divided into two phases (Tottoli et al., 2020). The early inflammatory phase usually starts after one to two days following the injury. In this phase, previously released growth factor TGF- β and provisional matrix will attract extracellular neutrophils to the wound site, which in turn will inactivate bacteria and foreign bodies through the phagocytosis process by releasing ROS and proteolytic enzymes (Velnar et al., 2009). After two to three days, the late inflammatory phase will start, and several chemoattractant cells, such as cytokines and clotting components, will attract monocytes to the wound site. Then they will undergo a phenotypic transition and become tissue macrophages, which tend to serve as the critical regulatory cells for repair. Macrophage cells have two distinct phenotypes: pro-inflammatory (released during the early phase of inflammation) and reparative (late inflammation phase) (Novak and Koh, 2013).

Following exposure to pro-inflammatory cytokines, such as IL-1, IL-6, interferon- γ , and TNF- α , pro-inflammatory macrophages are activated and release a wide variety of pro-inflammatory mediators and cytokines, including IL-1, IL-12, and TNF- α (Koh and DiPietro, 2011). In addition, anti-inflammatory mediators are expressed: IL-1 receptor antagonist and IL-10 stimulate anti-inflammatory macrophage activation in conjunction with the production of certain growth factors. They serve as phagocytic cells in addition to being the primary source of growth factors that promote proliferation, TGF- β in particular, but also other mediators

(heparin-binding epidermal growth factor, fibroblast growth factor). Additionally, macrophages secrete proteolytic enzymes (e.g., collagenase) that aid in wound debridement (Enoch and Leaper, 2008).

Consequently, macrophages are a key contributor to the shift from inflammation to proliferation (Landén et al., 2016). Bleeding or reduced tissue formation was seen in wound healing experiments in which macrophages were absent during the inflammatory or proliferation phases. There was also an issue in progressing to the next phase, as anticipated. Dermis-resident macrophages, as well as those differentiated from migrating monocytes, are activated by damage-associated molecular patterns and pathogen-specific patterns (Lucas et al., 2010).

The differentiation of monocytes in the early phase of the wound healing process will lead to the formation and differentiation of macrophages into the M1 subset. Phagocytic activity, scavenging, and the production of pro-inflammatory mediators are all related to M1 macrophages (Mosser and Edwards, 2008). A reparative phenotype of macrophages is produced when M1 macrophages transform into the M2 subset. Anti-inflammatory, angiogenesis, and the triggering of fibroblast proliferation are all activities that M2 macrophages are involved in (Brancato and Albina, 2011). They also produce extracellular matrix (ECM) and synthesise anti-inflammatory mediators (Sindrilaru and Scharffetter-Kochanek, 2013).

M1 macrophages phagocytose neutrophils, bacteria, and cell debris to avoid unnecessary damage to the wound site throughout the healing process. Non-healing or chronic wounds like venous and diabetic ulcers can arise if the M1-M2 transition does not occur (Landén et al.,

2016). During the initial phases of wound healing, neutrophils enter the site and then undergo apoptosis after performing their duties of removing pathogens and debris. These wasted neutrophils are eliminated by macrophages, which is thought to result in the macrophage's transition to an anti-inflammatory M2 phenotype that promotes wounds healing by suppressing inflammation. Hyperglycemia impairs macrophage's ability to phagocytose apoptotic neutrophils. Consequently, diabetic wounds feature elevated levels of neutrophils. In chronic wounds, a rise in apoptotic cell burden results in an increase in inflammation (Khanna et al., 2010; Hesketh et al., 2017).

1.6.2.3 Proliferative Phase

The acute wound transition to the tissue repair phase occurs once the injury has been halted, haemostasis has been achieved, and immune response has been successfully established. The proliferative process begins three days after a wound and lasts around 14 days. It is characterised by the migration and differentiation of fibroblasts into myofibroblasts, the deposition of newly synthesised extracellular matrix, and the contraction of the wound.

Keratinocytes, macrophages, endothelial cells, and platelets release extracellular signals such as TNF- α , IL-1, TGF- β 1 (Xu et al., 2009), and fibroblast growth factor-2, that fibroblasts can respond to (Kaltalioglu and Cevher, 2015). These cytokines and growth factors stimulate the proliferation of fibroblasts (Wynn and Barron, 2010). Mature fibroblasts move into granulation tissue, commence collagen synthesis, and replace the provisional fibrin matrix (Greaves et al., 2013). They then differentiate into myofibroblasts, which increase collagen deposition and induce wound contraction (Werner and Grose, 2003).

The epithelialization of the wound completes the proliferative process (Velnar et al., 2009). Re-epithelialization refers to the process of resurfacing a skin wound with new epithelium, is responsible for up to 80% of wound closure and it continues till the wound remodeling phase. The location, depth, and size of a skin wound, as well as microbial contamination, patient-related health factors, genetics, and epigenetics, all affect the epithelialization process (Volk and Bohling, 2013).

When keratinocytes at the wound edges are stimulated for migration, re-epithelialization of the wound commences. Throughout the initial re-epithelialization of cutaneous wounds, migrating keratinocyte cells move through a path between the fibrin clot and the collagen-rich dermis. On the other hand, suprabasal keratinocytes located on the leading edge proliferate to provide additional cells to fill in the gap. Near the leading edge, suprabasal keratinocytes reshape and move on top of basal keratinocytes to become leading cells (Pastar et al., 2014).

During the last stage of re-epithelialization, cells differentiate into epithelial cells that remain firmly adhered to the basal membrane. Cell-extracellular matrix and cell-cell interactions, cytokines, and growth factors secreted by various cell types stimulate keratinocytes to migrate over the provisional matrix deposited in the clot to cover the wound, whereas keratinocytes at the wound margins begin to proliferate and follow the migrating front (Rousselle et al., 2019). The extracellular matrix is vital to the process of re-epithelialization (Pastar et al., 2014; Rousselle et al., 2019).

Reduced blood supply and the rapid metabolism of cells repairing an injury result in hypoxic wound tissues, which is a primary stimulator for angiogenesis along with ROS. In macrophages (Willenborg et al., 2012), fibroblasts (Greaves et al., 2013), vascular endothelial cells, and

keratinocytes, hypoxic conditions stimulate the production of hypoxia-inducible factor-1 (HIF1); this is followed by the release of angiogenic factors such as vascular endothelial growth factor (VEGF), fibroblast growth factors (FGF), PDGF, and TGF- β 1 by these cells, resulting in neovascularization (Skuli et al., 2012; Duscher et al., 2015).

Neovascularization is a crucial aspect of wound healing because of its basic influence from the start of skin damage until the completion of wound remodelling. This wound microenvironment is the beginning site for new vessel formation and regeneration, providing nutritive circulation and the transport of immune cells that remove cell debris (Demidova-Rice et al., 2012). The neovascularization process may be described as the formation of a circle with inner circles of roundly arranged vessels at the wound border, followed by radially-shaped vessels that supply the inner circles and connect them to the undamaged skin. The neovascularization process is disrupted in venous insufficiency, arteriosclerotic illness, or diabetic foot sores, which results in wound healing difficulties or chronic ulcers (Dulmovits and Herman, 2012).

The role of keratinocytes is essential for maintaining the epidermis and restoring it after injury. In the basal layer, proliferative keratinocytes are distinguished by an infrastructure of K5 and K14 keratin (K) intermediate filaments. While moving toward the surface, the cells cross the spinous layer, granular layer, and stratum corneum. As they elevate, they undergo differentiation, which is defined by the shift from K5 and K14 synthesis in the basal layer to K1 and K10 synthesis in the suprabasal layers (Tomic-Canic et al., 1998). Keratinocytes constantly renew, migrating upward from the basal to differentiated layers. Epidermal stem cells sustain a constant, dynamic renewal during homeostasis and following the rupture of the epidermal barrier (Taylor et al., 2000). As an acute skin injury disrupts the barrier, neutrophils,

monocytes, and macrophages are attracted to the injury site. Afterward, keratinocytes are activated by releasing several cytokines and growth factors. The active phenotype is characterized by alterations in the cytoskeleton network and the expression of cell surface receptors important for re-epithelialization, especially K6, and K16, prompting keratinocytes to migrate into the wound and fill the void (Coulombe, 1997; Barrientos et al., 2008). Several regulators control keratinocyte migration, including cytokines and growth factors, chemokines, integrins, keratins, extracellular macromolecules, and MMPs (Raja et al., 2007; Barrientos et al., 2008). Keratinocytes in the first layer that covers the wound begin to proliferate to guarantee an adequate supply of cells to cover the wound. The control of keratinocyte proliferation relies on growth factors, cell adhesion to the substrate, and the degree of cell differentiation. Only basal keratinocytes can proliferate, while suprabasal keratinocytes that have undergone terminal differentiation lack this function. Epidermal growth factors, insulin-like growth factors, and transforming growth factor- α all play an essential role in the proliferative process during the re-epithelialization process (Marikovsky et al., 1996; Gniadecki, 1998).

Chronic wound edges are lined by keratinocytes that are phenotypically and physiologically distinct from the keratinocytes that make up the epidermis or the keratinocytes that line the edge of an acute wound. Keratinocytes in chronic wounds proliferate across the suprabasal layers, as opposed to normal skin, that only has mitotically active keratinocytes in the basal layer. The presence of nuclei in the cornified layer and a thick cornified layer also characterizes chronic wound keratinocytes. As a result of the dysregulation of differentiation and activation pathways, the distinct epidermal structure can also be explained. These characteristics result in

an epidermis that is hyperproliferative, nonmigratory, and unable to re-epithelialize and rebuild the barrier (Pastar et al., 2008; Stojadinovic et al., 2008).

24–48 hours after injury, at the end of the inflammatory phase and the beginning of the proliferative phase, fibroblasts start to emerge at the injury site. Fibroblasts infiltrate and degrade the fibrin clot by secreting various MMPs, replacing it with ECM components, such as collagen, laminin, thrombospondin, glycoproteins, glycosaminoglycans, hyaluronic acid, and proteoglycans. The release of growth factors such as TGF- β and PDGF from a previously formed clot stimulates fibroblasts' proliferation and migration to the wound. This newly formed ECM regulates and supports the process of angiogenesis, granulation-tissue production, and re-epithelialization. In addition, it regulates fibroblast activity and migration (Rozario and DeSimone, 2010; Li and Wang, 2011). During normal conditions, fibroblasts regulate the renewal of ECM to preserve tissue homeostasis. However, when tissues are injured, fibroblasts in the injury site differentiate into myofibroblasts, highly contractile cells that generate an excess of ECM proteins. Both fibroblasts and myofibroblasts are crucial for wound healing. In particular, it is thought that wound contraction and closure are due to the fibroblasts' traction forces and myofibroblasts' coordinated contraction (Tomasek et al., 2002).

The resolution of the inflammation is crucial for the successful progression of healing. Excessive accumulation of pro-inflammatory mediators by fibroblasts with prolonged macrophage-fibroblast activation state, and recruitment of immune cells, will lead to altered healing processes from chronic wounds to fibrosis and scarring (Grinnell and Petroll, 2010; Wynn and Ramalingam, 2012).

1.6.2.4 Remodeling Phase

The wound healing remodelling process is responsible for the formation of new epithelium and the formation of scar tissue (Kujath and Michelsen, 2008). In this phase, the extracellular matrix is synthesized and remodeled simultaneously with the formation of granulation tissue and continues for an extended time. Collagen is regularly synthesised and degraded while the extracellular matrix is remodelled, reaching a steady state approximately 21 days following the injury. In addition, numerous cytokines, including PDGF and FGF, mediate wound contraction caused by fibroblasts interacting with the surrounding extracellular matrix (Guo and DiPietro, 2010).

1.6.3 Natural Products in Wound Management

The wound healing process can be accelerated with natural products having therapeutic properties. Numerous research has been undertaken on the healing properties of natural products having antimicrobial, anti-inflammatory, antioxidant, and promoting collagen synthesis activity. The bioactive phytochemical constituents of the different chemical families, including phenolic, flavonoids, essential oils, terpenoids, tannins, saponins, and alkaloids, may contribute to their therapeutic effects (Thakur et al., 2011).

In recent years, the mechanism of herbal medications and natural products in wound healing has gained much attention. Some herbal medications appear to display their healing activity at various stages of the wound healing process and via multiple mechanisms. Several *in vitro* and *in vivo* studies demonstrate that numerous plant extracts possess different favorable effects. Antioxidants can improve wound healing and prevent oxidative damage to tissues. Herbal medicines stimulate fibroblast or keratinocyte cell proliferation, angiogenesis, and extracellular

matrix production (ECM). The wound healing process is enhanced by the immunomodulatory and anti-inflammatory actions of herbal extracts and natural products (Mohan et al., 2018).

Several wound care products and therapies have been created to accelerate the healing process, reduce scar formation, and enhance the properties of the newly formed skin. In addition, compounds derived from herbal remedies have been used for a long time to stimulate skin regeneration and avoid the failure of the wound healing process due to their simple accessibility, therapeutic characteristics, affordability and low cost (WHO).

Extreme pain, infection, and loss of function or movement are common symptoms of chronic wounds, resulting in amputation or even mortality from complications. Due to the high cost of conventional medical care and the rising incidence of wounds, many people, especially in developing countries, are turning to herbal medicines instead. Therefore, there is an overwhelming need to discover and integrate wound care products that are safe and effective in clinical practice (Pastar et al., 2018; Zhang et al., 2019). Traditional medical systems worldwide rely heavily on medicinal plants for the treatment of acute and chronic wounds. As a result, several plants native to different regions worldwide have been examined for their ability to treat wounds. Even yet, many more medicinal plants need to be investigated to develop more effective, affordable wound healing agents (Agyare et al., 2019).

1.6.3.1 Wound Dressings

Conventional wound dressings such as cotton, wool, and gauze do not actively participate in wound healing. Instead, modern wound dressings are intended to be biologically active either on their own or by the release of bioactive constituents integrated into the dressing (Boateng and Catanzano, 2015).

Novel wound dressings utilising medicinal plant extracts or their purified bioactive constituents have attracted much attention as an application of herbal medicines in the wound care domain in recent years. The wound healing process is quite complex, making it challenging to develop a suitable dressing for acute or chronic wounds. Maintaining a moist wound environment at the wound site, transferring bioactive constituents to wound sites, promoting growth factors, enabling gas exchange, being biocompatible and biodegradable, non-toxic, allowing dressing ease change and removal, and protecting wounds from infections and growth of microorganisms are all essential for an optimum wound dressing (Kokabi et al., 2007; Ghomi et al., 2019). Given the ideal environment for the growth of microorganisms, infection is one of the leading causes of wound complications. The development of innovative wound dressings with significant antimicrobial activity and considerable wound healing abilities is made more difficult by the evolution of multidrug-resistant pathogens. Bioactive constituents found in medicinal plants with antimicrobial activities can accelerate and enhance wound healing. In addition, some herbal treatments can work through multiple mechanisms and demonstrate their healing effects at different phases during the wound healing process (Bowler et al., 2001; Mohan et al., 2018; Khalifa et al., 2021).

1.6.4 Wounds Infection and Biofilm Formation

Many of the defensive mechanisms found in the skin are missing in open skin wounds. Without causing clinical complications, normal intact skin flora is often colonized with microcolonies of bacteria. However, in open wounds, where the lack of an intact epithelium provides an ideal

environment for bacteria to thrive, this level of bacterial load is often associated with infection (Edwards and Harding, 2004).

Inflammation is a vital aspect of the wound healing process and contributes to the clearance of contaminating bacteria. However, inflammation can be prolonged without successful decontamination due to inadequate bacterial clearance. Both bacteria and endotoxins can prolong the inflammatory process by causing sustained elevations of pro-inflammatory cytokines such as interleukin-1 (IL-1) and TNF- α . If this pattern continues, the wound can develop a chronic state and become infected (Toy and Macera, 2011).

It is critical to differentiate between infections caused by planktonic microorganisms and those caused by biofilm-forming bacteria. Bacteria have typically been investigated in their planktonic stage as free-floating organisms in their environment (Walker et al., 2001; Percival et al., 2010). On the other hand, a biofilm is a form of life in which bacteria cluster on a surface or air-liquid contact and develop, enclosing themselves in a self-produced matrix made of polymeric extracellular components, including polysaccharides, proteins, and lipids (Thomson, 2011). The stages of biofilm formation are presented in Figure 15.

The biofilm matrix is more than just an adhesion medium; it forms a microenvironment by itself, with characteristics and capabilities distinct from those seen in the surrounding environment (Thomson, 2011). For example, bacteria proliferative rate and metabolic activity can be modified when placed in this environment (Fisher et al., 2010). Additionally, microorganisms in the biofilm matrix develop quorum sensing, a mechanism by which bacteria may communicate via signaling molecules in response to the density of the population (Miller and Bassler, 2001). Biofilm production, adaptability, and damage response are all regulated by

this signaling network, which resembles these in a multicellular organism (Li and Tian, 2012).

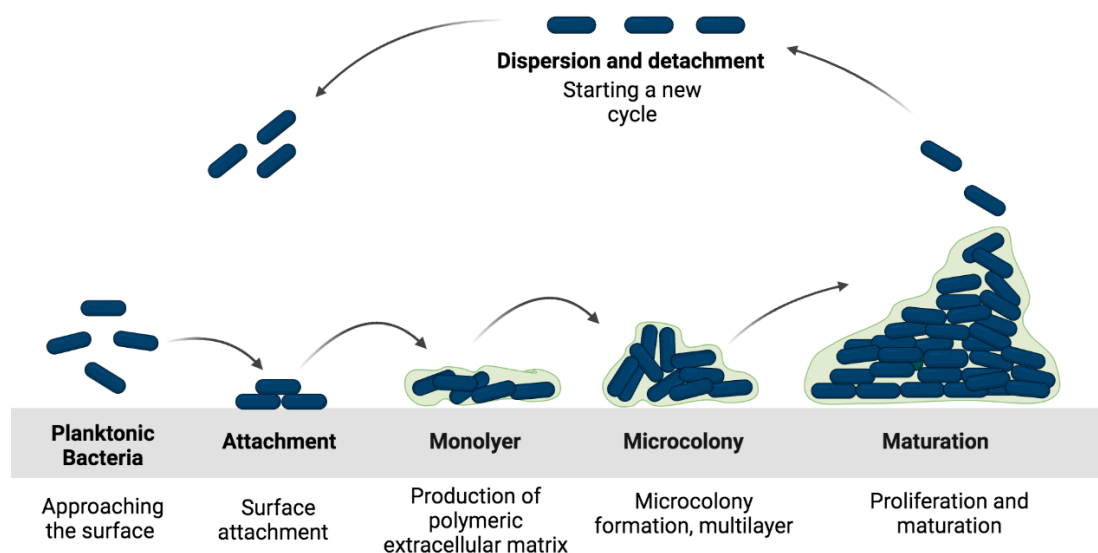


Figure 15 Different stages of bacterial biofilm formation (created with BioRender.com)

The biofilm provides its forming bacteria with significantly better resistance to mechanical, chemical, immunological, and antimicrobial effects than their planktonic counterparts (Fisher et al., 2010). In addition, the formed biofilm is highly resistant to removal or eradication from the outside, with enhanced resistance to antimicrobial agents (Fisher et al., 2010). Biofilms also increase metabolic efficiency, make substrates more accessible, and provide more capacity for self-healing and regeneration following damage (Kite et al., 2004; Percival, 2005). Chronic wounds provide a favorable environment for biofilm formation. In chronic cases, the surface debris and necrotic tissues are easily vulnerable to infection. In addition, the altered vascularization and associated ischemia hinder the immune system from developing an efficient defensive response (Zhao et al., 2013). A previous study reported that about 60% of chronic wounds are colonised by biofilm-forming bacteria, compared with just 6% of acute wounds (James et al., 2008).

S. aureus and *P. aeruginosa* are the most frequently encountered bacteria in contaminated and clinically non-infected wounds (Guo and DiPietro, 2010). *P. aeruginosa* and *S. aureus* play a significant role in wound infection. Chronic ulcers are difficult to heal due to *P. aeruginosa* biofilms, which protect the bacteria from the phagocytic action of invading neutrophils. This mechanism may account for antibiotics failings as a treatment for chronic wounds (Bjarnsholt et al., 2008).

1.6.4.1 Management of Bacterial Biofilm Infections

Biofilm bacterial infections are typically treated with antibiotics, which are currently part of the standard medical practice. Alternative conventional treatments include bacteriophage therapy, antisense nucleic acid approach, quorum sensing (QS) system inhibitors, monoclonal antibodies, immunomodulators, and antibiotic potentiators (Tse et a., 2017). In order to ensure that an adequate concentration of antibiotics reaches the biofilm-infected area, it is standard practice to administer large dosages of antibiotics that are both effective and highly penetrative (Hengzhuang et al., 2012; Wu et al., 2015). However, antibiotics efficacy has steadily declined due to the emergence of antibiotic-resistant microbes and the increased risk of adverse effects. Moreover, some drawbacks of alternative treatments are that they call for a proper diagnostic evaluation first, are expensive, and questionable safety profile (Tse et a., 2017; Theuretzbacher and Piddock, 2019).

Using herbal medicine has been common practice for centuries. They have exceptional efficacy in both preventing and treating infections caused by bacterial biofilms. Plant extracts can inhibit biofilm formation and the quorum sensing system that controls biofilms. They exert their antibiofilm action by preventing bacterial cell attachment and adhesion, inhibiting the

production of bacterial virulence factors, and inhibiting the production of polymeric extracellular matrix, hence preventing the formation of biofilms and the QS system. Herbal medicines are being regarded as a significant step toward the discovery of novel antibiofilm treatments. They can serve alternative and complementary functions when added to standard medical care. As a result of their inhibitory effect on biofilms, antibiotics may be more effective against bacteria and overcome antibiotic resistance (Karbasizade et al., 2017; Lu et al., 2019).

1.7 Aims and Objectives

1.7.1 Project Aim

This project aims to investigate the medicinal properties of five plants traditionally used in Saudi Arabia in terms of antimicrobial, antibiofilm, cytotoxic, anti-proliferative, anti-inflammatory, antioxidant activities, and wound healing potential. The treatment of SSTIs and chronic wounds will receive special emphasis, particularly against skin infection-causing microorganisms such as: *Staphylococcus aureus*, *Staphylococcus epidermidis*, *MRSA*, *Pseudomonas aeruginosa*, *Escherichia coli*, and, where appropriate, determine to what extent our findings support the plant's traditional, folkloric use. In addition, the study aims to identify the active compounds in plant extracts responsible for antimicrobial properties.

1.7.2 Project Objectives

- To select and collect five traditionally used medicinal plants indigenous to the western region of Saudi Arabia.
- To develop and optimize an extraction and fractionation process of selected plants through bioassay-guided fractionation.

- To determine the cytotoxic and cell growth effects of plant extracts on HaCaT keratinocyte cell line.
- To determine the antioxidant activity of selected plant extracts in cell-based and non-cell-based modules.
- To develop and optimize assays to determine the antimicrobial activity of plant extracts against clinically relevant bacteria.
- To identify compounds from plant extracts responsible for the antimicrobial activity.
- To determine the wound healing potential of selected plant extracts.
- To determine the anti-inflammatory activity of selected plant extracts.

Chapter 2: Plant Material Collection, Extraction and Fractionation

2.1 Introduction

Worldwide, medicinal plants have been utilised for centuries, and many communities rely on indigenous medicinal herbs for primary health care. Several studies have discovered that Saudi Arabia possesses valuable medicinal plants (Gamal et al., 2010; Daur, 2012). The Saudi Arabian environment covers a vast region with diverse habitats and climates. Therefore, there is a wide variety in plant distribution throughout the country, with over 2,250 species in 142 families making up the natural flora (Aati et al., 2019). Due to the region's consistent precipitation, around 70% of the flora is cultivated in the Southwest region of Saudi Arabia. In addition, the flora of the Kingdom of Saudi Arabia is a rich source of agricultural and medicinal plants (Collenette, 1998).

For drug discovery, one of the most common methods for selecting medicinal plants is based on ethnomedical or traditional use. The ethnomedical method selects and evaluates plants based on oral and written evidence of their medicinal usage. Different sources, including books, herbals, and review papers such as ethnobotanical surveys of medicinal plants by geographic location or ethnic culture, provide access to information about established traditional medical systems. Another method for choosing medicinal plants involves randomly collecting all relevant plant parts and screening them for antimicrobial activity. However, the panel of tested microorganisms and the activity criteria utilised are crucial to the success or failure of this method, which is time-consuming and costly. Finally, the chemotaxonomy method of selecting botanically similar medicinal plants typically contains the same or nearly identical secondary metabolites. Consequently, if it is known that a specific plant possesses antimicrobial activity or secondary metabolites with antimicrobial activity, it is possible to determine related plants with the same or similar active principles. This procedure is still widely used in underdeveloped

nations due to the simplicity of the testing. Nevertheless, false-positive findings sometimes make it challenging to analyse the results (Mothana and Lindequist, 2005; Cos et al., 2006; Almeida et al., 2012; Atanasov et al., 2015).

Traditional medicine is still widely used and accepted in modern Saudi society. People are used to seeking relief from their disease with the help of herbal products and other alternative treatments. They often assume that this approach will guarantee a full recovery. Myrrh, bee-honey, fenugreek, black seed, and many others are all natural products used in such a manner. The continuity of these traditions from one generation to the next is a testament to their value (Al-Yahya, 1984; Aati et al., 2019).

Eighty % of Saudi survey respondents for an ethnopharmacological study on the usage of medicinal plants reported using such therapies at some point in their lives. According to the survey, about 20% of those who were surveyed were taking herbal medicine for chronic conditions, whereas 70% were using it for acute conditions. Colds account for half of the acute conditions that were treated with herbs, and myrrh was the most often used medicinal plant (Alanzi et al., 2016).

Five medicinal plants from the Southwest region of Saudi Arabia were identified as having an established traditional use and, therefore, candidates for the potential development of drugs via a bioassay-guided fractionation approach. Fractioning a crude extract into fractions using chromatographic methods and then subjecting each fraction to biological assessment (bioassay) is an example of bioassay-guided fractionation. As a result of the bioassay, only those fractions demonstrating biological activity are chosen for further fractionation. A pure compound with the desired activity is separated by repeating the cycle of fractionation, testing,

and further fractionation (Weller, 2012). Figure 16 shows the stages of the bioassay-guided fractionation approach.

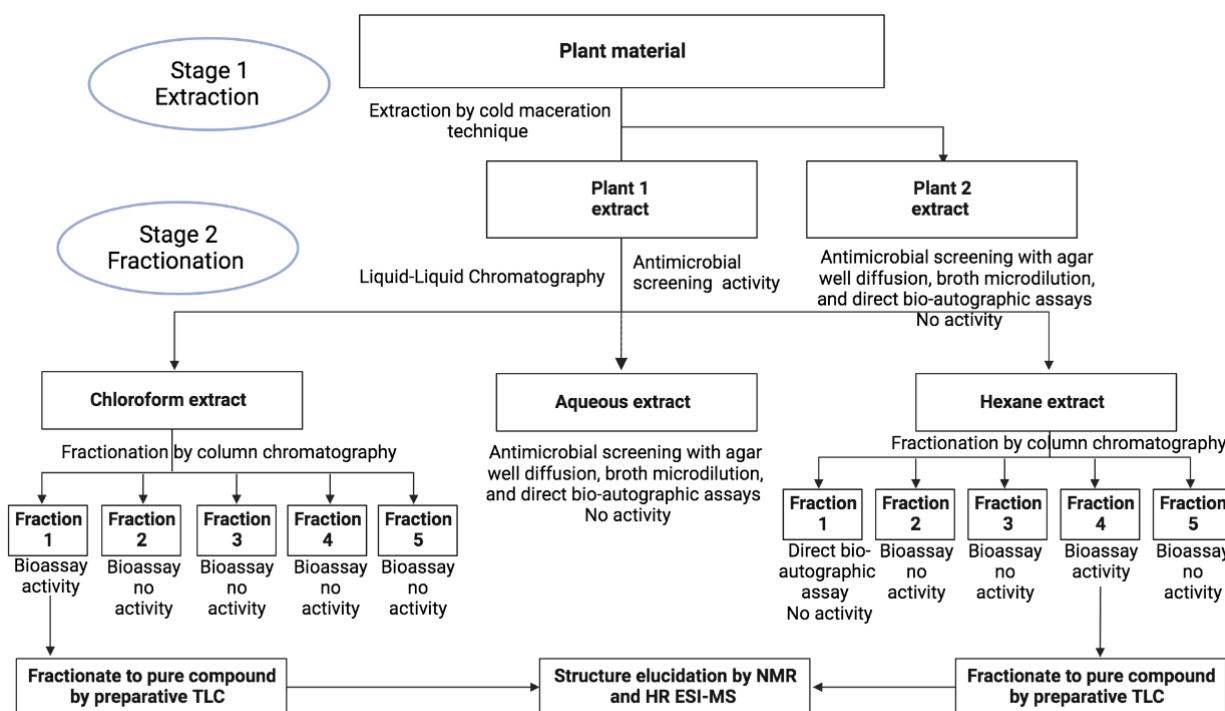


Figure 16 The stages of the bioassay-guided fractionation approach

2.2 Chapter Aim and Objectives

This chapter aims to identify and collect plant materials, develop and optimize extraction and separation techniques of plant extract, and identify active compounds.

- Identify and collect five traditionally used medicinal plants indigenous to the western region of Saudi Arabia.
- To develop and optimize an extraction process of plant materials.

- To develop and optimize a liquid-liquid chromatography separation technique for active plant extracts
- To develop and optimize a thin layer chromatography separation technique for future evaluation of separated compounds within active extracts.
- To develop and optimize a fractionation process of plant extracts through a column chromatography system.

2.3 Materials

All materials were obtained from ThermoFisher Scientific, Loughborough, UK, unless stated otherwise; methanol, ethanol, hexane, chloroform, and ethyl acetate HPLC grade were purchased from Sigma-Aldrich Company Ltd (Poole, UK). Aluminum sheet silica gel 60 F254 was obtained from Sigma-Aldrich Company Ltd.

2.4 Methods

2.4.1 Plant Material Collection

Aerial parts of *A. canariense* and *T. macropterus*, including the leaves, stems, seeds, flowers, and fruits were collected from the Northwestern region of Saudi Arabia Medina City in March 2017 with Dr. Hossam Afifi, Lecturer in Pharmacognosy at Department of Natural Products, faculty of pharmacy, King Abdulaziz University, Saudi Arabia. The authentication process was carried out by taxonomist (local flora guide), Dr. Emad A. Al Sherif, Lecturer in Plant Ecology, Department of Biology, Faculty of Science & Arts, Khulais, King Abdulaziz University, Saudi Arabia. Specimens were deposited in the herbarium of the Faculty of Pharmacy (AC 1330 & TM 1331), King Abdulaziz University.

Aerial parts of *C. colocynthis* and *M. crassifolia*, including the leaves, stems, seeds, flowers, and fruits were collected from the Southwestern Saudi Arabia, Al-Taif City, Al-Sail Al-Kabeer area (Table 1) in April 2018. Soil samples were collected from the site, and taxonomist (local flora guide), Dr. Emad A. Al Sherif, carried out the authentication process. Two specimens (CC 1431 & MC 1432) were kept in the herbarium at the Faculty of Pharmacy, King Abdulaziz University. Aerial parts of *R. stricta*, including the leaves, stems, seeds, flowers, and fruits were collected from the southwestern region of Saudi Arabia, Al-Shafa Mountains, and Al Taif City (Table 2) in April 2018. A soil sample was collected from the site, and the authentication was made by taxonomist (local flora guide), Dr. Emad A. Al Sherif, specimen (RS 1433) stored at the Faculty of Pharmacy, King Abdulaziz University.

Table 1 Site A of collected plants



Site A			
Temperature	GPS coordinates	Altitude	Photo
34 °C	Latitude N 21° 33'38.671" Longitude E 40° 07'23.149"	601 (m)	

Table 2 Site B of the collected plant

Site B			
Temperature	GPS coordinates	Altitude	Photo
26 °C	Latitude N 21° 17'24.967" Longitude E 40° 22'06.631"	1739 (m)	

2.4.2 Plant Extraction

After grinding 1 Kg of *A. canariense* and *T. macropterus* dried aerial parts, 800 g was extracted with 8 L of methanol for 72 h by cold maceration technique (ratio 1 g:10 mL). Evaporation processes were carried out under low pressure at 34 °C to remove methanol from the extract. For *M. crassifolia* and *R. stricta*, 1.5 Kg of plant aerial parts were ground, followed by extraction of 800 g with 8 L methanol for 72 h by cold maceration technique (ratio 1 g:10 mL). Extracts were concentrated through evaporation under low pressure at 34 °C. Finally, 700 g of *C. colocynthis* aerial parts were ground and then extracted with 7L methanol for 72 hours by cold maceration technique (ratio 1 g:10 mL). Evaporation processes were carried out under low pressure at 34° C to remove methanol from the extract (Mitscher et al., 1972).

2.4.3 Liquid-Liquid Chromatography

This separation technique involves partitioning compounds within plant extract between two immiscible liquid phases, and the separation process will depend on the solute's different partition coefficients (Colegate and Molyneux, 2008). Plant extracts that exhibited antimicrobial activity were further subjected to a liquid-liquid partitioning. Hexane extracts were obtained by dissolving the crude extract in 90% methanol and then carrying out a liquid-liquid partition between methanol and n-hexane three times, with 100 mL of n-hexane added each time (Figure 17A).

The chloroform and aqueous extracts were obtained by dissolving the extract in 10% methanol, followed by subjecting the methanol extract to liquid-liquid partition with chloroform three times (Figure 17B). The n-hexane and chloroform extracts were concentrated under low

pressure at 34 °C, and the water was removed from the aqueous extract via a freeze-drying process. Hexane, chloroform, and aqueous extracts were stored at -4 °C for further assessment.

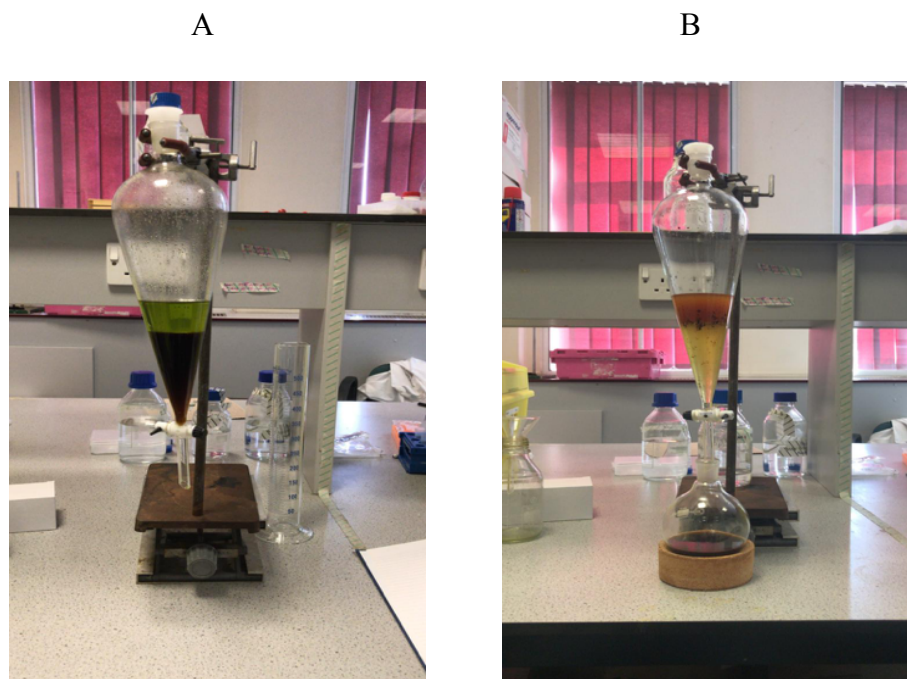


Figure 17 *R. stricta* liquid-liquid partition between two immiscible liquid phases, solutes are separated based on their differing partition coefficients (A) solutes with low polarity will favor the hexane phase (B) chloroform

2.4.4 Thin-Layer Chromatography (TLC)

The chemical profile of each extract and fraction were compared using analytical TLC analysis, which is an efficient, convenient, and rapid approach. Following the extraction and drying process of plant materials that were previously described (Section 2.4.2), a stock solution of plant extracts was prepared by re-suspending 10 mg in 1 mL of methanol to give a final 10 mg/mL concentration. Following that, a serial dilution with a ratio of 1:10 was carried out to prepare the following range of concentrations: 10, 1, 0.1, 0.01 mg/mL, then each dilution was mixed gently for 20 s with a vortex (ZX4 IR Vortex Mixer, Fisherbrand, UK). With the aid of fresh capillary pipettes, 25 μ L each concentration was spotted onto the surface of aluminum

sheet silica gel 60 F254 (Merck Life Science, Darmstadt, Germany) TLC plates 2 cm from the bottom of the plates. To ensure the evaporation of the excess solvent, the plates were positioned horizontally in a fume cupboard for 10 min. The mobile phase (solvent system) for separating extracts was optimized according to the optimum separation of bands within extracts. The following organic solvents were used in different ratios and combinations: ethyl acetate, hexane, methanol, and chloroform.

TLC developing tank was filled with 50 mL of selected mobile phase; then, spotted TLC plates were placed in the tank for 30 min or until the solvent covered 80% of the plate. Following that, plates were removed from the tank and the distance that the solvent traveled was marked and recorded. Bands were further observed by spraying the plates with anisaldehyde and sulphuric acid reagent and heating at 110 °C for 3 min (Murthy and Mishra, 2008). UV active compounds were visualized at 254 or 366 nm UV light.

The R_f values for each band were calculated with the following equation:

$$R_f = \frac{\text{Total distance traveled of the band (mm)}}{\text{Total distance traveled of solvent (mm)}}$$

Recorded R_f values can be compared with reference standards to identify compounds. Furthermore, TLC was also utilised to purify and isolate compounds from active fractions. The sample was diluted in a solvent and spotted as a band to the bottom of the preparative normal TLC plate (TLC Silica gel F₂₅₄, 20 x 20 cm, 0.5 mm, Merck Life Science, Darmstadt, Germany) or reverse-phase TLC plate (20 x 20 cm, 0.2 mm, Merck Life Science, Darmstadt, Germany). After developing the plate with the suitable mobile phase, the band was scraped off the plate,

and the compound was liberated through extraction with the suitable solvent. Finally, the solvent was evaporated, and the compounds were stored at -4 °C for further evaluation.

2.4.5 Column Chromatography (CC)

One of the most common techniques for the purification and separation of plant extracts and fractions at a preparative scale is column chromatography. After preparing the column, the sample will be loaded into the column, then eluting the column with a suitable mobile phase and recovering the constituents. Based on the different stationary phases, there are several types of column chromatography, such as adsorption chromatography, ion-exchange chromatography, affinity chromatography, and size exclusion chromatography. The selection of column type is determined by the characteristics of the sample to be separated (Jiang et al., 2021).

The glass column (50 mm x 61 cm) was packed to almost 65% with 45 g of silica (0.060- 0.200 mm, 4 nm) for this method. The column was then conditioned with 1 L of a 1:1 mixture of hexane and ethyl acetate, and 500 mL was eluted and discarded. Plant extracts that exhibited antimicrobial activity were further fractionated, and active plant extracts collected previously (Section 2.4.3) (1-2 g), were re-suspended in 10 mL of the same solvent at different concentrations. Using a Pasteur pipette, the solution was loaded uniformly onto the walls of the column after being mixed with a desktop vortex. Once the sample was applied, different hexane and ethyl acetate ratios were used to elute it. The obtained eluates were evaluated by TLC analysis, merged based on their TLC patterns, then concentrated in a vacuum at 34 °C and stored at -4 °C until needed.

2.4.6 Nuclear Magnetic Resonance (NMR)

^1H and ^{13}C -NMR spectroscopy is used to determine the structures of natural products and newly synthesised compounds. NMR is an essential spectroscopic technique for elucidating the structure of isolated compounds (Elyashberg, 2015; Reynolds and Mazzola, 2015). The isolated compounds were dissolved in deuterated methanol- d_4 or DMSO- d_6 solvents, then transferred to an NMR tube (Norell Standard Series 5, North Carolina, USA). ^1H -NMR and ^{13}C -NMR, as well as 2D experiments, including COSY, and NOESY for isolated compounds, were recorded. The chemical shift values were recorded and represented in parts per million (ppm) using the Bruker AVANCE 500 MHz NMR spectrometer (Bruker, Germany). Obtained spectra were calibrated with reference to the solvent peak by Topspin (version 3.6.3, Bruker, Germany).

2.4.6.1 ^1H -NMR

Hydrogen (^1H) is the most common isotope of the hydrogen atom and is the primary component of most organic molecules. Therefore, it is a valuable tool for structural identification of molecules, since it reveals critical information such as chemical shift (δ), integration, coupling constants, and hydrogen multiplicity pattern. The chemical shift (δ) reveals the proton surrounding the chemical environment, whereas integration reveals the number of hydrogens in that environment. The neighboring functional groups induce a chemical shift by shifting the proton peak in the spectrum downfield to the left (higher ppm) or upfield to the right (lower ppm). Deshielding refer to the presence of an electron-withdrawing group, such as double bonds and aromatic rings, carbonyl groups, and heteroatoms e.g. oxygen causes a leftward shift of the proton peak in the spectrum. Integration reveals how many protons are associated with

a group. Coupling constants or J values indicate how strongly one group is coupled to another. Finally, the splitting pattern reveals the number of hydrogens close to the examined atom, which is determined using the n+1 rule, where n is the number of hydrogens adjacent to that atom that yield a singlet, doublet or triplet if connected to zero, one, or two protons, respectively (Kwan and Huang, 2008; Elyashberg, 2015; Reynolds and Mazzola, 2015).

2.4.6.2 ^{13}C -NMR

Structure elucidation can also be performed via ^{13}C -NMR, which depends on the resonance of the isotope ^{13}C , which is not very abundant. ^{13}C represents only 1.1% of C in nature compared to the primary ^{12}C , which has no observable NMR spin. Consequently, the number of scans needs to be increased as its signal is weaker than the ^1H -NMR. Similar principles to ^1H -NMR apply for the chemical shift; a higher ppm atom is more deshielded by electron-withdrawing groups and appears downfield, whereas a lower ppm is more shielded by electron donating groups and atom appears upfield in the spectrum. Wide range of chemical shifts from 0 to 220 ppm due to shielding the environment's nature.

Typically, the nearby C is a ^{12}C , which lacks nuclear spin; hence C-C coupling cannot be detected. Furthermore, the number of hydrogens attached to it determines the peak intensity (i.e., the peak). The intensity of CH_3 is consequently more significant than that of quaternary carbon, which has no associated H (Kwan and Huang, 2008; Elyashberg, 2015; Reynolds and Mazzola, 2015).

2.4.6.3 Distortionless Enhancement by Polarisation Transfer (DEPT-135)

Data on the molecule carbon types (CH, CH₂, CH₃, or quaternary) was also obtained using DEPT-135. These spectra are compared against the ¹³C-NMR to identify the carbon type. In DEPT-135, the carbon signals are displayed as either positive peaks, negative peaks, or not exhibited at all, as for the quaternary carbon. The spectra of the CH and CH₃ group of positive magnitude, and the CH₂ groups are of negative magnitude (Kwan and Huang, 2008; Elyashberg, 2015; Reynolds and Mazzola, 2015).

2.4.6.4 Correlation Spectroscopy (COSY)

COSY is a homonuclear two-dimensional NMR that might be regarded three-dimensional owing to the intensity of the correlations observed in the spectrum. Offering insight into the ¹H-¹H coupling correlation over two or three and sometimes four bonds in the molecule. In rare cases, coupling occurs over longer distances, e.g., five bonds. The spectrum will show which protons are directly coupled to other protons. The ¹H-NMR spectrum is plotted in both axes within that set of experiments, with the diagonal peaks representing 1D ¹H-NMR signals and the cross peaks representing proton-proton couplings (Kwan and Huang, 2008; Elyashberg, 2015; Reynolds and Mazzola, 2015).

2.4.6.5 Nuclear Overhauser Effect Spectroscopy (NOESY)

The correlations between ¹H-¹H in space are shown as cross peaks in the NOESY spectrum. In this method, the stereochemistry of a molecule can be determined. NOESY spectra demonstrate coupling through space rather than through bonds (scalar coupling). Similar to the COSY spectrum layout, the ¹H-NMR spectrum is plotted along both axes, and the cross peaks

correspond to the NOESY correlation (Kwan and Huang, 2008; Elyashberg, 2015; Reynolds and Mazzola, 2015).

2.4.6.6 Heteronuclear Multiple Quantum Coherence (HMQC)

The direct ^{13}C - ^1H coupling is shown by the two-dimensional experiment, which provides information about which protons are directly attached to which carbons, known as Heteronuclear Correlation Spectroscopy, because correlations between different nuclei are observed, such as ^1H and ^{13}C . The top axis of the HMQC spectrum corresponds to ^1H -NMR, while the left axis corresponds to ^{13}C -NMR; ^1H - ^{13}C coupling is displayed as cross peaks (Kwan and Huang, 2008; Elyashberg, 2015; Reynolds and Mazzola, 2015).

2.4.6.7 Heteronuclear Multiple Bond Coherence (HMBC)

Heteronuclear Multiple Bond Coherence (HMBC) demonstrates correlations between protons and carbons distanced by two and three bonds. This heteronuclear experiment is precious since it allows the assembly of fragments and develops the molecule's structure. Similar to HMQC, with the ^1H spectrum on the right axis and the ^{13}C spectrum on the left (Kwan and Huang, 2008; Elyashberg, 2015; Reynolds and Mazzola, 2015).

2.4.7 Mass Spectroscopy (MS)

Mass-spectroscopy (MS) is an essential analytical technique for identifying isolated compounds by providing their specific molecular weight and fragments. MS works by forming the gas phase of the molecule, after which the volatile particles are ionised and separated according to their mass-to-charge ratio. Following that, the molecule is identified by the MS detector according to its abundance. After ionisation, the molecular weight is determined, or

the sample is fragmented to aid in the elucidation of the structure (Mirsaleh-Kohan et al., 2008; Pitt, 2009). Dr. Ann Hunter carried out low and high (accurate) mass resolution analysis at the National Mass Spectrometry Facility (NMSF), Swansea University, Swansea, UK. Thermo Scientific Orbitrap LTQ XL mass spectrometer (ThermoFisher Scientific) was used for the analysis.

2.5 Results and Discussion

2.5.1 Plant Extractions Yields

Using the maceration technique, the aerial parts of *A. canariense*, *C. colocynthis*, *M. crassifolia*, *R. stricta*, and *T. macropterus* were extracted with methanol for approximately 72 h. Extraction yield is the ratio of the amount of plant components dissolved in the solvent during the extraction procedure to the initial weight of plant material. *R. stricta* extract yielded the maximum extraction yield (12.18 % w/w), whereas *M. crassifolia* extract yielded the lowest (4.43 % w/w).

This variance in yield across different plant extracts can be due to differences in phytochemical constituents, which are influenced by several factors, including plant origin, climate, time of collection, extraction method, duration, and temperature (Karakaya et al., 2011; Efthymiopoulos et al., 2018). Taxonomist, Dr. Emad A. Al Sherif, carried out the authentication process of all plants. Table 3 presents summary of the yields of different plant extracts.

Table 3 The yield (solid matter residue, w/w) following plant extraction with methanol for 72 h

Extract	Yield
<i>A. canariense</i>	5.59%
<i>C. colocynthis</i>	8.65%
<i>M. crassifolia</i>	4.43%
<i>R. stricta</i>	12.18%
<i>T. macropterus</i>	5.26%

2.5.2 Plant Extract Liquid-Liquid Partition Yield

Plant extract with a promising antioxidant and antimicrobial activity *A. canariense* (3 g), *R. stricta* (10 g), and *T. macropterus* (3 g) were further subjected to a liquid-liquid partition process. The yield of hexane extract was (19.3, 12.9, 15.9 % w/w) and (32.5, 31.4, 16.7 % w/w) for the chloroform extract. In contrast, the aqueous extract demonstrated the highest yield with (45.2, 51.9, and 61.4 % w/w) and thus indicated the presence of a high number of polar compounds in separated extracts. Figure 18 shows a comparison of *R. stricta* liquid-liquid partition extraction yields.

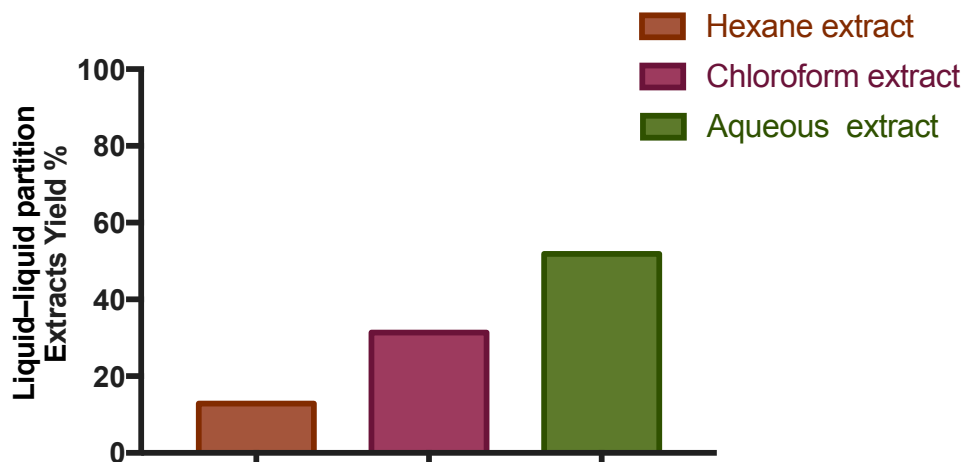


Figure 18 A comparison of *R. stricta* liquid-liquid partition extraction yields a total of 97%. The highest yield obtained with aqueous extract indicate the presence of many polar compounds in this extract

2.5.3 Fractionation of Plant Extracts by Column Chromatography

2.5.3.1 *Aizoon canariense*

Active hexane and chloroform extract (1 g) were subjected to fractionating with silica column chromatography, with hexane and ethyl acetate as the elution system by increasing the polar solvent gradient system. Nine collected fractions from *A. canariense* hexane extracts with an elution system are shown in Table 4.

Table 4 *A. canariense* hexane extract collected fractions by column chromatography

Number	Fractions (mg, dry weight)	Elution System
1	22.33	100% hexane
2	4.2	2.5% ethyl acetate
3	3.5	5% ethyl acetate
4	2.1	10% ethyl acetate
5	46.92	20% ethyl acetate
6	55.27	30% ethyl acetate
7	70.03	40% ethyl acetate
8	6.22	50% ethyl acetate
9	87.44	100% ethyl acetate

Fourteen fractions from *A. canariense* chloroform extracts were obtained after being eluted with hexane and ethyl acetate in 10% increments and washed with methanol (up to 20%) are shown in Table 5.

Table 5 *A. canariense* chloroform extract collected fractions by column chromatography

Number	Fractions (mg, dry weight)	Elution System
1	3.8	100% hexane
2	6.5	2.5% ethyl acetate
3	8.02	5% ethyl acetate
4	4.42	10% ethyl acetate
5	33.54	20% ethyl acetate
6	94.56	30% ethyl acetate
7	69.10	40% ethyl acetate
8	79.92	50% ethyl acetate
9	82.56	100% ethyl acetate
10	97.36	5% methanol in ethyl acetate
11	40.52	10% methanol in ethyl acetate
12	46.01	15% methanol in ethyl acetate
13	38.31	20% methanol in ethyl acetate
14	61	100% methanol

A. canariense hexane and chloroform fractions were evaluated against *Staphylococcus aureus* and MRSA through bacterial bio-autographic assay, and R_f values were recorded (Section 5.5.3). Chloroform fraction eight that demonstrated antimicrobial activity was further purified by preparative TLC normal silica mobile phase: 50% ethyl acetate: 25% hexane: 25% methanol, developed three times to yield compound ACC8 (18.43 mg, dry weight). ACC8 showed antimicrobial activity against *Staphylococcus aureus* and MRSA strain.

2.5.3.2 *Rhazya stricta*

Active hexane extract (2 g) was subjected to fractionating with silica column chromatography. Ten fractions were eluted using a gradient from 100% hexane to 100% ethyl acetate as the mobile phase. Ten fractions from *R. stricta* hexane extracts with an elution system are shown in Table 6.

Table 6 *R. stricta* hexane extract collected fractions by column chromatography

Number	Fractions (mg, dry weight)	Elution System
1	1.15	100% hexane
2	2.87	2.5% ethyl acetate
3	5.02	5% ethyl acetate
4	59.5	10% ethyl acetate
5	91.5	20% ethyl acetate
6	66.04	30% ethyl acetate
7	108	40% ethyl acetate
8	86.30	50% ethyl acetate
9	112.17	40% ethyl acetate
10	180.73	100% ethyl acetate

R. stricta hexane fractions were evaluated against *S. aureus*, MRSA, and *P. aeruginosa* through bacterial bio-autographic assay, and R_f values were recorded (Section 5.5.3). Fractions 5 and 6 exhibited antimicrobial activity. These fractions were investigated further. Using preparative TLC on normal silica (50% ethyl acetate: 50% hexane) developed three times, two compounds

were isolated: 1 (14.33 mg, dry weight) and 2 (11.44 mg, dry weight). Both RSH6 and RSH5 exhibited antimicrobial activity against strains of *Staphylococcus aureus* and MRSA.

2.5.3.3 *Tribulus macropterus*

T. macropterus hexane and chloroform extracts (1 g) were fractionated using silica columns chromatography, with hexane and ethyl acetate as the elution system. The polarity was gradually increased from 100% hexane to 100% ethyl acetate, and nine fractions were collected and evaluated for antimicrobial properties against *Staphylococcus aureus* and MRSA through bacterial bio-autographic assay. Rf values were recorded (Section 5.5.3). Table 7 shows summary of nine fractions recovered from *T. macropterus* hexane extract using a gradient elution system.

Table 7 *T. macropterus* hexane extract collected fractions using a gradient elution system

Number	Fractions (mg, dry weight)	Elution System
1	0.34	100% hexane
2	7.23	2.5% ethyl acetate
3	15.60	5% ethyl acetate
4	27.05	10% ethyl acetate
5	52.22	20% ethyl acetate
6	37.6	30% ethyl acetate
7	32.93	40% ethyl acetate
8	53.51	50% ethyl acetate
9	80.74	100% ethyl acetate

Chloroform extract showed antimicrobial activity and was further fractionated by a silica column as a separation method. A combination of 100 % hexane to 100 % ethyl acetate and methanol was used for the elution system. Fourteen collected fractions were evaluated against *Staphylococcus aureus* and MRSA through bacterial bio-autographic assay; Rf values were recorded (Section 5.5.3). Table 8 presents summary of *T. macropterus* chloroform extract 14 obtained fractions.

Table 8 *T. macropterus* chloroform extract collected fractions by column chromatography

Number	Fractions (mg, dry weight)	Elution System
1	83.88	100% hexane
2	41.42	2.5% ethyl acetate
3	55.8	5% ethyl acetate
4	74.36	10% ethyl acetate
5	46.44	20% ethyl acetate
6	34.81	30% ethyl acetate
7	180.57	40% ethyl acetate
8	13.80	50% ethyl acetate
9	63.20	100% ethyl acetate
10	34.09	5% methanol in ethyl acetate
11	29.76	10% methanol in ethyl acetate
12	20.37	15% methanol in ethyl acetate
13	74.51	20% methanol in ethyl acetate
14	95.5	100% methanol

2.5.4 Thin-Layer Chromatography (TLC)

2.5.4.1 Optimise the Organic Solvent System for the Separation of Plant Extracts

The separation of compounds through TLC depends on selecting the most appropriate solvent system consisting of one or more organic solvents. Different organic solvents have been used to select the most suitable separation method for five medicinal plant extracts, including hexane, ethyl acetate, methanol, and chloroform. Table 9 illustrates the different ratios of organic solvents typically used in TLC separation methods for natural products and was employed to separate the plant extracts and fractions.

Table 9 The different ratios of organic solvents are typically used in TLC separation methods for natural products and were employed to separate the plant extracts and fractions

Ratio number	Hexane	Ethyl Acetate	Methanol	Chloroform
1	1	1	1	1
2	2	8	0	0
3	3	7	0	0
4	4	6	0	0
5	5	5	0	0
6	6	4	0	0
7	7	3	0	0
8	8	2	0	0
9	0	2	8	0
10	0	3	7	0
11	0	4	6	0
12	0	5	5	0
13	0	6	4	0
14	0	7	3	0
15	0	2	8	0
16	5	0	0	5
17	2	4	4	0
18	0	0	1	9

Upon visualization of optimum separated bands on TLC plates, organic solvents ratio number five and seven were selected for further separation of five plant extracts plus hexane fractions. Finally, ratio twelve was selected for separating chloroform and aqueous fractions. The R_f

distribution of the separated compounds in the selected organic solvents fell within the desirable R_f value range of 0.20 to 0.85 (Shewiyo et al., 2012). TLC separation process rely on the polarity of compounds within plant extracts. Moreover, the rationale behind achieving the optimum separation with the above-selected solvent system is that using a non-polar solvent (hexane) with a relatively polar solvent (ethyl acetate) will improve the separation of polar from non-polar compounds. Figure 19 presents developed TLC plates spotted with *M. crassifolia* comparing two solvents system ratio five plate on the right (hexane 5: ethyl acetate 5) and ratio 16 plate on the left (hexane 5: chloroform 5) (Hostettmann et al., 1998; Owen et al., 2019).

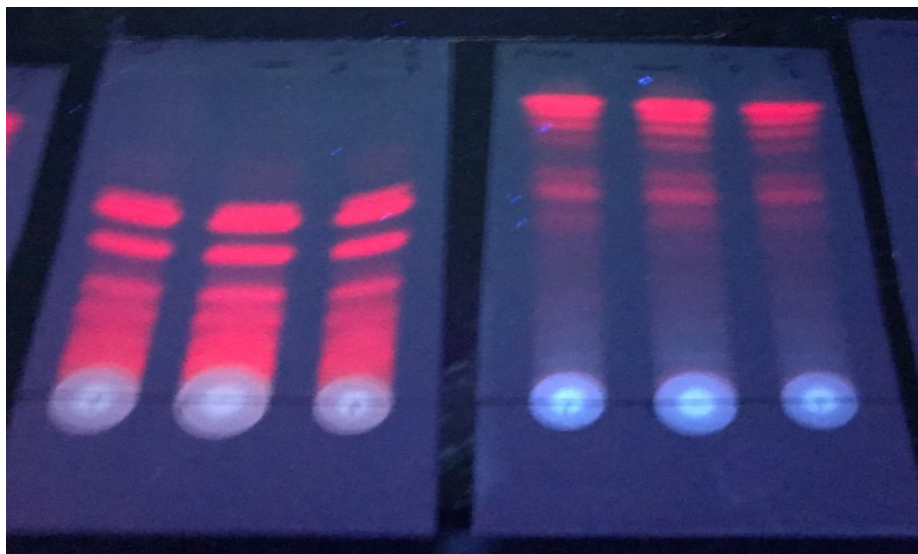


Figure 19 Shows developed TLC plates spotted with *M. crassifolia* comparing two solvent systems. The TLC plate on the right was developed with solvent system hexane 50%: ethyl acetate 50%, TLC plate on the left was developed with solvent system hexane 50%: chloroform 50%

2.5.4.2 Separation of Plant Extracts by Thin-Layer Chromatography

Five methanolic plant extracts (10 mg/mL) were spotted on aluminum sheet silica gel 60 F254 TLC plates, then eluted with 70% hexane with 30% ethyl acetate and 50% hexane with 50%

ethyl acetate. The rationale behind selecting these solvent systems is that they showed the optimum separation of bands. It was mainly based on trial and error (Figure 20), followed by spraying the plates with sulphuric acid reagent and heating at 110 °C for 3 min. This reagent is a general non-selective and destructive staining reagent that reveals a variety of chemical constituents, including; glycosides, alkaloids, terpenoids, steroids, phenolics, tannins and proteins. Rf values were recorded (Table 10). These findings will aid the fractionation process of extracts with column chromatography and support the antimicrobial bio-autographic assay to determine bioactive analytes within plant extracts (Section 5.5.3).

Table 10 Rf values of different phytochemical bands in plant extracts

Plant extracts	Rf value 1 ± S.D.	Rf value 2 ± S.D.	Rf value 3 ± S.D.	Rf value 4 ± S.D.	Rf value 5 ± S.D.	Rf value 6 ± S.D.	Rf value 7 ± S.D.
<i>R. stricta</i>	0.2 ± 0.003	0.44 ± 0.02	0.51 ± 0.01	0.63 ± 0.03	0.84 ± 0.02		
<i>A. canariense</i>	0.09 ± 0.003	0.17 ± 0.01	0.90 ± 0.007	0.94 ± 0.01			
<i>C. colocynthis</i>	0.08 ± 0.009	0.17 ± 0.009	0.33 ± 0.01	0.63 ± 0.01	0.74 ± 0.01	0.79 ± 0.01	0.87 ± 0.01
<i>M. crassifolia</i>	0.49 ± 0.005	0.58 ± 0.01	0.65 ± 0.01	0.74 ± 0.01	0.79 ± 0.007	0.85 ± 0.01	0.88 ± 0.01
<i>T. macropterus</i>	0.18 ± 0.003	0.65 ± 0.01	0.86 ± 0.006	0.88 ± 0.01	0.91 ± 0.007	0.93 ± 0.01	

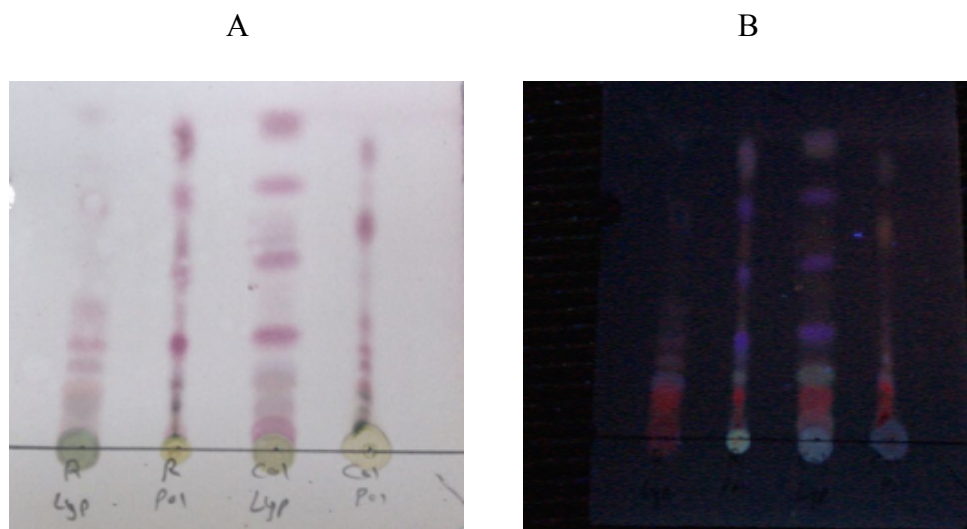


Figure 20 *R. stricta* and *C. colocynthis* TLC plates developed with 30% ethyl acetate and 70% hexane, it indicate the presence of many compounds in these two extract (A) The plate was sprayed with p-anisaldehyde and sulphuric acid reagent and heated at 110 °C for three min (B) UV active compounds were visualized at 254 nm UV light

2.5.5 Structure Elucidation of the Isolated Compounds

Previously isolated compounds (Section 2.5.3) were evaluated via NMR and MS spectrometry techniques, to elucidate the structure of the molecules in question. NMR data are also presented in this Section.

2.5.5.1 Identification of RSH6 as Vincadifformine

RSH6 was isolated from *R. stricta* hexane extract with the appearance of beige to brown solid. TLC development with a mobile phase of 50% ethyl acetate and 50% hexane reveals a blue spot under UV light (254, 365 nm). The accurate mass obtained by a high-resolution electrospray ionisation mass spectrometry (ESI-MS) indicated the molecular formula of $C_{21}H_{26}N_2O_2$ and generated the $[M+H]^+$ ion at m/z 339.2058 (Figure 21).

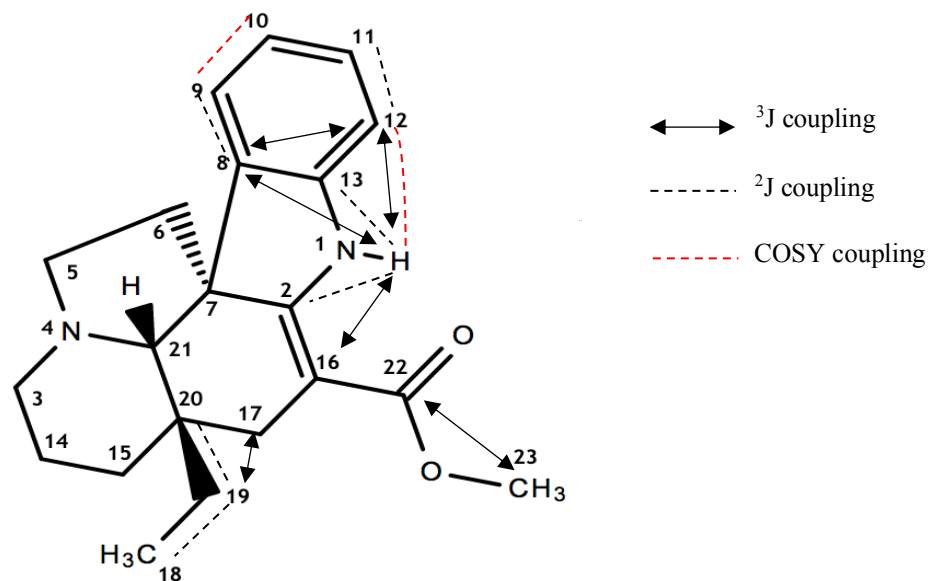


Figure 21 Chemical structure of RSH6 (vincadifformine). Demonstrating 2D NMR correlations; HMBC (2J , 3J couplings), and COSY (created with ChemDraw)

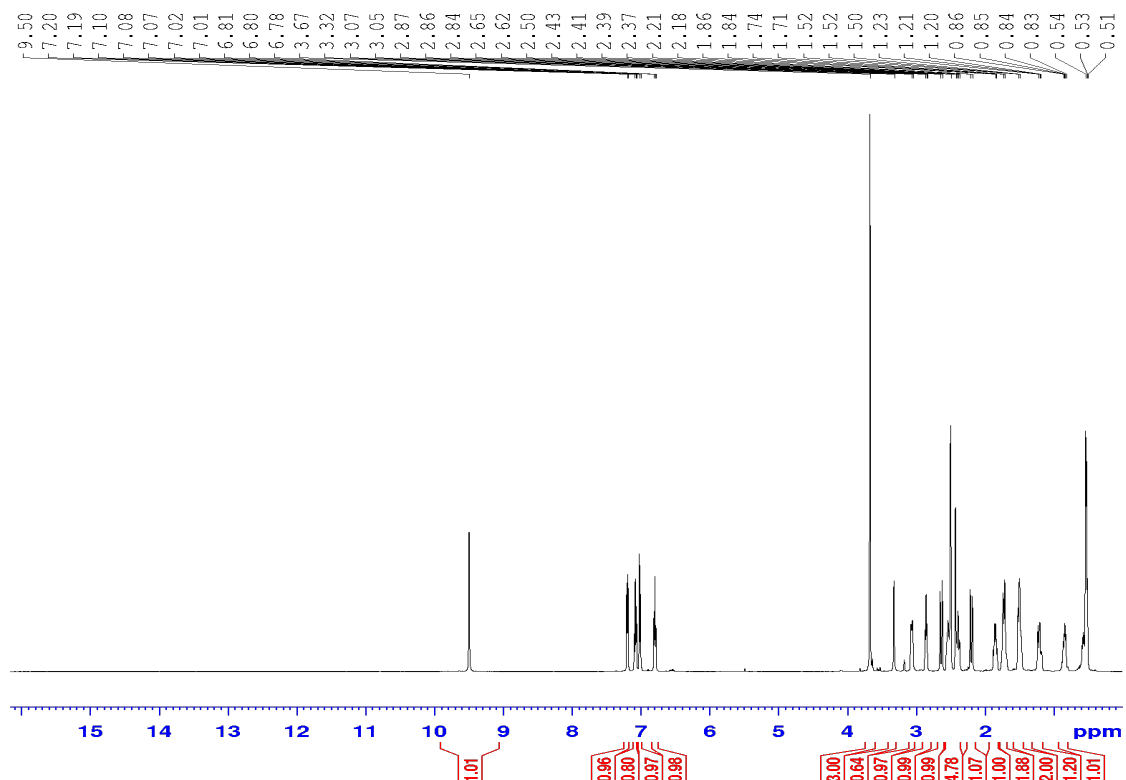


Figure 22 1H -NMR spectrum of RSH6

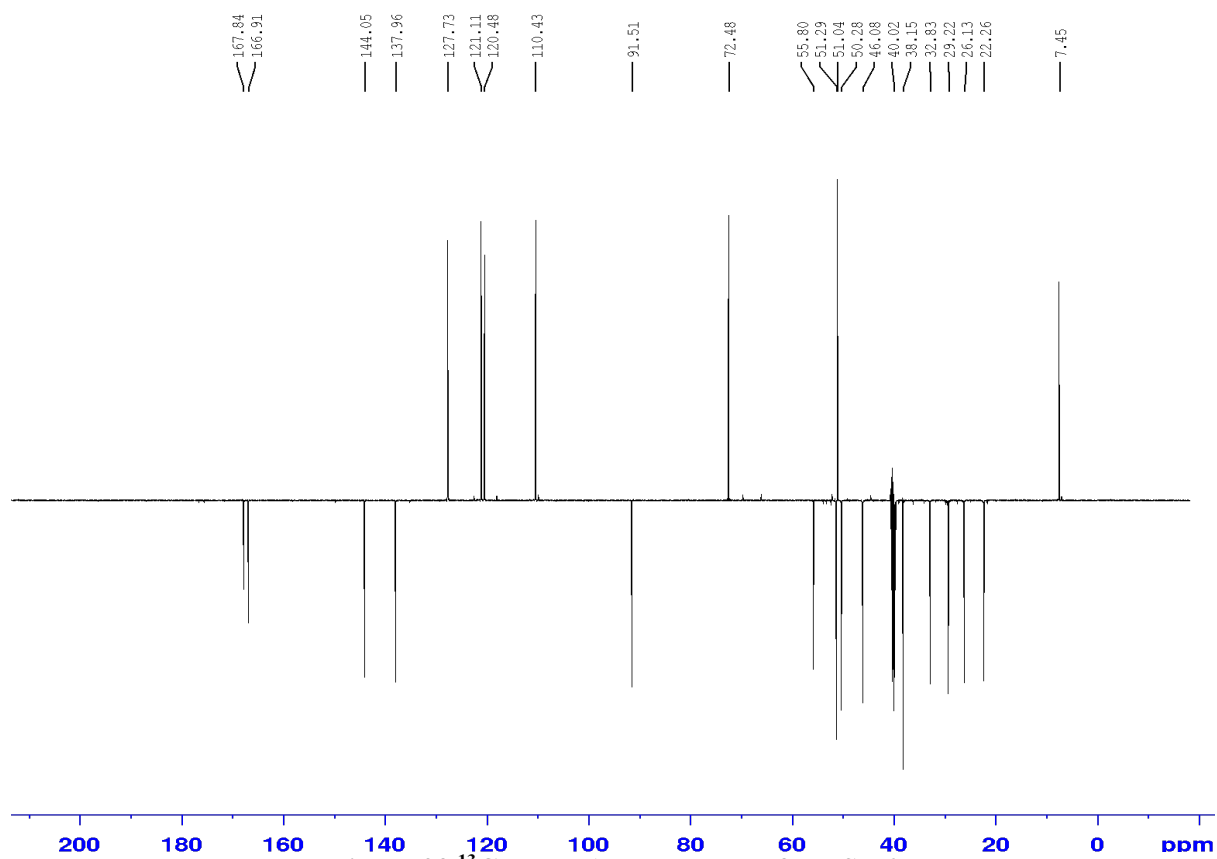


Figure 23 ^{13}C -NMR APT spectrum for RSH6

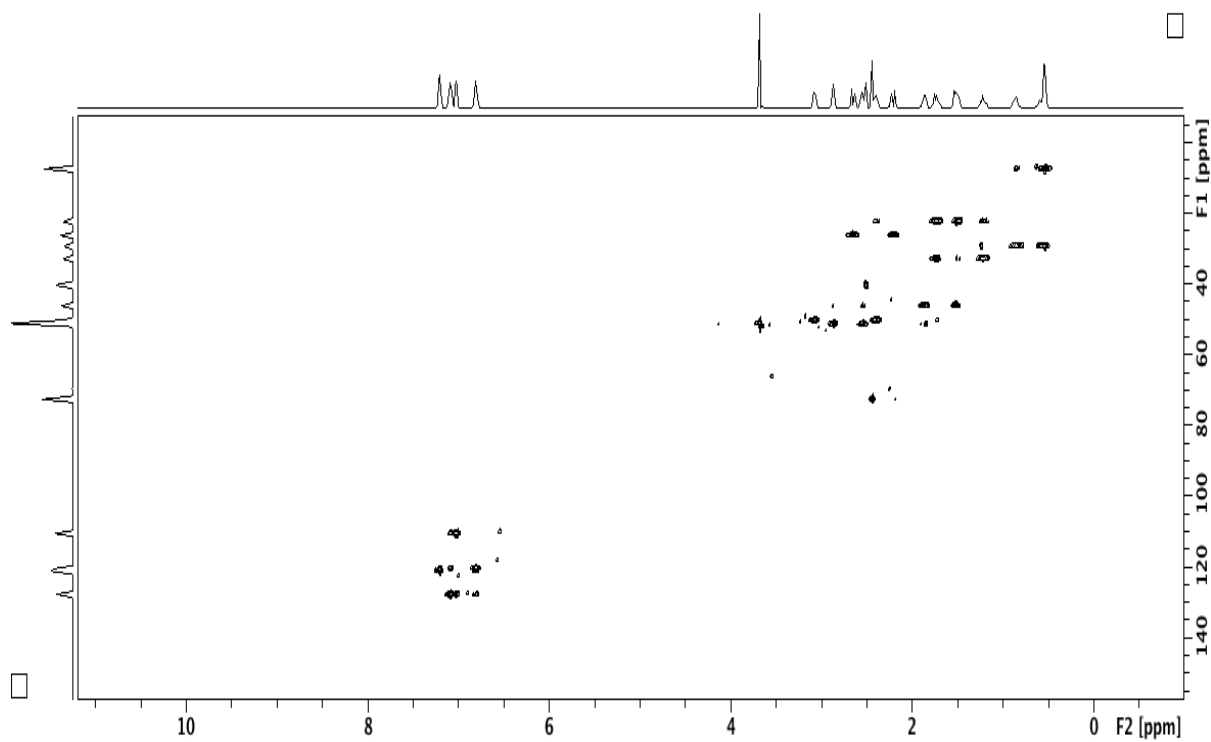


Figure 24 HMQC spectrum for RSH6

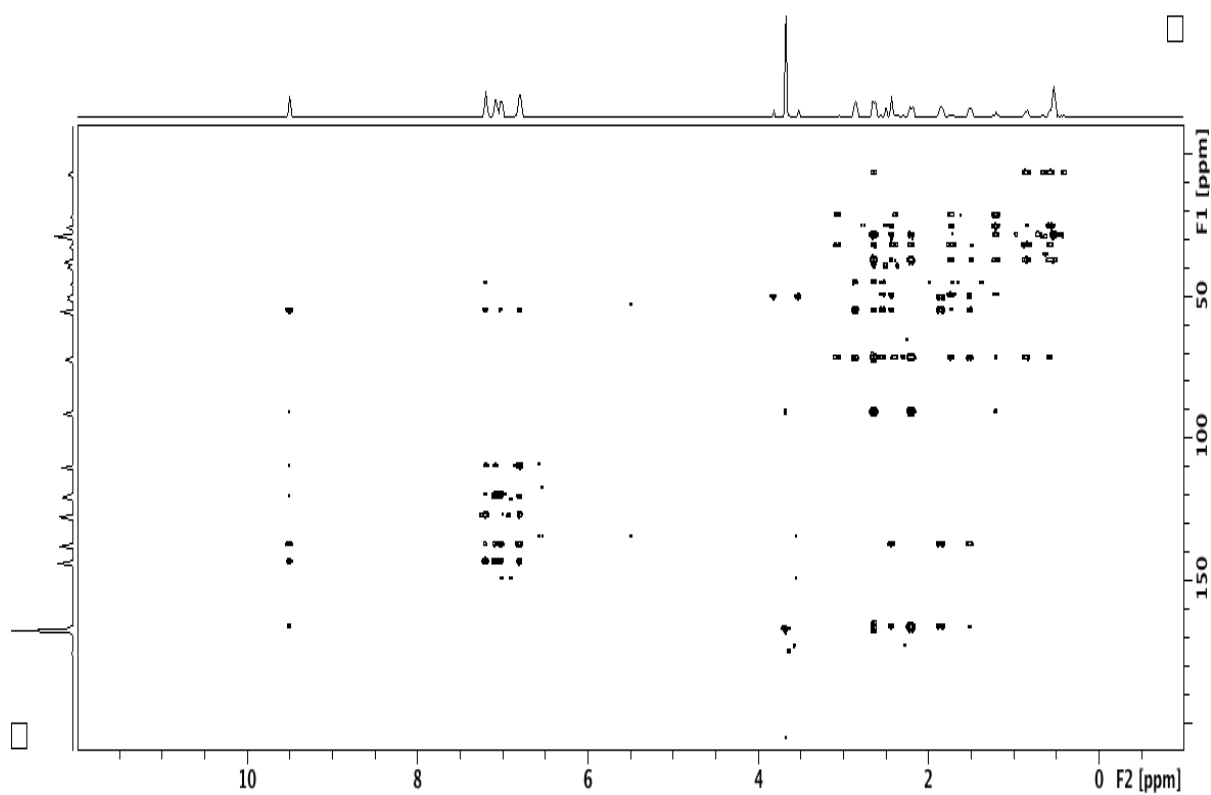


Figure 25 HMBC ^1H - ^{13}C NMR for RSH6

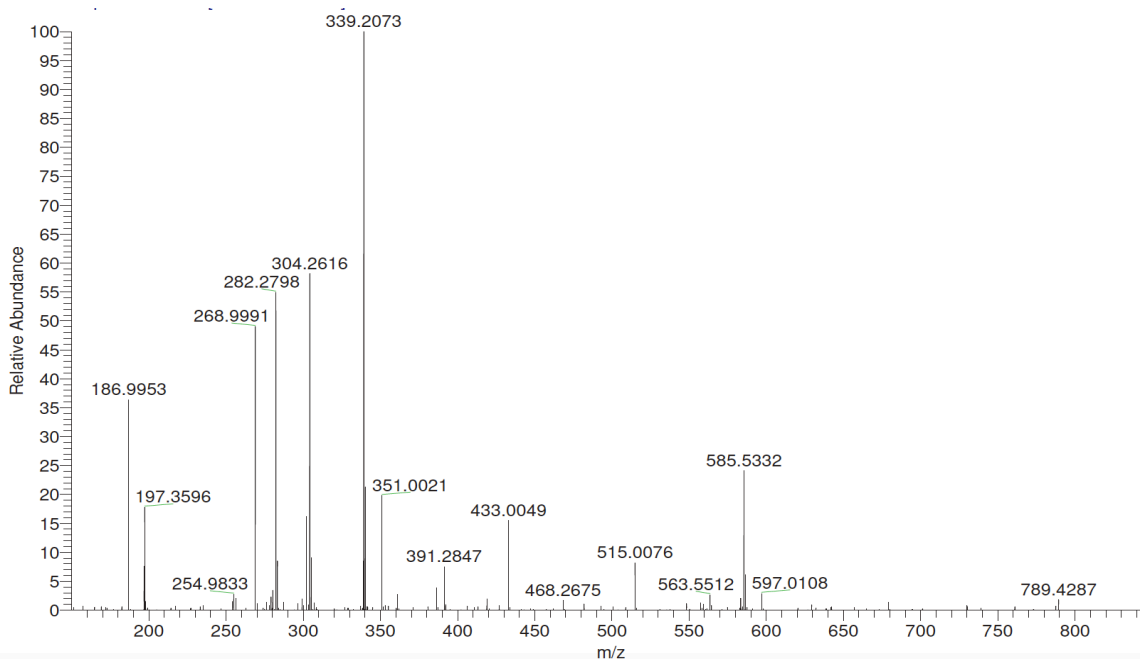


Figure 26 Mass spectrum of RSH6

RSH6 ^1H and ^{13}C NMR data are presented in Table 11. The ^1H NMR spectrum reveals the presence of terminal methyl and methylene protons signals coupled to each other in the upfield region at δ 0.52 appears as triplet peaks (2H, t, $J_{\text{ortho}} = 6.5$ Hz, H18) and δ 0.82 as quartet peaks (3H, t, $J_{\text{ortho}} = 6.5$ Hz, H19), respectively. Furthermore, the spectrum demonstrated characteristic resonances of a proton from a secondary amine (NH) with a deshielded singlet downfield at δ 9.49 (1H, s, H1), another distinguished resonance of a terminal methyl ester appears typically at δ 3.67 as a singlet (3H, s, H23). Four signals from aromatic protons in the downfield region between δ 6.8-7.2 were detected with two coupled aromatic protons at δ 6.8 (1H, t, $J_{\text{ortho}} = 7.3$ Hz, H10) and δ 7 (1H, d, $J_{\text{ortho}} = 7.3$ Hz, H9). Another coupling was observed

at δ 7.08 (1H, t, $J_{\text{ortho}} = 7.5$ Hz, H11) and δ 7.2 (1H, d, $J_{\text{ortho}} = 7.5$ Hz, H12). In addition to the deshielded methylene signal observed at δ 2.85 attributed to electron withdrawing tertiary amine next to it, five other methylene signals were detected at (δ 2.63, 2.4, 1.75, 1.5, and 1.2), a singlet peak of methine group observed at δ 3.17.

The ^{13}C NMR spectrum indicated the presence of twenty-one carbon signals (Table 11). The results of ^{13}C APT and DEPT-135 spectrum peaks concluded with the presence of two methyls, six methylene, five methine groups, and eight quaternary carbons. The ^{13}C NMR spectrum confirmed the obtained ^1H NMR data with the presence of distinct quaternary carbon resonance (δ 167.83) corresponding to the ester group. Another downfield alkenyl carbon signal was observed at δ 166.7, corresponding to the quaternary carbon part of the distinctive indole ring of RSH6. Two terminal methyl and methylene signals were detected upfield at the chemical shift δ 7.44 and δ 29.22. A quaternary carbon and methyl signal appeared downfield at δ 91.51 δ 51.03 deshielded as it is attached to an oxygen atom of ester group. Resonances of methylene carbons were observed at δ 51.28, 50.27, 32.82, 26.13 and 22.26.

Signals from two quaternary carbons were seen at δ 55.80 and δ 38.15. Moreover, methylene and methine resonance at δ 72.48 and δ 46.08 were detected. The remaining carbon atoms (two methines and two quaternary) were located in the downfield region of the ^{13}C spectrum between δ 144-110, related to aromatic carbons in the aromatic ring.

The functional groups' positions were determined by employing HMBC and COSY NMR experiments in which the ester group demonstrated ^3J coupling with δ 3.67, thus locating the ester group at C22 and placing the methyl at C23. The secondary amine was positioned at one as the proton showed ^2J coupling with δ 166.7 (C2) and δ 144.05 (C13). In contrast, ^3J coupling

with δ 137.95 (C8), 110.43 (C12), 91.51 (C16), and 55.51 (C7), furthermore, the COSY spectrum revealed the secondary amine proton long range coupling with methine from the aromatic ring at δ 7.2 (H12) placing it at position 12. The aromatic proton δ 7.2 showed a 2J coupling with other aromatic quaternary carbon at δ 144.05 (C13) and a methine δ 127.73 (C11) with 3J coupling with the rest of the aromatic carbons at δ 137.95 (C8) and δ 120.48 (C10), respectively and displayed other COSY correlations to aromatic protons at δ 7.08 (H11), the other aromatic proton at δ 7 (H9) of methine group via the HMBC spectrum it demonstrated a 2J coupling with quaternary carbon at δ 137.95 (C8) and methine at δ 120.48 (C10) and a 3J coupling with two quaternary carbons at δ 144.05 (C13) and at δ 127.73 (C11) along with methine at δ 55.51 (C7). Also, the COSY proton-proton coupling showed a coupling with a proton at δ 6.8 (H10); consequently, these data lead to their positioning in the aromatic ring. HMBC spectrum revealed that the terminal methylene at δ 0.82 (H19) has a 2J coupling at δ 38.15 (C20) and δ 7.45 (C18). Furthermore, 3J coupling with a methine at δ 72.48 (C21) and two methylene groups at δ 32.82 (C15) and δ 26.13 (C17), as well as the COSY correlation between δ 0.82 (H19), δ 0.52 (H18) and δ 1.2 (H15). The signals at δ 0.52 and 0.82 were placed at positions 18 and 19, respectively.

These findings, together with the HMBC and COSY spectrum analyses of RSH6, were in close alliance with those for vincadifformine, which was previously isolated from *R. stricta* (Kumara, 2010; Akhgari et al., 2015).

Table 11 ^1H and ^{13}C NMR data for RSH6, obtained in DMSO- d_6 (500 MHz)

Position	^1H	^{13}C	^2J	^3J	(Kumara C., 2010) in chloroform- d ^1H	^{13}C
1	9.49 (1H, s, H1)	-	C2, C13	C7, C8, C12, C16	8.89	
2	-	166.7	-	-	-	166.7
3	2.4 (2H, t, H3)	51.2	C14	C15, C5, C21	2.43- 2.35	50.66
4	-	-	-	-	-	-
5	2.85 (2H, t, H3)	50.27	C6	C3, C7, C21	2.91	51.71
6	1.5 (2H, t, H6)	46.07	C5, C7	C2, C8, C21	1.69	45.25
7	-	55.51	-	-	-	55.45
8	-	137.95	-	-	-	137.94
9	7 (1H, d, H9)	121.1	C8, C10	C11, C13, C7	6.78	121
10	6.8 (1H, t, H10)	120.48	C9, C11	C8, C12	7.11	120.45
11	7.08 (1H, t, H11)	127.73	C10, C12	C9, C13	6.84	127.40
12	7.2 (1H, d, H12)	110.43	C11, C13	C8, C10	7.18	109.29
13	-	144.05	-	-	-	143.27
14	1.75 (2H, m, H14)	22.26	C3, C15	C20	1.81	22.14
15	1.2 (2H, t, H15)	32.82	C14, C20	C3, C17, C19, C21	1.27-1.20	32.86
16	-	91.51	-	-	-	92.62
17	2.63 (2H, s, H17)	26.13	C16, C20	C2, C19, C21, C22	2.71	25.52
18	0.52 (3H, t, H18)	7.44	C19	C20	0.56	7.14
19	0.82 (2H, q, H19)	29.22	C18, C20	C15, C17, C21	0.96	29.29
20	-	38.15	-	-	-	38.15
21	3.17 (1H, s, H21)	72.48	C7, C20	C2, C6, C8, C15, C19,	2.45	72.66
22	-	167.83	-	-	-	169.19
23	3.67 (3H, s, H23)	51.03	-	C22	3.75	50.98

2.5.5.2 Identification of ACC8 as γ -Linolenic Acid

ACC8 was isolated from *A. canariense* chloroform fraction eight via preparative TLC with a mobile phase of 50% ethyl acetate: 25% hexane: 25% methanol. Under long and shortwave UV light (365, 254 nm), the ACC8 spot exhibited a blue fluorescence. HR ESI-MS determined the molecular formula of $C_{18}H_{30}O_2$ based on the $[M+H]^+$ ion at 279.2342 m/z. Figure 27 presents the chemical structure of ACC8.

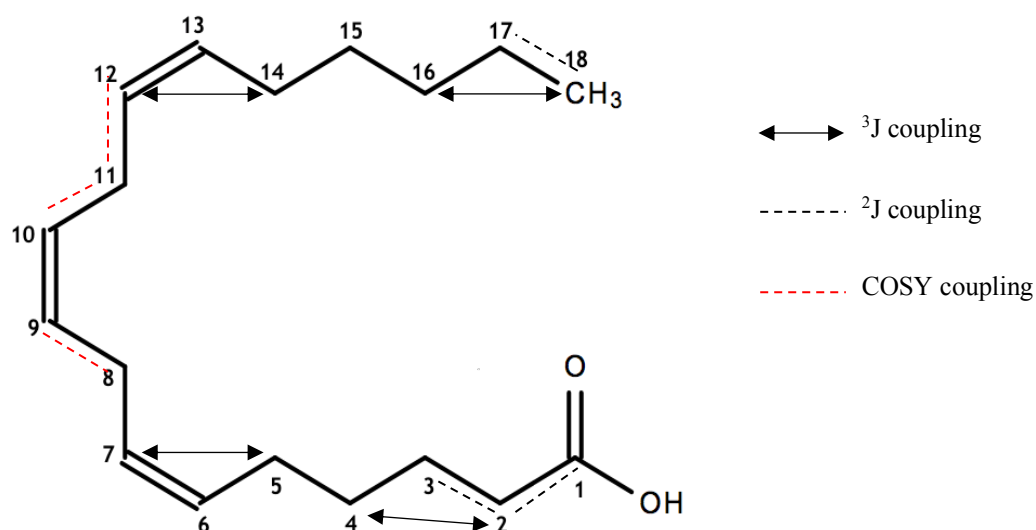


Figure 27 Chemical structure of ACC8 (γ -linolenic acid). Demonstrating 2D NMR correlations; HMBC (2J , 3J couplings), and COSY (created with ChemDraw)

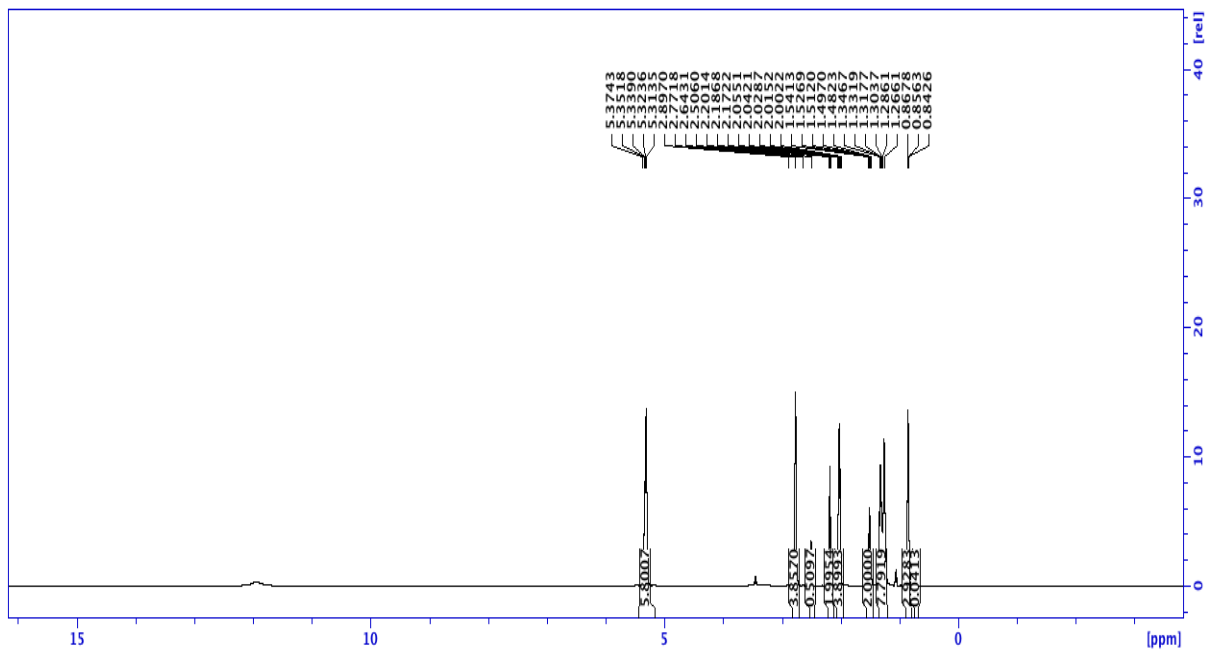


Figure 28 ¹H-NMR spectrum of ACC8

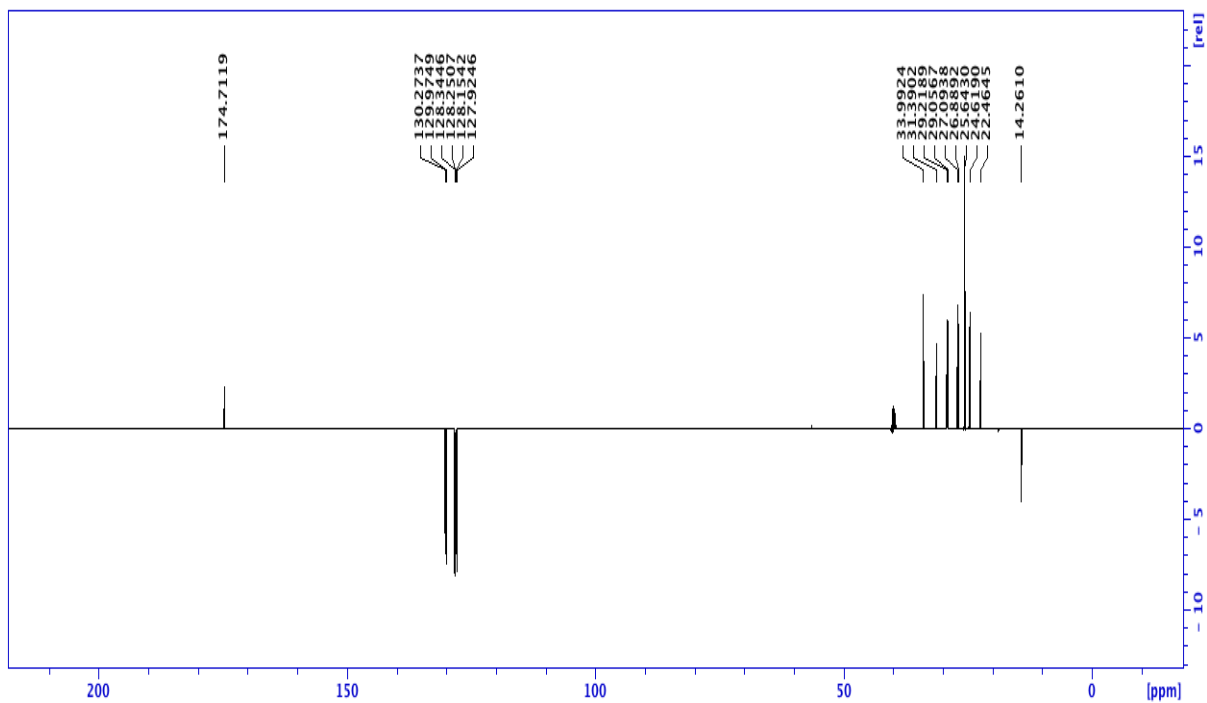


Figure 29 ¹³C-NMR APT spectrum of ACC8

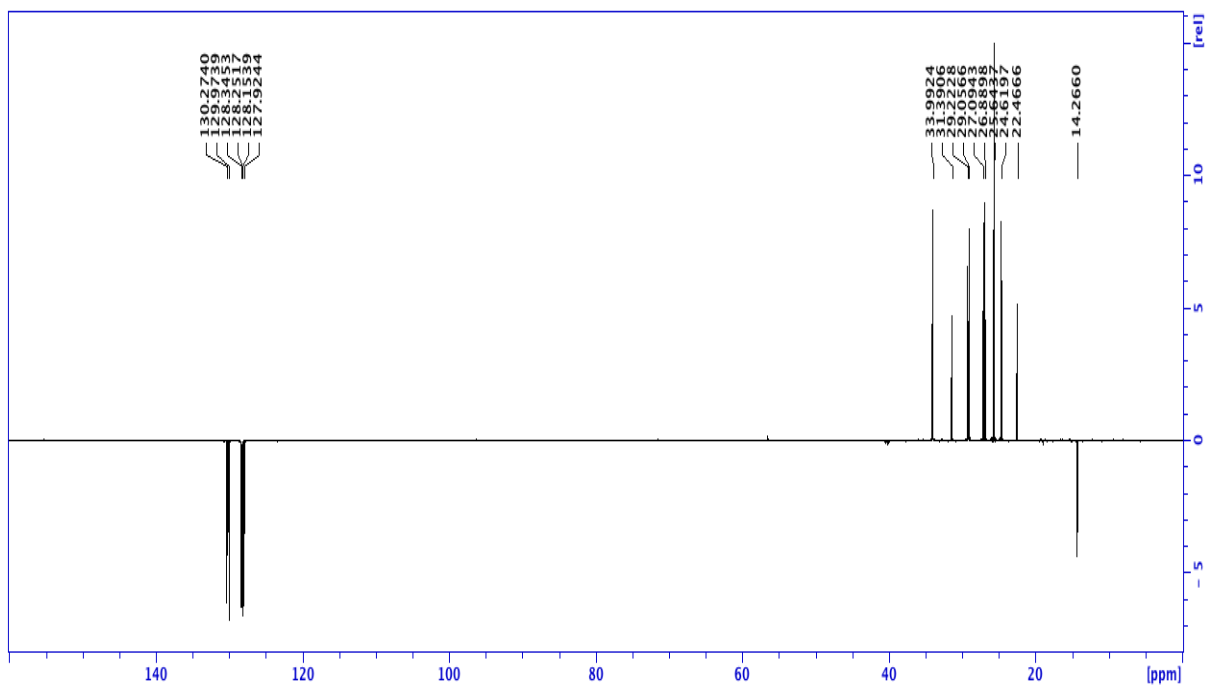


Figure 30 ^{13}C -NMR DEPT-135 spectrum of ACC8

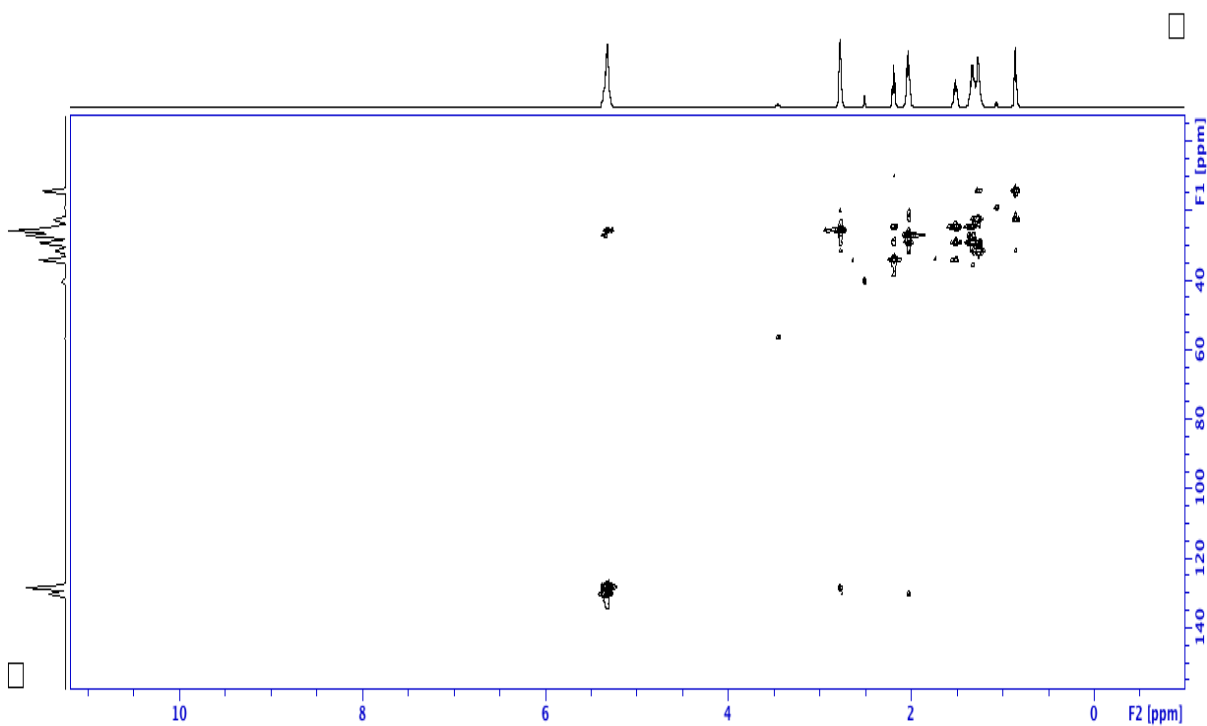


Figure 31 HMQC spectrum for ACC8

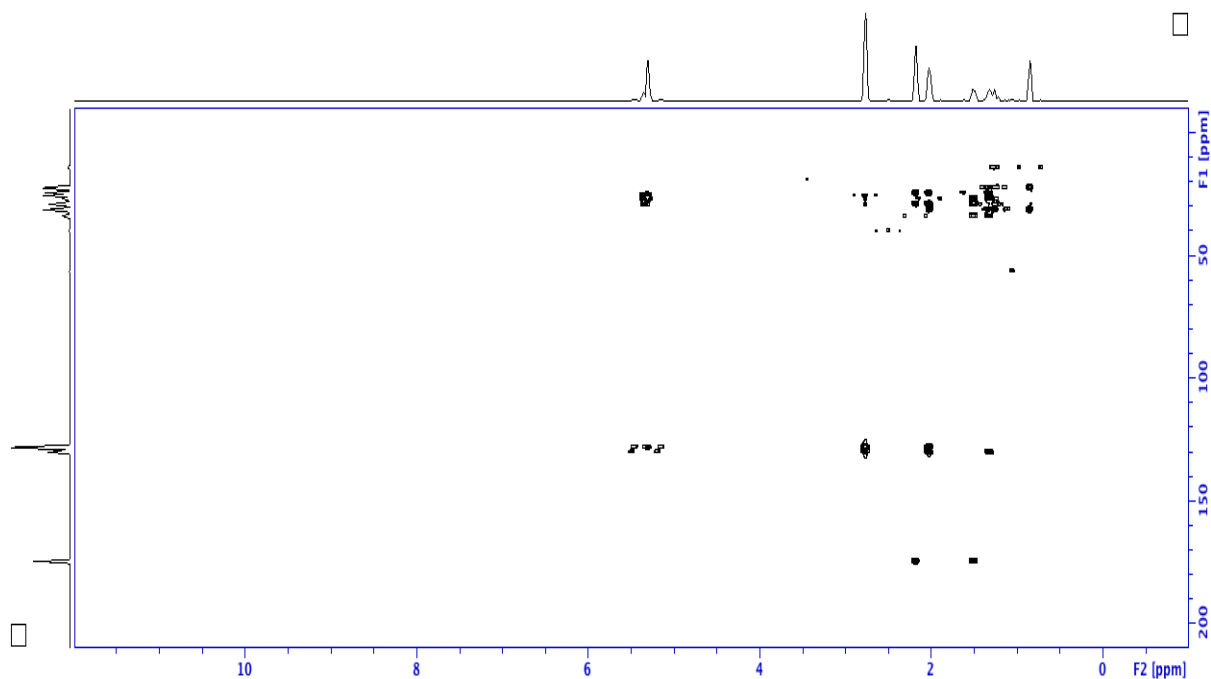


Figure 32 HMBC spectrum of ACC8

^1H and ^{13}C NMR data of ACC8 demonstrated the presence of a downfield triplet signal of α -methylene proton at δ 2.17- 2.2 (2H, t, H2) due to their neighboring terminal carboxylic acid group, and a signal from a β -methylene proton was detected at 1.48-1.54 (2H, m, H3).

^1H spectrum revealed characteristic overlapping signals of triple unsaturated chain, indicating the existence of three double bonds and six olefinic protons at δ 5.31- 5.37 (6H, m, H6, 7, 9, 10, 12, 13). In addition, a terminal methyl proton triplet signal appeared upfield at δ 0.84-0.86 (3H, t, H18), with and adjacent methylene protons signal at δ 1.26-1.34 (2H, m, H17), furthermore, the COSY characteristic cross peaks between those two protons validated their adjacent to each other.

Other distinguished overlapping signals appeared at δ 2.77 and δ 2.0- 2.05 to confirm the presence of two allylic methylene (4H, m, H5, H14) and two bis-methylene groups (4H, m,

H8, H11), respectively. Gathered COSY data confirmed the correlation between olefinic protons with the bis-methylene ones; in addition to the long coupling with the allylic protons, these data confirmed placing them next to each other.

^{13}C NMR data showed a downfield signal at δ 174.71(C1) corresponding to the carbon of the carboxylic acid (electron withdrawing). Six olefinic carbons gave six downfield peaks at δ 127.92, 128.15, 128.25, 128.34, 129.97, and 130.27 (C12, C7, C10, C9, C6, and C13), and HMBC spectrum reveals the ^2J and ^3J coupling of olefinic protons at δ 5.31- 5.37 (6H, m, H6, 7, 9, 10, 12, 13) with the carbons of each other. The signal from α -methylene generated downfield at δ 33.99 (C2) due to the presence of the electron withdrawing effect of neighboring carboxylic acid, and HMBC showed the long rang correlation ^2J between α -methylene proton δ 2.17- 2.2 (2H, t, H2) and carbon at δ 174.71 (C1) along with carbon δ 31.39 (C3). Moreover, a coupling over three bonds at δ 29.8 (C4) confirming their positions in the chain. Terminal methyl carbon signal appeared upfield at δ 14.26 (C18), moreover, it is proton at δ 0.84-0.86 (3H, t, H18) demonstrated a ^2J correlation with carbon at δ 22.61 (C17) and a ^3J coupling at δ 24.61 (C16). Comparing the above NMR data with literature data (Park et al., 2013) aids in identifying ACC8 as γ -linolenic acid (Table 12). The isolated compound was identified in *A. canariense* (Freije et al., 2013).

Table 12 ^1H and ^{13}C NMR data for ACC8, obtained in DMSO-d₆ (500 MHz)

Position	^1H	^{13}C	^2J	^3J	(Park et al., 2013) in methanol-d ^1H	^{13}C
1	-	174.71	-	-	-	177.68
2	2.17-2.2 (2H, t, H2)	33.99	C1, C3	C4	2.24-2.26	34.95
3	1.48-1.54 (2H, m, H3)	31.39	C2, C4	C1, C5	1.57-1.60	30.3
4	1.26-1.34 (2H, m, H4)	29.8	C3, C5	C2, C6	1.32	29.9
5	2.0-2.05 (2H, m, H5)	29.21	C4, C6	C3, C7	2.04-2.09	29.8
6	5.31-5.37 (1H, m, H6)	129.97	C5, C7	C4, C8	5.32-5.34	130.5
7	5.31-5.37 (1H, m, H7)	128.15	C6, C8	C5, C9	5.32-5.34	128.3
8	2.77 (2H, m, H8)	29.05	C7, C9	C6, C10	2.78- 2.84	29.8
9	5.31-5.37 (1H, m, H9)	128.34	C8, C10	C7, C11	5.32-5.34	128.7
10	5.31-5.37 (1H, m, H10)	128.25	C9, C11	C8, C12	5.32-5.34	128.7
11	2.77 (2H, m, H11)	27.09	C10, C12	C9, C13	2.78- 2.84	27.8
12	5.31-5.37 (1H, m, H12)	127.92	C11, C13	C10, C14	5.32-5.34	127.8
13	5.31-5.37 (1H, m, H13)	130.27	C12, C14	C11, C15	5.32-5.34	132.72
14	2.0-2.05 (2H, m, H14)	26.88	C13, C15	C12, C16	2.04-2.09	26.52
15	1.26- 1.34 (2H, m, H15)	25.64	C14, C16	C13, C17	1.32	26.1
16	1.26- 1.34 (2H, m, H16)	24.61	C15, C17	C14, C18	1.32	26.08
17	1.26- 1.34 (2H, m, H17)	22.61	C16, C18	C15, C19	1.32	21.48
18	0.84-0.86 (3H, t, H18)	14.26	C17	C16	0.96	14.64

2.6 Conclusion

After identifying five promising medicinal plants through an ethnomedical approach, aerial parts were collected from the Southwest region of Saudi Arabia. An established process was

followed to extract plants with the cold maceration technique. Next, a bioassay-guided fractionation approach was employed to fractionate *A. canariense*, *R. stricta*, and *T. macropterus* with several chromatographic techniques, including liquid-liquid partitioning, silica column chromatography, and thin-layer chromatography. Two compounds were successfully isolated with the aid of preparative TLC and identified from *A. canariense* and *R. stricta*. Finally, spectroscopy techniques, NMR and MS completed the structural elucidation of isolated compounds.

Chapter 3: The Effect of Plant Extracts on Human Skin Keratinocyte Cell Proliferation and Survival

3.1 Introduction

Despite widespread recognition as being safe, not all medicinal plants lack the risk of adverse reactions or toxicity and various medicinal plants' chemical constituents could result in varying toxicity. Even low-toxicity extracts from herbal medicines have the potential for toxicity, if used in large doses or for prolonged periods (Ferreira-Machado, 2004; Mounanga et al., 2015). Different factors influence the toxicity of a particular plant, including the plant parts utilised, the amount consumed, the concentration of secondary metabolites, the duration of exposure, genetic variations within the species, climate, and soil. In the light of this, it is evident that medicinal plants should be used carefully and that toxicological studies should be undertaken to expand understanding of medicinal plants used in local communities (Celik et al., 2012).

In vitro cell culture anti-proliferative and cytotoxicity assays could be utilised to examine and evaluate plant extracts, assess the safety of the extracts for use on a normal host cell line, and ensure the selectivity of the extracts in terms of their pharmacological action (Cos et al., 2006). The site of administration and delivery method will influence the cell type chosen for utilisation. For example, hepatocyte cell lines, such as HepG2, are evaluated with orally administered drugs in development since the liver is the principal site of toxicological effects following systemic administration due to first-pass metabolism (Krithika et al., 2009). In contrast, the spontaneously transformed HaCaT human keratinocyte cell line is commonly utilised for evaluating topical agents (Rezk et al., 2015).

Preliminary experiments involving the human skin-immortalized keratinocytes (HaCaT) cell line were conducted to develop a topical product for treating infections. The immortalization of the HaCaT cell line was first achieved through the reactivation of the telomerase enzyme,

which renders HaCaT cells capable of undergoing more than 140 passages (Boukamp et al., 1988; Bachor and Boukamp, 1996). The HaCaT cell line has also been widely used as a robust model for demonstrating the anti-proliferative activity of many agents. Plants of the Brazilian Cerrado biome, *Galenia Africana*, *Picea abies L.* and *Fagus sylvatica L.* are some examples of plant extracts to have been evaluated against the HaCaT cell line (Elias et al., 2015; Coşarcă et al., 2019; Ndlovu et al., 2021).

The evaluation of cell viability is one of the cornerstones of cytotoxicity studies. Dye exclusion assays are commonly used to assess cells' viability such that a viable cell with an intact cell membrane can repel these dyes. In contrast, dead cells allow the stain to enter, making viable cells visible in suspension. Trypan blue dye has been extensively used to determine the viability of cells in a given population; some of its advantages include its simplicity, usefulness in evaluating cell membrane integrity, and low cost. However, in this method, cells are counted using a hemacytometer, which increases the possibility of counting errors, is time demanding, and makes it challenging to analyse many samples concurrently. These drawbacks, together with the huge number of plant extracts to be investigated (23 samples), necessitated the use of another colorimetric assay, the 3-(4,5-dimethylthiazol-2-yl)-2,5-diphenyl tetrazolium bromide reduction (MTT) (Adan et al., 2016).

Due to its simplicity and sensitivity, the MTT test is one of the most commonly used assays for assessing the cell proliferation activity of plant extracts against a wide variety of cell lines. It is also considered to be a suitable assay for a 96-well plate screening. When mixed with PBS, the salt of MTT results in a yellowish solution that, upon reduction using dehydrogenases and other reducing agents within metabolically active cells like nicotinamide adenine dinucleotide (NADH) coenzyme and ascorbic acid, will turn the colour of the solution into a non-water-

soluble violet-blue formazan (Figure 33). The formed formazan then draws needle-shaped crystals from the cells through exocytosis; the activity of the dehydrogenases enzyme in the viable cells will be directly proportional to the quantity of the formazan.

As MTT determines a single marker, it is often helpful to supplement such data with others to provide a more unequivocal result. In order to differentiate between the anti-proliferative action of plant extracts and necrotic cell death, additional cytotoxicity experiments were conducted using Fluorescence-Activated Cell Sorting (FACS) and Confocal Laser Scanning Microscopy (CLSM) (Mosmann, 1983; Liu et al., 2002; Stockert et al., 2012).

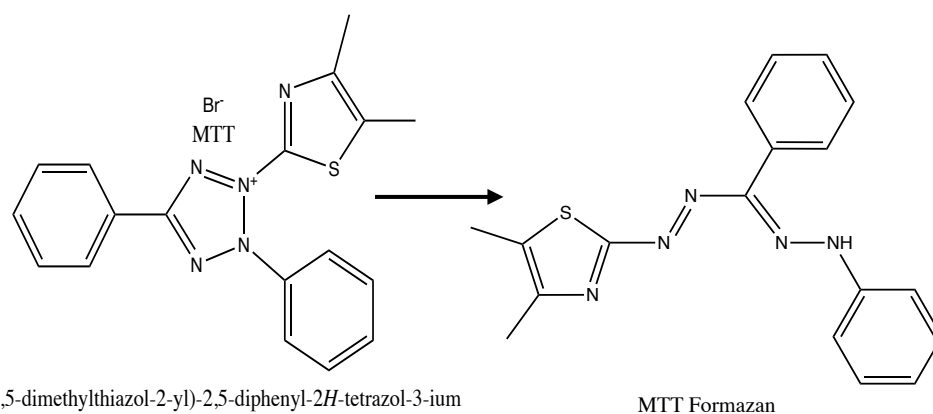


Figure 33 MTT reduction reaction in metabolically active cells will result in the formation of formazan (Stockert et al., 2012)

Numerous approaches for determining the cytotoxicity of plant extracts were explored, one of which used FACS to assess the cytotoxicity of plant extracts and other agents (Oyama and Masuda, 2001; Lau, 2008; Kuete et al., 2013).

One of these methods to test the cytotoxicity of drugs using FACS utilizes a dual staining approach with two fluorescent dyes, fluorescein diacetate (FD) and propidium iodide (PI). FD, a non-polar dye that can penetrate an intact cell membrane and undergo hydrolyzation through

intercellular esterase to produce the polar compound fluorescein, will accumulate inside the cell and produce strong green fluorescein upon excitation; cells with a damaged membrane or with low metabolic activity will not be able to do so. PI, on the other hand, will pass through the damaged cell membrane and interact with the DNA and RNA of the cell to produce red fluorescein within dead cell nuclei. Using these dyes yielded more precise quantification of viable and non-viable cells, allowing for a more comprehensive knowledge of the cytotoxicity of the studied plant extracts (Jones and Senfet, 1985; Berglund et al., 1987).

Using CLSM, the cytotoxicity of a specific plant extract was confirmed qualitatively. This method has been extensively used in cell biology and microbiology. The double staining approach using PI/FD was then conducted to identify the viable and non-viable cells. For example, one study utilised the PI/FD double staining method to stain dentin infected with *Enterococcus faecalis* to distinguish between live and dead bacteria (Zapata et al., 2008), while another study used the method to evaluate the presence of viable chondrocytes in osteochondral articular cartilage (Ohlendorf et al., 1996).

3.2 Chapter Aim and Objectives

This chapter aims to determine the effects of plant extracts on the viability and cytotoxicity towards the keratinocyte (HaCaT) cell line, considering the following objectives:

- To establish the optimal HaCaT cell growth pattern and time using a growth curve study to be used in subsequent experimental work.
- To optimize an assay to investigate the pro or anti-proliferative activity of plant extracts through MTT cell viability assay.

- To optimize an assay for the study of the cytotoxic activity of plant extracts using the FD/PI dual staining approach with FACS.
- To achieve qualitative confirmation of plant extracts' cytotoxic effect on an HaCaT cell line by using a PI/FD dual staining approach with PI/FD and collecting images via CLSM.

3.3 Materials

Unless otherwise specified, all materials were purchased from ThermoFisher Scientific (Loughborough, UK). In addition, a solution of phosphate-buffered saline (PBS) was made by adding one tablet of PBS to 200 mL of deionized water. In this study, Dulbecco's Modified Eagle Medium (Gibco DMEM 1X) contains 4.5 g/L glucose and 0.11 g/L sodium pyruvate stored at 4°C was utilised, and the antibiotic employed was composed of 100 µg/ mL streptomycin sulphate, 0.25 µg/mL amphotericin B, and 100 U/mL penicillin G sodium.

24- and 96-well microplates (flat bottom, transparent, sterile, tissue culture-treated surface, polystyrene plate), and fluorescence-activated cell sorting (FACS) tubes were acquired from Sarstedt (Leicester, UK), while Gibco foetal bovine serum (FBS), thiazolyl blue tetrazolium bromide (MTT) powder, and dimethyl sulfoxide DMSO were acquired from Sigma-Aldrich. FD and PI were obtained from Sigma-Aldrich Company Ltd. Before use, PBS solution and all plastic materials, including tips and reagent reservoirs, were sterilized via an autoclaving process at 123°C for 15 min. All equipment required for the experiments were kept and stored in the tissue culture laboratory to minimize contamination. A microtiter plate reader was employed to determine absorbance (Infinite 200 Pro, Tecan, Switzerland). An aliquot of

HaCaT cells was donated by Amal Al-Rashidi, a PhD student at the School of Pharmacy and Pharmaceutical Sciences, Cardiff University.

3.4 Methods

3.4.1 Preparation of the Stock Solution of Extracts

Stock solutions of 5 mg/mL of plant extracts were made by dissolving 50 mg of plant extracts in 100 μ L of 90% methanol, and followed by the addition of 9.9 mL of DMEM to prepare the final volume of 10 mL in preparation for cytotoxic assay evaluation. The final methanol concentration was 1%, and stock solutions were filtered, sterilized, and stored at 4°C. The plant extracts' final stock concentration was 5 mg/mL.

3.4.2 Culturing of HaCaT Cell Line

A Heraeus class II safety cabinet was used to carry out all cell culturing procedures. Sterile conditions were kept through regular cleaning and spraying of the hood with 70% ethanol, both before and after use. Furthermore, all materials were decontaminated with 70% ethanol before being placed in the hood. The safety cabinets, water baths, and incubator were cleaned every week.

3.4.2.1 Cell Culture Medium Preparation

FBS 500 mL was stored at -20 °C to preserve its protein content and prevent the formation of turbidity. Serum aliquots were prepared by thawing the FBS at 2-8 °C overnight; the serum was then heated in the water bath at 56 °C for 30 min to render the complement proteins inactive. Finally, serum aliquots were stored at 2-8°C for 2-4 weeks for short-term use and at

-20 °C for long-term use for up to 6 months. Serum-containing culture medium (CCM) was made using DMEM, 10% heat-inactivated FBS, 1% antibiotics, and 1% L-glutamine. In a 75 cm² culturing flask, 1.5x10⁵ HaCaT cells were seeded, and the flask was kept in an incubator at 37 °C, 5% CO₂, and 95% humidified air. Every 24 to 48 h, the medium was changed with a fresh CCM. The cells were inspected under a light microscope at the ideal magnification to detect the cells (CK2 Inverted Microscope, Olympus Ltd., Middlesex, UK) for any sign of contamination. A water bath at 37 °C was used to warm up the media and solutions for about 15 min.

3.4.2.2 HaCaT Cell Passaging and Counting

When the cell density in a given 75 cm² tissue culture flask reached 70%-90% confluence, a sub-culturing process was used to maintain continuous cell growth and bring cells to the desired density. During this process, the medium was discarded before the cells were washed with 10 mL of PBS; all traces of PBS were removed from the cells to facilitate their detachment from the flask's surface. Next, 3 mL of proteolytic enzyme trypsin-EDTA was added; this enzyme cleaves proteins at the carboxyl position, thus breaking down the essential amino acids arginine and lysine, while EDTA acts as a calcium chelating agent. To achieve full detachment, cells were placed in the incubator for approximately 10 min, after which the attached cells were dislodged by tapping the side of the flask with the palm. Six mL of complete culture medium was added to render the trypsin inactive prior to centrifuging the suspension for 5 min at 1500 rpm.

The supernatants were then removed, and the HaCaT pellets resuspended with 10 mL of complete culture medium CCM. To determine viable cell count in a HaCaT cell suspension,

10 μL of cell suspension were combined with 10 μL of trypan blue dye. The mixture (10 μL +10 μL) was then injected into the haemocytometer chamber (ThermoFisher Scientific). Following the staining procedure, viable cells with intact cell membranes will reject the dye while non-viable cells with damaged membranes will not. thus, only transparent cells located on the squares from one to four were counted using a light microscope at x100 magnification (Figure 34). Finally, cell suspensions were diluted according to the desired cell counts.

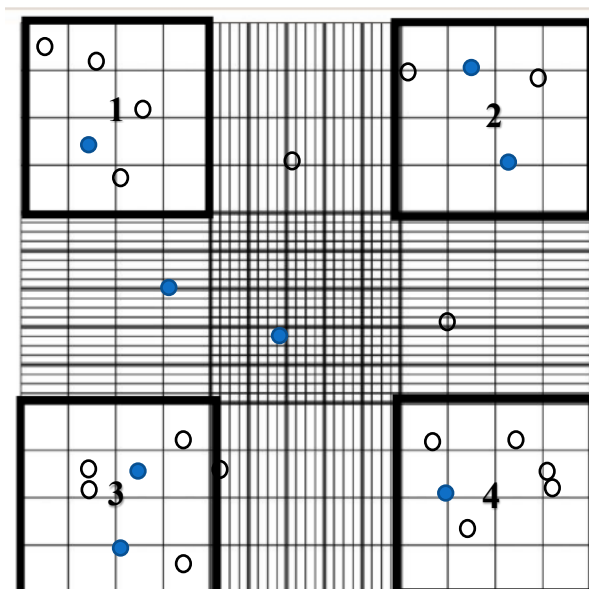


Figure 34 Illustration of a haemocytometer's gridded areas: Transparent cells inside the borders of gridded squares labelled from one to four were counted, and the average was multiplied by two to account for the dilution factor of trypan blue

3.4.2.3 HaCaT cell Freezing and Thawing

To preserve the cells for future work and ensure a continuous supply of HaCaT cells with low passages, a process of freezing the cells was conducted. First, HaCaT cells underwent passaging, and the pellets were suspended in 10% DMSO and 90% FBS before being transferred to cryovials; the DMSO acted as a cryoprotective agent that prevented the formation of ice crystals, protecting the cells from any damage. Then, with the aid of a freezing container

(Mr. Frosty, Sigma-Aldrich), containing isopropanol, the cell mixture was gradually cryopreserved to -80 °C at the rate of -1°C per min. Finally, the cell mixture was placed in liquid nitrogen at -196 °C after 24 h.

When needed, cryovials containing cells were retrieved from the liquid nitrogen and placed in a water bath at 37 °C; 9 mL of CCM was added to the cell mixture before 5 min centrifugation at 1500 rpm. The supernatant was removed, and 10 mL of fresh CCM was added to the pellets, which were then placed in a tissue culture flask and kept in an incubator set to 37 °C, 5% CO₂, and 95% relative humidity.

3.4.3 Cell Growth Study

A growth study curve was determined for this specific cell line to assess cell growth time, determine the pattern of the HaCaT cells, identify the time required to double the number of cells, and find the optimum cell density achievable by this cell line. Therefore, after trypsinization, the haemocytometer was utilised to count the cells. The cells were then diluted with CCM to a density of 2×10^4 cells per mL. Next, 1 mL of the suspension was added to each well of three 24-well plates. Twenty-four h after placing the plates in the incubator at 37 °C, 5% CO₂, and 95% relative humidity, the initial seeding time was recorded. The next day, at the same time, cell counts were performed; the medium from each well was removed before the wells were washed twice with 1 mL of PBS per well. After incubating the plates for 5-10 min, the cells were detached from the flask using 100 µL of trypsin-EDTA. Trypsin activity was neutralized by adding 1 mL of CCM before transferring the suspension to a marked Eppendorf; the suspension in the vials was mixed well by pipetting up and down three times.

Finally, the cell count was measured two times every 24 h for 6 days, using a haemocytometer; the media was replaced every 3 days. This experiment was carried out 3 times and in triplicates.

3.4.4 MTT Assay (3-(4,5-dimethylthiazol-2-yl)-2,5-diphenyl tetrazolium bromide reduction)

Five plant extracts were evaluated for their ability to inhibit the proliferation of HaCaT keratinocytes using the MTT assay, which is widely recognised as a standard cytotoxic and anti-proliferative tool for evaluating various compounds. Mosmann introduced it as a quantitative colorimetric method to detect viable mammalian cells (Mosmann, 1983). Following the trypsinization procedure, the cells were counted with a haemocytometer before being diluted with CCM. Density was adjusted to 5×10^4 cells per mL, and 100 μ L of cells and CCM solution were added to four 96-well plates; experimental plates were labelled with the dates, and day 1, day 3, day 5 and day 7, before being placed in the incubator.

On the next day, the CCM in each plate was changed with 100 μ L of serum-free media before placing the plates in the incubator, and the sample treatment medium was made with DMEM, 1% FBS, antibiotics, and L-glutamine. On the third day, the serum-free media were discarded from the wells, and 6 replicates of each treatment medium concentration were added to the same plate. The treatment medium was replaced daily. After 24 h (day 1 of MTT), thiazolyl blue tetrazolium bromide (MTT) powder was prepared with PBS. The MTT solution was filtered through a 0.2 μ m sterile syringe filter, and 25 μ L was added to the day one plate before the plate was stored in the incubator at 37 °C, 5% CO₂, and 95% relative humidity for 4 hours. The treatment media and MTT were removed from each well, and the addition of 100 μ L DMSO solubilized the formazan crystals. The plates were then covered in clingfilm and

incubated for 30 min. The absorbance was determined using a microtiter plate reader (Infinite 200 Pro, Tecan Trading, Männedorf, Switzerland) at 570 nm. The exact process was repeated for MTT plates at days 3, 5, and 7. The MTT experiment was conducted in triplicate for every plant extract, and concentration was examined. The following equation was used to calculate the percentage of cell growth for plant extracts that were tested:

$$\text{Cell Growth Percentage} = 100 \times \frac{\text{(the mean absorbance of treatment wells)}}{\text{(the mean absorbance of control wells)}}$$

IC₅₀ values (the concentration that inhibits 50% of the growth of the HaCaT cells) were determined using GraphPad Prism 7.0 (GraphPad Software Inc., San Diego, CA). Data from the MTT experiment were presented as a percentage against each plant extract concentration.

3.4.5 Fluorescein Diacetate and Propidium Iodide-based Fluorescence-Activated Cell Sorting (FACS) Analysis

HaCaT cells were counted and diluted with serum-containing culture media to reach a cell density of 5×10^4 cells/mL for the FACS investigation. First, 1 mL of cell suspension in culture media was added to a 24-well plate, and overnight incubation was maintained at 37 °C, 5% CO₂ and 95% humidity. The next day, the culture media was discarded from each well and replaced with various concentrations of each plant extract, using the same concentration ratio as the MTT investigation (Section 3.4.4). For each experiment, 5 separate controls were constructed as follows:

1. Vehicle control: serum-containing culture media with 1% methanol.
2. A control of untreated, unstained cells was added to select the target population and adjust the FACS.

3. A control of untreated cells was stained with FD to detect viable cells.
4. A control of untreated cells was fixed with 200 μ L of ethanol for 10 min and stained with PI to detect non-viable cells.
5. A control of untreated cells stained with PI and FD to calibrate dual stains.

After incubation for 24 h, the media from every well was recovered in Eppendorf tubes to examine the presence of dead cells. After centrifuging at 500 g for 5 min, the supernatant was removed from the tubes. Cells attached to the surface of the 24-well plate were washed multiple times with 1 mL PBS, prior to adding 200 μ L of trypsin and incubating for 10 min. The trypsin activity was neutralised by the addition of 800 μ L of culture media. Each well's cell suspension was transferred to its matching Eppendorf tube, then centrifuged at 500 g for 5 min. The supernatant was discarded, and the cells were washed multiple times with 1 mL PBS to eliminate the culture media.

The cell pellets were dislodged by shaking the tubes carefully. In each Eppendorf tube, 300 μ L of an FD solution (10 μ g/mL in 0.2% DMSO/PBS) and a PI solution (5 μ g/mL in PBS) were added. Cells were carefully mixed and kept in the dark for 5 min, finally stored on ice for flow cytometry analysis within 1 h (FACSCalibur, Becton Dickinson, Heidelberg, Germany). FACS system was calibrated using the previously discussed controls, and the fluorescence generated was analysed on two distinct channels, one dedicated to the FD and another to the PI. To place the cells in the optimal region, the FACS threshold and voltage were modified. It was set to collect 20,000 events. The FACS assay was performed in triplicate for every plant extract and concentration evaluated. The following equation was utilised to calculate the percentage of FD/PI-stained cells in plant extracts:

$$\text{FD/PI-stained cells percentage} = 100 \times \frac{(\text{Geo Mean for FD/PI in treatment wells})}{(\text{Geo Mean for FD/PI in control wells})}$$

3.4.6 Fluorescein Diacetate and Propidium Iodide-based Confocal Laser Scanning Microscopy Analysis (CLSM)

Using Confocal Microscopy, viable and non-viable cells were qualitatively validated using the PI/FD dual staining technique. After trypsinization, the cells were counted using a haemocytometer, and the cell suspensions were diluted with CCM. The density was adjusted to 10×10^4 cells per mL, and 2 mL of cell suspension was added to each cell culture dish (MatTek 35 mm Dish, 1.5 Coverslip, 14 mm Glass Diameter, MatTek, Ashland, USA), before the plates were kept overnight in an incubator at 37 °C, 5% CO₂, and 95% humidity levels.

Media in each well was discarded and replaced using treatments at the highest concentration evaluated previously in the MTT and FACS assays. The next day, the media was gently discarded from each plate and replaced with a solution of 600 µL of an FD (10 µg/mL in 0.2% DMSO/PBS) and PI (5 µg/mL in PBS). The cells were mixed gently and stored in the dark for 10 min before getting rinsed twice with 1 mL PBS for every wash. Finally, 1 mL of the imaging medium (DMEM, Phenol red-free) was applied to each dish, before image collection utilising CLSM with a Leica SP5 Laser Scanning Microscope, fitted with a 65x oil-immersion objective. The laser was adjusted to 488 nm for FD and 543 nm for PI.

Gain and offset parameters were optimised for each experiment to ensure optimal imaging. The medical imaging software, ImageJ, was used to analyse the CLSM-collected images, which were separated into distinct channels and then combined using the software. The thresholding and 8-bit conversion enabled us to optimise the precision of each image.

3.4.7 Statistical Analysis

The acquired data were statistically analysed using GraphPad Prism 7.0a (GraphPad Software Inc., San Diego, USA); all data is reported as the mean \pm standard error (SE), and all experiments were conducted three times each. The means and standard errors were calculated using Excel (Microsoft) software. The statistical analysis was performed using a one-way analysis of variance (ANOVA) Dunnett post-test to assess the significance of the difference between the means of the control and experimental groups. The statistically significant difference between groups was determined using Tukey's post-test, with a threshold of $p < 0.05$ deemed to indicate statistical significance.

3.5 Results and Discussion

3.5.1 HaCaT Cell Growth

The HaCaT cell line, like other cell lines, goes through four distinct growth phases. The first is the lag phase; cells will not proliferate at this stage but will adapt to culturing conditions and grow in size. The duration of this phase depends on several factors, including seeding density, time of culture, and cell growth pattern. Then, in the logarithmic (log) phase, cells are at their most viable, meaning that their density increases exponentially at this point. This phase is considered the most suitable for experimental work and determining the cells' doubling time. Next, in the stationary (plateau) phase, the cells' proliferation rate decreases as they reach confluence; cells will be in close contact with adjacent cells, leading to a smaller surface area in the medium. These conditions, along with the depletion of nutrients and the accumulation of catabolite, will reduce cell growth; the percentage of cells in their viable stage will be 0-

10%. Finally, the death phase is the last stage of the cycle, during which the shortage of nutrients will cause cell death.

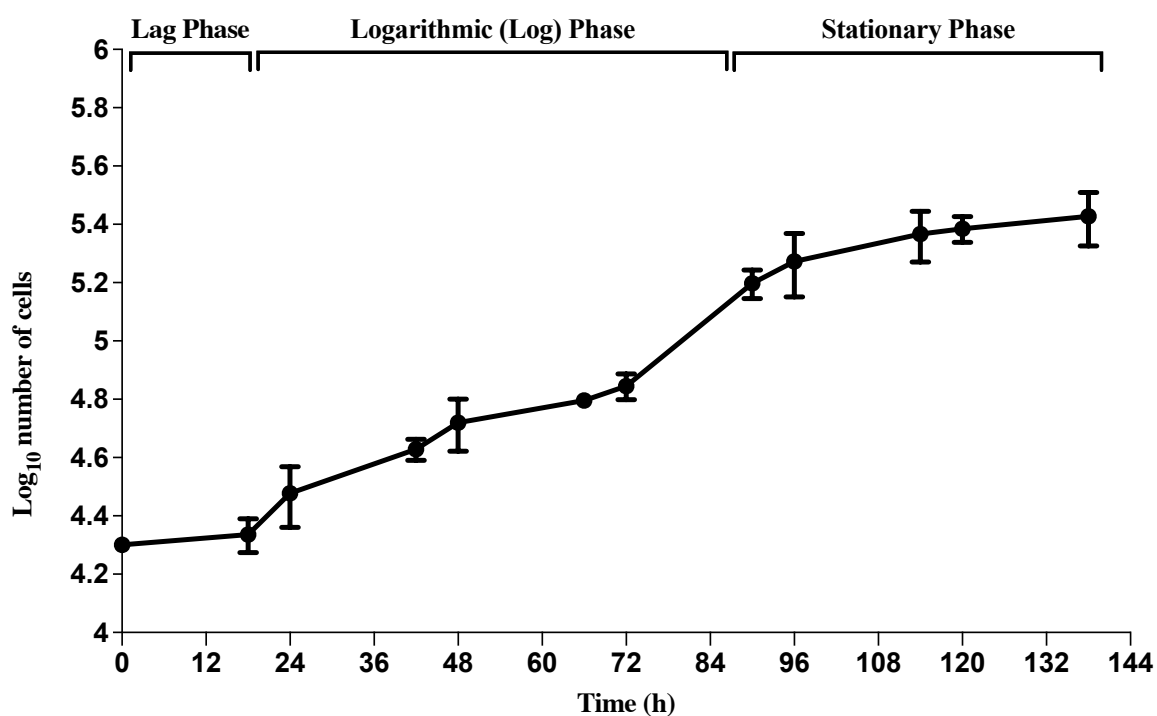


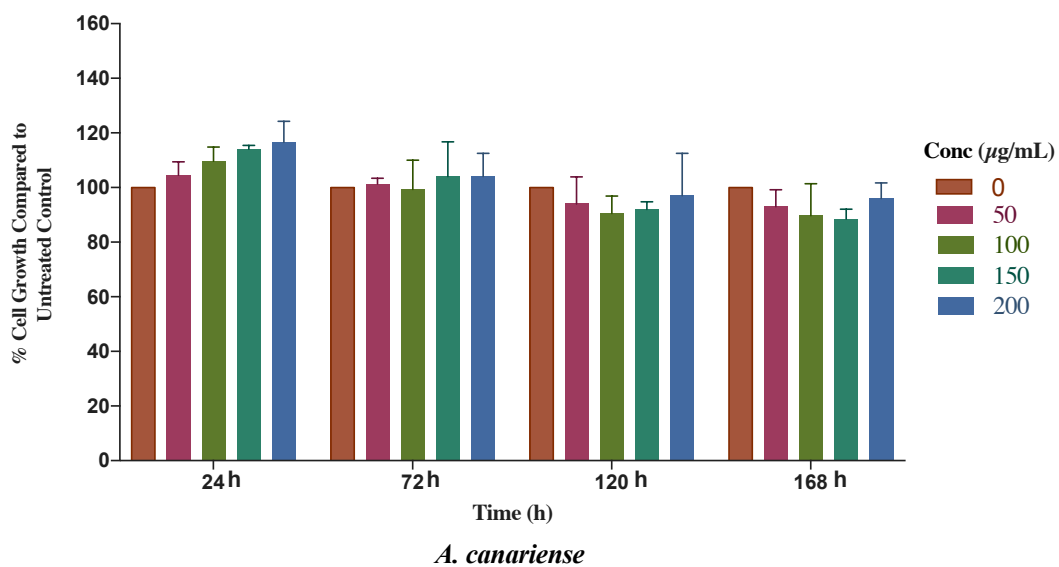
Figure 35 HaCaT growth curve with normal culturing conditions (mean \pm SE). Experiments were done in three replicates across three independent experiments

The log of a given number of cells was plotted against time to determine its lag phase, the time required for it to reach 80-100% confluence and cover most of the plate surface, and the population doubling time for the HaCaT cells (Figure 35). The linear correlation curve of the log phase was used to estimate the doubling time of the population, which was found to be 35 h. Lag time was calculated from the graph; the result was 18.5 h. Overall, it took about 4 days for the HaCaT cells to reach the stationary phase.

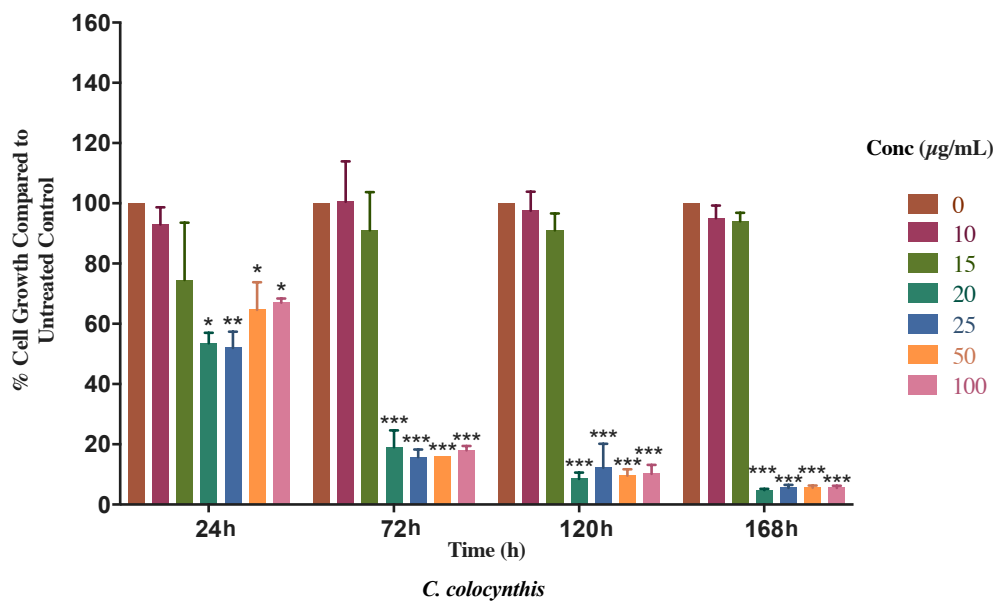
3.5.2 Evaluating the Effects of Plant Extracts on the Viability of HaCaT

Different concentrations of plant extracts were used for the investigation.; *A. canariense*, *M. crassifolia*, and *T. macropterus* were evaluated at 200, 150, 100, and 50 $\mu\text{g/mL}$, while *C. colocynthis* was investigated at values of 100, 50, 25, 20, 15, and 10 $\mu\text{g/mL}$. The concentrations of *R. stricta* were 100, 75, 50, 25, and 12.5 $\mu\text{g/mL}$. In addition, non-treated controls with vehicle-only (1% methanol, 1% FBS, DMEM) were introduced for comparative reasons. Furthermore, CCM (DMEM/1%FBS) was added as a control for normal cell proliferation, revealing that adding of 1% methanol did not significantly inhibit the proliferation of HaCaT cells (*data not shown*). Preliminary results (*data not shown*) from a three days MTT assay suggested that several plant extracts, even at a high concentration, failed to achieve the 50% inhibition of cell proliferation. Consequently, the MTT assay was extended to 7 days, and the average absorbance of each extracts at different concentrations was measured at 24 h, 72 h, 120 h, and 168 h. For every concentration and time point, the cell growth percentage was determined and compared to the vehicle controls (Figure 36 A-E).

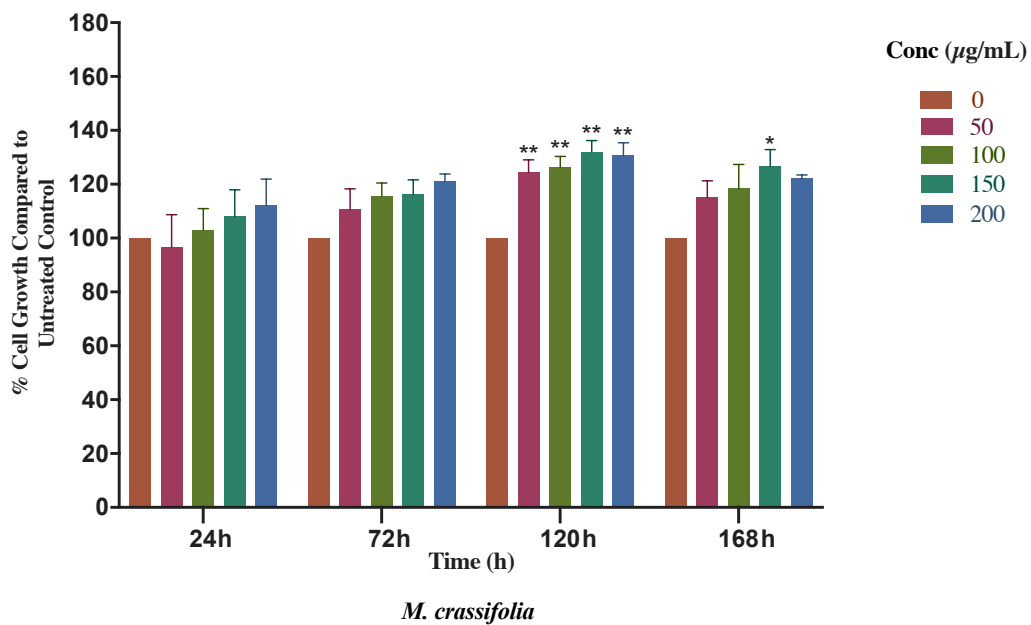
A)



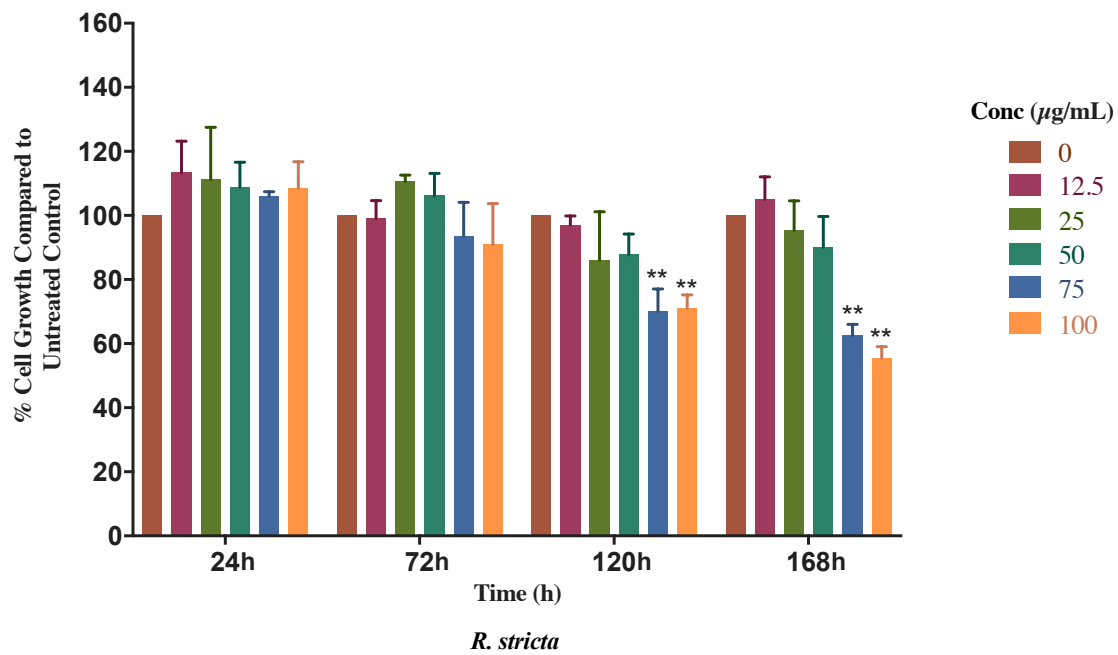
B)



C)



D)



E)

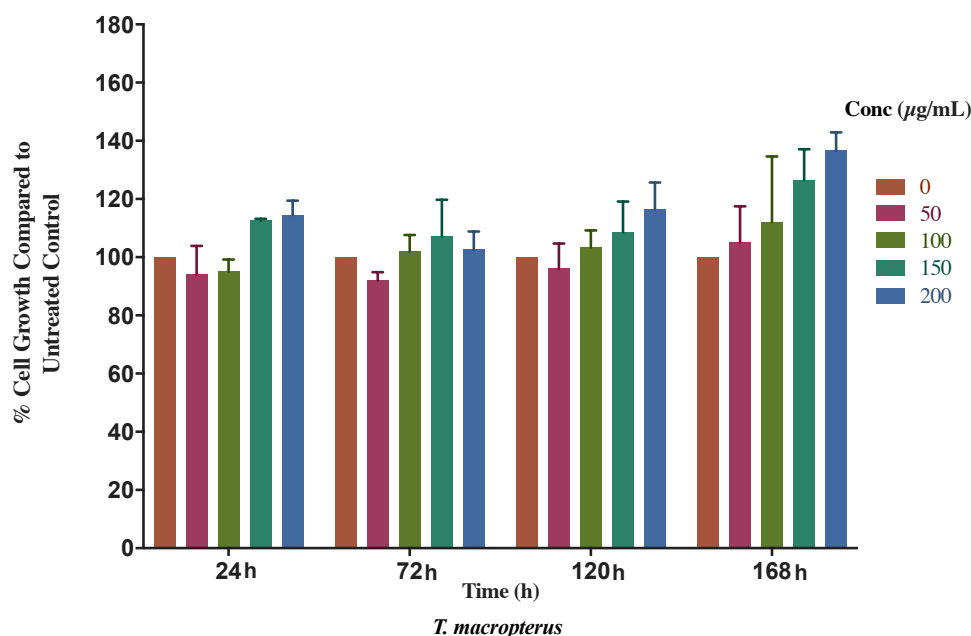


Figure 36 Proliferation percentage of HaCaT cells treated with (A) *A. canariense* extract (200, 150, 100, and 50 µg/mL in CCM), (B) *C. colocynthis* extract (100, 50, 25, 20, 15, and 10 µg/mL in CCM), (C) *M. crassifolia* extract (200, 150, 100, and 50 µg/mL in CCM), (D) *R. stricta* extract (100, 75, 50, 25, and 12.5 µg/mL in CCM), (E) *T. macropteris* extract (200, 150, 100, and 50 µg/mL in CCM), at 24 h, 72 h, 120 h, and 168 h, compared to untreated control (mean ± SE). Three separate experiments were conducted to acquire findings. Analysis of statistically significant differences between treated cells and untreated controls via Dunnett post-test (* $p < 0.05$, ** $p < 0.01$, * $p < 0.001$)**

Compared to controls, *A. canariense* and *T. macropteris* had no impact on HaCaT cell proliferation. However, *T. macropteris* extract enhanced proliferative activity at 200 and 150 µg/mL concentrations after 5 and 7 days of treatment. This stimulating effect was subsequently insignificant ($p > 0.05$), and neither plant extract exhibited anti-proliferative activity toward HaCaT cells.

On the other hand, cells treated with *C. colocynthis* at concentrations of 100, 50, 25, and 20 µg/mL demonstrated a significant dose-dependent reduction of cell growth after 24 h, with potent inhibition of cell growth occurring after 72 h of treatment ($p < 0.001$) (Figure 36B), suggesting that *C. colocynthis* may elicit a cytotoxic activity towards HaCaTs, further

investigation are required to determine the cytotoxicity of this plant against HaCaT cells. When evaluated at concentrations of 100 and 75 $\mu\text{g}/\text{mL}$, *R. stricta* demonstrated a delayed but significant suppression of cell proliferation after 5 and 7 days of treatment ($p < 0.01$) (Figure 34D). *M. crassifolia* was the only used plant extract that resulted in a significant increase in cell proliferation in the concentration range of 200 to 50 $\mu\text{g}/\text{mL}$ at 120 h ($p < 0.01$). This stimulation effect continued at 168h, though it was deemed to be non-significant ($p > 0.05$), except in cells treated with a concentration of 150 $\mu\text{g}/\text{mL}$ ($p < 0.05$) (Figure 36C).

The concentration needed to suppress 50% of HaCaT cell growth (IC_{50}) for *C. colocynthis* and *R. stricta* was determined using a graph with a best-fit line where the R^2 value was more than 0.90 (Table 13). *C. colocynthis* inhibited cell growth with an IC_{50} of 17.32 $\mu\text{g}/\text{mL}$ after 5 days of treatment and 16.91 $\mu\text{g}/\text{mL}$ after 7 days. During the last days of treatment, *R. stricta* demonstrated delayed inhibitory action, with an IC_{50} of 175 $\mu\text{g}/\text{mL}$ after 5 days and 105.3 $\mu\text{g}/\text{mL}$ after 7 days. To the best of our knowledge, this is the first study to investigate the cell proliferation activity of selected plant extracts using the HaCaT cell line.

Table 13 The IC₅₀ of *C. colocynthis*, *R. stricta*, *A. canariense*, *M. crassifolia* and *T. macropterus* as measured by the MTT test after five and seven days of treatment using the best-fitting line. Three separate experiments were conducted to acquire findings

Plant Extract	IC ₅₀ µg/mL	
	Day 5	Day 7
<i>C. colocynthis</i>	17.32	16.91
<i>R. stricta</i>	175	105.3
<i>A. canariense</i>	IC ₅₀ > 200	IC ₅₀ > 200
<i>M. crassifolia</i>	IC ₅₀ > 200	IC ₅₀ > 200
<i>T. macropterus</i>	IC ₅₀ > 200	IC ₅₀ > 200

3.5.3 Evaluating the Cytotoxic Effect of Plant Extracts on HaCaT

Utilising FACS, CLSM, and dual staining with PI and FD, cytotoxic analyses of the plant extracts were conducted to validate the previously reported HaCaT cell proliferation suppression in the MTT assay was attributable to the anti-proliferative action of the plant extract rather than induction of cell death. Throughout the FACS study, the percentages of PI-stained cells and FD-stained cells, compared to the controls, were determined for plant extracts at a concentration specified by the MTT experiment.

3.5.3.1 Determining Cytotoxicity Using Fluorescence-Activated Cell Sorting

To investigate the cytotoxic effect of plant extracts at different concentrations, PI/FD dual staining FACS analysis was conducted; the gating sequence of the flow cytometer consisted of the following procedure:

- 1- Twenty thousand cells were aspirated into the flow cytometer from the unstained, untreated control. To identify the optimal population and confirm the elimination of any debris, forward scatter (FSC) was plotted versus side scatter (SSC) (Figure 37). The P1 gate-selected population was then utilised for subsequent gating of PI- and FD-stained cells.
- 2- A scatter plot of PI-h against FD-h, with PI-stained cells gated in the upper left region (Figure 38) and FD-stained cells gated in the lower right region of the plot (Figure 39).
- 3- The PI-stained red cells in the upper left region of the plot were differentiated from the FD-stained cells in the lower right region of the plot using a non-treated, stained control.

PI-stained dead cells were retrieved from the culture media, and adherent cells were recovered from the well. The percentage of PI-stained cells (dead cells) corresponding to untreated controls is shown.

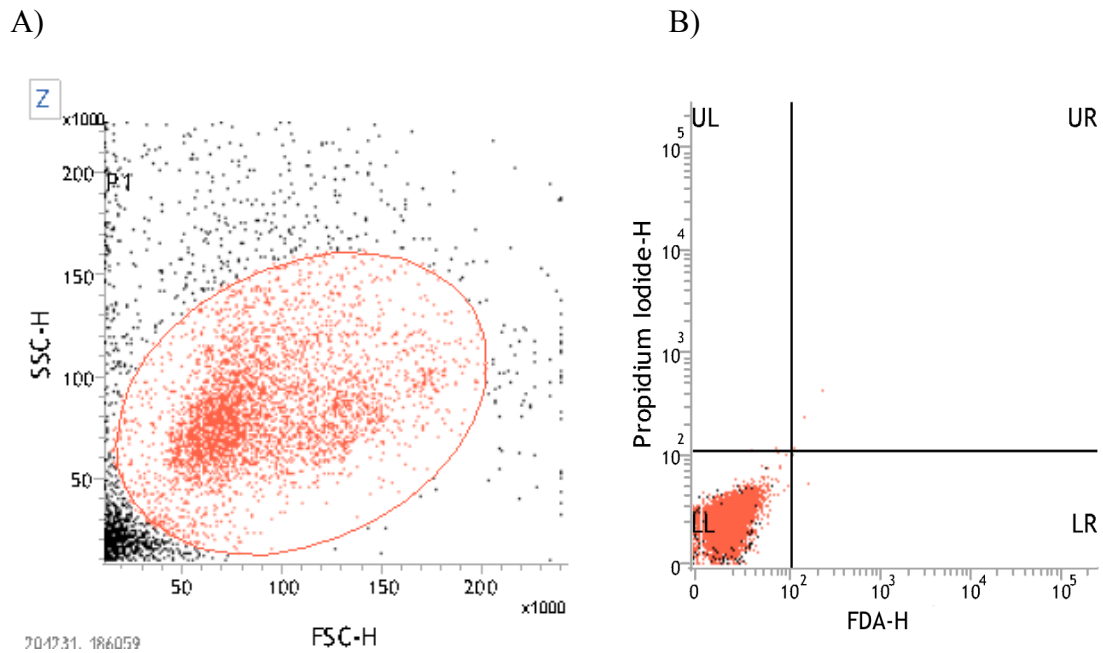


Figure 37 Red dots represent population 1 (P1) cells chosen from the untreated, unstained control. (A) dot plot of FSC against SSC, and (B) dot plot of PI-H against FDA-H; non-stained cells are shown in the lower left quadrant

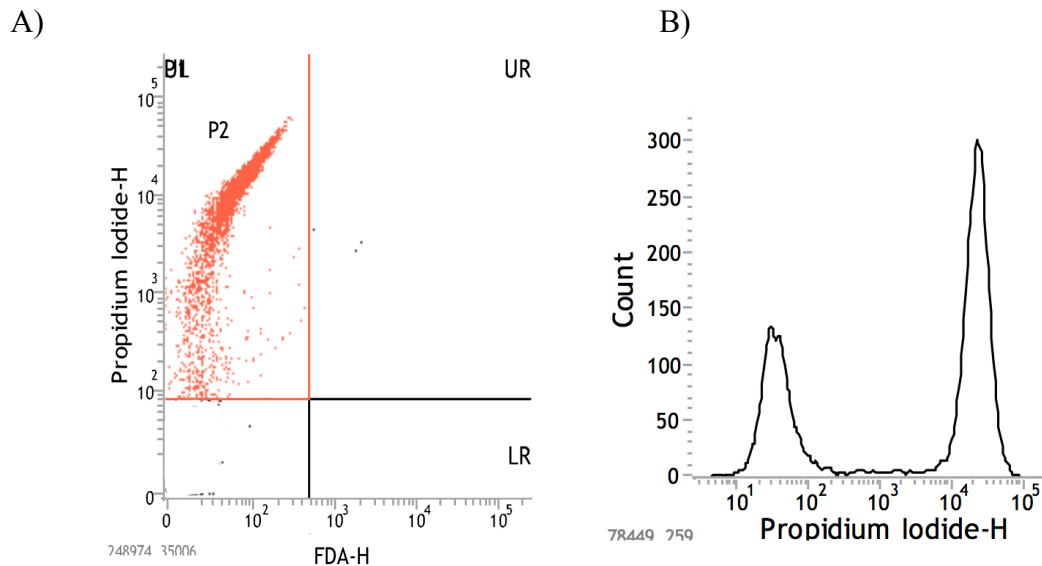


Figure 38 Defining the area of PI-stained cells utilising FACS analysis. (A) The PI stain will collect within the nucleus of dead cells and emit a red fluorescence, which can be seen as red spots in the upper left region. (B) Histogram for PI-H

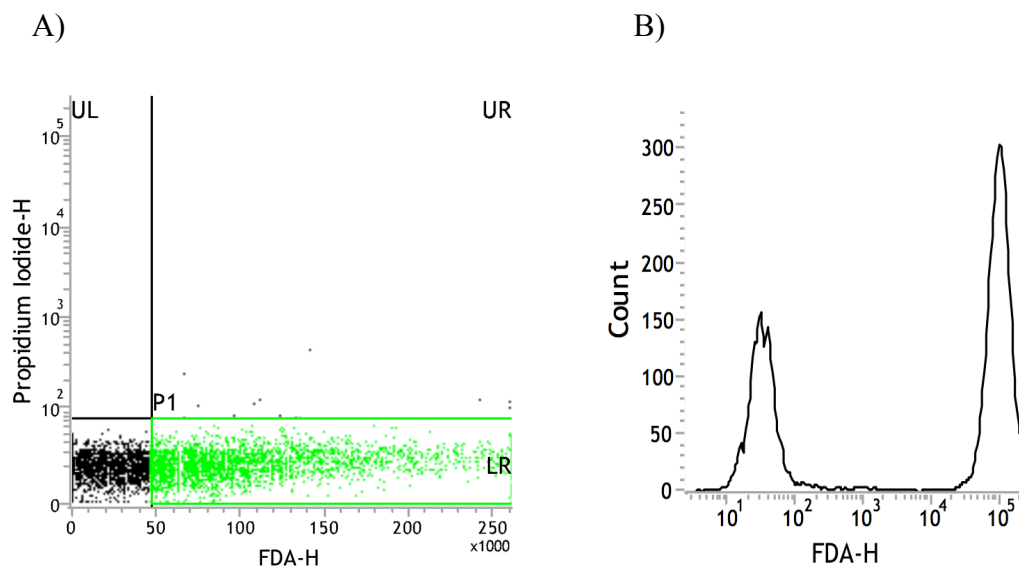
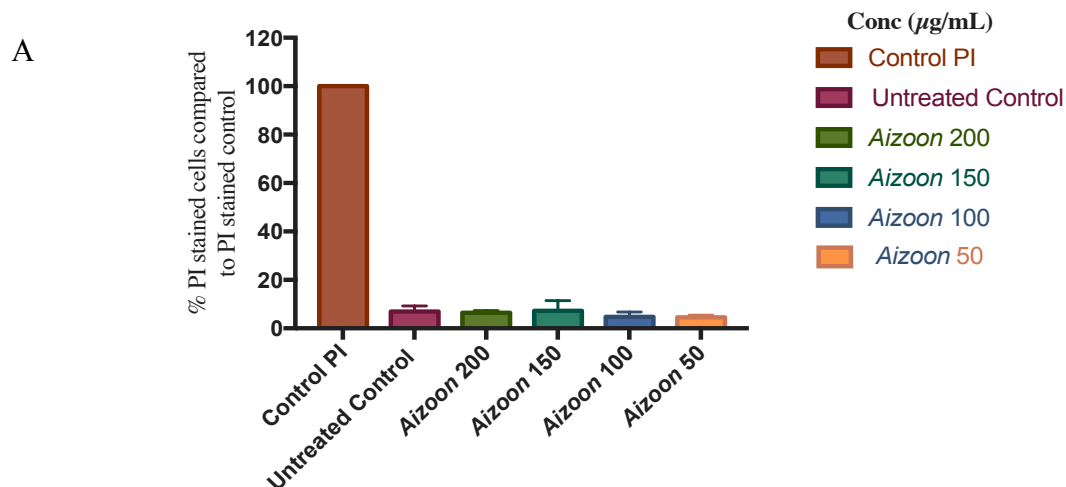
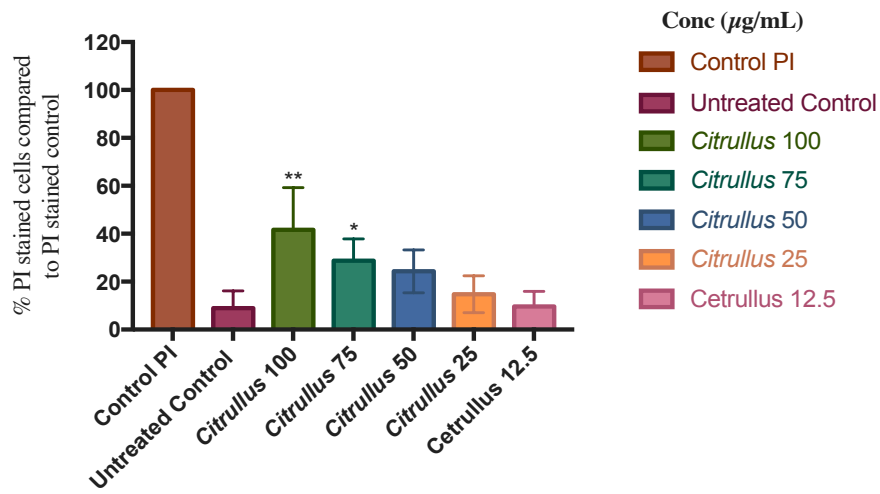


Figure 39 Dot plot depicting cells stained with FD. FD stain will enter the membrane of living cells, which will subsequently hydrolyse the dye to emit green fluorescence. (A) The green spots in the lower right region are FD-stained cells, and, (B) Histogram of the FDA-H

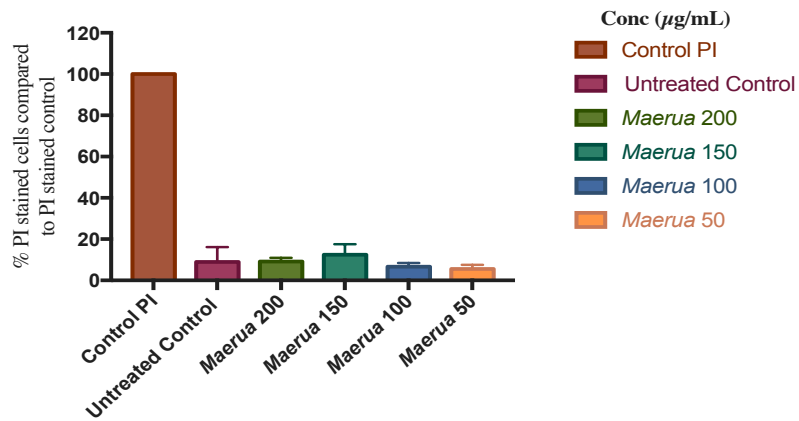
To further assess the toxicity, plant extracts were tested at the same concentrations as the MTT experiment: 200, 150, 100, and 50 $\mu\text{g/mL}$, for *A. canariense*, *M. crassifolia*, *R. stricta*, and *T. macropterus*. In addition, the *C. colocynthis* concentrations examined were 100, 75, 50, 25, and 12.5 $\mu\text{g/mL}$. Results are shown below (Figure 40 A-E).



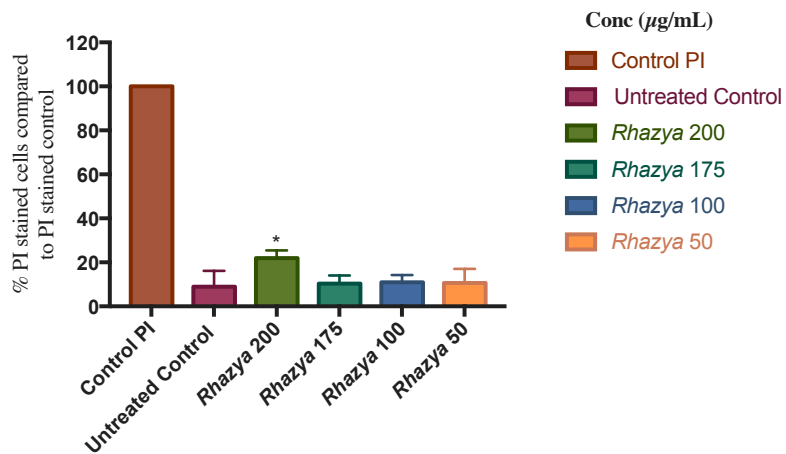
B



C



D



E

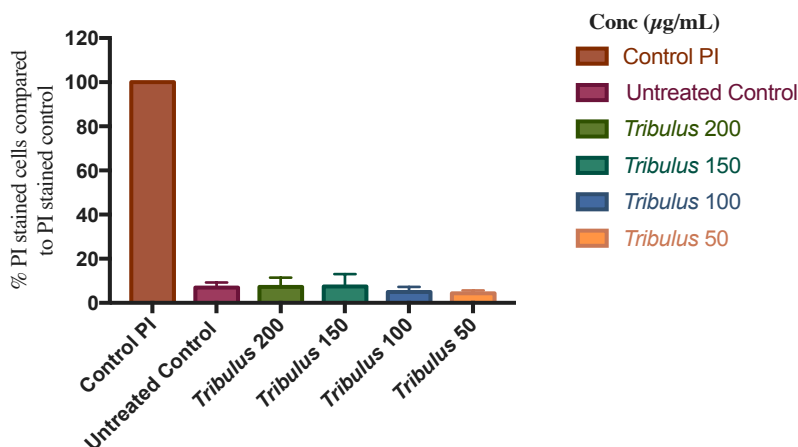


Figure 40 Percentage of PI-stained HaCaT cells treated with plant extracts in comparison to the PI control cells (fixed cells) at varying concentrations (mean \pm SE). (A) *A. canariense*, (B) *C. colocynthis*, (C) *M. crassifolia*, (D) *R. stricta*, (E) *T. macropterus*. Three separate experiments were conducted to acquire findings. Analysis of statistically significant differences between treated cells and untreated controls via Dunnett post-test (* $p < 0.05$, ** $p < 0.01$)

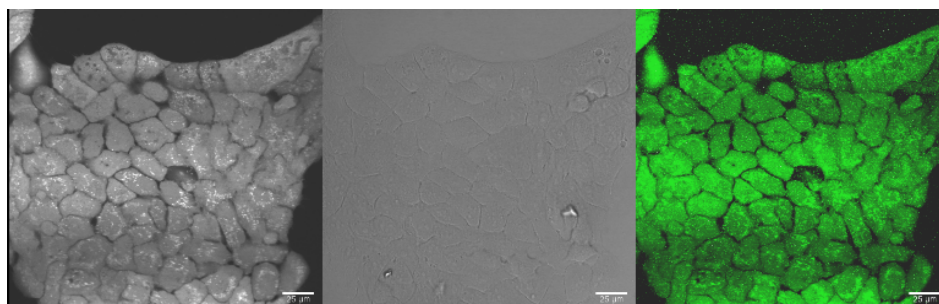
Corresponding to the MTT viability experiment, the FACS PI/FDA dual staining findings evaluating cytotoxicity demonstrated that *C. colocynthis* at a concentration of 100 $\mu\text{g/mL}$ and 75 $\mu\text{g/mL}$ exhibited a significant cytotoxic effect against HaCaT cells after 24 h ($p < 0.05$) (Figure 40B). The data collected by FACS is regarded as a tool for measuring cell damage and death. Thus, it demonstrates that the growth suppression seen in the MTT experiment results from *C. colocynthis* potent toxicity to HaCaT cells. *R. stricta* exhibited considerable cytotoxicity to HaCaT cells at 200 $\mu\text{g/mL}$ only at maximum concentration after 24 h ($p < 0.05$) (Figure 40D). The remaining plant extracts revealed similar trends to those observed in the MTT assay and were non-toxic to the HaCaT cell line. This study presented the cytotoxic activity of selected plant extracts against the HaCaT cell line for the first time.

3.5.3.2 Confocal Laser Scanning Microscopy (CLSM)

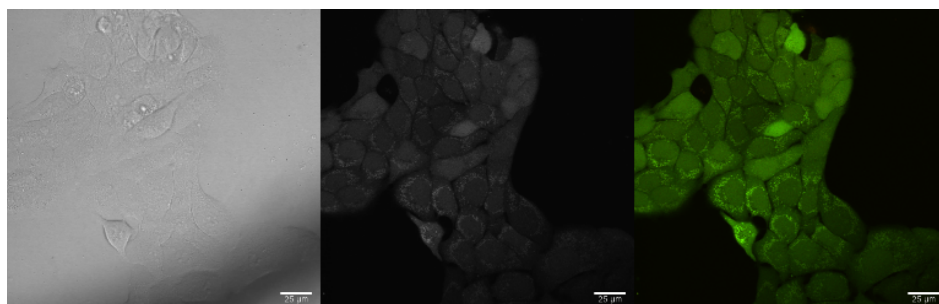
Utilising confocal microscopy and the PI/FD dual staining technique, viable and non-viable cells were distinguished to provide qualitative validation of the viability and cytotoxicity data

stated previously. Cells treated with *A. canariense*, *M. crassifolia*, *R. stricta*, and *T. macropterus* extracts were evaluated at 200 $\mu\text{g}/\text{mL}$, while *C. colocynthis* were evaluated at 100 $\mu\text{g}/\text{mL}$ (Figure 41 A-F).

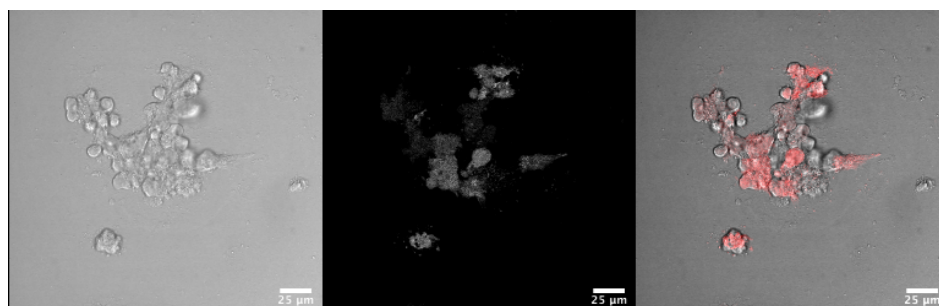
(A)



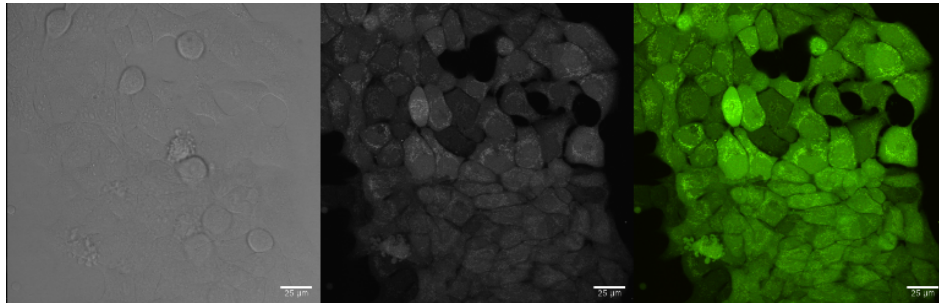
(B)



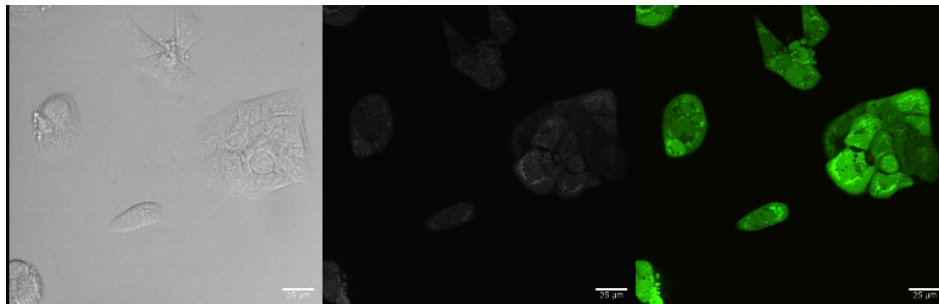
(C)



(D)



(E)



(F)

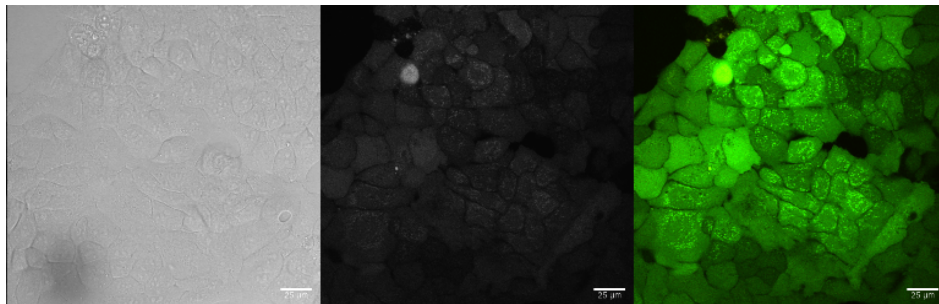


Figure 41 Obtained images via CLSM of dual-stained HaCaT cells using PI and FD (red and green fluorescent). (A) illustrates the non-treated control; the cells appear to be typical polygonal cells with elevated confluence and consistent form. (B), (D) and (F) represent cells treated with *A. canariense*, *M. crassifolia*, and *T. macropterus* and appeared to be well-formed and normally spread across the area. (E) displays cells treated with *R. stricta*; although they appear viable, their confluence was poor (approximately 20%). Cells treated with *C. colocynthis* exhibit severe morphological alterations and poor confluence, as shown in (C)

Overall, the CLSM images were consistent with the viability and cytotoxicity findings. HaCaT cells treated with *A. canariense*, *M. crassifolia*, and *T. macropterus* were stained with FD alone rather than PI. They seemed to be normal, regularly shaped polygonal cells with elevated confluence (around 90%) and uniformly distributed without any morphological alterations compared to the control. *R. stricta*-treated cells that were stained with FD seemed to be viable

polygonal cells without morphological abnormalities. Nevertheless, their confluence seemed to be poor (roughly 20%), and some cells were labelled with PI, causing them to appear red. Substantial morphological alterations were observed in *C. colocynthis* treated cells, which were also very low in confluence and mostly PI-stained. *C. colocynthis* showed significant toxicity against HaCaT cell lines, correlating with the results from the MTT and Flow Cytometry analysis.

New actives, including plant extracts, must have a good safety profile to be of therapeutic use. Therefore, it is common to subject new actives to normal cell lines and evaluate their effects to provide a preliminary indication of safety. Thus, the effect on cell growth and cytotoxic potentials of the 5 plant extracts were evaluated through different methods against the HaCaT keratinocyte cell line to ensure selectivity of targeted pharmacological action.

Although this is the first time, these 5 plant extracts were evaluated against the HaCaT cell line, the effect of *C. colocynthis* plant extract has been examined against different cancerous cell lines via MTT assay. In one report, *C. colocynthis* extract at a concentration of 100 µg/mL inhibited the growth of the MCF-7 and AGS cell lines by around 90% after 72 h exposure (Rezai et al., 2017). Additionally, the IC₅₀ of 17.2 µg/mL against MCF-7 following 48 h and 72 h exposure and the IC₅₀ of 12.54 µg/mL against HepG-2 cells after 48 h and 72 h exposure were determined with *C. colocynthis* extract (Mukherjee and Patil, 2012), both of which were lower than the IC₅₀ of 17.32 µg/mL and 16.91 µg/mL against HaCaT after 120 h and 168 h exposure, as reported in this study. Although the IC₅₀ would decrease in direct proportion to the length of exposure in normal conditions, this disparity is unsurprising given the known variation in the susceptibility of different cell types to cytotoxic agents.

To distinguish between cell growth inhibition and the cytotoxic effect of the plant extracts, cytotoxic actions were evaluated using FACS and CLSM by employing a double staining approach of PI/FD. Both techniques revealed that *C. colocynthis* showed a cytotoxic effect on the HaCaT cell line that was statistically significant at concentrations of 100 and 75 $\mu\text{g/mL}$ after 24 h exposure ($p < 0.01$, $p < 0.05$). In summary, *C. colocynthis* inhibited the growth of and killed HaCaTs in a dose- and time-dependent manner. These data suggest that *C. colocynthis* may be a promising source for anti-tumor drug discovery through the bioassay-guided fractionation approach.

Several bioactive compounds known as cucurbitacin glucosides have been isolated from *C. colocynthis*. These compounds are members of tetracyclic triterpenoid molecules well-known for their bitterness and toxicity, among other characteristics (Chawech et al., 2015). Cucurbitacin B and E, for example, have been isolated from *C. colocynthis* and shown to inhibit the growth of several cancerous cell lines, including the breast cancer cell line (Saeed et al., 2019). Traditionally, *C. colocynthis* plant extracts have been used in local communities in Saudi Arabia to treat several conditions; one of these traditional methods involves applying the extract topically to treat skin infections (Tounekti et al., 2019). Therefore, the potential toxicity of *C. colocynthis* on human skin should be further explored.

This study was mainly concerned with short-term exposure to different treatments, though long-term exposure was also conducted to explore other application possibilities. *R. stricta* showed no growth inhibition of HaCaT after 72 h treatment at 100, 75, 50, 25, and 12.5 $\mu\text{g/mL}$ concentrations. However, significantly delayed inhibition was observed following 120 h and 168 h treatment with an IC_{50} of 175 $\mu\text{g/mL}$ and 105 $\mu\text{g/mL}$ against HaCaTs. Other studies have reported lower IC_{50} numbers of 30 $\mu\text{g/mL}$ after 24 h against the HepG2 cell line (Al-Dabbagh

et al., 2018); and 160 µg/mL and 177 µg/mL against the MCF-7 and MDA-MB-231 cancerous cell lines after 48 h (Al-Zharani et al., 2019). As stated above, these variations in growth inhibition are due to the different susceptibility levels of different cell types. They may be explained by variations in the percentage of bioactive compounds in the plant extract (Sasidharan et al., 2011). In our study, analysis with FACS using a double staining method, showed that *R. stricta* had a significant cytotoxic effect on HaCaT at a concentration of 200 µg/mL, following 24 h exposure ($p < 0.05$).

The rest of the plant extracts, namely *A. canariense*, *M. crassifolia*, and *T. macropterus*, showed no antiproliferative or cytotoxic activity on HaCaT cells at concentrations of 200, 150, 100, and 50 µg/mL. However, It is important to note, that a recent study of *A. canariense*-based growth inhibition of the HCT-116, MCF-7, and HepG-2 cancerous cell lines resulted in a reported IC₅₀ of 21, 40, and 26 µg/mL, following 48 h exposure (Bakr et al., 2021). In addition, *M. crassifolia* was the only plant extract that showed a significant increase in cell proliferation after 120 h ($p < 0.01$), which may indicate that it possesses a wound-healing effect; this would be in alignment with a previous report of its traditional use (Volpato et al., 2012).

3.6 Conclusion

C. colocynthis exhibited a potent cytotoxic activity on HaCaT cells, as evidenced by a significant reduction in cell proliferation beginning at 24 h observed with the MTT experiment, and toxicity toward HaCaT was observed with FACS analysis and validated by CLSM images, whereas *R. stricta* inhibited cell growth after 5 and 7 days of treatment. The 50% inhibitory concentration (IC₅₀) values were calculated for both plant extracts. After 5 days, the IC₅₀ for *C. colocynthis* was 17.32 µg/mL, and after 7 days, it was 16.91 µg/mL. For *R. stricta*, after 5

days the IC₅₀ values were 175 µg/mL, and after 7 days, it was 105.3 µg/mL. MTT results were complemented by those from the FACS and CLSM analyses. The safety profile of the 5 selected medicinal plants varied greatly. *C. colocynthis* toxicity toward human skin keratinocytes can be further investigated with different skin cell line models (fibroblast) to validate its toxicity toward human skin. Moreover, *C. colocynthis* can serve as a promising source of anti-tumour drugs. *M. crassifolia* wound healing activity can be further evaluated through a scratch testing model of wound healing to detect cell migration and wound closure in HaCaT cell culture.

Chapter 4: Antioxidant and Wound Healing Properties of Plant Extracts

4.1 Introduction

Damage to the skin, such as burns, ulcers, and wounds, will cause the body to launch a series of complicated biological processes to repair and regenerate the damaged tissue. Several mediators, such as cytokines, growth factors, platelets, extracellular matrix (ECM), chemokines, and inflammatory cells, interact with one another in a coordinated and integrated manner during the various phases of the wound healing process hemostasis, inflammation, proliferation, and tissue remodelling phase (Zahedi et al., 2010; Pereira et al., 2013).

The re-epithelialization process, which refers to regenerating an intact epidermal layer, is crucial to effective wound healing. Re-epithelialization of the wound depends on the consequence of three overlapping keratinocyte functions: migration, proliferation, and differentiation. It is commonly considered that the set of events by which keratinocytes complete re-epithelialization begins with the breakdown of cell-cell and cell-matrix connections. Basal and suprabasal keratinocytes then polarise and migrate over the provisional wound matrix.

Mitosis occurs in a group of keratinocytes, close to, but not within the wound bed. The process concludes with developing a newly multilayered epidermis and activating differentiation-specific gene products to recover the functional capacity of the epidermis. Impairment in the migration process, but not proliferation or differentiation, is associated with chronic wounds which do not heal (Andriessen et al., 1995; Santoro and Gaudino, 2005; Stojadinovic et al., 2005). The inability to re-epithelialize is one of the most evident signs of a chronic wound (Pastar et al., 2014). Figure 42 presents a diagram of skin re-epithelialization process.

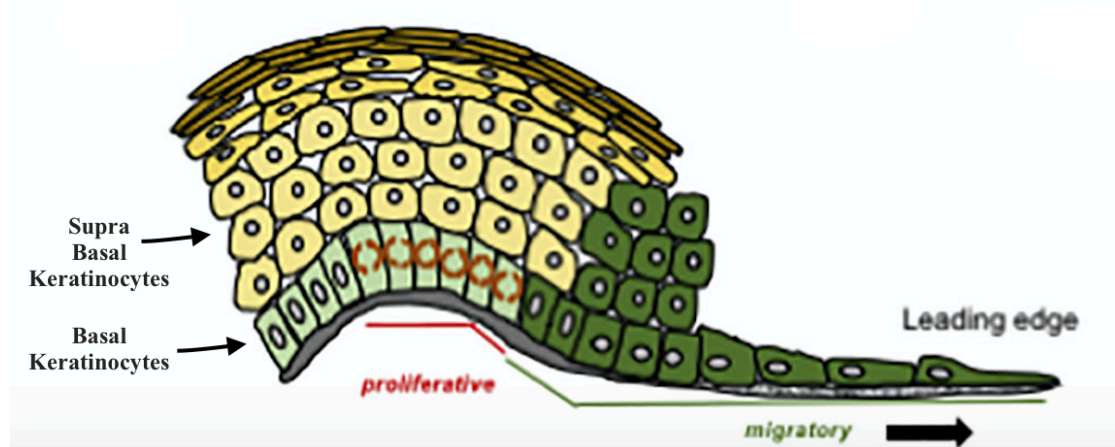


Figure 42 The two overlapping functions of keratinocyte migration and proliferation are illustrated in a diagram of the skin re-epithelialization process. It was hypothesised that layers above Basal keratinocytes, including Supra Basal keratinocytes, would be dragged together as a block when basal keratinocytes migrate across the wound bed and basal keratinocytes situated behind undergo proliferation (Adapted from Rousselle et al., 2019)

Chronic wounds and poor keratinocyte cell turnover are common in the elderly, making it difficult for wounds to re-epithelialize (Grove and Kligman, 1983). In addition, frequent relapses are seen with chronic wounds once they enter a persistent inflammatory and non-healing state. Infection, diabetes, malnutrition, age, renal impairment, pressure necrosis, and inflammation can cause a normal wound to fail to heal (Harding et al., 2002; Mekkes et al., 2003).

Wound dressings, tissue-engineered substitutes, and surgical reconstruction procedures using autografts or allografts are current therapeutic options for skin wounds that aim to promote wound re-epithelialization. However, clinically beneficial as they may be, these approaches are nevertheless faced with significant drawbacks, such as high production costs, low wound bed adhesion, limited vascularization, and the inability to duplicate skin appendages (Rousselle et al., 2019).

The primary healthcare systems of 80% of the world's developing and underdeveloped countries rely heavily on herbal medicine. Several plants and their extracts have been utilised for wound care and treatment due to their remarkable healing abilities (Agyare et al., 2019). Wound healing and tissue regeneration are promoted by herbal medicines that use multiple mechanisms linked with one another. For example, the same whole-plant extract contains antimicrobials, antioxidants, anti-inflammatory compounds, and other molecules that can promote keratinocyte or fibroblast cells proliferation, angiogenesis, and the formation of provisional extracellular matrix (ECM) (Akbik et al., 2014; El-Ashram et al., 2021). Herbal medicines are easily accessible and inexpensive. However, growing knowledge of their activities and potential and possible safety concerns underlines the need for scientific validation, standardisation, and strict safety evaluation prior to their successful introduction to wound management (Gupta and Jain, 2010).

4.1.1 The Role of Reactive Oxygen Species (ROS) in Wound Healing

Reactive oxygen species (ROS), such as nitric oxide, superoxide, hydroxyl radicals, and hydrogen peroxide (H_2O_2), participate in several crucial cellular functions, including gene transcription, signal transmission, antimicrobial, and immunological response. However, excessive ROS production has been linked to several disorders, including cancer, diabetes, neurodegenerative, and cardiovascular disorders. In addition, ROS production has been associated with wound healing. At low concentrations, ROS supports the healing process by eliminating invading microorganisms; nevertheless, elevated ROS production will lead to oxidative damage to the cells and impairment of wound healing (Rogers et al., 2014; Zuo et al., 2015; Sanchez et al., 2018). The high levels of ROS or the absence of antioxidant ROS scavenging compounds, such as vitamins C and glutathione, are standard features of chronic

wounds. Elevated levels of ROS via multiple ROS-generating enzymes observed in diabetic wounds will result in impaired wound healing as a consequence of elevated oxidative stress, protein modification, lipid peroxidation, and oxidative damage to DNA along with apoptosis of cells (Schäfer and Werner, 2008). An upsurge triggers increased intracellular ROS production in serum glucose and the buildup of advanced glycation end products (potent pro-oxidants). Consequently, it activates intracellular metabolic pathways like the protein kinase C signalling and polyol pathway, inhibiting antioxidant enzymes and molecules (Evans et al., 2002). Excessive ROS production disrupts redox balance in diabetic wounds, leading to a depletion of antioxidants, oxidative damage to cells, and impairment of wound healing (Figure 43) (Evans et al., 2002; Monnier et al., 2006; Zhang et al., 2018).

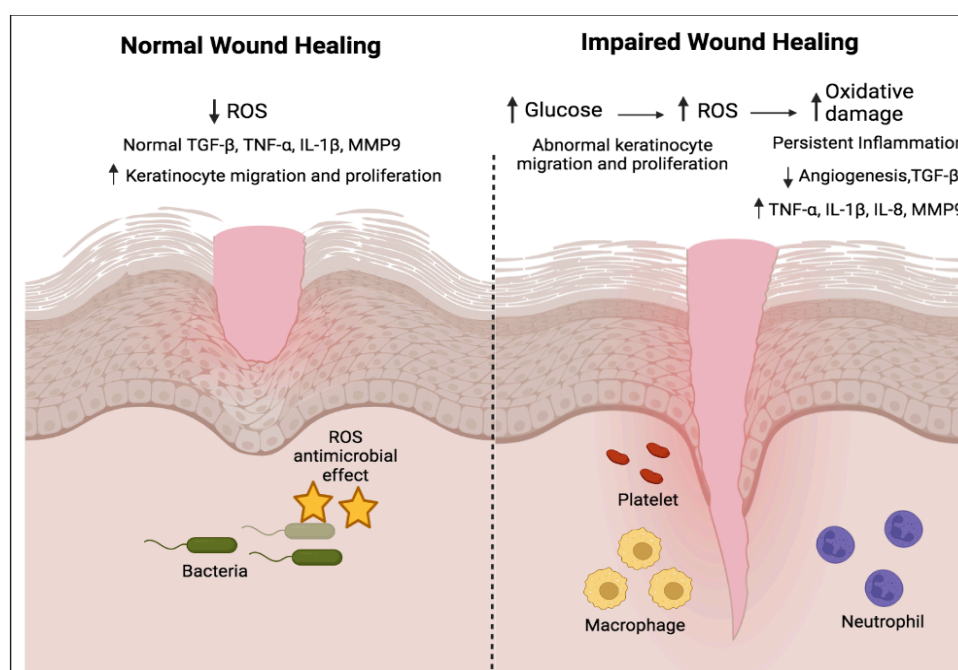


Figure 43 Role of reactive oxygen species (ROS) in normal wound healing and diabetic chronic wounds causing impaired wound healing (created with BioRender.com)

Notably, the levels of wound antioxidants decrease with age, which correlates to the slowed wound healing responses observed in elderly individuals. As a result, wound ROS activities

can continue uncontrolled, leading to increased tissue damage and impaired or delayed wound healing (Schäfer and Werner, 2008). Antioxidant effects of several herbal extracts have been demonstrated in various *in vitro* and *in vivo* assays. Antioxidants can promote wound healing, and tissues can be protected from oxidative damage (Shetty et al., 2008).

Antioxidant-rich medicinal plants can mitigate the harmful effects of reactive oxygen species (ROS) by donating one electron to free radicals and neutralise it to create a more stable byproduct. In addition to significant antioxidant activity, phenolic compounds can also exhibit antibacterial and anti-inflammatory properties. Phenolic is one of plants' four major classes of secondary metabolites (alkaloids, glycosides, terpenes, and phenolic compounds) (Balasundram et al., 2006; Wang et al., 2007; Moldovan et al., 2017). Figure 44 shows an example of a phenolic antioxidant, natural product (PPH), donating an electron to unstable peroxy radical (ROO[•]) to form a stable alkyl hydroperoxide (ROOH).



Figure 44 The Formation of stable alkyl hydroperoxide through a donation of electron by phenolic antioxidant natural product

Among the various antioxidant methods used to explore plant extract free radical scavenging potential, a widely used method employs the organic radical 1,1-diphenyl-2-picrylhydrazyl (DPPH) to evaluate natural products' ROS scavenging ability. In this chemical-based experiment, the addition of an antioxidant causes the purple colour of the DPPH solution to diminish. Because of its ease of use, high sensitivity, and consistent output, this experiment has achieved widespread use (Noipa et al., 2011; Boylan et al., 2015; Kim, 2016). However, due to the complexity of the mechanisms of action of natural products, a single chemical-based approach is inadequate for analysing and comparing their antioxidant effects. Furthermore, the

observed antioxidant capacity index may not adequately represent the antioxidant effects since these chemical-based assays do not account for critical biological factors, such as the ability of antioxidants to reach the site of ROS and their bioavailability. Consequently, it is vital to determine whether or not natural products may induce antioxidant activity at the cellular level (Lü et al., 2010; López-Alarcón and Denicola, 2013; Nwachukwu et al., 2021).

ROS-Glo H_2O_2 technique was employed to investigate antioxidant capacity in a cellular system. This technique is effective in detecting ROS in cultured cells. It serves as a fast and precise luminescence assay that directly evaluates the amount of hydrogen peroxide (H_2O_2) in the cellular system to more accurately identify compounds and plant extracts with ROS scavenging properties. Numerous other ROS are generated in cell culture media, such as superoxide and hydroxyl radicals. However, H_2O_2 has the most extended half-life compared to all other ROS, so changes are more readily detected. In this assay, the interaction between H_2O_2 substrate (added) and H_2O_2 will result in the production of luciferin precursor, which will be converted to luciferin at a later stage through the addition of ROS-Glo detection reagent containing D-cysteine. The amount of luminescent signal generated is proportional to the level of H_2O_2 in the medium. Immortalized human skin keratinocytes (HaCaT) cells were employed to investigate the ROS scavenging activities of plant extracts. Menadione, a chemical compound identified for its ability to generate ROS at high concentrations through a redox cycle, was introduced to HaCaT to stimulate ROS production (O'Brien and Dawes, 1998; Loor et al., 2010). Employing HaCaT cells for the evaluation of the antioxidant activity of plant extracts allowed for the simulation of a distinct characteristic of pathological skin conditions, particularly the elevation of ROS observed with chronic wounds.

4.2 Chapter Aim and Objectives

This chapter investigates selected medicinal plants' wound healing potential and antioxidant properties through chemical-based and cellular-based modules.

- Develop and optimize technique to determine the total phenolic content of 5 selected medicinal plants as gallic acid equivalents, through Folin-Ciocalteu (FC) assay.
- Develop and optimize a technique to evaluate the antioxidant capacity of selected medicinal plants utilising DPPH assay.
- Develop and optimize a cell-based technique for evaluating the antioxidant properties of selected medicinal plants utilising the ROS-Glo H₂O₂ Assay and the HaCaT cell line.
- Develop and optimize technique to evaluate the effect of selected medicinal plants on keratinocyte migration, a critical wound healing response.

4.3 Materials

Unless otherwise indicated, all materials were purchased from ThermoFisher Scientific (Loughborough, UK). HaCaT cell line supplies were described in a previous section (Section 3.2). 96- and 24-well microplates (flat bottom, transparent, sterile, tissue culture-treated surface, polystyrene plate) were acquired from Sarstedt (Leicester, UK). ROS-Glo™ H₂O₂ Assay kit was acquired from Promega (Promega, Southampton, UK Ltd), and 96-well plates (white, flat bottom, clear bottom, sterile, tissue culture-treated surface, lid with condensation rings, polystyrene plate) were obtained from Greiner (Greiner Bio-One Ltd., Stonehouse, UK). Menadione powder, Folin Ciocalteu reagent, 1,1-diphenyl-2-picrylhydrazyl (DPPH) powder, ascorbic acid, and methanol were purchased from Sigma-Aldrich Company Ltd (Poole,

UK). The absorbance (515 nm) was determined using a microtiter plate reader (Infinite 200 Pro, Tecan Trading, Männedorf, Switzerland).

4.4 Methods

4.4.1 Preparation of Samples

Five selected plant extracts, namely *A. canariense*, *C. colocynthis*, *M. crassifolia*, *R. stricta*, and *T. macropterus*, were dissolved in methanol to a final concentration of 10 mg/mL to produce stock solutions.

4.4.2 Determination of Extracts Total Phenolic Content

The Folin Ciocalteu (FC) method, with some modifications from the original methodology described by Mancini et al. (2015), was employed to determine the total phenolic content of five plant extracts. Standard solutions of 0.05, 0.1, 0.15, 0.25, and 0.5 mg/mL of gallic acid were made, and samples of plant extracts with a concentration of (1mg/mL) were made by dissolving 5 mg in 5 mL methanol. Each test tube included 0.5 mL of the sample under investigation, then 2.5 mL of Folin-Ciocalteu reagent (10% concentration), and incubated for approximately 8 min. The samples were then diluted to a final volume of 5 mL with 2 mL of a 20% sodium carbonate solution, combined, and kept in the dark for 2 h. Absorbance at 760 nm was measured using a Cary 60 UV/Vis spectrophotometer (Agilent Technologies Ltd., Oxford, UK) compared to a blank solution. A calibration curve was established using the above-stated gallic acid concentrations. The findings were reported in mg of gallic acid equivalents (GAE) per gram of dry plant extract.

4.4.3 DPPH (1,1-diphenyl-2-picrylhydrazyl) Free Radical Scavenging Assay

The 96-well plate is split into columns including only DPPH radical, columns including only the sample, and columns containing both the sample and DPPH radical. The samples in each plate were serially diluted (1000, 500, 250, 125, 62.5, 31.25, 15.625, 7.8125 µg/mL), the plates were covered with adhesive foil for 30 min, and the absorbance at 515 nm was measured using a microplate reader.

For determining the percentage of radical scavenging, the following equation was used:

The percentage DPPH scavenging = $100 \times \frac{[(\text{Absorbance of Sample and DPPH}) - (\text{Absorbance of Sample blank})]}{[(\text{Absorbance DPPH}) - (\text{Absorbance of Solvent})]}$.

The inhibitory concentration (IC₅₀) (concentration required to achieve a 50% antioxidant action) was determined by interpolating the $[(\text{Absorbance of the sample} - \text{Absorbance of the sample blank})]$ onto a calibration line formed by the absorbance of DPPH at various concentrations.

4.4.3.1 Preparation of DPPH Radical

Solution of DPPH with a concentration of 0.2 mM was made by dissolving 39.4 mg in 1 mL methanol, transferring the solution to a 500 mL volumetric flask, and then filling out the flask with the solvent. The solution was wrapped with aluminium foil to reduce light-induced deterioration and kept at 4 °C.

4.4.4 ROS-Glo H₂O₂ Assay

ROS-Glo™ H₂O₂ Kit (Promega) was used to examine the potential of plant extracts further to scavenge H₂O₂ from cell culture; the experiment was performed following the manufacturer's instructions. First, luminescence signals were amplified using clear-bottomed white 96-well plates. White plates are ideal since they reflect light and increase the signal output (Loh et al., 2020). Next, the HaCaT cells were trypsinized and counted using a haemocytometer. Afterward, cells were diluted with CCM, and their density was adjusted to 10 x 10⁴ cells per mL; 100 µL of cell suspension was applied to every well; the following day, the media was removed from every well, and 80 µL of treatment with menadione was added. Menadione, an aromatic ketone molecule that acts as a precursor for producing Vitamin K, is known to produce ROS at high concentrations via the redox cycle (O'Brien and Dawes, 1998; Loor et al., 2010).

The following were employed as controls for each experiment:

- 1- Cell-free media with vehicle control (1% methanol).
- 2- Cell-free media with treatments.
- 3- Media containing cells and 1% methanol.
- 4- Menadione 50 µM as a positive control with and without cells.
- 5- Ascorbic acid 5 µg/mL serves as a positive control.

The final volume of each well was brought to 100 µL by adding 20 µL of 125 µM H₂O₂ substrate dilution buffer, followed by 4 h of incubation. Finally, 100 µL of ROS-Glo detection solution was applied to each well. Signals of luminescence were obtained using a CLARIOstar Plate Reader (BMG Labtech Ltd., Aylesbury, UK). Obtained signal values were adjusted

downward by the mean of media devoid of cells. The percentage of H₂O₂ decrease was determined by comparing the treatments to a menadione positive control, with data normalised against a control containing only cells.

4.4.5 Scratch Wound Assay

One of the most prominent features of chronic wounds is an upsurge in ROS levels, which leads to increased tissue damage and hinders or delays wound healing (Schäfer and Werner, 2008). Therefore, following the investigation of plant extract's antioxidant properties, their effect on keratinocyte migration was evaluated. Keratinocyte migration is an essential function throughout the wound healing process. The experiment was carried out according to Moses et al. (2020) procedure with slight modifications. HaCaTs were trypsinized and counted utilising Scepter 3.0 Cell Counter (ThermoFisher Scientific). Cells were seeded at 12.5×10^5 per mL density in serum-containing culture media (DMEM, 10% FBS, 1% antibiotics and L-glutamine). 1 mL was applied to a 24-well plate before being kept in an incubator for 48 h at 37 °C, 5% CO₂, and 95% humidity. After incubation, the culture media were replaced with serum-free media and incubated for 24 h. After 24 h, the supernatant was carefully removed from every well. Each cell layer was artificially scratched with a sterile 200 µL pipette and rinsed a couple of times with 1 mL PBS to remove cell debris. Subsequently, 1 mL of 1% serum culture media with various concentrations of *A. canariense*, *M. crassifolia*, and *T. macropterus* (200, 150, 100, and 50 µg/mL), *R. stricta* (100, 75, 50, 25, and 12.5 µg/mL), and *C. colocynthis* (25, and 10 µg/mL) added to each well. Untreated control of 1% methanol was included in each experiment.

The monitoring of the migration of cells into the unpopulated area was done with the use of the EVOS M7000 Live Cell Imaging System (ThermoFisher Scientific). The plate was kept in the system incubator for 48 h at 37 °C, 5% CO₂, and 95% humidity. EVOS system software was configured to capture digital images from each well every 20 min for 48 h. LAS AF Lite (Leica Software, Version 4.0, Leica Microsystems Ltd., UK) was utilised to convert these images to video. Images of HaCaTs were analysed using ImageJ software (National Institute of Health Software, Version 1.48). At 24 h and 48 h, each treatment's percentage of wound closure was computed and expressed as the mean \pm Standard Error (SE).

4.4.6 Statistical Analysis

The acquired data were statistically analysed using GraphPad Prism 7.0a (GraphPad Software Inc., San Diego, USA); all data is reported as the mean \pm SE, and all experiments were conducted three times each. The means and standard errors were calculated using Excel (Microsoft) software. The statistical analysis was performed using a one-way analysis of variance (ANOVA) Dunnett post-test, to assess the significance of the difference between the means of the control and experimental groups. The statistically significant difference between groups was determined using Tukey's post-test, with a threshold of $p < 0.05$ deemed to indicate statistical significance.

4.5 Results and Discussion

4.5.1 Total Phenolic Content

The total phenolic contents of five plant extracts are presented in Table 14. TFC was measured using a gallic acid calibration curve. Many studies showed that high amounts of antioxidant

activity were demonstrated to have a direct relationship with the overall phenolic content of a given sample (Li et al., 2008; Bahri-Sahloul et al., 2014).

Table 14 Total phenolic content (TPC) of 5 plant extracts reported as equivalent gallic acid per gram dry powder extract (GAE/g) (mean \pm SE). The findings were collected from three separate experiments performed in triplicate

Sample	TPC (mg GAE/ g dry extract)
<i>A. canariense</i>	7.85 \pm 2.48
<i>C. colocynthis</i>	37 \pm 1.55
<i>M. crassifolia</i>	24.89 \pm 1.06
<i>R. stricta</i>	64.04 \pm 2.84
<i>T. macropterus</i>	21.97 \pm 0.74

4.5.2 Chemical-Based Assessment of Antioxidant Activity

A chemical-based method employing DPPH was exploited to investigate the antioxidant properties of *A. canariense*, *C. colocynthis*, *M. crassifolia*, *R. stricta*, and *T. macropterus* extracts. Results were compared to a positive control of ascorbic acid. DPPH is a stable free radical that exhibits a purplish colour. This assay's method relies on the potential antioxidant's capacity to donate one of its hydrogens to the free radical DPPH, resulting in DPPH's reduction to DPPH-H and the development of yellow colour as opposed to a purple one. The concentration of plant extracts needed to scavenge 50% of the starting DPPH (IC₅₀) is listed in Table 15, along with the IC₅₀ value of ascorbic acid using the DPPH test. Figure 45 demonstrates the DPPH-scavenging properties of selected plant extracts.

Table 15 IC₅₀ values (µg/mL) of plant extracts as determined by the DPPH test following half an hour (mean ± SE) compared with TPC. Ascorbic acid was the reference standard for this investigation. The obtained values represent the concentration needed to scavenge 50% of the DPPH radicals produced at the beginning of the experiment; hence, lower values suggest higher antioxidant properties. Three separate experiments done in triplicate provided the findings

Plant Extracts	IC ₅₀ (µg/mL) (average ± SE)	TPC (mg GAE/ g dry extract)
<i>A. canariense</i>	IC ₅₀ ≈ 822 ± 54.37	7.85 ± 2.48
<i>C. colocynthis</i>	IC ₅₀ ≈ 824 ± 40.74	37 ± 1.55
<i>M. crassifolia</i>	IC ₅₀ ≈ 448 ± 25.7	24.89 ± 1.06
<i>R. stricta</i>	IC ₅₀ ≈ 335 ± 20.7	64.04 ± 2.84
<i>T. macropterus</i>	IC ₅₀ ≈ 787 ± 24.5	21.97 ± 0.74
<i>Ascorbic acid</i>	IC ₅₀ ≈ 3.92 ± 0.32	

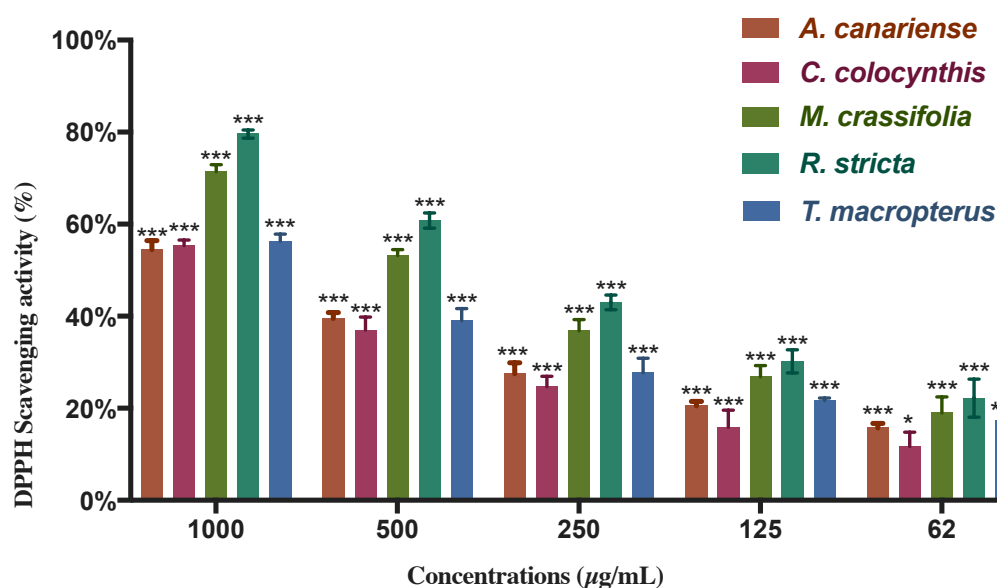


Figure 45 The percentage of DPPH free radical scavenging ability over a range of concentrations of selected plant extracts in µg/mL (mean ± SE). Three separate experiments were performed to acquire findings. Analyses of statistically significant differences compared to a control group (*p<0.05, **p<0.01, ***p<0.001)

With IC₅₀ values of 335 and 448 µg/mL, respectively, *R. stricta* and *M. crassifolia* exhibited the most significant ability to scavenge DPPH radicals. These two extracts were able to neutralise 50% of the harmful radicals at these low concentrations. To some extent, the observed antioxidant activity of *R. stricta* can be attributed to its high total phenolic content (TPC). In contrast, the demonstrated antioxidant activity of *A. canariense* is related to its low

TPC. Several phytochemical studies have identified phenolic components, including luteolin, isoquercetin, quercetin-3-rhamnoside, quercetin, kaempferol, apigenin, apigenin-8-C-glucoside, hesperetin, rutin, acacetin, and rhazianoside A & B in *R. stricta*. Such compounds are responsible for the plant's activity (Marwat et al., 2012; Bukhari et al., 2017). On the other hand, antioxidant activity in *M. crassifolia* can be indicated by the presence of phenolic substances not reported in phytochemical investigations. Such findings suggest that these two plants have a superior ratio of phenolic compounds and are a potential source of natural antioxidants that can be used to reduce the damaging effects of free radicals ROS. Excessive production of free radicals has been linked to various health conditions, including coronary heart disease, arthritis, muscular degeneration, and cancer (Rogers et al., 2014). The correlations between the phenolic content of plant extracts and their antioxidant properties have been established by many studies (Kim et al., 2007; Piluzza et al., 2011; Aryal et al., 2019). Several studies investigated the antioxidant properties of *M. crassifolia* methanolic extract using the DPPH method, showing lower IC₅₀ values of 122.9 and 58.9 µg/mL (Chaib et al., 2015; Ckilaka et al., 2015). This fluctuation may be attributed to the fact that the amounts of active components in plant extracts fluctuate considerably based on the local climate and other environmental factors. In addition, different compounds and their modes of action within extracts can be influenced by factors, such as growing location, harvesting time, processing techniques, and used plant parts. In light of this, it may not be easy to make firm conclusions regarding the antioxidant activity of plant extracts from a comparison of the various data in the research literature (Radulovic et al., 2013).

4.5.3 Cell-Based Assessment of Antioxidant Activity

To better understand the potential of antioxidants to reach the site of ROS and their bioavailability, it was necessary to evaluate the antioxidant activity at the cellular level after applying a chemical-based technique. Consequently, the ROS-Glo H₂O₂ Assay Kit was utilised to examine the H₂O₂ scavenging properties of *C. colocynthis*, *M. crassifolia*, and *R. stricta* in HaCaT cell culture. The introduction of the menadione molecule triggered the production of free radicals H₂O₂ in HaCaT cells. The amount of H₂O₂ radicals was directly proportional to the luminescence signal intensity. Figure 46 provides a comparison of plant extracts inhibiting H₂O₂ radicals generation.

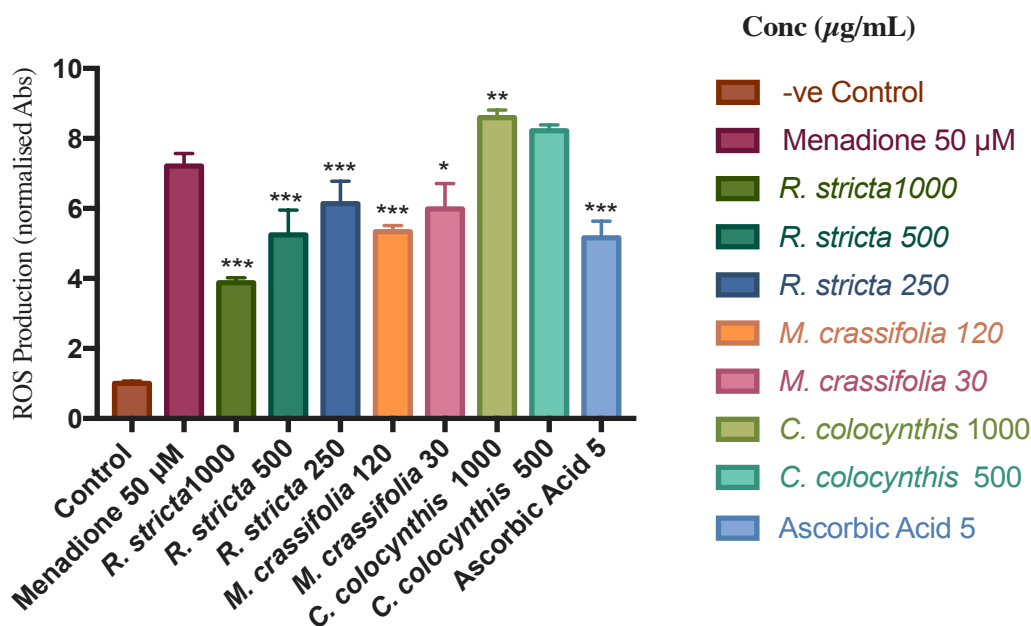


Figure 46 Inhibition of H₂O₂ radicals generation by various plant extracts at different concentrations (µg /mL) (mean ± SE). The data was collected from three separate experiments. Significant differences between treatments and the control group were analysed statistically (*p<0.05, **p<0.01, *p<0.001)**

R. stricta exhibited a significant ability to scavenge H₂O₂ radicals with 46%, 27%, and 14% at 1000, 500, and 250 µg/mL, respectively (p<0.001) compared to menadione control. Even

though *M. crassifolia* exhibits no scavenging response at concentrations of 1000, 500, and 250 $\mu\text{g/mL}$, it did exhibit modest activity at concentrations of 120 and 30 $\mu\text{g/mL}$, with inhibition percentages of 25% and 16%, respectively ($p < 0.001$; $p < 0.05$). These findings were in alignment with the DPPH findings. At 1000 and 500 $\mu\text{g/mL}$, *C. colocynthis* recorded higher levels of H_2O_2 radicals than the menadione control ($p < 0.01$). Furthermore, to recognise cell-dependent from cell-independent variations in free radicals level, *C. colocynthis* control without cells was evaluated and demonstrated a higher amount of hydrogen peroxide ($p < 0.01$). Such an observation could be due to the ability of *C. colocynthis* to generate H_2O_2 directly or simply it contains polyphenolic substances that undergo a chemical interaction with components of the cell culture medium, resulting in the generation of H_2O_2 (Long et al., 2010). In any case, the previously observed findings of cytotoxic action of *C. colocynthis* could be due to the excessive generation of hydrogen peroxide that damages HaCaT cells. Figure 47 shows *C. colocynthis* extract control without cells compared to *C. colocynthis* extract.

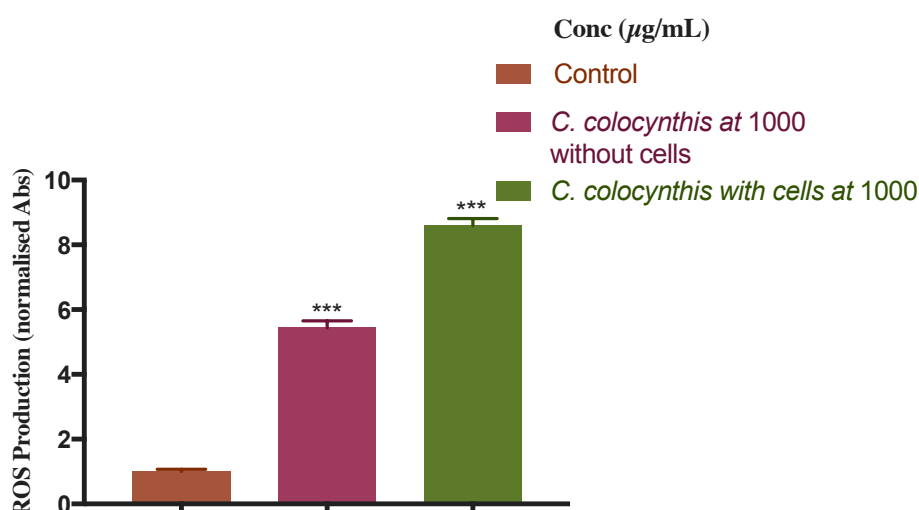
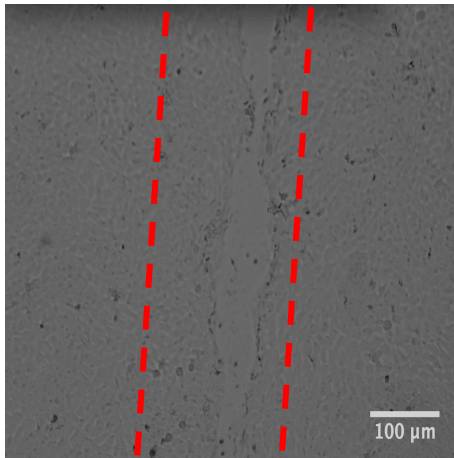


Figure 47 The difference in H_2O_2 production between *C. colocynthis* with and without cells. The capacity of this plant extract to produce H_2O_2 was evidenced by the finding of a greater H_2O_2 level in samples evaluated in the absence of cells (mean \pm SE). Three separate experiments were conducted to acquire data. Significant differences between treatments and the control group were analysed statistically (***) $p < 0.001$

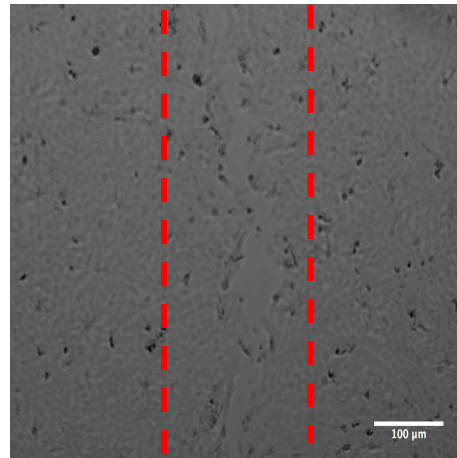
4.5.4 Effects of Plant Extracts on HaCaT Migration

HaCaTs migrated across the scratched regions during the period of 48 h, as seen by the EVOS System digital images (Figure 48). At different concentrations cells were cultured in *A. canariense*, *M. crassifolia*, and *T. macropterus* (200, 150, 100, and 50 µg/mL), *R. stricta* (100, 75, 50, 25, and 12.5 µg/mL), and *C. colocynthis* (25, 20, 15 and 10 µg/mL) and findings were compared with untreated solvent vehicle control (0 µg/mL). *A. canariense*, *R. stricta*, and *T. macropterus* at the concentrations evaluated showed no effect on the migration of HaCaT cells over the scratched region, in comparison to untreated controls (Figure 49) ($p > 0.05$). Although *M. crassifolia* at 100 and 50 µg/mL showed no effect on the migratory patterns of HaCaT in comparison to untreated control ($p > 0.05$), when *M. crassifolia* was examined at concentrations of 200 and 150 µg/mL, it demonstrated significantly enhanced migratory activity compared to untreated controls, but only following 48 h ($p < 0.05$, $p < 0.001$). *C. colocynthis* at (25, 20, and 15 µg/mL) revealed a cytotoxic effect on HaCaT cells over a period of 48 hours, with noticeable morphological changes starting 12 h after treatment, validating the Section 3.5.3 findings. Moreover, it demonstrated a significant inhibition of keratinocytes migration compared to untreated controls ($p < 0.001$) (Figure 48 H, I).

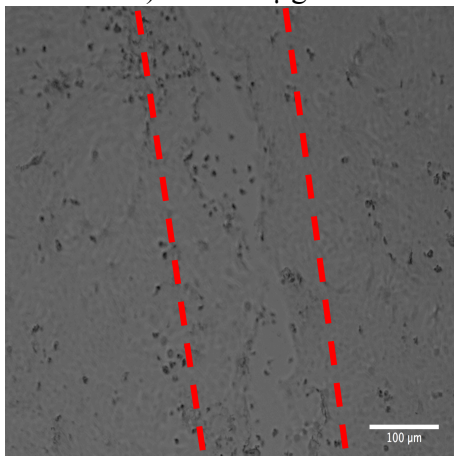
A) Control



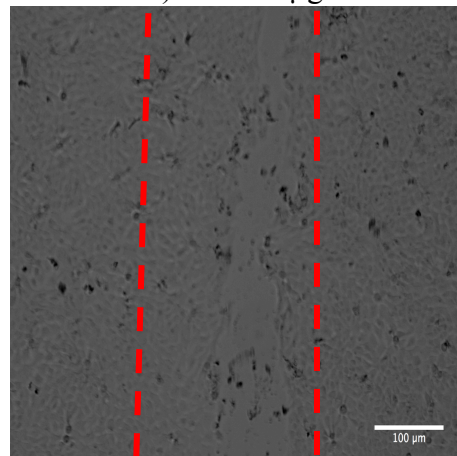
B) AC 50 μg/mL



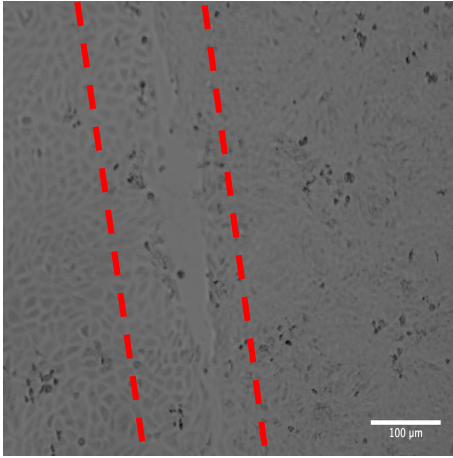
C) AC 100 μg/mL



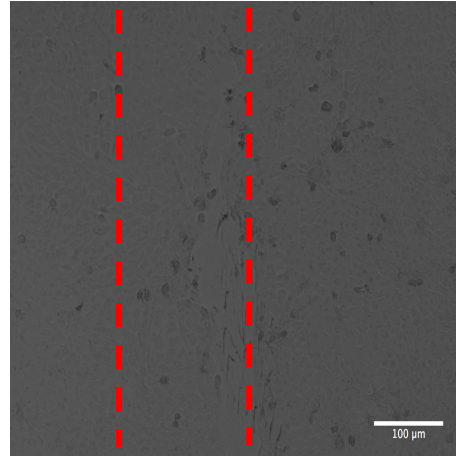
D) AC 150 μg/mL



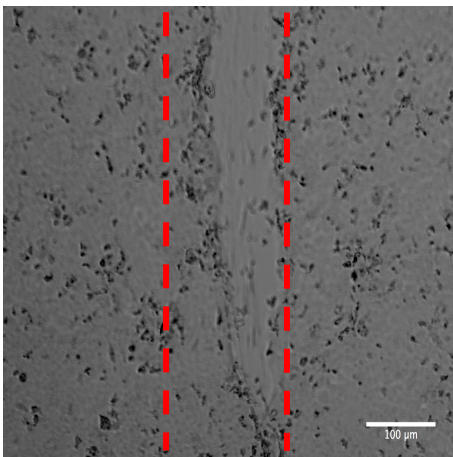
E) AC 200 $\mu\text{g}/\text{mL}$



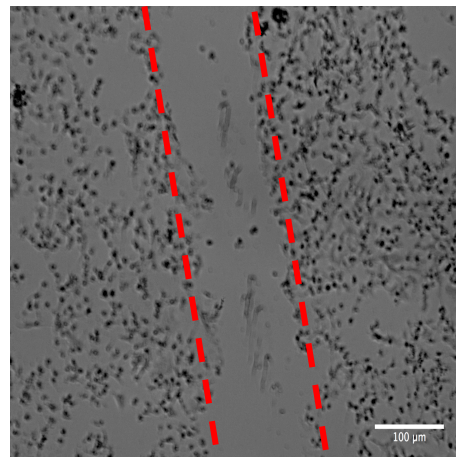
F) CC 10 $\mu\text{g}/\text{mL}$



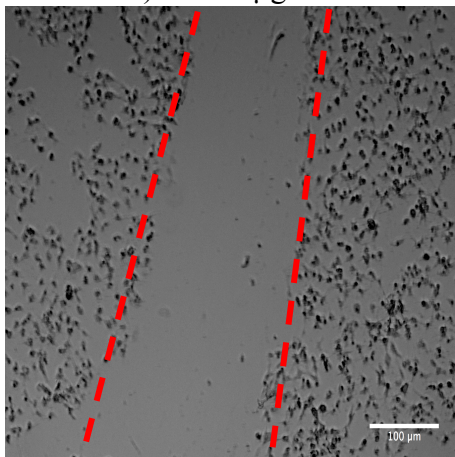
G) CC 15 $\mu\text{g}/\text{mL}$



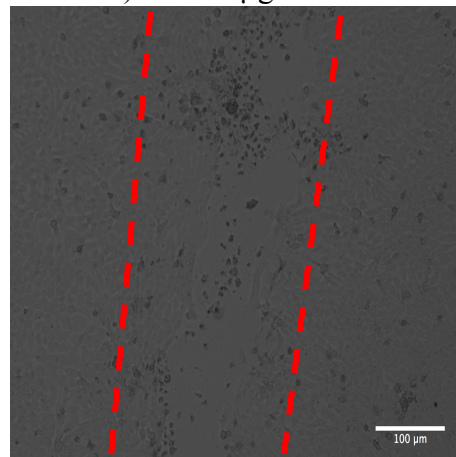
H) CC 20 $\mu\text{g}/\text{mL}$



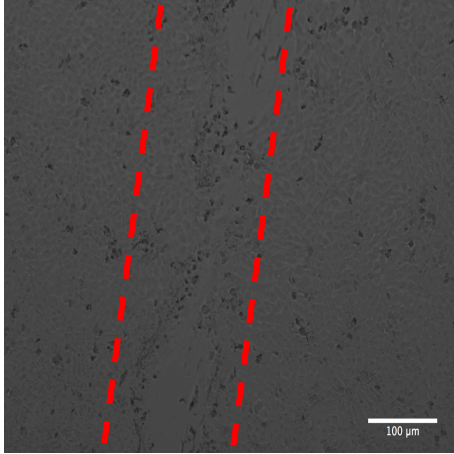
I) CC 25 $\mu\text{g}/\text{mL}$



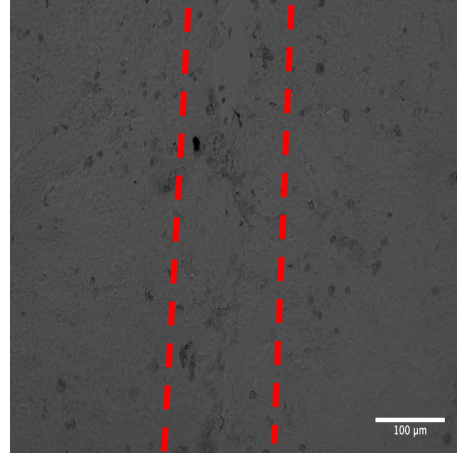
J) MC 50 $\mu\text{g}/\text{mL}$



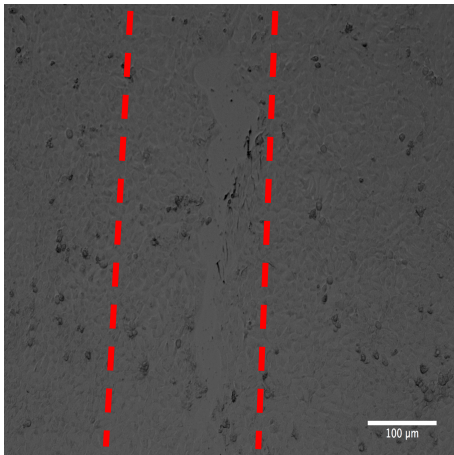
K) MC 100 $\mu\text{g/mL}$



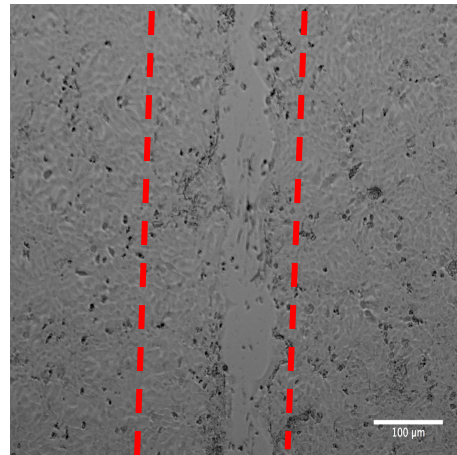
L) MC 150 $\mu\text{g/mL}$



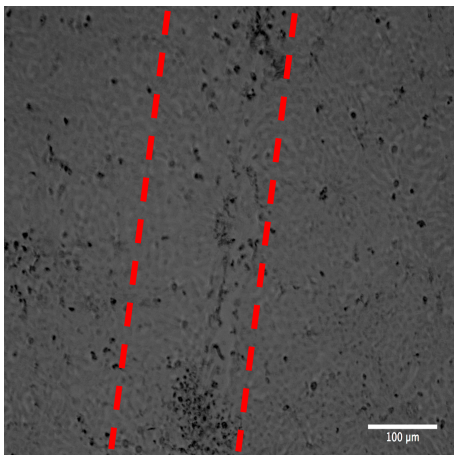
M) MC 200 $\mu\text{g/mL}$



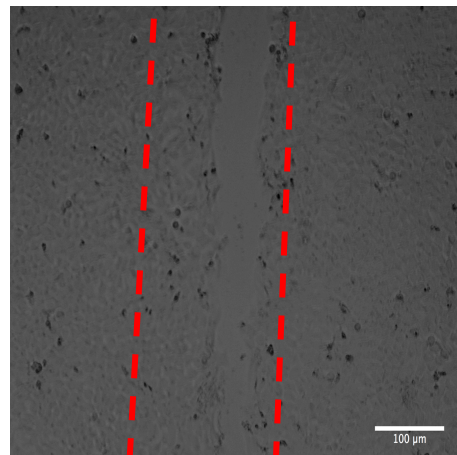
N) RS 12.5 $\mu\text{g/mL}$



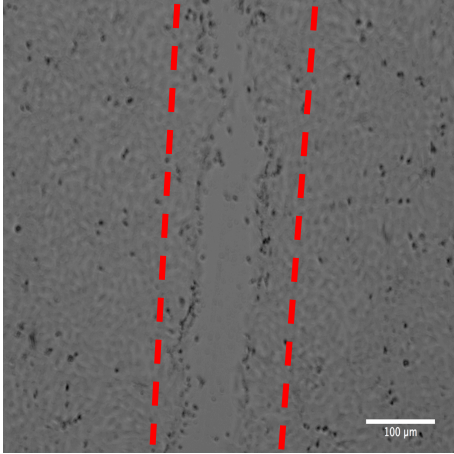
O) RS 25 $\mu\text{g/mL}$



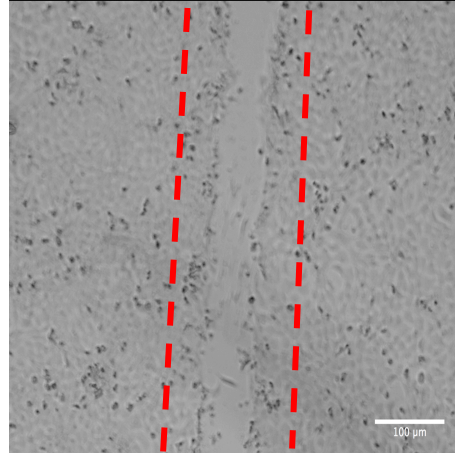
P) RS 50 $\mu\text{g/mL}$



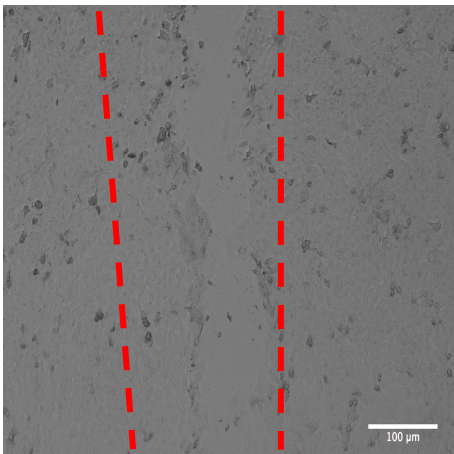
Q) RS 75 $\mu\text{g/mL}$



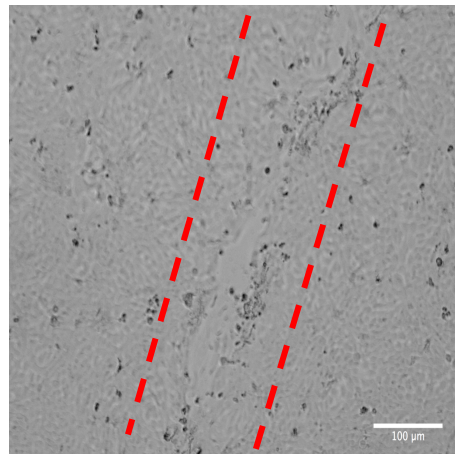
R) RS 100 $\mu\text{g/mL}$



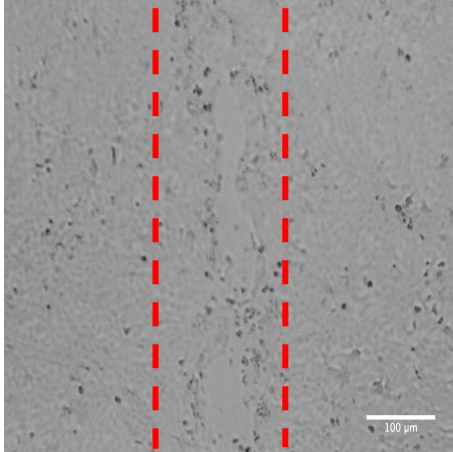
S) TM 50 $\mu\text{g/mL}$



T) TM 100 $\mu\text{g/mL}$



U) TM 150 $\mu\text{g}/\text{mL}$



V) TM 200 $\mu\text{g}/\text{mL}$

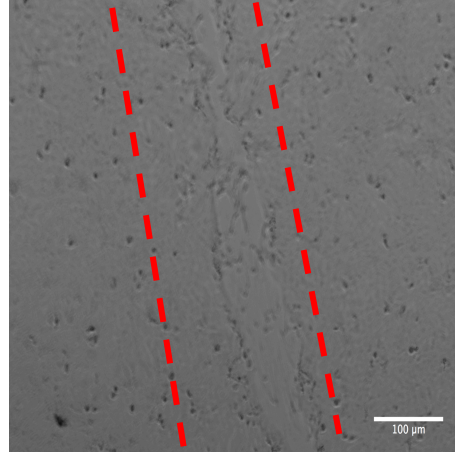
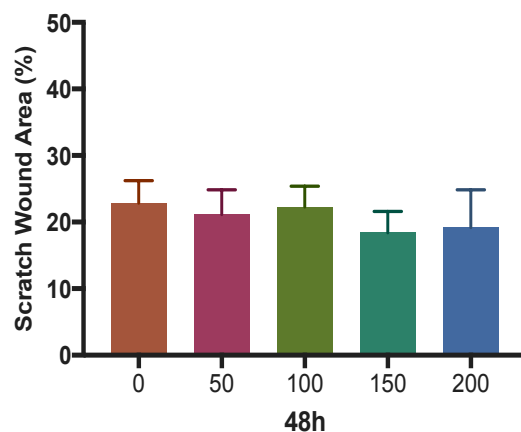
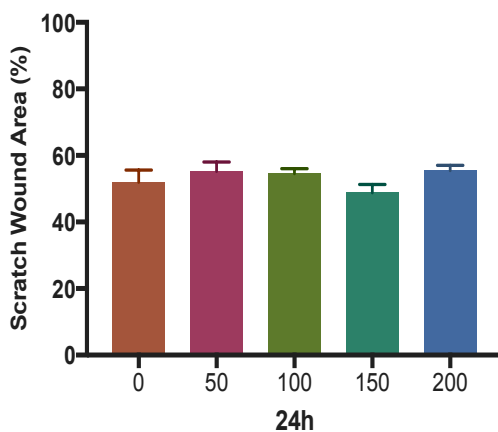
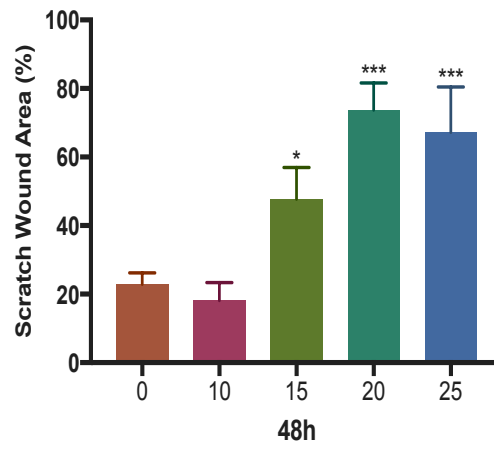
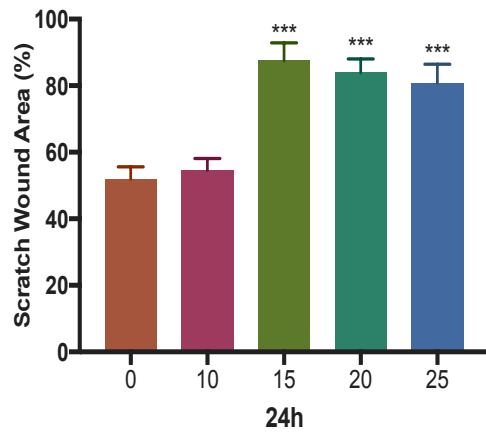


Figure 48 EVOS images of wound area in HaCaT cells monolayer by employing scratch assay *in vitro* in the presence of untreated control (A) 0 $\mu\text{g}/\text{mL}$, *A. canariense* (B) 50 $\mu\text{g}/\text{mL}$, (C) 100 $\mu\text{g}/\text{mL}$, (D) 150 $\mu\text{g}/\text{mL}$, (E) 200 $\mu\text{g}/\text{mL}$, *C. colocynthis* (F) 10 $\mu\text{g}/\text{mL}$, (G) 15 $\mu\text{g}/\text{mL}$, (H) 20 $\mu\text{g}/\text{mL}$, (I) 25 $\mu\text{g}/\text{mL}$, *M. crassifolia* (J) 50 $\mu\text{g}/\text{mL}$, (K) 100 $\mu\text{g}/\text{mL}$, (L) 150 $\mu\text{g}/\text{mL}$, (M) 200 $\mu\text{g}/\text{mL}$, *R. stricta* (N) 12.5 $\mu\text{g}/\text{mL}$, (O) 25 $\mu\text{g}/\text{mL}$, (P) 50 $\mu\text{g}/\text{mL}$, (Q) 75 $\mu\text{g}/\text{mL}$, (R) 100 $\mu\text{g}/\text{mL}$, *T. macropterus* (S) 50 $\mu\text{g}/\text{mL}$, (T) 100 $\mu\text{g}/\text{mL}$, (U) 150 $\mu\text{g}/\text{mL}$, (V) 200 $\mu\text{g}/\text{mL}$, over 48 h (N=3). The red dashed lines at 0 h represent the initial scratch wound. Images were obtained at a magnification of 10x, and each scale bar represents 100 μm

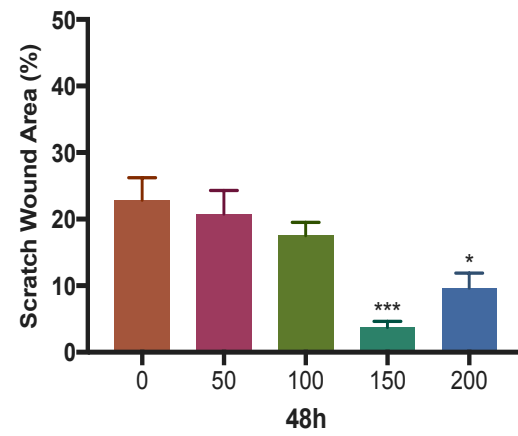
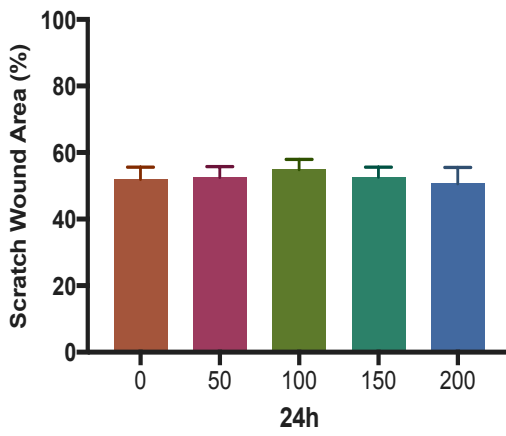
A)



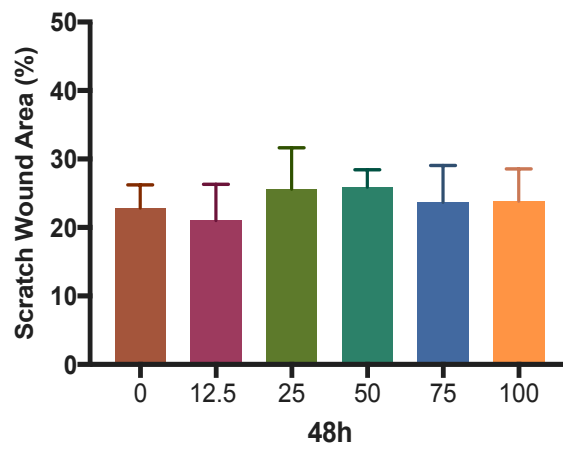
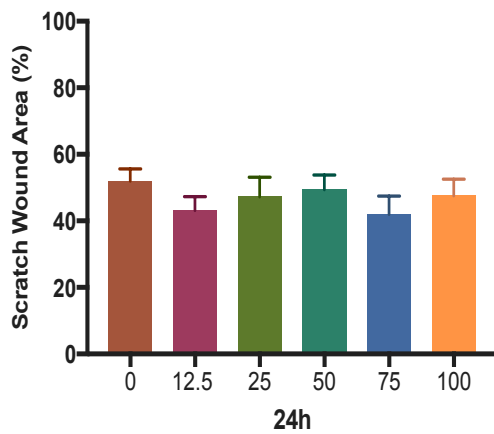
B)



C)



D)



E)

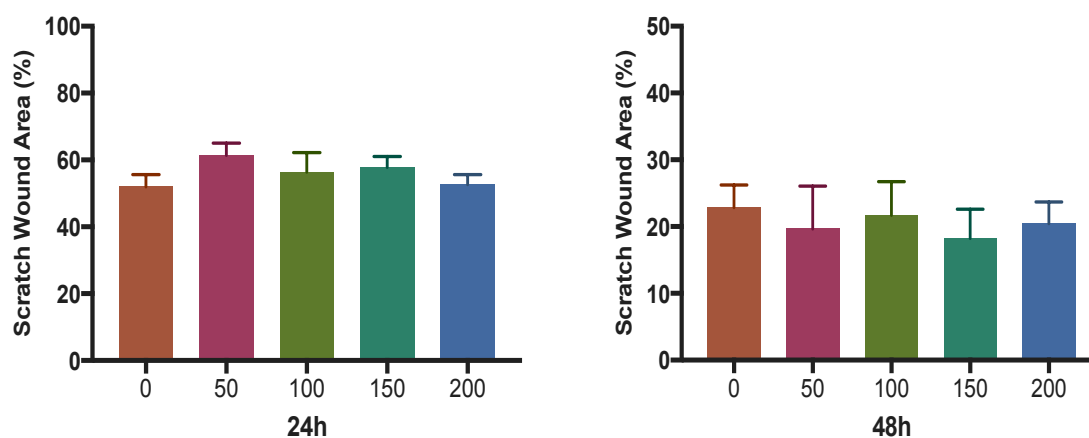


Figure 49 Analysis of wound area (uncovered area) in HaCaT cells following scratch wound, treated with (A) *A. canariense* (200, 150, 100, and 50 µg/mL), (B) *C. colocynthis* (25, 20, 15 and 10 µg/mL), (C) *M. crassifolia* (200, 150, 100, and 50 µg/mL), (D) *R. stricta* (100, 75, 50, 25, and 12.5 µg/mL), and (E) *T. macropterus* (200, 150, 100, and 50 µg/mL) at 24 h and 48 h. (mean ± SE). Results were obtained through three independent experiments. Statistical analysis of significant changes compared to control (0 µg/mL) (*p<0.05, **p<0.01, *p<0.001)**

Keratinocyte migration and proliferation are the key factors of the epidermal wound healing process. Since cells migrate early in the wound healing process, their inability to do so delays healing even when proliferation is maintained. As a result, wound healing relies heavily on cell migration (Ettenson and Gotlieb, 1994; Shaw and Martin, 2009).

In this study, we examined the effect of selected medicinal plants on HaCaTs migration. HaCaTs are immortalised cells that can carry the functional activities and express all the primary surface markers of primary keratinocytes. Furthermore, they can be cultured for a long term without growth factors (Schürer et al., 1993; Micallef et al., 2009). Therefore, many studies have utilized the HaCaT cell line to evaluate the wound healing potential of different treatments (Fouché et al., 2020; Moses et al., 2020).

Figure 48 (M, L) and Figure 49 (C) indicates that *M. crassifolia* promotes cell proliferation and migration in HaCaT cells. Moreover, this could explain it is traditional to use by applying it to the wounds (Volpato et al., 2012). Volpato et al. (2012) reported the plant usage by Sahrawi refugees displaced to refugee camps in southwestern Algeria. Burned plant leaves are used as a poultice, antiseptic for wounds, boils, and irritation. The leaves are administered as a powder or combined with water to form a poultice. Another ethnobotanical study conducted in Tarfaya, Morocco, showed a similar traditional application of the medicinal plant to wounds by local populations (Idm'hand et al., 2020). Although methanol and water have similar profiles for extracting various compounds, both have a high extraction efficiency (Borges et al., 2020). Furthermore, water extraction might enhance polyphenol yield by increasing diffusion through plant tissues (Altiok et al., 2008). Therefore, it would be interesting to investigate the effect of *M. crassifolia* aqueous extracts on the migration and proliferation of HaCaT.

Few studies have examined the antiinflammatory, antimicrobial, and antioxidant properties of *M. crassifolia* (Akuodor et al., 2014; Ckilaka et al., 2015). However, to the best of our knowledge, wound-healing abilities of *M. crassifolia* have not been examined. Chronic wounds often display several features, including elevated levels of pro-inflammatory cytokines, proteases, and ROS, persistent infection, and reduced migration (Dickinson and Gerecht, 2016). Thus, *M. crassifolia* could be a potential alternative therapy for chronic wounds, since it can induce keratinocyte proliferation and migration. This could be related to its capacity to ROS and inhibit inflammatory mediators.

It is crucial to identify if the previously established enhanced proliferation could influence the findings of scratch repopulation, since the increased number of cells will accelerate wound closure. Therefore, future studies are required to assess the migratory action in the presence of

an anti-proliferative agent and utilise fibroblast cell line to determine the proliferative and migratory abilities on a different skin layer. Furthermore, the mechanism through which *M. crassifolia* reveals wound-healing characteristics need to be investigated in more depth through gene analysis.

Although *R. stricta* did not influence the proliferation or migration of HaCaT cells, a previous study examining the wound healing capacity of *R. stricta* in rats using an *in vivo* model reported a delayed acceleration in the wound closure, following topical administration for seven days (Khaksari et al., 2000).

4.6 Conclusion

R. stricta and *M. crassifolia* showed the maximum capacity for DPPH radical scavenging, with IC₅₀ values of 335 and 448 µg/mL, respectively. Moreover, *R. stricta* exhibited the highest H₂O₂ scavenging activity in the cell-based antioxidant assay and it demonstrated the highest total phenolic content among others. In addition, HaCaT cells treated with *M. crassifolia* at concentrations of 200 and 150 µg/mL exhibited increased migratory activity, which could accelerate the wound healing response by reducing wound-associated ROS activity. Although the topical application of these medicinal plants requires further investigation in terms of penetrations of different skin layers, the findings reveal a promising potential for *R. stricta* and *M. crassifolia* applications.

Chapter 5: Antimicrobial Activities of Plant Extracts and Fractions

5.1 Introduction

Skin and soft tissue infections (SSTIs) have a wide range of clinical presentation, origin, and severity, ranging from minor to life-threatening infections. In addition to the aging population, increased critical illness, the increase in immunocompromised patients, and the introduction of multidrug-resistant bacteria, there has been an increase in the cases of SSTIs (Esposito et al., 2011; Moffarah et al., 2016). SSTIs affects 7-10% of hospitalised patients and are highly common in emergency care (Vinh and Embil, 2005). Due to the variable presentation of SSTIs, estimating their prevalence and incidence has been challenging. Nevertheless, the incidence rate of SSTIs is predicted to be 24.6 per 1000 person-year (Simonsen et al., 2006).

The skin serves as a barrier to the external environment that is also host to a diverse surface microbiota of bacteria, viruses, and fungi. The skin microbiota supports body defense and immunological responses, prevents colonization by pathogenic or opportunistic microorganisms, promotes tissue regeneration, and supports barrier functions. On the other hand, the skin provides habitats and nutrients for the existence, competition, and collaboration of microorganisms within the skin (Fredricks, 2001; Lee et al., 2006; Chambers and Vukmanovic-Stejić, 2020).

A variety of factors influence skin microbiota. Age, gender, skin site, level of hygiene and the type of cleansers used, climate, occupation, and if an individual is hospitalised are all factors considered. Temperature and humidity can also substantially impact microbial populations and composition (Wilburg et al., 1984; Larson et al., 2000). Microbiota is almost composed entirely of bacteria. Gram-positive microorganisms such as *Staphylococcus aureus*, *Staphylococcus epidermidis*, *Corynebacterium* species, and *Streptococcus pyogenes* colonise the skin above the waist. Moreover, the common microorganisms colonizing the skin below the waist include

Gram-positive and Gram-negative species (Ki and Rotstein, 2008). These microorganisms may cause infection if the delicate balance between the host and microorganism is disrupted. Exogenous (such as hand washing) and endogenous (for instance, genetic variation that promotes a particular microbial population) disturbances can influence the host–microorganism relationship (Moellering, 2010; Grice and Segre, 2011). Even though commensal microorganisms usually live in human bodies in a non-pathogenic manner, many are capable of causing illness under the appropriate circumstances. In addition, various opportunistic bacteria prevalent in the normal skin microbiome often cause infection in chronic, non-healing wounds, which are frequent in diabetes patients and the geriatric population. The immune response to these microorganisms will cause persistent inflammation, exacerbating the condition (Grice et al., 2010; Grice and Segre, 2012; Gardner et al., 2013; Misisic et al., 2014).

Chronic wounds result from impaired multifactorial elements in the wound healing process. They are characterised by failing to proceed through the usual phases of wound healing in the same order and time as acute wounds (Järbrink et al., 2016). In chronic wound infection, bacteria can live as free-floating organisms or as colonies enclosed in a protective extracellular polymeric substance (EPS), called biofilm. Polysaccharides, proteins, lipids, and extracellular DNA makes up the usual EPS matrix (Roche et al., 2012). Chronic wounds provide a desirable environment for biofilm development; skin debris and necrotic tissues are prone to infection, and abnormal vascularisation and associated ischemia hinder the immune system from establishing an adequate defensive response (Zhao et al., 2013). Biofilm-forming bacteria are thought to colonise 60% of chronic wounds, compared to just 6% of acute wounds (James et al., 2008). However, many species are capable of forming biofilm, including *Staphylococcus*

aureus and *Pseudomonas aeruginosa*; they are the two most prevalent microorganisms responsible for wound biofilm formation (Percival et al., 2012). The most common chronic wounds are diabetic ulcers, pressure ulcers, and venous stasis ulcers. Chronic wounds facilitate bacterial growth due to reduced oxygen, necrotic debris, microenvironment, and a weakened immune system (Wu et al., 2019). One of the major complications of chronic wounds is the life-threatening sepsis associated with bacteraemia (Brem et al., 2001). Comparison between planktonic and biofilm bacteria is presented in Figure 50.

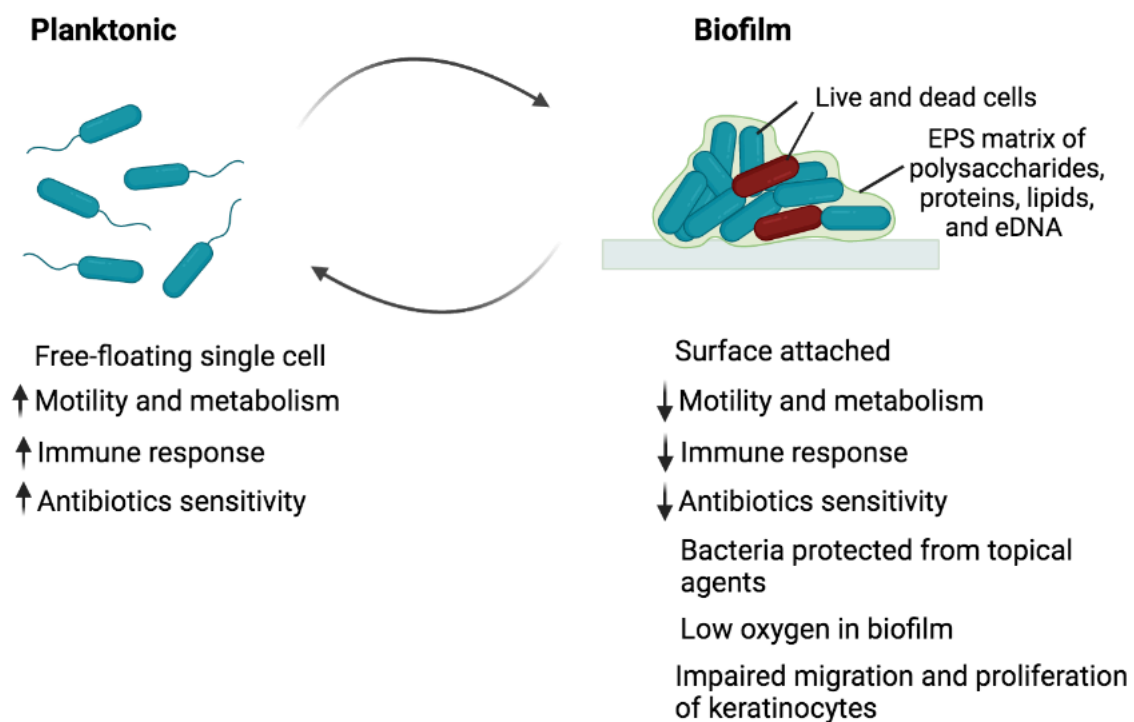


Figure 50 Characteristics of planktonic and biofilm bacteria. The biofilm's extracellular polymeric substance (EPS) matrix provides further antibiotic resistance, resulting in the emergence of multi-drug resistant microorganisms. Cell-to-cell communication inside the biofilm is achieved through quorum sensing (QS) (created using BioRender.com)

5.1.1 Antibiotics Resistance in Bacterial Biofilm

Bacterial biofilm development poses a significant challenge in the treatment of wound infections, as the biofilm matrix is believed to be one of the significant reasons that antibiotics become ineffective. Chronic infections are facilitated by the antibiotic resistance of bacteria in biofilm colonies. Biofilm bacteria are responsible for about 80% of chronic and recurring microbial infections in the human body. Microorganisms inside biofilm are 10 to 1,000 times more resistant to antibiotics than planktonic microbes (Mah, 2012). The resistance mechanisms of biofilm cultures, such as drug-neutralising proteins, efflux pumps, decreased cell permeability, drug-modifying enzymes, and target site mutations, differ from those of planktonic cultures (Beauclerk and Cundliffe, 1987; Walsh, 2000; Magnet et al., 2001; Nikaido, 2003; Kumar et al., 2013; Lata et al., 2015; Sharma et al., 2016). However, it has previously been reported that antibiotic resistance is made possible by conventional resistance mechanisms expressed in biofilms. Biofilm-forming *P. aeruginosa*, for instance, can produce chromosomal β -lactamase, enabling it to develop resistance to ceftazidime (Bagge et al., 2000).

The efflux pumps formed in *P. aeruginosa* biofilms have been shown to eliminate antibiotics. In addition, the complexity of these biofilms enhances their potential to cause infections by protecting bacteria from the host immune system and antibiotics (De Kievit et al., 2001; Stewart and Franklin, 2008). Antibiotic resistance emerges within biofilm cultures through a variety of mechanisms, including the biofilm's ability to change the chemical microenvironment (Zhang and Bishop, 1996; Xu et al., 2000), a subpopulation of microorganisms within the biofilm (Das et al., 1998; Cochran et al., 2000), the antibiotics' inability to fully or partially penetrate the biofilm due to the EPS matrix (Stewart, 1998; Mah and O'Toole, 2001). These processes contribute to the antibiotic resistance observed in biofilm

cultures and directly result from biofilms' multicellular structure (Davies, 2003). Mupirocin and fusidic acid are routinely prescribed topical antimicrobial agents for the treatment of skin and soft tissue infections (Banerjee and Argáez, 2018). The resistance rate to those topical antibiotics is rising rapidly against many strains of *S. aureus* (Simor et al., 2007; Alsterholm et al., 2010; Chaturvedi et al., 2014).

Currently, antibiotics are the first-line treatment for bacterial biofilm infections. Bacteriophage therapy, antisense nucleic acid approach, quorum sensing (QS) system inhibitors, monoclonal antibodies, immunomodulators, and antibiotic potentiators are some of the alternative conventional therapies that have been developed (Tse et al., 2017). Large doses of effective and highly penetrative antibiotics are frequently used to ensure that an appropriate concentration of antibiotics reaches the biofilm-infected site (Hengzhuang et al., 2012; Wu et al., 2015). However, the efficacy of antibiotics has declined over time due to the emergence of resistance and the growing concern over their adverse effects. Alternative therapies have many limitations, including the need for a comprehensive diagnostic evaluation before therapy, high costs, and a poor safety profile (Tse et al., 2017; Theuretzbacher and Piddock, 2019). The effectiveness of medicinal plants in preventing and treating infections caused by bacterial biofilms is unique. *In vitro*, several plant extracts display antibacterial and antibiofilm activities. Plant extracts can inhibit biofilm formation and the biofilm-regulating quorum sensing mechanism. They prevent the formation of biofilms and the QS system by blocking the attachment and adhesion of bacterial cells, the production of bacterial virulence factors, and the creation of a polymeric extracellular matrix. Medicinal plants present a crucial step toward developing innovative antibiofilm treatments (Karbasizade et al., 2017; Lu et al., 2019).

In the context of this study, the following bacteria, *S. aureus*, MRSA, and *P. aeruginosa*, are of particular interest. *Staphylococcus aureus* is a Gram-positive extracellular species that is the leading cause of skin and soft tissue infections, such as impetigo and infected abrasions, and complicated SSTI such as cellulitis, folliculitis, and wounds and infected ulcers (McCaig et al., 2006). *S. aureus* is a common component of human skin microbiota. Furthermore, it colonises the nasal mucosa and exhibits opportunistic pathogen activity (Gordon and Lowy, 2008). The pathogenicity of *S. aureus* is attributed to a range of virulence factors, such as exfoliative toxins, enterotoxins, and panton-valentine leukocidin (Otto, 2014); as a result, the expression of these virulence factors can cause infections in healthy persons. In addition, different strains of *S. aureus* exhibit methicillin resistance (MRSA) or multi-drug resistance (MDR). MDR, in contrast, is defined as acquired resistance to three or more classes of antibiotics (Archer et al., 2011). Methicillin resistance is often caused by *mecA* and *mecC*, found on the *Staphylococcal* chromosomal cassette *mec*, leading to broad-spectrum resistance to all β -lactam antibiotics (Paterson et al., 2014).

P. aeruginosa is a widely distributed Gram-negative rod-shaped bacterium that thrive in various environments (Crone et al., 2020). It is regarded as an opportunistic infection for humans and linked with significant morbidity and mortality (Dolan, 2020). *P. aeruginosa* expresses a variety of virulence factors, and its ability to switch between planktonic and biofilm-based formation allows it to avoid the immune system and antimicrobial agents (Thi et al., 2020). Antibiotic-resistant strains of bacteria, such as MRSA, have been a significant issue in treating this type of infection (Lim et., 2018).

Natural products have been used to treat microbial infections since ancient times. They have provided antimicrobial agents for many years, beginning with the breakthrough discovery of

penicillin from *Penicillium rubens*. However, in the last decade, trends have shifted from discovering new agents to improving currently existing antimicrobial agents by discovering new analogs (Moloney, 2016). Reasons behind such a change could be credited to the regulatory guidelines for approving a new class of antimicrobial agents. Furthermore, the escalating cost of discovering new agents has rendered it not worth the risk financially. Consequently, no new class of antimicrobial agent against Gram-negative bacteria have been discovered since the late-1980s (Silver, 2011; Hoffman, 2020). One of the main challenges with current antimicrobial agents is widespread antimicrobial resistance (AMR), which accounts for 25,000 deaths per year in the EU (European Centre for Disease Prevention and Control). The evolution of multidrug-resistant bacteria capable of resisting commonly used antibiotics has recently been a significant concern.

The continually emerging AMR has called for drastic changes in discovering new antimicrobial agents. Antimicrobial resistance is a growing problem, yet it is not unprecedented. Microbes have always possessed the ability to develop mechanisms to resist antibiotics. Medicinal plants are affordable and easily accessible; and plant extracts could have a broad spectrum of activity against several microbes, and frequently have immunomodulatory effects. In addition, the diverse chemical structures of the broad array of plant-derived secondary metabolites can be exploited in the search for new therapeutic agents (Freire-Moran et al., 2011; Subramani et al., 2017; Gorlenko et al., 2020).

5.2 Chapter Aim and Objectives

This chapter aims to demonstrate the antibacterial and bactericidal activity of different plant extracts and fractions, following a bioassay-guided fractionation approach, against a panel of pathogens clinically implicated in skin infections.

- To determine the number of colonies forming units of a bacterial suspension for experimental work using the Miles and Misra drop count method.
- To develop and optimize an assay capable of determining the antibacterial activity of plant extracts through agar well diffusion assay.
- To develop and optimize an assay capable of determining minimum inhibitory and minimum bactericidal concentrations of plant extracts through broth microdilution assay.
- To develop and optimize a method for identifying compounds exhibiting antibacterial activity within active plant extracts using the bio-autographic assay.
- To develop a method for determining the ability of plant extracts on *S. aureus*, *MRSA*, *S. epidermidis*, *E. coli*, and *P. aeruginosa* bacterial biofilm formation and eradication.

5.3 Materials

5.3.1 Chemicals and Culture Media

Chemicals, reagents, solvents, Mueller Hinton agar (MHA), and broth (MHB) were acquired from ThermoFisher Scientific (Loughborough, UK). In addition, 96-well plates (black, flat bottom, clear glass bottom, sterile, treated, individually wrapped with lid, polystyrene plate) were purchased from Greiner Bio-One Ltd (Stonehouse, UK), and 96-well microplates (flat

bottom, transparent, sterile, tissue culture-treated surface, polystyrene plate) were acquired from Sarstedt (Leicester, UK). All supplemented media were prepared according to manufacturer instructions and were sterilized through an autoclaving process at 123 °C for 15 min.

5.3.2 Bacterial Cultures

SSTI-causing microorganisms were used to investigate the antibacterial activity of plant extracts: *Staphylococcus aureus* 12973 from the National Collection of Type Cultures (NCTC, UK), Methicillin-resistant *Staphylococcus aureus* (MRSA) 13373 from the National Collection of Type Cultures (NCTC, UK), *Staphylococcus epidermidis* 14990 from the American Type Culture Collection (ATCC, USA), *Pseudomonas aeruginosa* 6749 from the National Collection of Type Cultures (NCTC, UK), *Escherichia coli* (MS2) 15597 from the American Type Culture Collection (ATCC, USA), *Propionibacterium acnes* 737 from the National Collection of Type Cultures (NCTC, UK). In addition, Microbank cryoprotective beads purchased from Pro-Lab Diagnostics Ltd (Birkenhead, UK) were utilized to freeze bacterial cultures at -80 °C until needed.

5.4 Methods

5.4.1 Preparation of Samples

Five samples of the five plant extracts; *A. canariense*, *C. colocynthis*, *M. crassifolia*, *R. stricta*, and *T. macropterus*, were prepared by dissolving in 1% methanol at a final concentration of 20 mg/mL and a control vehicle of 1% methanol was prepared.

5.4.2 Freezing Bacterial Strains

The continuous supply of required bacterial strains was accomplished by utilising cryoprotective beads according to manufacturer instructions for long-term storage at -80 °C. Then, using a sterile inoculating loop, 3-5 colonies of pure overnight culture (18 to 24h) were introduced to the beads, followed by shaking the beads for seconds and allowing them to sit to ensure the binding of bacteria to the beads. Finally, the beads solution was carefully aspirated, tightly closed, and stored at -80 °C.

5.4.3 Bacterial Overnight Culture

50 mL falcon tubes containing 20 mL of MHB were inoculated with pure colonies from required bacteria through inoculation loops or directly from stored inoculated cryoprotective beads. Tubes were placed in a shaker (Thermo Scientific MAXQ 4450) at 100 rpm for overnight incubation at 37 °C. The following day, tubes were centrifuged at 4000 rpm for 10 min, the supernatant was removed, and the pellet was resuspended in 1 mL PBS. The pellet was washed twice with PBS, and the optical density (OD) at 600 nm was adjusted based on the needed bacterial cell count.

5.4.4 Preparation of Bacterial Slope

50 mL falcon tubes were filled with 25 mL of MHA and placed at a 45° angle for a while. Subsequently, the slope's surface was coated with a loop from an overnight culture of bacteria (Section 5.4.3). Bacterial slopes were placed in the incubator at 37 °C for 24 h and then stored in the fridge at 2-4 °C to be used for 2 weeks.

5.4.5 Bacterial Counting by Miles and Misra Method

Following the Miles and Misra approach, the number of colony-forming units in a bacterial solution was calculated (Miles and Misra, 1931). In which an overnight culture of required bacteria was centrifuged at 4000 rpm (Mistral 1000. London, UK) for 10 min, the supernatant was discarded. The pellet was reconstituted in 1 mL PBS and transferred to an Eppendorf tube to be further washed multiple times with 1 mL PBS and centrifuged at 10,000 g for 1 min before being resuspended in PBS and mixed thoroughly to ensure the full suspension of microbes. Using a spectrophotometer (Ultrospec 3100 pro, Amersham BioSciences Ltd., Buckinghamshire, UK), optical density (OD) was measured at 600 nm and suspension was adjusted to the following readings; 0.9, 0.7, 0.5, 0.3, 0.1, 0.05. Each OD was serially diluted by adding 100 μ L of bacterial suspension to 900 μ L of PBS until the desired 8 to 10 dilutions were attained. Then 20 μ L of each dilution was applied to the surface of MHA agar plates in three replicates. The drops were then dried and incubated for 24 h at 37 °C. The next day, colonies in each drop were counted, and colony-forming units (CFU) were determined using the following equation:

$$\text{CFU per mL} = 100 \times \text{average number of colonies for each dilution} \times \text{dilution factor}$$

Average colony-forming units were plotted against average optical density, and standard curves were produced according to the Miles and Misra method. Finally, a linear equation from each curve would be used to determine the desired bacterial concentration CFU/mL. Figures 51, 52, and 53 presents standard curve graphs of *MRSA*, *P. aeruginosa*, and *E. coli*.

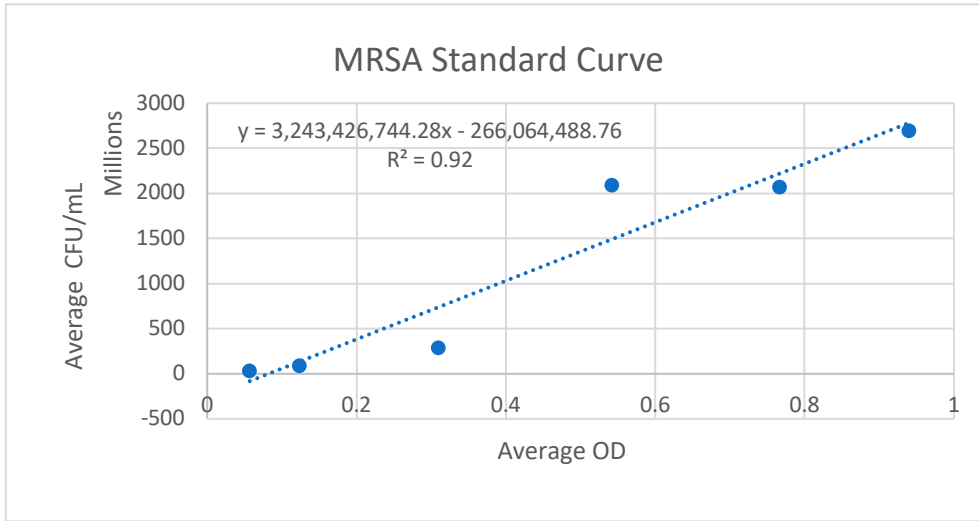


Figure 51 MRSA standard curve

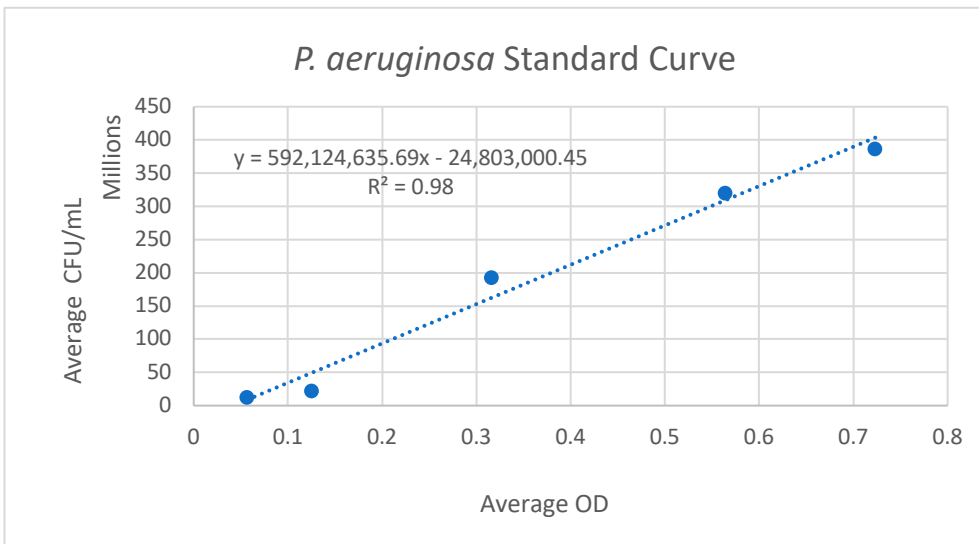


Figure 52 *P. aeruginosa* standard curve

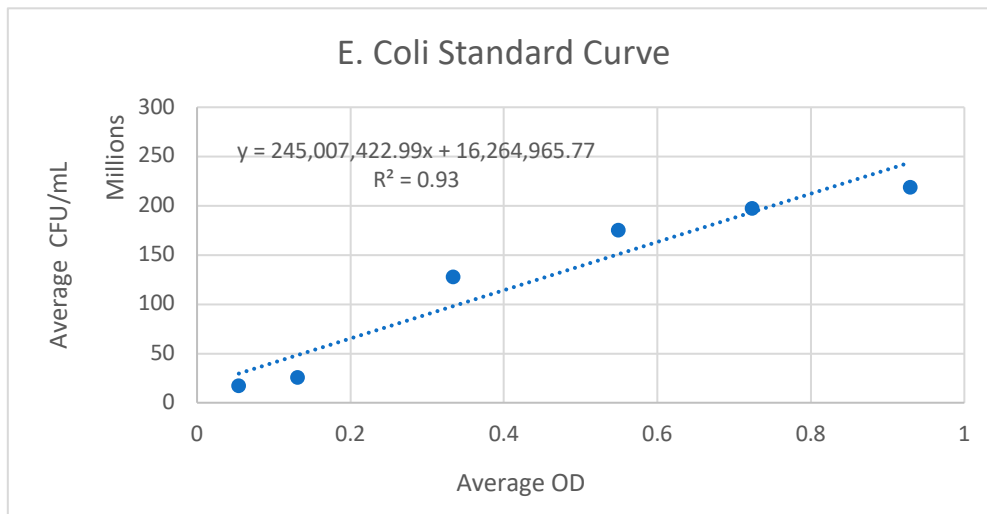


Figure 53 *E. coli* standard curve

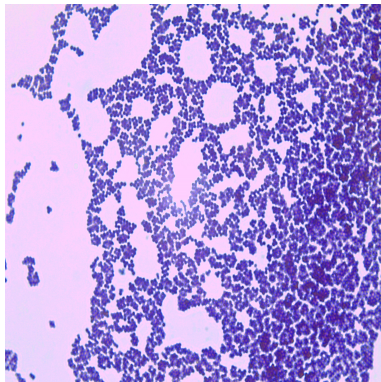
5.4.6 Bacteria Gram Staining

To examine the structure of bacteria and distinguish between Gram-positive and negative bacteria under microscope, the Gram staining method was performed. A few drops of sterile distilled water were added to the surface of the microscope slide, then an inoculated loop of desired bacteria colony was spread across the slide and left to dry, then fixed with heat. Finally, the following reagents were added to the slide:

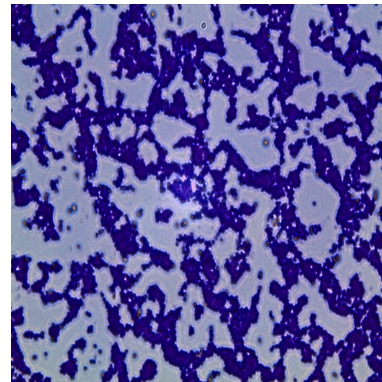
- The slide was submerged in crystal violet solution for 1 min.
- Water was applied to remove unwanted stains from the slide.
- Gram's iodine solution was poured over the slide and left for 1 min.
- Water was applied to remove unwanted stains from the slide.
- The additional colour was removed from the slide by adding 95% ethanol.
- Water was applied to eliminate ethanol from the slide.
- The slide was flooded with Safranin solution and allowed to sit for 10 s.

- The slide was cleaned with water to remove excess stain and then dried with paper towels by gently blotting.
- Slides were examined under a light microscope using an oil immersion (100x) objective (Figure 54 A-E).

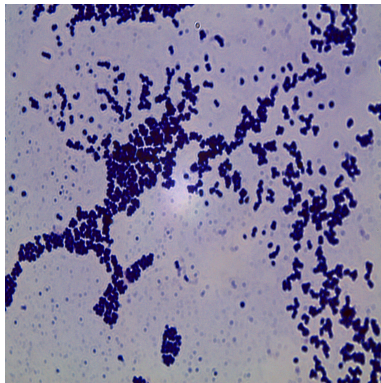
A



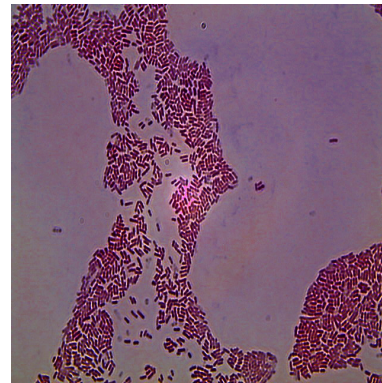
B



C



D



E

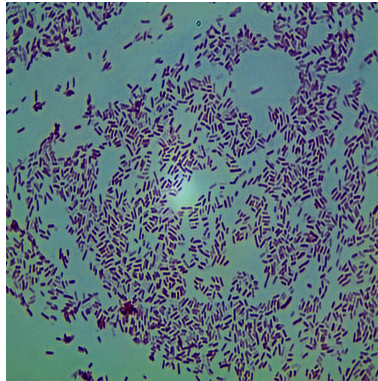


Figure 54 Obtained images under a light microscope of Gram-stained (A) *Staphylococcus aureus*, (B) MRSA, (C) *Staphylococcus epidermidis*, (D) *P. aeruginosa*, and (E) *E. coli*

5.4.7 Agar Well Diffusion Assay

It is regarded as one of the most commonly used qualitative methods for screening the antimicrobial property of plant extract, first introduced by Heatley in the 1940s for testing penicillin activity (Heatley, 1944). The benefits of the application of the well diffusion method include the low sample volume needed and the ability to compare up to six samples against the same microbe on a single plate. However, it is not suitable for samples with low polarity or hard to diffuse into the aqueous agar (King et al., 2008; Klančnik et al., 2010). In this method, a well is punched from the surface of the agar plate that was previously inoculated with bacterial suspension. Subsequently, the well is filled with plant extract at a given concentration then plant extract will diffuse through the agar and form a clear zone. The diameter of the clear zone is directly proportional to the concentration of antimicrobial compounds present in the extract and diffusion rate through the agar. Consequently, this approach was used to examine the antibacterial properties of several plant extracts, including *A. canariense*, *C. colocynthis*, *M. crassifolia*, *R. stricta* and *T. macropterus*.

The supernatant from an overnight culture of the desired bacteria was removed, and the pellet was reconstituted in PBS and mixed thoroughly to achieve the total suspension of the bacteria. The OD₆₀₀ of bacterial suspension was measured and adjusted to the desired concentration of 1×10^6 CFU/mL. Next, 150 μ L of bacterial suspension was added to the agar plate then a bacterial spreader was used to spread bacteria on a clockwise rotation evenly. Plates were left to dry for a few minutes then a cork borer (sterilized with 95% ethanol) was utilized to punch four wells in each plate to produce a well with a diameter of 5 mm. Finally, 100 μ L of plant extract was applied to each well, and then plates were incubated for 24 h at 37 °C.

Negative control of 1% methanol and positive control of 0.1% thymol 1 mg/mL (Sigma-Aldrich Company Ltd, Poole, UK) was included in each experiment. Thymol is a phenolic compound isolated from plant extract belonging to the *Lamiaceae* family (Thymus and Origanum) with an established antimicrobial activity (Marino et al., 1999; Mancini et al., 2015). Thymol exhibits antibacterial activity by disrupting bacterial cell membranes (Kachur and Suntres, 2020). Following 24 h incubation zone of inhibition for extracts and controls was measured in millimeters using a digital caliper (Traceable™, ThermoFisher Scientific). The diameter of the well was subtracted from each reading.

5.4.8 Broth Microdilution Assay to Determine Minimum Inhibitory and Minimum Bactericidal Concentrations

The method used was adapted from the Clinical and Laboratory Standards Institute (CLSI) published guidelines, with minor modifications to evaluate the antimicrobial activity of natural products. The benefits of this method include greater sensitivity for lower extract quantities, a quantitative approach, the ability to distinguish between the bacteriostatic and bactericidal

action of the extracts, and the ability utilise high-throughput screening with 96-well plates to identify the exact concentrations that inhibit growth (MIC) and that eradicate it (MBC) (Langfield et al., 2004).

An overnight culture of desired bacteria was prepared, and sterile filtered (0.22 μm) samples (plant extracts) were prepared with 1% methanol at a final concentration of 80 mg/mL and diluted with double strength MHB to prevent the loss of MHB nutrition by the dilution process at a ratio of 1:1. A serial dilution of samples was carried out across the 96-well plates with 100 μL MHB in each well starting from the concentration of 20 mg/mL to 156.25 $\mu\text{g/mL}$ negative control of 1 % methanol and positive control thymol concentration of 5 mg/mL to 39 $\mu\text{g/mL}$. Each experiment also contained sterility well with 100 μL of broth. Directions for making the bacterial suspension for the agar well diffusion experiment were followed (Section 5.4.7).

The OD600 of bacterial suspension was measured and adjusted to the desired concentration of 1×10^6 CFU/mL, according to the previously described Miles and Misra Drop Counting Method. Apart from sterility wells, each well was inoculated with 100 μL of bacterial suspension with a final bacterial concentration of 5×10^5 CFU/mL. After 24 h of incubation at 37 °C, MIC we measured by visualization of each well turbidity (bacterial growth) following CLSI standards. The minimum sample concentration with clear wells was set as MIC.

The MBC of each sample was determined by sub-culturing wells into a freshly prepared MH agar plate by dropping 10 μL aliquots from each well in triplicate onto the agar surface and then incubating it for 24 h at 37 °C. The minimum concentration of samples that showed no

growth of bacterial colonies was recorded as an MBC. All experiments were conducted in three replicates, and each run included positive and negative controls.

5.4.9 Detecting Antimicrobial Compounds Through Bio-Autographic Assay

The paper-based bio-autography assay was introduced first by Goodall and Levi, to identify the presence and estimate the amount of Penicillin in a mixture. Later in the 1960s, thin layer chromatography was utilized to identify antibiotics. This assay employs the previously described TLC separation technique (Section 2.4.4), to detect the presence of active antimicrobial compounds within a plant extract or fraction (Goodall and Levi, 1946).

Stock solutions of five plant extracts were prepared in methanol (concentration 10 mg/mL), and positive control of 0.1% thymol in methanol (1 mg/mL) was included in each experiment. Extracts and fractions were spotted on the surface of TLC plates and then placed into a developing tank filled with a suitable solvent system for optimum separation of analytes. Once developed, plates were transferred to the fume cupboard to remove any trace of solvents.

Overnight cultures of *S. aureus*, MRSA and *P. aeruginosa* were centrifuged at 4,000 RPM for 10 min, then the supernatant was discarded, and the pellet was reconstituted in PBS and mixed thoroughly to ensure the complete suspension of bacteria. Bacteria suspension was rinsed multiple times with PBS, and then the pallet was reconstituted in MHB and gently mixed with a vortex. The optical density (OD) was adjusted to 1×10^6 CFU/mL using the Miles and Misra Drops Counting Method. Each TLC plate was sprayed evenly with inoculated broth and positioned horizontally in a cabinet with the laminar flow for 5 min, to allow any excess solution to evaporate. The plates were then placed in a sterile container and incubated vertically at 37 °C for 24 h.

The next day, plates were placed in a laminar flow cabinet and sprayed with the visualising agent tetrazolium salt, 2,3,5-triphenyl tetrazolium chloride, which was prepared by suspending 2 mg/mL in distilled water. Plates were then incubated at 37 °C for 4 h. The tetrazolium salt will be converted to a brightly coloured formazan by metabolically active bacteria; antimicrobial compounds will exhibit a clear zone on a red background. The Rf values of active antimicrobial compounds within extracts and fractions were recorded in three separate experiments. This assay has been intensively used as a qualitative tool for identifying active compounds within a mixture of plant extracts. Moreover, it has been successfully utilised to determine antioxidant and antimicrobial and to screen for inhibitory compounds against specific enzymes (Purkait et al., 2020; Legerska et al., 2020).

5.4.10 *In Vitro* Assessment of Plant Extracts on Biofilm Formation and Biofilm Eradication

5.4.10.1 Evaluating the Ability of Selected Bacterial Species to Form a Reproducible Biofilm

This experiment was conducted to examine the capacity of the selected microorganisms to adhere to and form a biofilm. In addition, crystal violet was utilised to determine the biofilm's biomass. Each well of a 96-well plate was inoculated with an overnight bacterial suspension containing 10^8 CFU/mL, and the plate was then incubated for 24 h at 37 °C in aerobic conditions (Coffey and Anderson, 2014). After 24 h, each well's supernatant was gently removed not to disrupt the biofilm at the bottom of every well. To eliminate free-floating bacteria, wells were rinsed multiple times with 100 µL of distilled water. Next, the plate lid was slightly opened for 15 min, to air dry the wells and remove traces of the previous washing

step. Next, the wells were stained using 1% crystal violet (100 µL/well) made with distilled water, and the plate was then incubated at room temperature for 30 min. The unbound crystal violet was eliminated by washing the wells three times with 100 µL of distilled water per well and air-drying them for 15 min at room temperature. Next, 100 µL of 95% ethanol was applied to each well to dissolve the bound crystal violet, and the plate was incubated for 20 min with gentle shaking to achieve total dissolution. The absorbance at 570 nm was recorded using a microtiter plate reader (Tecan Infinite, Tecan Trading, Männedorf, Switzerland). The results were presented as the mean for each strain \pm standard error (SE), and results were obtained through three independent experiments.

5.4.10.2 Assessment of Plant Extracts Effect on Biofilm Formation and Biofilm Eradication

As previously described, overnight bacterial suspensions were prepared. The adapted spectrophotometric technique was utilised to conduct biofilm inhibition experiments in a 96-well plate (Celiksoy et al., 2021). First, 100 µL of plant extracts showed antimicrobial activity at different concentrations for *R. stricta* MIC concentration and one-half of the minimum inhibitory concentration (MIC/2), and 1.25, 2.5 mg/mL for *A. canariense* and *T. macropterus* were added to each well. Then 100 µL bacterial suspension (10^8 CFU/mL) was added to each well. Next, separate background 96 well plates (tissue culture-treated surface, polystyrene plate) without bacterial inoculation were prepared by adding 100 µL of previously prepared treatments at specific concentrations with 100 µL MH broth. Twenty-four hours were dedicated to incubating plates under aerobic conditions at 37 °C. Following the initial incubation period, the solution was carefully removed from each well, rinsed multiple times with 100 µL of distilled water per well, and air-dried for 15 min. After adding 100 µL of 1%

solution of crystal violet, the mixture was incubated for 30 min at room temperature. After removing the crystal violet and carefully washing the wells three times, 95 % ethanol was added (100 μ L/well) and incubated for 20 min. The OD of plates was measured at 570 nm. To minimise the non-specific binding of crystal violet, OD treatments and OD controls were calculated by subtracting the background OD values of compounds (without bacterial inoculation) from the original OD values. The below equation was used to determine the percentage of biofilm inhibition:

$$\text{Percentage of biofilm inhibition} = 100 - [(\text{OD of treatment}/\text{OD of control}) \times 100].$$

Using a similar methodology, the potential of plant extracts to eradicate biofilms was examined. In summary, a plate containing the investigated bacteria was developed and incubated for 24 h at 37 °C under aerobic conditions to assure biofilm formation. After the incubation period, the supernatant was gently removed from every well, fresh plant extracts at the previously determined concentration were added, and the biofilm inhibition procedure was repeated. Finally, the percentage of biofilm eradication was estimated using the same procedure and equation applied in inhibiting biofilm formation.

5.4.10.3 Live/Dead Imaging of Plant Extract-Treated Biofilms Using Confocal Laser Scanning Microscopy

In order to determine the effect of active plant extracts on biofilms in 96-well glass bottom plates (Greiner Bio-One Ltd, Kremsmünster, Austria), a Live/Dead BacLight™ (ThermoFisher Scientific) bacterial viability experiment was conducted. This assay was adapted from Celiksoy et al. (2021). First, an overnight bacterial suspension was adjusted to the desired concentration of 1×10^8 CFU/mL, then 100 μ L was applied to a 96-well glass bottom plate, which was then

incubated at 37 °C for 24 h. The next day, the supernatant was carefully aspirated from every well, and freshly prepared plant extracts at the same concentration stated previously (Section 5.4.10.2) were applied. The plate was then incubated at 37 °C for an additional 24 h.

The plate's supernatant was discarded after the incubation time. Then, each well was stained with 4 µL/well of Live/Dead stain, which was made according to the directions of the Live/Dead Bacterial Viability kit by mixing 2 µL of SYTO 9 (stain live cells) and 2 µL of propidium iodide (stain dead cells) diluted in 1 mL of PBS. The stain was carefully applied to the middle of the well to avoid disturbing the biofilm. The plate was incubated at 37 °C for ten min at room temperature and then covered with aluminium foil to prevent light-induced damage. Finally, 47 µL of PBS was added to each well before image acquisition using a Leica TCS SP5 Confocal Microscope (Leica Microsystems Ltd, Buckinghamshire, UK). Images were viewed using a 60 x 1.8 oil objective with a one µm z-step. Four channels of view were chosen for each well, and the captured images were processed using COMSTAT2 and ImageJ to generate image sequences to quantify biofilm properties and unattached bacteria. Using automated thresholding employed by Otsu to each image, slice separated bacterial fluorescence from background noise. Several parameters, including mean biofilm thickness, biomass, roughness coefficient, and dead/live ratio, were quantified by analysing Image sequences in COMSTAT2. The COMSTAT2 analysis of findings was provided as the mean and standard error for each parameter, and assays were performed on 3 separate occasions.

5.4.11 Statistical Analysis

The acquired data were statistically analysed using GraphPad Prism 7.0a (GraphPad Software Inc., San Diego, USA); all data is reported as the mean ± standard error (SE), and all

experiments were conducted three times each. The means and standard errors were calculated using Excel (Microsoft) software. The statistical analysis was performed using a one-way analysis of variance (ANOVA) with Dunnett post-test, to assess the significance of the difference between the means of the control and experimental groups. The statistically significant difference between groups was determined using Tukey's post-test, with a threshold of $p < 0.05$ deemed to indicate statistical significance.

5.5 Results and Discussion

5.5.1 Agar Well Diffusion Assay

The antimicrobial activities of five plant extracts were evaluated with an agar diffusion method using MHA. Extracts at different concentrations were tested in triplicate over three independent experiments. Standard errors was calculated to evaluate the variation between experiments. Negative and positive controls of 0.1 % thymol were adapted to each experiment; no antimicrobial activity was observed with the negative control. The following bacterial strains associated with skin infections were used to determine plant extracts activity *Staphylococcus aureus* NCTC 12973, MRSA NCTC 13373, *Staphylococcus epidermidis* ATCC 14990, *Pseudomonas aeruginosa* NCTC 6749, *Escherichia coli* ATCC 15597, and *Propionibacterium acne* NCTC 737. Tables 16-21 presents summary of the antibacterial activity of plant extracts in terms of zone of inhibition diameter.

Table 16 Summary of antibacterial activities of plant extracts against *Staphylococcus aureus* (mean \pm SE). Three separate experiments were conducted to acquire findings, performed in triplicate (Key - NC: Not a complete inhibition of bacterial growth in the clear zone; NI: no inhibition observed)

Plant Extract	Concentration (mg/mL)	Zone of Inhibition diameter (mm) \pm SE
<i>R. stricta</i>	2	5.56 \pm 1.05
<i>R. stricta</i>	4	8.97 \pm 0.68
<i>R. stricta</i>	6	9.76 \pm 1.33
<i>R. stricta</i>	10	11.73 \pm 1.06
<i>R. stricta</i>	20	12.7 \pm 0.48
<i>A. canariense</i>	5	5.33 \pm 0.57 (NC)
<i>A. canariense</i>	10	4.83 \pm 0.75 (NC)
<i>T. macropterus</i>	5	4.25 \pm 0.5 (NC)
<i>T. macropterus</i>	10	4.33 \pm 0.81 (NC)
<i>C. colocynthis</i>	2,4,6,10	NI
<i>M. crassifolia</i>	2,4,6,10	NI
Thymol	0.1% (w/v)	13.74 \pm 1.62

Table 17 Summary of antibacterial activities of plant extracts against MRSA (mean \pm SE). Three separate experiments were conducted to acquire findings, performed in triplicate (Key - NC: Not a complete inhibition of bacterial growth in the clear zone; NI: no inhibition observed)

Plant Extract	Concentration (mg/mL)	Zone of Inhibition diameter (mm) \pm SE
<i>R. stricta</i>	2	3.95 \pm 0.42
<i>R. stricta</i>	4	8.7 \pm 0.79
<i>R. stricta</i>	6	8.75 \pm 0.46
<i>R. stricta</i>	10	12.78 \pm 0.41
<i>R. stricta</i>	20	13.48 \pm 1.67
<i>A. canariense</i>	5	NI
<i>A. canariense</i>	10	6.68 \pm 0.87 (NC)
<i>T. macropterus</i>	5	NI
<i>T. macropterus</i>	10	5.85 \pm 0.73 (NC)
<i>C. colocynthis</i>	2,4,6,10	NI
<i>M. crassifolia</i>	2,4,6,10	NI
Thymol	0.1% (w/v)	12.40 \pm 2.75

Table 18 Summary of antibacterial activities of plant extracts against *Staphylococcus epidermidis* (mean \pm SE). Three separate experiments were conducted to acquire findings, performed in triplicate (Key - NC: Not a complete inhibition of bacterial growth in the clear zone; NI: no inhibition observed)

Plant Extract	Concentration (mg/mL)	Zone of Inhibition diameter (mm) \pm SE
<i>R. stricta</i>	2	3.7 \pm 0.94
<i>R. stricta</i>	4	8.5 \pm 1.26
<i>R. stricta</i>	6	9.2 \pm 1.3
<i>R. stricta</i>	10	11.8 \pm 0.83
<i>A. canariense</i>	5	4.5 \pm 0.54 (NC)
<i>A. canariense</i>	10	5 \pm 0.6 (NC)
<i>T. macropterus</i>	5	5.5 \pm 0.54 (NC)
<i>T. macropterus</i>	10	6.5 \pm 1.29 (NC)
<i>C. colocynthis</i>	2,4,6,10	NI
<i>M. crassifolia</i>	2,4,6,10	NI
Thymol	0.1% (w/v)	15.73 \pm 1.99

Table 19 Summary of antibacterial activities of plant extracts against *Pseudomonas aeruginosa* (mean \pm SE). Three separate experiments were conducted to acquire findings, performed in triplicate (Key - NC: Not a complete inhibition of bacterial growth in the clear zone; NI: no inhibition observed)

Plant Extract	Concentration (mg/mL)	Zone of Inhibition diameter (mm) \pm SE
<i>R. stricta</i>	2	5.47 \pm 1.15
<i>R. stricta</i>	4	8 \pm 2.24
<i>R. stricta</i>	6	9.57 \pm 1.13
<i>R. stricta</i>	10	10.25 \pm 0.43
<i>R. stricta</i>	20	12.97 \pm 0.84
<i>A. canariense</i>	5,10,20	NI
<i>T. macropterus</i>	5,10,20	NI
<i>C. colocynthis</i>	2,4,6,10, 20	NI
<i>M. crassifolia</i>	2,4,6,10,20	NI
Thymol	0.1% (w/v)	14.85 \pm 1.24

Table 20 Summary of antibacterial activities of plant extracts against *Propionibacterium acne* (mean \pm SE). Three separate experiments were conducted to acquire findings, performed in triplicate (Key - NC: Not a complete inhibition of bacterial growth in the clear zone; NI: no inhibition observed)

Plant Extract	Concentration (mg/mL)	Zone of Inhibition diameter (mm) \pm SE
<i>R. stricta</i>	2	4.3 \pm 0.64
<i>R. stricta</i>	4	4.98 \pm 1.01
<i>R. stricta</i>	6	6.67 \pm 1.06
<i>R. stricta</i>	10	11.08 \pm 0.82
<i>R. stricta</i>	20	11.96 \pm 0.83
<i>A. canariense</i>	5	NI
<i>A. canariense</i>	10	6.18 \pm 1.20 (NC)
<i>T. macropterus</i>	5	NI
<i>T. macropterus</i>	10	6.52 \pm 0.89 (NC)
<i>C. colocynthis</i>	2,4,6,10,20	NI
<i>M. crassifolia</i>	2,4,6,10,20	NI
Thymol	0.1% (w/v)	9.17 \pm 1.40

Table 21 Summary of antibacterial activities of plant extracts against *Escherichia coli* (mean \pm SE). Three separate experiments were conducted to acquire findings, performed in triplicate (Key - NC: Not a complete inhibition of bacterial growth in the clear zone; NI: no inhibition observed)

Plant Extract	Concentration (mg/mL)	Zone of Inhibition diameter (mm) \pm SE
<i>R. stricta</i>	2	5.5 \pm 0.71 (NC)
<i>R. stricta</i>	4	7.5 \pm 0.70 (NC)
<i>R. stricta</i>	6	1.33 \pm 0.57
<i>R. stricta</i>	10	2.66 \pm 0.51
<i>R. stricta</i>	20	5.25 \pm 1.25
<i>A. canariense</i>	5	6.5 \pm 0.577 (NC)
<i>A. canariense</i>	10	8.25 \pm 0.95 (NC)
<i>T. macropterus</i>	5	6.25 \pm 0.95 (NC)
<i>T. macropterus</i>	10	8 \pm 0.81 (NC)
<i>C. colocynthis</i>	2,4,6,10,20	NI
<i>M. crassifolia</i>	2,4,6,10,20	NI
Thymol	0.1% (w/v)	15.92 \pm 1.32

From the ZOI data obtained, *R. stricta* extract demonstrated activity against both Gram-positive and Gram-negative bacteria. It demonstrated varying degrees of inhibitory activity against strains of *S. aureus*, MRSA, *S. epidermidis*, *P. aeruginosa*, *E. coli*, and *P. acne*, and

activity was more noticeable against the Gram-positive bacteria. This could indicate the presence of compounds with antibacterial activity, and the whole extract could be further fractionated and purified to increase the availability of these active compounds. However, there is a chance of losing extract activity after fractionation as the extract may exhibit the activity as a combination (synergy effect) (Caesar and Cech, 2019). Although *A. canariense* and *T. macropterus* exhibited antibacterial activity against both Gram-positive and negative strains, this was a partial inhibition as traces of bacterial growth could be observed on the surface of the agar (Figure 55). This could indicate that the antimicrobial compounds in the plant extract are present in low concentrations. Moreover, it could be due to the presence of bacteriostatic compounds in the extract. Further fractionation of the extract could increase the potency and isolate the pure compound responsible for such activity. Both *C. colocynthis* and *M. crassifolia* demonstrated no effect against all tested strains.

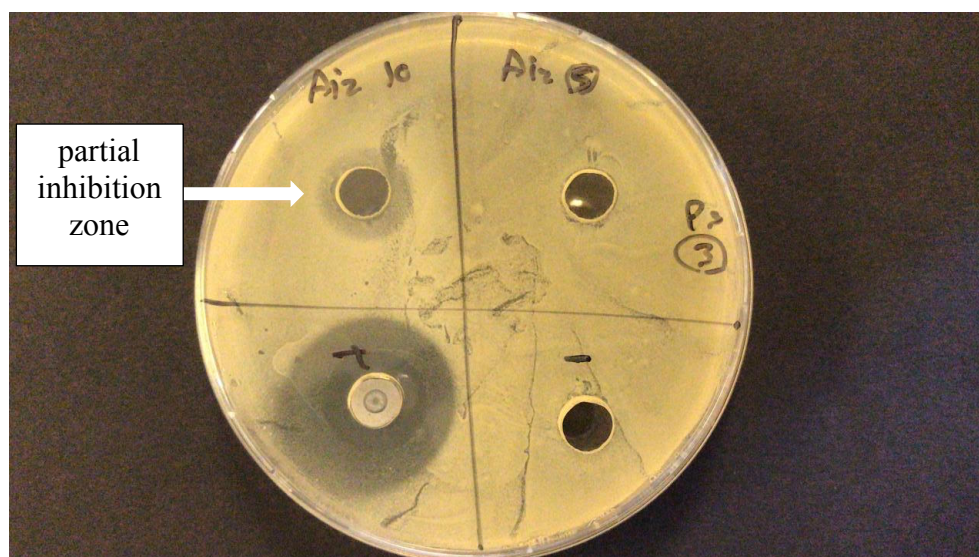


Figure 55 The well diffusion assay used to evaluate the antimicrobial activity of *A. canariense* exhibited a partial inhibitory zone towards MRSA. That could indicate the presence of low concentration antimicrobial components or bacteriostatic effect. Additionally, it could indicate the presence of compound-resistant mutants in the partial inhibitory zone. Three separate experiments were carried out to obtain results

The observed absence of activity of *A. canariense* and *T. macropterus*, moreover, the reduced activity of *R. stricta* towards Gram-negative strains under investigation are anticipated. Considering Gram-negative bacteria are surrounded by two membranes, the cytoplasmic cell membrane, and the outer membrane. The outer monolayer of the membrane is mainly composed of lipopolysaccharide (LPS), a lipid component only found in Gram-negative bacteria. The outer membrane is the principal cause of antibiotic resistance (Beutler, 2002; Breijyeh et al., 2020). Apart from *T. macropterus*, several studies have investigated the antimicrobial activities of the selected plant extracts via diffusion methods. Elkhalfi et al. (2013) reported that *A. canariense* methanolic extract exhibited a clear zone of 20 mm against *Pseudomonas syringae*. In addition, El-Amier et al. (2016) reported clear zones of 21, 6, and 5 mm against *Bacillus subtilis*, *Streptococcus pyogenes*, and *Klebsiella pneumoniae*. *R. stricta* extract demonstrated clear zones against *S. aureus*, MRSA, *B. subtilis*, and *P. aeruginosa* (Sultana and Khalid, 2010; Khan et al., 2016).

Although *C. colocynthis* and *M. crassifolia* showed no antimicrobial effect against tested strains, several studies reported that *C. colocynthis* showed clear inhibition zones against *Bacillus cereus*, *Staphylococcus aureus*, *Klebsiella pneumoniae*, *Escherichia coli*, and *Streptococcus agalactiae* (Ali et al., 2013; Bnyan et al., 2013). Another study reported that *M. crassifolia* produces clear inhibition zones against *S. aureus*, *S. typhi*, *B. subtilis* and *E. coli* (Ckilaka et al., 2015). These differences in reported activity could be due to the higher tested concentration of more than 50 mg/mL and the sensitivity of tested strains toward plant extract. In addition, plant-to-plant variation makes it difficult to assess the relative antibacterial efficacy of various extracts, mostly due to differences in physical properties like volatility, solubility, and diffusion rate in agar (King et al., 2008; Klančnik et al., 2010).

In general, these discrepancies in antibacterial properties and efficacy of selected plant extracts could be attributable to the fact that the concentrations of active constituents in plant extracts vary greatly dependent on the local climate and other environmental conditions. In addition, different constituents within extracts might be affected by factors, such as growing location, harvesting time, processing methods, plant development stage, and utilised plant parts (Radulovic et al., 2013).

5.5.2 Broth Microdilution Assay

The antimicrobial activity of the 5 plant extracts was examined by broth microdilution assay against the following bacterial strains: *S. aureus*, MRSA, *S. epidermidis*, *P. aeruginosa*, and *E. coli*, to determine the lowest concentration that inhibits the growth of bacteria (MIC) by assessing the turbidity of the wells. Moreover, the minimum concentration that kills bacteria was determined by sub-culturing samples on MHA plates. *R. stricta* extract showed the lowest inhibition concentration of 312.5 µg/mL against Gram-positive bacteria *S. aureus* and an MBC of 312.5 µg/mL. Table 22 summary of the MIC and MBC values of *R. stricta*. Table 23 summary of MIC and MBC values of positive control, thymol. All experiments were performed in triplicate, and positive and negative controls were included in each run.

Table 22 Summary of MIC and MBC values of *Rhazya stricta*. The results of three independent experiments conducted in six replicates

Bacterial Strain	MIC	MBC
<i>S. aureus</i> NCTC 12973	312.5 µg/mL	312.5 µg/mL
MRSA NCTC 13373	312.5 µg/mL	1.25 mg/mL
<i>S. epidermidis</i> ATCC 14990	625 µg/mL	2.5 mg/mL
<i>P. aeruginosa</i> NCTC 6749	1.25 mg/mL	NA
<i>E. coli</i> ATCC 15597	5 mg/mL	10 mg/mL

Table 23 Summary of MIC and MBC values of positive control thymol. The results of three independent experiments conducted in six replicates

Bacterial Strain	MIC	MBC
<i>S. aureus</i> NCTC 12973	153 µg/mL	153 µg/mL
MRSA NCTC 13373	153 µg/mL	153 mg/mL
<i>S. epidermidis</i> ATCC 14990	612 µg/mL	612 µg/mL
<i>P. aeruginosa</i> NCTC 6749	1.25 mg/mL	1.25 mg/mL
<i>E. coli</i> ATCC 15597	612 µg/mL	1.25 mg/mL

Numerous studies have demonstrated that *R. stricta* has a broad spectrum of antimicrobial effects against different microorganisms. For example, in one study, *R. stricta* leaf underwent five different extraction methods and was investigated for its antimicrobial properties against Gram-negative *E. coli* and Gram-positive MRSA bacteria. *R. stricta* organic alkaloid extract exhibited the most antimicrobial activity, and cell membrane disruption was visible with transmission electron microscopy (Khan et al., 2016). Thus, the antimicrobial activity could be related to the alkaloid constituents of *R. stricta*. In another study, silver nanoparticles were synthesised using silver nitrate and methanol root extract of *R. stricta*, and they demonstrated enhanced antibacterial activity against *B. subtilis* and *E. coli* (Shehzad et al., 2018). The bioavailability of natural products can be significantly improved by using nanoparticles, both *in vitro* and *in vivo*. Thus, the antimicrobial activity could be dramatically boosted by utilizing nanoparticles into the delivery system of *R. stricta* (Watkins et al., 2015; Patra et al., 2018).

5.5.3 Antibacterial Bio-Autographic Assay

Bioassay-guided fractionation was followed; thus, *A. canariense*, *T. macropterus*, and *R. stricta* extracts that showed antimicrobial activity with previously stated assays were further fractionated with liquid-liquid partitioning and column chromatography. This method will

guide the separation of active analytes within plant extracts, plant extracts and their hexane, chloroform, aqueous extracts, plus fractions collected from the fractionation process via column chromatography were developed on a surface of a TLC plate and then sprayed with bacterial strains: *Staphylococcus aureus*, MRSA, *Staphylococcus epidermidis*, *Pseudomonas aeruginosa*, and *E. coli* a visualizing agent active analytes will appear as clear spots against a red background (Begue and Kline, 1972). Rf values were recorded, experiments were performed in triplicate, and positive control thymol 0.1% (1 mg/mL) was included in each run. Figure 56 demonstrates an example of the bacterial bio-autographic assay with *R. stricta* hexane and chloroform extracts.

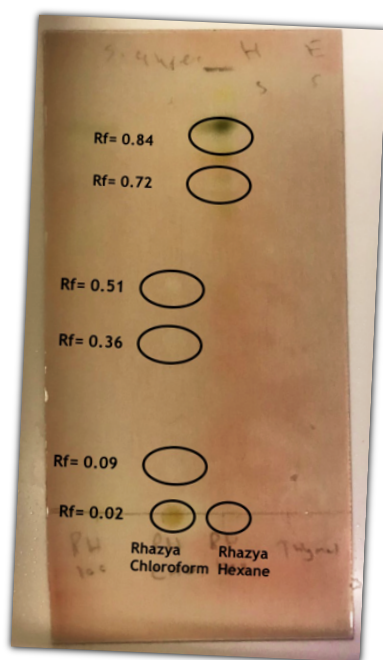


Figure 56 *R. stricta* hexane and chloroform extracts were examined utilising the bacterial bio-autographic method. Several observed clear zones suggest that extracts include antimicrobial compounds. The Rf values were recorded for future work. Three separate experiments were carried out to obtain results

The extract of *A. canariense*, *T. macropterus*, and *R. stricta* were evaluated, plus their hexane and chloroform extracts with previously selected solvent system ratio number five hexane 5:

ethyl acetate 5. Table 24 presents summary of Rf values of tested plant extracts and selected solvent system ratio number five against bacterial strains.

Table 24 Summary of Rf values of tested plant extracts and selected solvent system ratio number five against bacterial strains (mean \pm SE). Three separate experiments were carried out to obtain results

Plant extract	Rf value 1 \pm SE	Rf value 2 \pm SE	Rf value 3 \pm SE	Rf value 4 \pm SE	Rf value 5 \pm SE	Bacterial strain
<i>R. stricta</i>	0.02 \pm 0.001	0.45 \pm 0.01	0.64 \pm 0.03	0.72 \pm 0.04	0.86 \pm 0.01	<i>S. aureus</i>
<i>R. stricta</i>	0.02 \pm 0.001	0.42 \pm 0.01	0.64 \pm 0.03	0.71 \pm 0.02	0.85 \pm 0.005	MRSA
<i>R. stricta</i>	0.02 \pm 0.001	0.73 \pm 0.01	0.83 \pm 0.01			<i>P. aeruginosa</i>
<i>R. stricta</i>	0.02 \pm 0.001	0.62 \pm 0.01				<i>S. epidermidis</i>
<i>R. stricta</i>	0.02 \pm 0.001	0.74 \pm 0.02				<i>E. coli</i>
<i>R. stricta</i> Hexane	0.02 \pm 0.001	0.73 \pm 0.01	0.84 \pm 0.01			<i>S. aureus</i>
<i>R. stricta</i> Hexane	0.02 \pm 0.001	0.65 \pm 0.03				MRSA
<i>R. stricta</i> Hexane	0.02 \pm 0.001	0.77 \pm 0.02				<i>P. aeruginosa</i>
<i>R. stricta</i> Chloroform	0.02 \pm 0.001	0.09 \pm 0.02	0.36 \pm 0.02	0.51 \pm 0.01		<i>S. aureus</i>
<i>R. stricta</i> Chloroform	0.02 \pm 0.001	0.21 \pm 0.02	0.63 \pm 0.04			MRSA
<i>R. stricta</i> Chloroform	0.02 \pm 0.001	0.24 \pm 0.01	0.75 \pm 0.03			<i>P. aeruginosa</i>

<i>A. canariense</i> Hexane	0.02± 0.001	0.52± 0.02	0.67± 0.01			<i>S. aureus</i>
<i>A. canariense</i> Hexane	0.02± 0.001	0.58± 0.01	0.68± 0.01			MRSA
<i>A. canariense</i> Chloroform	0.02± 0.001	0.54± 0.01				<i>S. aureus</i>
<i>A. canariense</i> Chloroform	0.02± 0.001	0.57± 0.01	0.72± 0.008			MRSA
<i>T. macropterus</i> Hexane	0.02± 0.001	0.74± 0.008				<i>S. aureus</i>
<i>T. macropterus</i> Hexane	0.02± 0.001	0.57± 0.01				MRSA
<i>T. macropterus</i> Chloroform	0.02± 0.001	0.58± 0.01				<i>S. aureus</i>
<i>T. macropterus</i> Chloroform	0.02± 0.001	0.6± 0.009				MRSA
Thymol 1% (1mg /mL)	0.02± 0.001	0.93± 0.02				All tested bacterial strains

The results in Table 24 for different extracts show that *R. stricta* possessed the highest number of inhibitory compounds with five separated spots against Gram-positive bacteria (*S. aureus*, MRSA) and two inhibitory compounds against *S. epidermidis*. Moreover, it showed fewer inhibitory compounds against Gram-negative bacteria, with three against *P. aeruginosa* and two against *E. coli*. Those findings could indicate that *R. stricta* plant extract includes more compounds that inhibit Gram-positive bacteria than Gram-negative ones, which validates the low MIC and MBC that were recorded in previous broth microdilution assay (Section 5.5.2) against Gram-positive bacteria and the large clear zone that were observed in the zone of inhibition assay (Section 5.5.1).

The recovered hexane and chloroform extracts from previous liquid-liquid partitioning process were evaluated depending on the polarity of the *R. stricta* whole extract. Three inhibitory compounds against *S. aureus* and two against MRSA and *P. aeruginosa* were identified in the hexane extract. The chloroform extract contained four antimicrobial compounds against *S. aureus* and three against MRSA and *P. aeruginosa*. Based on these results, some of the inhibitory compounds (Rf 0.45; 0.64) in the whole extracts were lost during the fractionation process; other new inhibitory compounds (Rf 0.09; 0.51) appeared in the chloroform extract. This could be due to the concentration of these active constituents inside the extract and fractions, which may become more concentrated or even lose concentration during the fractionation process. Furthermore, it can be due to the synergy effect of two or more compounds exhibiting or losing their antimicrobial activity (Eloff et al., 2008). Moreover, the lack of action may be attributable to photo-oxidation degradation, evaporation of the active compounds, or a minimal concentration of the active compounds (Masoko and Eloff, 2005). Distinct bands with almost the same Rf value could indicate that the same components are responsible for the antimicrobial activity observed in the same extract when tested against various microorganisms. This indicates a lack of antimicrobial selectivity.

Ten fractions collected from the fractionations of *R. stricta* hexane extract through silica column chromatography (Section 2.5.3.2), were evaluated by bacterial bio-autographic assay, and active fractions 4, 5, 6, 7, 8, 9 and 10 were identified. Figure 57 presents active *R. stricta* hexane fractions against *S. aureus* with obtained Rf values.

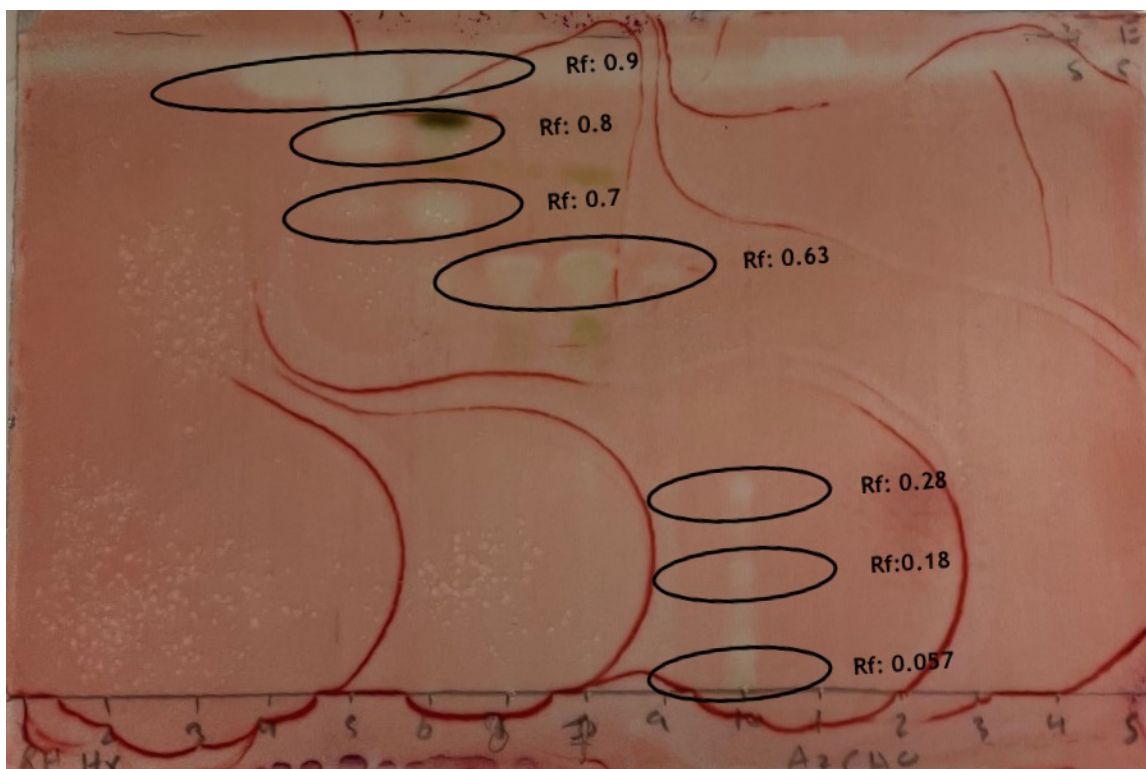


Figure 57 The antimicrobial activity of *R. stricta* hexane fractions was determined using a bacterial bio-autographic test against *Staphylococcus aureus*, and the Rf values were obtained. In addition, *R. stricta* hexane extracts active fractions of hexane (4, 5, 6, 7, 8, 9, and 10) were determined. Three separate experiments were conducted in order to acquire results

Although *A. canariense* and *T. macropterus* whole methanolic extract did not exhibit any activity against bacterial strains by this assay, the collected fractions from the liquid-liquid partition process revealed the presence of some antimicrobial compounds, *A. canariense* hexane extract, showed three inhibitory compounds against both *S. aureus* and MRSA. Only two inhibitory compounds were observed with chloroform extract in TLC plates inoculated with *S. aureus* and three with MRSA. The evaluation of both *T. macropterus* hexane and chloroform extracts revealed the presence of two antimicrobial compounds against *S. aureus* and MRSA. Finally, the bacterial bio-autographic assay was carried out on 23 fractions collected from *T. macropterus* hexane and chloroform extracts and on 23 fractions collected

from *A. canariense* hexane and chloroform. Table 25 summary of active *A. canariense* and *T. macropterus* fractions of hexane and chloroform extracts against *S. aureus*, MRSA.

Table 25 Active *A. canariense* and *T. macropterus* fractions of hexane and chloroform extracts were determined via bacterial bio-autographic test against *Staphylococcus aureus* and MRSA. Three separate experiments were conducted in order to acquire results

Plant extract	Active fractions	Bacterial Strains
<i>A. canariense</i> hexane	Fractions 4, 6, 7, 8	<i>S. aureus</i> , MRSA
<i>A. canariense</i> chloroform	Fractions 8, 9, 10, 11, 12	<i>S. aureus</i> , MRSA
<i>T. macropterus</i> hexane	Fractions 5, 6, 7, 8, 9	<i>S. aureus</i> , MRSA
<i>T. macropterus</i> chloroform	Fractions 9, 10, 11	<i>S. aureus</i> , MRSA

5.5.4 Evaluating the Ability of Tested Microorganism to Form a Reproducible Biofilm

The ability of investigated microorganisms to attach and retain their viability on 96-well plates was assessed to determine their *in vitro* biofilm formation capability. The crystal violet staining technique was utilised to evaluate the biofilm mass of each bacterial strain, following a 24 h incubation. This assay confirmed the ability of each bacterial strain to form a reproducible biofilm mass with variation in the biomass size between them. The mean OD was recorded, and statistical differences between strains were measured (Figure 58A). *E. coli* exhibited the highest OD value, indicating a superior crystal violet-stained biomass to other microorganisms ($p < 0.001$). The remaining bacterial strains produced a consistent biofilm mass with no significant variation. This indicates that some bacterial strains are more capable than others of forming biofilms *in vitro*. This variation in biofilm mass could be attributed to the difference

in bacterial virulence-associated genes even between different isolates of the same bacterial species. A study by Naves et al. (2008) examined the variation in the ability of *E. coli* clinical isolates to produce biofilm, and they found that specific virulence-related proteins such as phylogenetic group B2, were expressed in potent biofilm-producing *E. coli* isolates (Naves et al., 2008). Figure 58B shows the biofilm mass of *P. aeruginosa* stained with crystal violet and then dissolved with 95% ethanol.

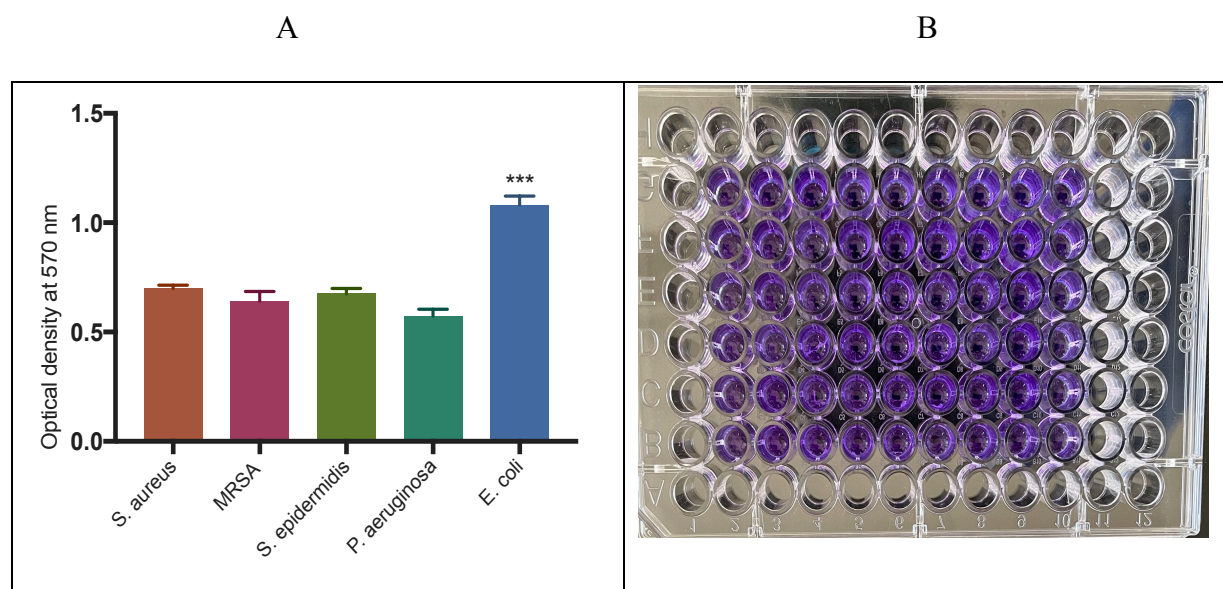


Figure 58 (A) After 24 h incubation in MH broth, the crystal violet staining technique was used to compare biofilm formation between the bacterial strains investigated. Data were reported as the mean \pm SE. Three separate experiments were conducted to acquire findings. Analysis of statistically significant differences between tested strains via Tukey's post-test (***) $p < 0.001$. **(B)** biofilm mass of *P. aeruginosa* stained with crystal violet and dissolved with 95% ethanol. The intensity of the colour is directly proportional to the biofilm mass

5.5.5 Inhibition of Biofilm Formation and Biofilm Eradication

Utilising the crystal violet *in vitro* method on a microtiter plate, the effects of *A. canariense*, *R. stricta*, and *T. macropterus* on the inhibition of biofilm formation (Figure 59) and the eradication of pre-formed biofilm (Figure 60), were examined. Examined concentrations for *R.*

stricta were 312 and 156 µg/mL (MIC and MIC/2) and 1.25, 2.5 mg/mL for *A. canariense* and *T. macropterus*.

The impact of *R. stricta* on *S. aureus* biofilm formation was significantly inhibited, and a comparable effect was found on the eradication of pre-formed biofilm at MIC and MIC/2 values ($p < 0.001$). Moreover, *A. canariense* and *T. macropterus* inhibited biofilm formation significantly at concentrations of 2.5 and 1.25 mg/mL ($p < 0.001$; $p < 0.01$). Moreover, *A. canarienses* significantly affected the eradication of pre-formed biofilm ($p < 0.01$). However, this impact diminished when *T. macropterus* treatment was administered at the same concentrations to pre-formed biofilm to evaluate the efficacy ($p > 0.05$).

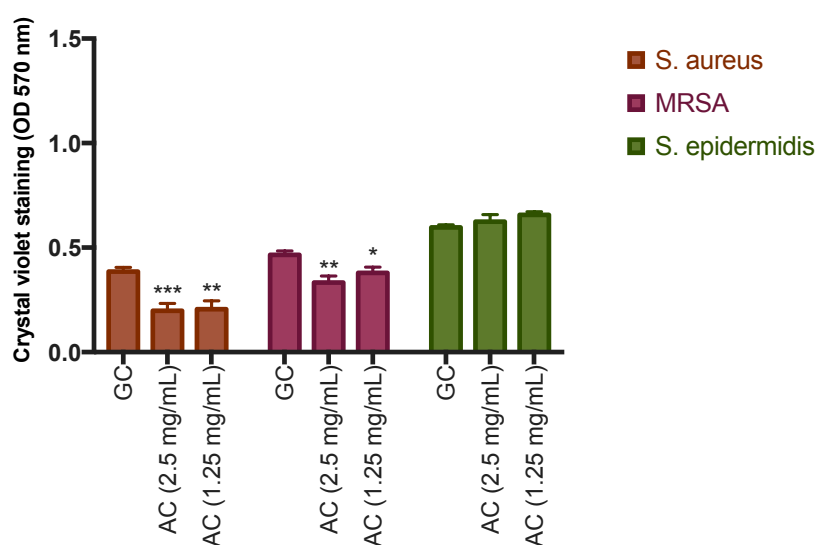
For MRSA, *R. stricta* inhibited biofilm formation significantly ($p < 0.001$), while pre-existing biofilm was eradicated to a lesser extent but was still considered significant ($p < 0.05$). *A. canariense* inhibited biofilm formation significantly at concentrations of 2.5 and 1.25 mg/mL ($p < 0.01$; $p < 0.05$) but had no impact on pre-formed MRSA biofilm ($p > 0.05$). Finally, extract of *T. macropterus* showed no impact on either biofilm inhibition or eradication of pre-formed one ($p > 0.05$).

For *S. epidermidis*, a similar pattern of a significant effect was observed with *R. stricta* on biofilm formation inhibition at MIC and MIC/2 concentrations ($p < 0.001$; $p < 0.01$). However, this effect was reduced when evaluating the eradication of pre-formed biofilm ($p < 0.01$) at MIC value and had no effect at MIC/2 concentration. *A. canariense* and *T. macropterus* demonstrated no effect on biofilm inhibition or eradication of pre-formed one ($p > 0.05$).

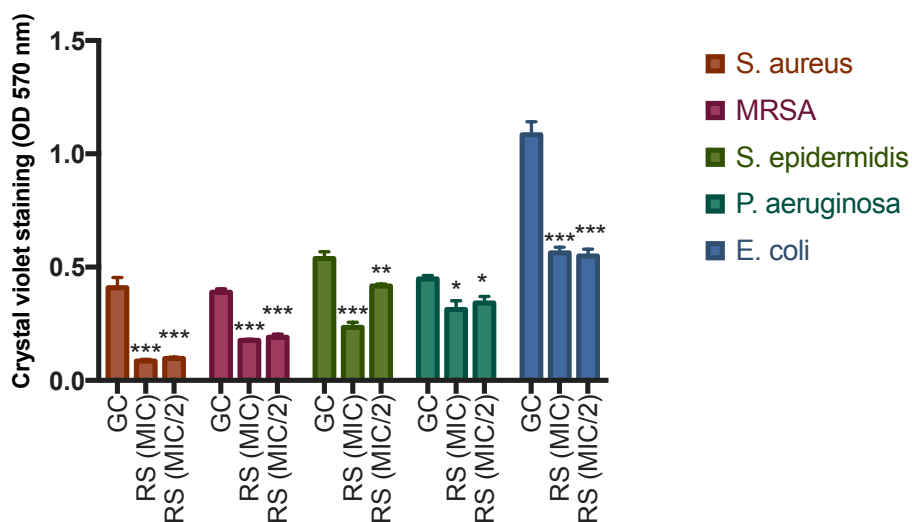
For *P. aeruginosa*, *R. stricta* significantly inhibited biofilm formation at both MIC and MIC/2 concentrations ($p < 0.05$). However, no effect was observed in eradicating biofilms at the same

concentrations. Moreover, *R. stricta* demonstrated a significant effect on biofilm formation of *E. coli* at MIC and MIC/2 concentrations ($p < 0.001$), and only MIC concentration showed a similar effect on the eradication of pre-formed biofilm of *E. coli* ($p < 0.01$). In contrast, the MIC/2 showed no effect ($p > 0.05$).

A)



B)



C)

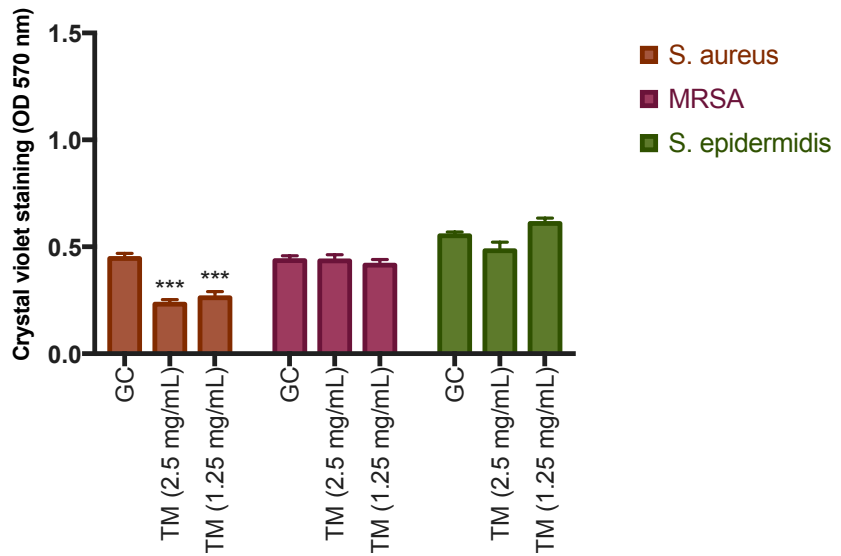
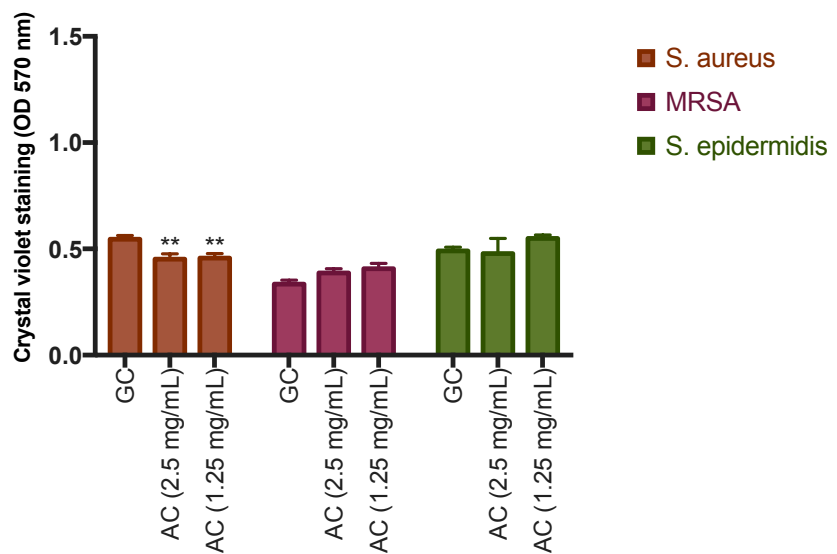
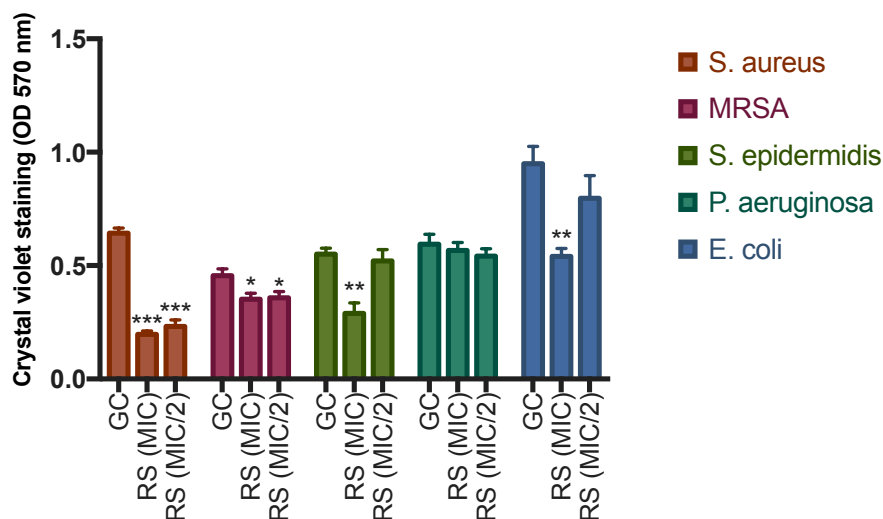


Figure 59 Comparison of the ability of plant extracts to inhibit biofilm formation for (A) *A. canariense* at concentrations 2.5 and 1.25 mg/mL (B) *R. stricta* at MIC and MIC/2 values (C) *T. macropterus* at concentrations of 2.5 and 1.25 mg/mL against selected microorganisms in MH broth, following 24 h incubation in 96-well plate using the crystal violet staining method. Data was reported as the mean \pm SE. Three separate experiments were conducted to acquire findings. Analysis of statistically significant differences between treatments and controls via Dunnett post-test (* $p < 0.05$, ** $p < 0.01$, *** $p < 0.001$)

A)



B)



C)

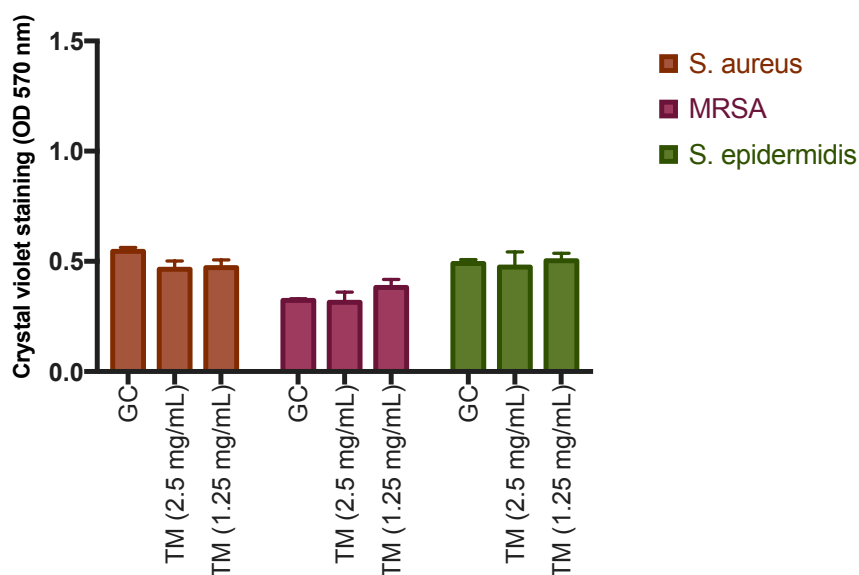


Figure 60 Comparison of the ability of plant extracts to eradicate pre-formed biofilm for (A) *A. canariense* at concentrations 2.5 and 1.25 mg/mL (B) *R. stricta* at MIC and MIC/2 values (C) *T. macropterus* at concentrations of 2.5 and 1.25 mg/mL against selected microorganisms in MH broth, following 24 h incubation in 96-well plate using the crystal violet staining method. Data was reported as the mean \pm SE. Three separate experiments were conducted to acquire findings. Analysis of statistically significant differences between treatments and controls via Dunnett post-test (*p < 0.05, **p < 0.01, ***p < 0.001)

Saudi Arabian communities have traditionally used *A. canariense*, *R. stricta*, and *T. macropterus* to treat several diseases, including infectious disorders such as cough, bronchitis, influenza, sore throats, and wounds (Al-Laith et al., 2015; Baeshen et al., 2016; Ksiksi et al., 2017).

In this study, we investigated the efficacy of several plant extracts used in folk medicine against SSTI-causing bacteria and their biofilm formation, which is closely associated with chronic infection and antimicrobial resistance. To the best of our knowledge, this is the first report of *A. canariense*, *R. stricta*, and *T. macropterus*, to which their antibiofilm properties against selected microorganisms are explored.

In recent years, *R. stricta* has been the subject of several studies, especially concerning its antioxidant (Iqbal et al., 2006; Mahmood et al., 2020), cytotoxic (Shaer, 2019; Al-Abbas and Shaer, 2021), anti-fungal (Khan and Khan, 2007), and antimicrobial (Khan et al., 2016; Shehzad et al., 2018; Alshehri et al., 2020) properties. In our study, *R. stricta* demonstrated antimicrobial effects against a panel of Gram-positive and Gram-negative bacteria: *S. aureus*, MRSA, *S. epidermidis*, *P. aeruginosa* and *E. coli*.

Given the significance of bacterial adherence in the early stages of the biofilm formation process, the potential to inhibit bacterial adhesion is an ideal strategy for combating bacterial pathogenesis. In addition, bacterial adhesion inhibition can be used as a preventative measure against infection (Cegelski et al., 2008). Therefore, applying natural compounds that effectively inhibit cell adhesion is a viable method for reducing bacteria growth and preventing biofilm formation (Bavington and Page, 2005). Furthermore, natural products with

antimicrobial activities have been shown in recent studies to have antibiofilm properties (Chaieb et al., 2011; Luna et al., 2011).

Therefore, the effect of *R. stricta* on biofilm formation was evaluated, and our results indicate a significant inhibition against all tested microorganisms at the MIC and below it (MIC/2). This could be due to its previously established direct antimicrobial effect, or it may prevent the adhesion of bacteria to the surface, consequently preventing it from colonising and eventually forming a biofilm. Moreover, it could be involved in inhibiting bacterial quorum sensing (QS), which controls the biofilm formation process and release of virulence factors.

To determine if *R. stricta* could eradicate the biofilm, *R. stricta* was applied to the pre-formed biofilm, and the quantity of biofilm was measured. The quantity of *S. aureus* and MRSA biofilm did significantly decrease at MIC and MIC/2 concentrations, and a similar effect was observed for *S. epidermidis* and *E. coli*, but only at MIC value. At the same time, it did not affect *P. aeruginosa* established biofilms. *P. aeruginosa* is a Gram-negative bacterium with a cell wall composed of a peptidoglycan layer and an additional outer membrane (Vadillo-Rodriguez et al., 2008). Moreover, several genes encoding efflux pumps have also been linked to the reduced antibacterial susceptibility of *P. aeruginosa* biofilms (Tseng et al., 2013), which might explain the lack of activity. Finally, in order to neutralise the bacterial cells, antimicrobial agents must be able to penetrate through the biofilm matrix. By affecting the transit rate to the deep biofilm layer, bacterial extracellular polymeric substances (EPS) are a powerful barrier for these compounds. Thus, *R. stricta* significant effect on the eradication of pre-formed biofilm of tested microorganisms could be due to its ability to penetrate the solid extracellular polymeric substances matrix (EPS) (Cochran et al., 2000).

Both *A. canariense* and *T. macropterus* showed significant activity in inhibiting *S. aureus* biofilm formation at 2.5 and 1.25 mg/mL. However, only *A. canariense* demonstrated a significant effect against MRSA biofilm and also eradicated a pre-formed biofilm of *S. aureus*. The formation of bacterial biofilm is a dynamic process that begins with adhesion and progresses to the formation and maturation of the created biofilm, all of which are regulated by several genes. As a result, biofilm prevention and eradication mechanisms differ. Future studies are needed to determine how these traditionally used plant extracts prevent biofilm formation and eradicate it.

5.5.6 CLSM Live/Dead Microbial Viability Method to Evaluate Biofilm Eradication

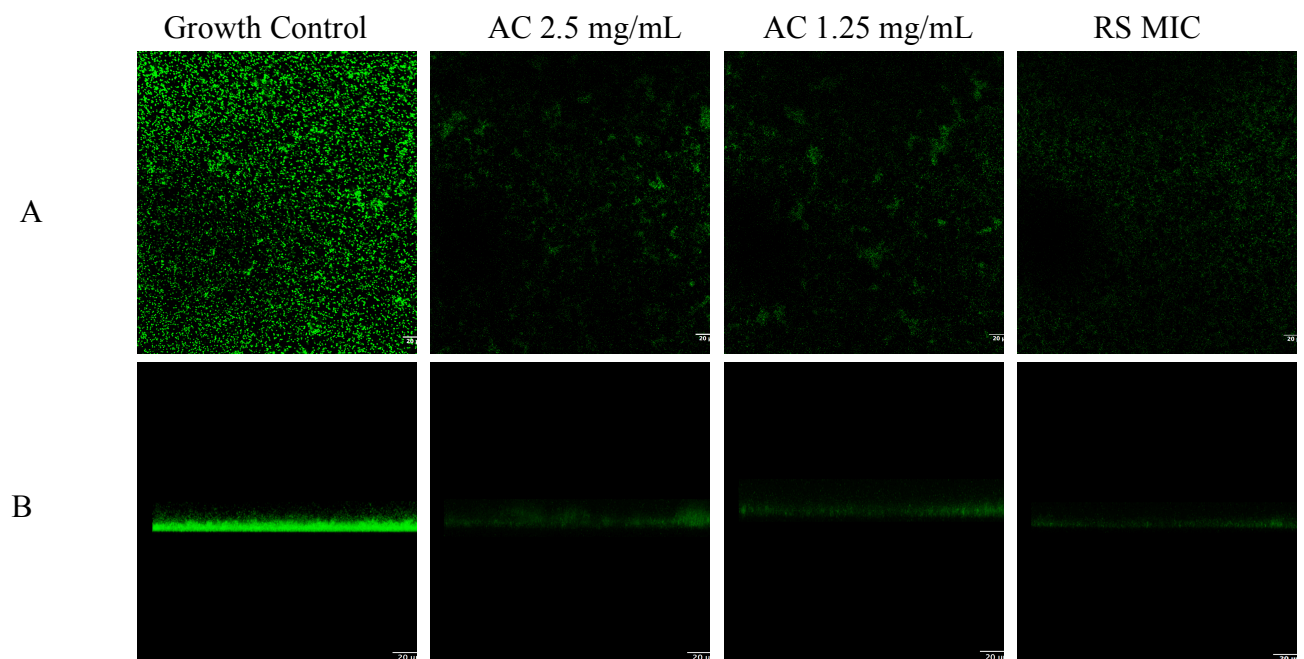
The BacLight Live/Dead Bacterial Viability Kit was utilized to investigate the structure of *S. aureus* and MRSA-formed biofilm and to evaluate the ability of *A. canariense*, *R. stricta* and *T. macropterus*, to eliminate the biofilm at different concentrations for *R. stricta* (MIC, MIC/2) and *A. canariense* and *T. macropterus* (2.5 and 1.25 mg/mL). CLSM images of control biofilm exhibited a dense and compact structure stained green with SYTO 9, indicating viable cells. Using ImageJ and COMSTAT 2.1 image analysis software, the acquired Z-stack images data were analysed to get further information on the biofilm structure, such as biofilm mass, mean thickness of biofilm, dead:live ratio and roughness coefficient (Heydorn et al., 2000). CLSM images were presented using ImageJ software. The tested concentrations of *A. canariense* and *T. macropterus* were selected since in a previous *in vitro* crystal violet assay, they were effective at the minimal concentrations that inhibited biofilm formation and eradicated pre-formed biofilm.

After 24 h incubation, adding *A. canariense* and *R. stricta* to *S. aureus* biofilm resulted in a significant decrease in biofilm biomass, compared to the untreated control ($p < 0.001$; $p < 0.01$, Figure 61). In addition, a significant increase in biofilm roughness coefficient was detected ($p < 0.001$; $p < 0.05$, Figure 61). This parameter is a direct indicator of biofilm heterogeneity since it quantifies the variation in biofilm thickness. In addition, all treatments considerably decreased the average biofilm thickness ($p < 0.001$; $p < 0.01$), as shown by the images provided (Figure 61). In comparison to the untreated control, both treatments resulted in a significant rise in the dead/live ratio ($p < 0.001$).

T. macropterus showed no effect on the biofilm properties as biofilm mass, roughness coefficient, and mean biofilm thickness. However, an interesting significant increase in the dead/live bacteria ratio was observed ($p < 0.001$). This could suggest that the extract adheres to the surface of the biofilm and then enters the biofilm through its pores, where it applies its previously observed antimicrobial activity without affecting other biofilm parameters.

For MRSA, *R. stricta* had a similar effect on biofilm parameters, decreasing biofilm biomass and increasing roughness coefficient significantly at both MIC and MIC/2 concentrations ($p < 0.01$; $p < 0.05$, Figure 62). The MIC value of *R. stricta* demonstrated a statistically significant decrease in biofilm thickness ($p < 0.05$), however, the MIC/2 value, despite demonstrating a reduction in thickness, was not statistically significant ($p > 0.05$). In addition, a significant rise in the ratio of dead/live bacteria was reported for both MIC values ($p < 0.001$). Both *A. canariense* and *T. macropterus* did not affect the biofilm of MRSA ($p > 0.05$, Figure 62).

In the previous section, we determined that tested plant extracts could effectively inhibit biofilm formation and eradicate pre-existing biofilm. Similarly, in this study, COMSTAT analysis confirmed that treatments with *A. canariense* and *R. stricta* decreased *S. aureus* biofilm biomass and thickness while increasing the roughness coefficient and dead/live ratio. The results indicated that both treatments could damage the *S. aureus* biofilm structure, rendering it less compact and homogenous and demonstrating a potent antibiofilm activity. In addition, *R. stricta* exhibited the same effect on MRSA biofilm; variation in efficiency against methicillin-sensitive *S. aureus* and MRSA may be attributable to different biofilm formation mechanisms. The acquisition of the *mecA* gene, which encodes penicillin-binding protein 2a (PBP2a), may change the cell wall architecture of methicillin-resistant bacteria, prevent the production of polysaccharide-type biofilms, and leads to the formation of proteinaceous-type biofilms which could explain the weaker activity (Pozzi et al., 2012).



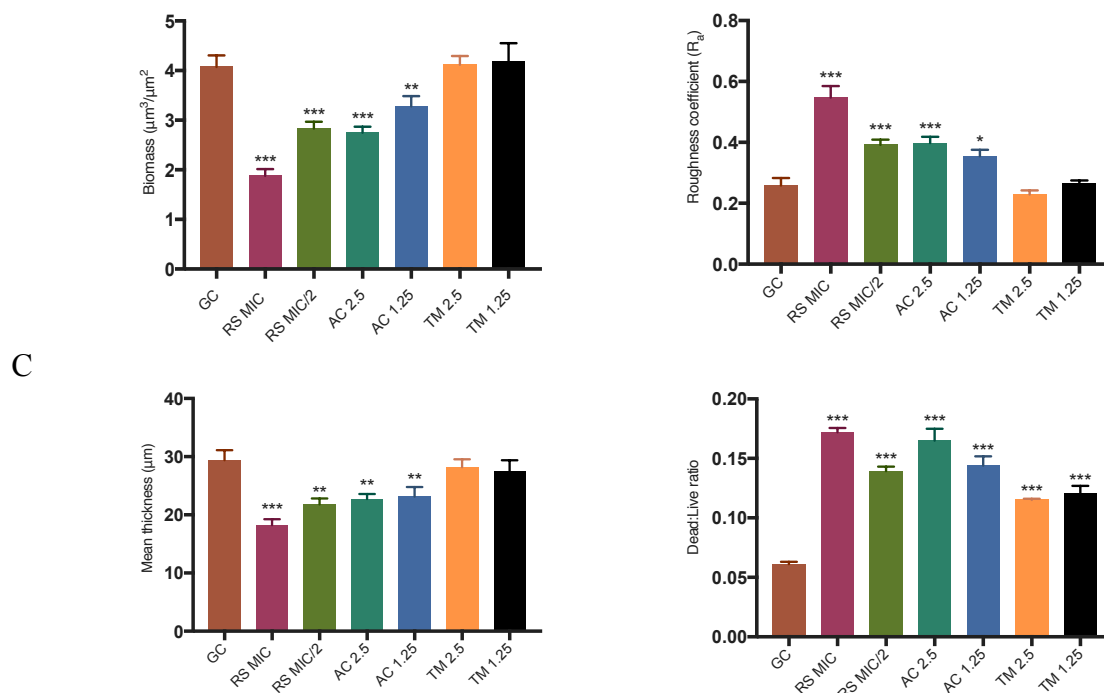
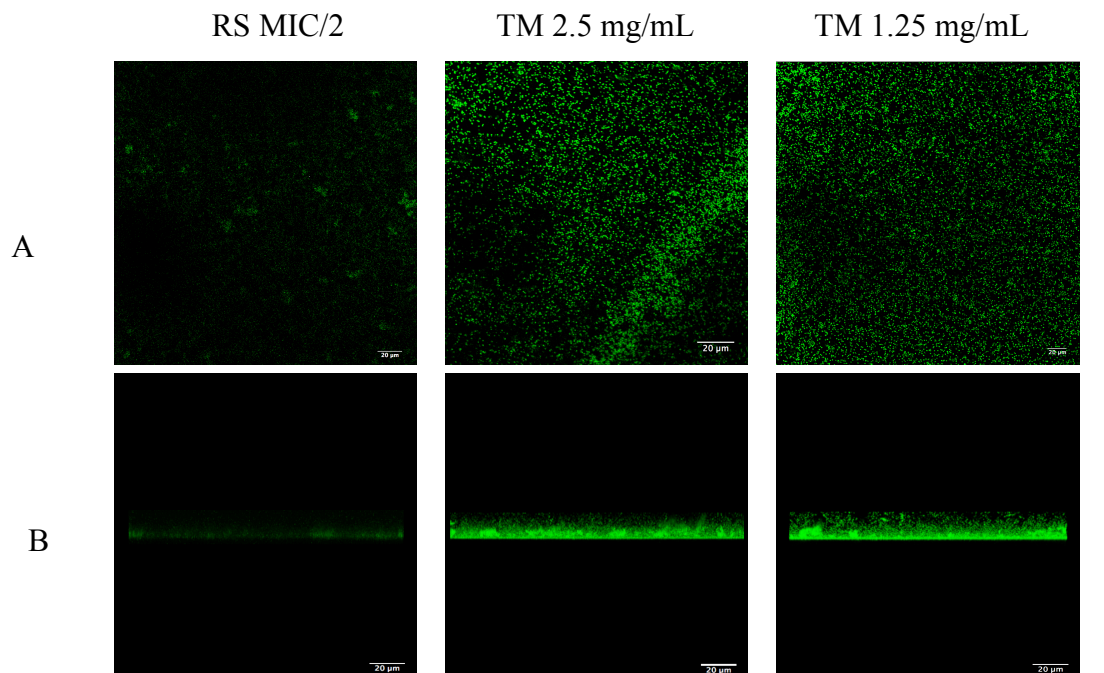
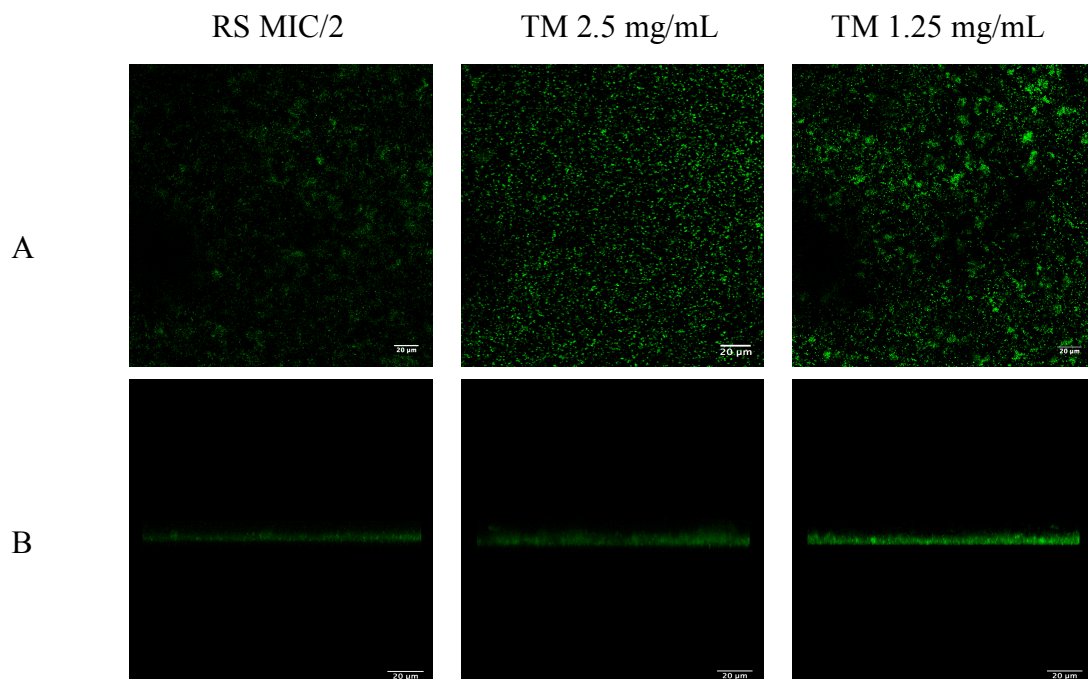
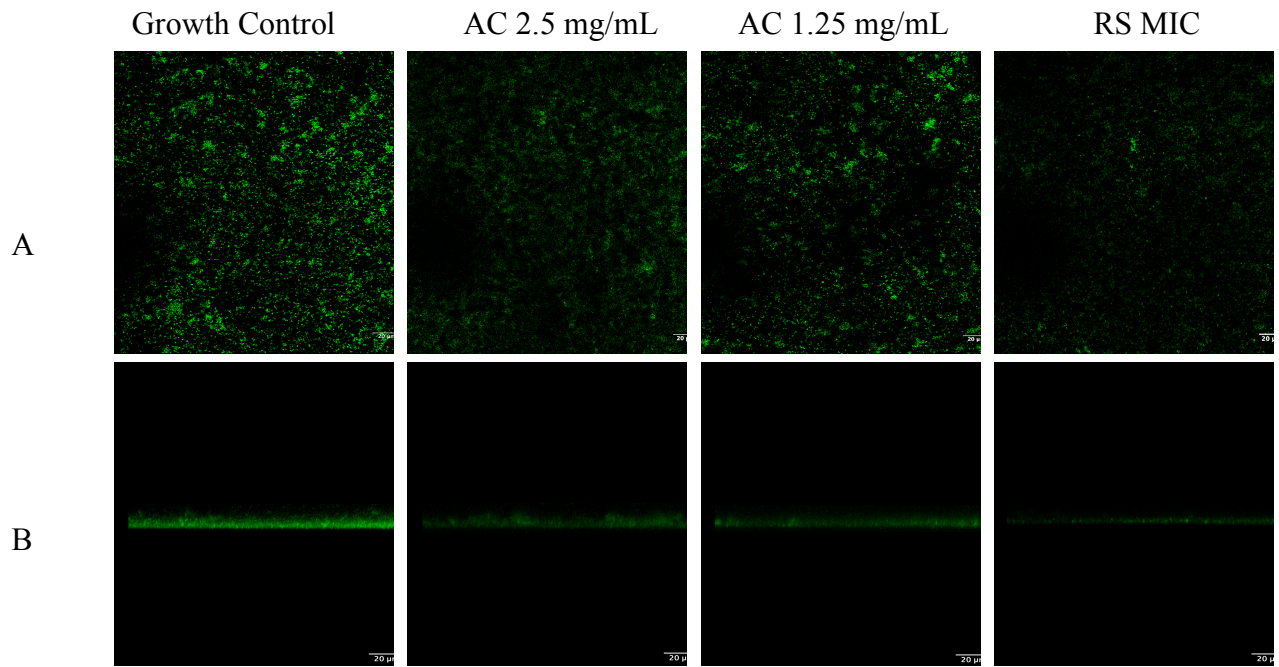


Figure 61 Effects of *A. canariense*, *R. stricta*, and *T. macropterus* on the biofilm eradication of *S. aureus* using a live/dead bacterial viability assay (A and B) showing CLSM images of *S. aureus* 24 h biofilms treated AC and TM (2.5 and 1.25 mg/mL), RS (MIC and MIC/2) compared to untreated controls. (C) Biofilm parameters obtained with the quantitative analysis of CLSM Z stack images via COMSTAT 2.1. Data presented as mean \pm standard error (SE) and experiments were performed three times. Statistical analysis of significant changes, compared to each others (* $p < 0.05$, ** $p < 0.01$, *** $p < 0.001$)



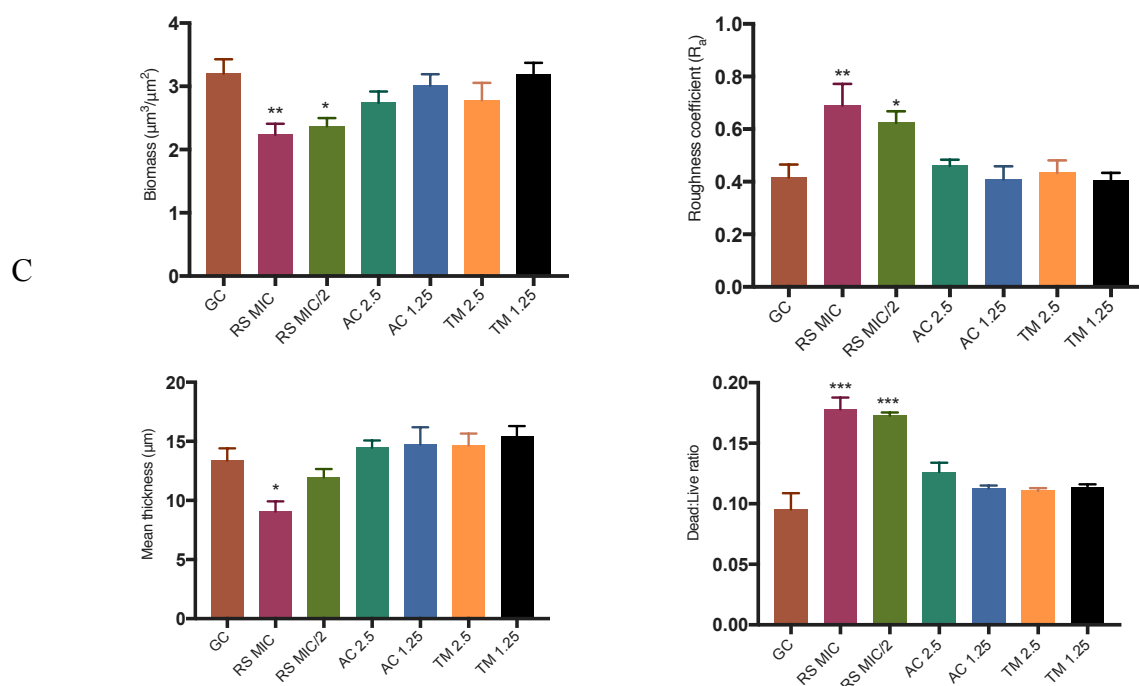


Figure 62 Effects of *A. canariense*, *R. stricta*, and *T. macropterus* on the biofilm eradication of MRSA using a live/dead bacterial viability assay (A and B) showing CLSM images of MRSA 24 h biofilms treated AC and TM (2.5 and 1.25 mg/mL), RS (MIC and MIC/2) compared to untreated controls. (C) Biofilm parameters obtained with the quantitative analysis of CLSM Z stack images via COMSTAT 2.1. Data presented as mean \pm standard error (SE) and experiments were performed three times. Statistical analysis of significant changes compared to each others (* $p < 0.05$, ** $p < 0.01$, *** $p < 0.001$)

5.6 Conclusion

Preliminary screening of five plant extracts through agar well diffusion assay revealed that *R. stricta* demonstrated broadspectrum antimicrobial activity against Gram-positive and Gram-negative tested strains. *A. canariense* and *T. macropterus* were active against all Gram-positive bacteria, only. *R. stricta* minimum inhibitory (MIC) and minimum bactericidal concentrations (MBC) were determined with broth microdilution assay against both Gram-positive and Gram-negative bacteria. Plant extracts and collected fractions were examined through bacterial bioautographic assay. Subsequently, active fractions were identified. Although *A.*

canariense and *T. macropterus* demonstrated a partial inhibition of bacterial growth in a well diffusion assay, a bacterial bio-autographic analysis confirmed the existence of antimicrobial compounds that inhibited *S. aureus* and MRSA strains. The results of a bacterial bio-autographic study indicate the presence of several antimicrobial compounds. *R. stricta* showed promising broad-spectrum antimicrobial activity against *S. aureus*, MRSA, *S. epidermidis*, *P. aeruginosa*, and *E. coli* through different antimicrobial screening techniques.

All three extracts inhibited the growth of *S. aureus* biofilms, demonstrating their antibiofilm properties. *A. canariense* and *R. stricta* effectively penetrated pre-formed *S. aureus* biofilms and eradicated them. Furthermore, CLSM images and COMSTAT 2.1 quantitative analysis of bacterial biofilm demonstrated that *R. stricta* has a potent antibiofilm effect with a broad-spectrum antimicrobial activity against planktonic and biofilm cultures.

Chapter 6: Antimicrobial Activities of Isolated Compounds

6.1 Introduction

Plants could be considered as sources of potential antiseptic or antimicrobial agents since they have developed complicated defensive mechanisms against microorganisms, such as the employment of chemical defenses utilising a wide variety of structurally distinct secondary metabolites known as natural products to combat invading microorganisms (Zaynab et al., 2018). In addition to their extensive chemical diversity with more than 370 thousand species of plants on earth, plants also possess additional distinguishing characteristics that are interesting for drug discovery and development (Christenhusz and Byng, 2016). These characteristics include their accessibility, the demonstrated clinical efficacy of plant extracts in traditional use across the globe in local communities, and the possibility for synergistic interactions between phytochemicals and other active compounds (Gurib-Fakim, 2006; Caesar and Cech, 2019).

Throughout history, natural products from plants have played a vital role in identifying and developing drugs. In addition, the hit rate for discovering new antimicrobial agents through synthetic combinatorial chemical library screening has fallen short of expectations. Since their primary purpose is to interact with biological systems, natural products also tend to have a higher hit rate than synthetic compounds because of the wide variety of chemical and structural diversity they possess (Harvey et al., 2015).

Alkaloids, terpenoids, phenolic acids, and phenols are examples of natural products. Although, many of these compounds are small compounds with antimicrobial effects, few are commercially available as antiseptics or food preservatives. That could be attributed to the lengthy process, which starts with detecting antimicrobial activity in a plant extract to isolating

and evaluating the active compounds. This process includes identification, purification, and *in vitro* and *in vivo* evaluation of the biological and pharmacological properties of the compounds, and confirmation through different phases of clinical trials. Many of the antimicrobial compounds that have reached medical practice in the past four decades are regarded to have been derived from natural products produced by bacteria and fungi (Newman and Cragg, 2020).

In order to isolate and identify bioactive constituents from complex plant extracts, a comprehensive range of techniques known as bioassay-guided fractionation is commonly used. Bioassay-guided fractionation is a repetitive process that alternates between chemical fractionation and targeted bioassays. As the mixture is fractionated, the level of complexity falls, making it possible to isolate and identify the compounds responsible for the observed biological action (Kinghorn, 1998). Camptothecin and taxol (Wall and Wani, 1996; Oberlies and Kroll, 2004), artemisinin (Tu, 2011) and vinblastine (Noble, 1990) were discovered using this approach, which has long been the gold standard in natural product discovery.

Although medicinal plants are frequently regarded as effective and safe and offer various benefits, they have a few disadvantages. First, there is a risk of consumers purchasing medicinal plants of poor quality due to the lack of standardization. Second, as the production process is not as strictly monitored as it is in the pharmaceutical industry, the quality of medicinal plants varies from batch to batch. Third, as most individuals self-administer these remedies, there is a risk of accidental overdose, which can result in adverse side effects. Moreover, medicinal plants include a diverse range of highly complex compounds, making it difficult to characterise all properties (Rafieian-Kopaei, 2012; Parasuraman, 2018; Howes et al., 2020). Adulteration is another severe issue with medicinal plants. Renal impairment may occur due to steroid and

heavy metal adulteration that has appeared in a few formulations (Hussin, 2001; Posadzki et al., 2013). Finally, variation in the constituents of medicinal plants and preparations owing to environmental, cultural, and genetic conditions has made the application of herbal remedies more difficult (Oluyemisi et al., 2012). Consequently, isolating a pure compound from medicinal plants might overcome all of these obstacles, and could display a superior antibacterial efficacy and safety profile with a low degree of unwanted and possibly toxic side effects (Hopkins, 2008). In addition, medicinal plants provide a source of antiseptics or antimicrobial lead molecules that could aid supply the drug discovery pipeline in response to the rising antibiotic resistance crisis (Harvey et al., 2015; Shen, 2015).

Chapter 5 investigated the antimicrobial effect of *A. canariense* and *R. stricta* whole extracts and fractions against a range of clinically relevant bacteria using a bioassay-guided fractionation process. Data indicated the presence of several active compounds. Two compounds were isolated and identified as vincadifformine from the hexane fraction of *R. stricta* (RSH6) and γ -linolenic acid from the chloroform fraction of *A. canariense* (ACC8).

R. stricta is a plant rich in alkaloids, with more than 100 alkaloids have been identified (Gilani et al., 2007). One of which is vincadifformine (Kumara, 2010; Akhgari et al., 2015), a terpenoid indole alkaloid that has been isolated from other plants, such as *Aspidosperma pyriformium* (Mustofa et al., 2006), *Kopsia arborea* (Cheenpracha et al., 2014), and *Amsonia hubrichtii* (Levac et al., 2016), with antiplasmodial and cytotoxic activity (Mustofa et al., 2006).

Alkaloids are one of the largest groups of natural products, with over 20,000 unique compounds and a wide range of biosynthetic routes and chemical structures (Matsuura and Fett-Neto, 2017). Alkaloids are nitrogen-containing molecules with low molecular weight that are often

alkaline due to the existence of a nitrogen-containing heterocyclic ring (Yang and Stöckigt, 2010). The amino acids tyrosine, lysine, tryptophan, ornithine, and phenylalanine are used to synthesize alkaloids. Alkaloids are classified based on their biogenesis, closely related to their molecular structure (Ncube et al., 2008). Alkaloids are believed to play a critical role in self-protection, communication, and competition inhibition. For example, some plants utilise alkaloids as natural insecticides or pesticides to protect themselves from the destructive effects of certain insects (Wink and Twardowski, 1992). They showed several pharmacological effects, including antiarrhythmic (quinidine), central nervous system stimulant (ephedrine), a vasodilator (vincamine), hypertension (reserpine), antineoplastic (vinblastine and vincristine), and antimalarial (quinine) properties. In addition to stimulant properties (caffeine and nicotine), alkaloids can exert an analgesic effect, as in the case of morphine. Moreover, alkaloids could possess antibacterial properties (Barbieri et al., 2017). For example, sanguinarine, a benzophenanthridine alkaloid isolated from the rhizomes of *Sanguinaria canadensis*, had broad-spectrum antimicrobial activity and anti-inflammatory properties (Godowski, 1989).

γ -linolenic acid (GLA) was isolated and identified from *A. canariense*; gamma-linolenic acid is an omega-6 polyunsaturated fatty acid with a carboxylic acid and 18-carbon chain including double bonds at positions 6, 9, and 12 (Fan and Chapkin, 1998). It can be found in human milk and several plants, including *Borago officinalis* (Asadi-Samani et al., 2014) and *Oenothera biennis* (Timoszuk et al., 2018), *Asperugo procumbens* (Łazarski, 2021) and *Ribes nigrum* (Guil-Guerrero et al., 2001). Their pharmacological activity has been extensively investigated over many years, with a particular focus on their anti-inflammatory effects, for example, their effect on atopic dermatitis (Andreassi et al., 1997; Foolad et al., 2013),

rheumatoid arthritis (Cameron et al., 2011; Macfarlane et al., 2011), and asthma (Arm et al., 2013). Furthermore, GLA is known to possess antimicrobial activities with many studies against Gram-positive and Gram-negative strains (Giamarellos-Bourboulis et al., 1995; McGaw et al., 2002; Desbois and Lawlor, 2013; Park et al., 2013; Yuyama et al., 2020).

This chapter will evaluate isolated compounds' antimicrobial and antibiofilm actions to better comprehend the rationale behind the traditional usage of *A. canariense* and *R. stricta*.

6.2 Chapter Aim and Objectives

This chapter aims to determine the antibacterial and antibiofilm activity of two isolated and identified pure compounds, γ -linolenic acid and vincadifformine from *A. canariense* and *R. stricta*, against a panel of bacteria clinically associated with skin infections to fully comprehend their foundations for traditional use.

- To develop an assay capable of determining minimum inhibitory and minimum bactericidal concentrations of isolated compounds through broth microdilution assay against *S. aureus*, MRSA, *S. epidermidis*, *E. coli* and *P. aeruginosa*.
- To develop a method for determining the ability of isolated compounds on *S. aureus*, MRSA, *S. epidermidis*, *E. coli* and *P. aeruginosa* bacterial biofilm formation and eradication.
- To develop a method for determining the ability of isolated compounds to affect *S. aureus* and MRSA formed biofilm biomass parameters by utilising Confocal Laser Scanning Microscopy (CLSM).

6.3 Materials

6.3.1 Chemicals and Culture Media

Chemicals, reagents, solvents, Mueller Hinton agar (MHA), and broth (MHB) were acquired from ThermoFisher Scientific (Loughborough, UK). In addition, 96-well plates (black, flat bottom, clear glass bottom, sterile, treated, individually wrapped with lid, polystyrene plate) were purchased from Greiner Bio-One Ltd (Stonehouse, UK), and 96-well microplates (flat bottom, transparent, sterile, tissue culture-treated surface, polystyrene plate) were acquired from Sarstedt (Leicester, UK). Standard vincadifformine with a minimum of 95% purity was purchased from Biosynth Carbosynth (Compton, UK). Standard γ -linolenic acid with a minimum of 98% purity was purchased from Cambridge Bioscience (Cambridge, UK). All supplemented media were prepared according to manufacturer instructions and were sterilized through an autoclaving process at 123 °C for 15 min.

6.3.2 Bacterial Cultures

SSTI-causing microorganisms were used to investigate the antibacterial activity of plant extracts: *Staphylococcus aureus* 12973 from the National Collection of Type Cultures (NCTC, UK), Methicillin-resistant *Staphylococcus aureus* (MRSA) 13373 from the National Collection of Type Cultures (NCTC, UK), *Staphylococcus epidermidis* 14990 from the American Type Culture Collection (ATCC, USA), *Pseudomonas aeruginosa* 6749 from the National Collection of Type Cultures (NCTC, UK), *Escherichia coli* (MS2) 15597 from the American Type Culture Collection (ATCC, USA). In addition, Microbank cryoprotective beads

purchased from Pro-Lab Diagnostics Ltd (Birkenhead, UK) were utilized to freeze bacterial cultures at -80 °C for future use.

6.4 Methods

6.4.1 Preparation of Samples

Vincadifformine stock solution was made by dissolving 100 mg in 1 mL Dimethyl sulfoxide (DMSO). Experimental samples were prepared by dissolving stock solution in 1% methanol at a final concentration of 2 mg/mL, with 1% methanol serving as the vehicle control. The γ -linolenic acid was made by dissolving it in 1% ethanol to a final concentration of 2 mg/mL, with 1% ethanol serving as the vehicle control.

6.4.2 Broth Microdilution Test to Determine Minimum Bactericidal and Minimum Inhibitory Concentrations

It was adapted with slight modifications from the published Clinical and Laboratory Standards Institute (CLSI) guidelines to evaluate the antimicrobial activity of natural products. It offers high-throughput screening by utilizing 96-well plates, and this approach can determine the precise concentration that inhibits the growth of bacteria (MIC) and the concentration that eradicates it (MBC). First, an overnight culture of the desired bacteria was prepared. Then, sterile filtered (0.22 μ m) samples (isolated compounds) were prepared, with 1% methanol or 1% ethanol at a final concentration of 1 mg/mL and diluted with double strength MHB to prevent the loss of MHB nutrition by the dilution process at a ratio of 1:1. A serial dilution of samples was carried out across the 96-well plates with 100 μ L MHB in each well starting from 1 mg/mL to 3.9 μ g/mL. The bacterial suspension was prepared according to the previously

described agar well diffusion assay (Section 5.4.7). According to the previously reported Miles and Misra Drop Counting Method, the OD600 of bacterial suspension was measured and adjusted to the target concentration of 1×10^6 CFU/mL. Excluding the sterility wells, each well was inoculated with 100 μ L of a bacterial suspension at a final concentration of 5×10^5 CFU/mL. Sterile normal strength MHB was also used to prepare a 96-well plate with identical sample dilutions to test plates without bacterial inoculation. Blank plates provided baseline adjustment against any colouration generated by the test agents over tested concentrations. Blank and inoculated plates were incubated at 37 °C for 24 h.

After the incubation period, the absorbance in each well of the test and blank plates was measured at 600 nm using a Tecan Infinite F200 PRO Spectrophotometric Microplate Reader.

Background correction was performed by subtracting each well reading from its corresponding background well. Moreover, the percentage of inhibition was calculated according to the following equation:

$$\text{Percentage of inhibition} = \left(1 - \frac{\text{mean absorbance of corrected treatment wells}}{\text{mean absorbance of corrected control wells}} \right) \times 100$$

The MBC of each sample was determined by sub-culturing wells into a freshly prepared MH agar plate by dropping 10 μ L aliquots from each well in triplicate onto the surface of the agar and incubating it for 24 h at 37 °C. The MIC₉₀ of each treatment was determined as the lowest concentration needed to inhibit growth by at least 90% of the mean. In addition, the minimum concentration of samples that exhibited no bacterial colony growth was recorded as the MBC. All experiments were conducted in triplicate, and each run included positive and negative controls.

6.4.3 *In Vitro* Assessment of Isolated Compounds on Biofilm Formation and Biofilm Eradication

6.4.3.1 Assessment of Isolated Compounds on Biofilm Formation and Biofilm Eradication

An overnight bacterial suspension was prepared, as described previously (Section 5.4.10.2). In addition, an adapted spectrophotometric technique was utilised to conduct biofilm inhibition investigations in a 96-well plate (Celiksoy et al., 2021). First, 100 μL of isolated compounds at MIC values were added to each well then 100 μL of bacterial solution (10^8 CFU/mL) was added to each well. Next, to prepare a separate background plate without bacterial inoculation, 100 μL of previously prepared treatments were added to 100 μL of MH broth at similar concentrations. Twenty-four h were devoted to incubating plates under aerobic conditions at 37 °C. After incubation, the solution was removed from each well, washed twice with 100 μL of distilled water per well, and air-dried for 15 min. After adding 100 μL of 1% crystal violet solution made with distilled water, the mixture was incubated for 30 min at room temperature. Following rinsing three times to remove any residual crystal violet, 100 μL of 95% ethanol was added to each well, and the plate was incubated for 20 min. The measured OD of plates was set at 570 nm.

To reduce non-specific crystal violet binding, the background OD values of compounds (without bacterial inoculation) were deducted from the OD treatments and controls. The percentage of biofilm inhibition was determined using the following equation:

$$\text{Percentage of biofilm inhibition} = 100 - [(\text{OD of treatment}/\text{OD of control}) \times 100].$$

Using a similar methodology, the potential of isolated compounds to eradicate biofilms was examined. In summary, a plate containing the investigated bacteria was developed and incubated for 24 h at 37 °C under aerobic conditions to assure biofilm formation. After the incubation period, the supernatant was gently removed from every well, fresh treatments at the previously determined concentration were added, and the biofilm inhibition procedure was repeated. Finally, the percentage of biofilm eradication was estimated using the same procedure and equation applied in inhibiting biofilm formation.

6.4.3.2 Live/Dead Imaging of Biofilms Treated with Compounds through Confocal Laser Scanning Microscopy

The effect of isolated compounds on biofilms grown in 96-well glass bottom plates (Greiner Bio-One Ltd, Kremsmünster, Austria) was investigated by a Live/Dead BacLight™ bacterial viability investigation was performed. This experiment was adapted from Celiksoy et al. (2021). 96-well glass bottom plates were incubated for 24 h at 37 °C, with a bacterial suspension that had been adjusted from an overnight subculture to contain 1×10^8 CFU/mL. The next day, the supernatant was carefully removed from each well, and freshly prepared treatments at the same concentration (Section 6.4.3.1) were added before the plate was incubated at 37 °C for an additional 24 h. The plate's supernatant was discarded after the incubation time. Then, each well was stained with 4 µL/well of Living/Dead stain, which was prepared following the Living/Dead Bacterial Viability kit's instructions by combining 2 µL of SYTO 9 (live stain cells) and 2 µL of propidium iodide (dead stain cells) in 1 mL of PBS. The stain was applied gently to the centre of the well to minimize upsetting the formed biofilm.

Furthermore, the plate was incubated at 37 °C for 10 min at room temperature, while wrapped with aluminium foil to prevent light-induced damage. Finally, 47 µL of PBS was added to each well before image acquisition using a Leica TCS SP5 Confocal Microscope (Leica Microsystems Ltd, Buckinghamshire, UK). Images were viewed using a 60 x 1.8 oil objective with a one µm z-step. Four channels of view were chosen for each well, and captured images were processed using COMSTAT2 and ImageJ to generate image sequences to quantify biofilm properties and unattached bacteria. Automated thresholding employed by Otsu to each image slice, separated bacterial fluorescence from background noise. Several parameters, including mean biofilm thickness, biomass, roughness coefficient, and dead:live ratio, were quantified by analysing Image sequences in COMSTAT2. The COMSTAT2 analysis of findings was provided as the mean and standard error for each parameter, and assays were performed three times.

6.4.4 Statistical Analysis

The acquired data were statistically analysed using GraphPad Prism 7.0a (GraphPad Software Inc., San Diego, USA); all data is reported as the mean \pm standard error (SE), and all experiments were conducted three times each. The means and standard errors were calculated using Excel (Microsoft) software. The statistical analysis was performed using a one-way analysis of variance with Dunnett post-test, to assess the significance of the difference between the means of the control and experimental groups. The statistically significant difference between groups was determined using Tukey's post-test, with a threshold of $p < 0.05$ deemed to indicate statistical significance.

6.5 Results and Discussion

6.5.1 Broth Microdilution Assay

The antimicrobial activity of isolated compounds was evaluated using a broth microdilution assay against the following bacterial strains: *S. aureus*, MRSA, *S. epidermidis*, *P. aeruginosa*, and *E. coli*. The lowest concentration that inhibits bacterial growth (MIC) was determined by measuring the absorbance of the wells, and sub-culturing samples into MHA plates determined the minimum concentration that kills bacteria (MBC). Vincadifformine showed a weak antimicrobial activity against both Gram-positive and negative microorganisms with an MIC₉₀ of 500 µg/mL and MBC value > 2 mg/mL against Gram-positive strains. MIC₉₀ and MBC values for Gram-negative strains were more than 2 mg/mL, despite a 40% suppression of *P. aeruginosa* growth at a concentration of 500 µg/mL (Figure 63). The weaker antimicrobial activity of the isolated compound, compared to the whole extract of *R. stricta* indicates that synergistic interaction or multifactorial effects between constituents of *R. stricta* extracts is of great importance. Other possible explanations include cumulative effects, improved bioavailability, or simply the additive characteristics of the components (Williamson, 2001). In addition, it shows plant extracts' immense variability and complexity (Gilbert and Alves, 2003).

Several studies have reported that the total activity of natural extracts might arise from the combination of synergistic or antagonistic compounds (Tegos et al., 2008; Stermitz et al., 2002; Wagner and Ulrich-Merzenich, 2009). A study by Junio et al., 2011 identified the three flavonoids 6-desmethyl-sideroxylin, 8-desmethyl-sideroxylin, and sideroxylin from *Hydrastis canadensis* extract. The antimicrobial activity of the alkaloid berberine, another active

constituent in the extract, was synergistically enhanced by these three flavonoids. They improve activity by inhibiting the NorA multidrug resistance pump of *Staphylococcus aureus* without possessing a direct antimicrobial activity. Although the mechanism of action of vincadifformine is unknown, natural products could inhibit the growth of bacteria via a number of mechanisms, such as inducing damage to the cell membrane and cell wall, suppression of efflux pumps, suppression of the bacterial nucleic acid and protein synthesis, suppression of bacterial metabolism, and alteration of the bacterial membrane permeability (Zhang et al., 2020).

γ -linolenic acid exhibited a superior antimicrobial activity with an MIC₉₀ of 31.2 $\mu\text{g/mL}$ against *S. aureus* and 62.5 $\mu\text{g/mL}$ against MRSA and *S. epidermidis*. Furthermore, MBC was 62.5 $\mu\text{g/mL}$ for all three strains (Figure 64). A lesser effect was observed with Gram-negative bacteria with an MIC₉₀ of 2 mg/mL and 1 mg/mL against *P. aeruginosa* and *E. coli*, respectively.

Many studies reported MIC and MBC values comparable to ours, while others reported values distinct from ours. This may result from methodological variations in assessing antimicrobial activity and inoculation procedure, as well as the utilisation of various bacterial strains and growth conditions (Giamarellos-Bourboulis et al., 1995; McGaw et al., 2002; Zhang et al., 2012; Park et al., 2013; Yuyama et al., 2020). Finally, The OH group of the terminal carboxyl group seems critical for the antimicrobial action of γ -linolenic acid since the methylation process often decreases or renders it inactive (Zheng et al., 2005). Table 26 presents MIC₉₀ and MBC values of tested isolated compounds and positive controls.

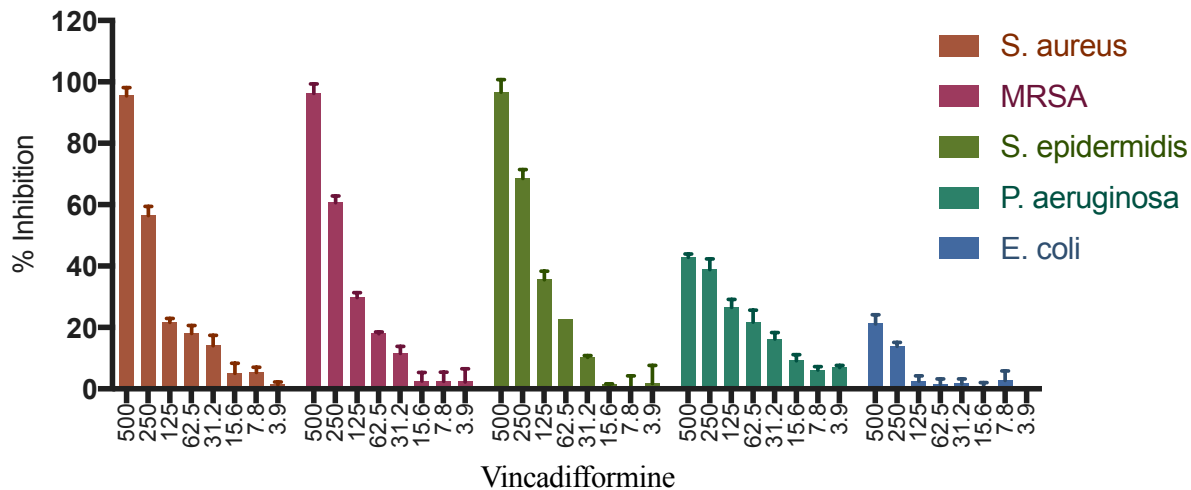


Figure 63 Inhibitory effect of vincadifformine at different concentrations ($\mu\text{g/mL}$) on the growth of selected bacterial strains in MH broth after incubation for 24 h. Data were reported as the mean \pm SE. Three separate experiments were conducted in triplicate to acquire findings

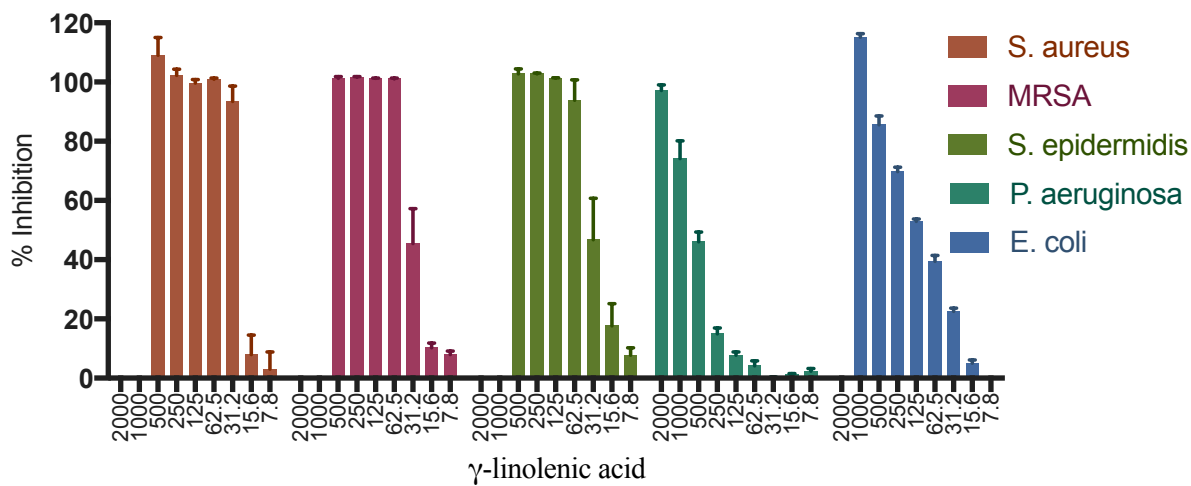


Figure 64 Inhibitory effect of γ -linolenic acid at different concentrations ($\mu\text{g/mL}$) on the growth of selected bacterial strains in MH broth after incubation for 24 h. Data were reported as the mean \pm SE. Three separate experiments were conducted in triplicate to acquire findings

Table 26 Present MIC₉₀ and MBC values of tested isolated compounds and positive controls against selected bacterial stains. Three separate experiments were conducted to acquire findings

Tested Compound	MIC ₉₀	MBC	Bacterial Strain
Vincadifformine	500 µg /mL	> 2 mg/mL	<i>S. aureus</i> , MRSA, and <i>S. epidermidis</i>
Vincadifformine	> 2 mg/mL	> 2 mg/mL	<i>P. aeruginosa</i> and <i>E. coli</i>
γ-linolenic acid	31.2 µg /mL	62.5 µg /mL	<i>S. aureus</i>
γ-linolenic acid	62.5 µg /mL	62.5 µg /mL	MRSA and <i>S. epidermidis</i>
γ-linolenic acid	2 mg/mL	> 2 mg/mL	<i>P. aeruginosa</i>
γ-linolenic acid	1 mg/mL	> 2 mg/mL	<i>E. coli</i>
Vancomycin	1.95 µg /mL	3.9 µg /mL	<i>S. aureus</i> , MRSA, and <i>S. epidermidis</i>
Ofloxacin	1.95 µg /mL	15 µg /mL	<i>P. aeruginosa</i>

6.5.2 The Effect of Isolated Compounds on the Inhibition of Biofilm Formation and Biofilm Eradication

Vincadifformine and γ-linolenic acid were investigated for their abilities to prevent biofilm formation (Figure 65) and eliminate pre-formed biofilm (Figure 66) by employing an *in vitro* crystal violet technique on a microtiter plate. Concentrations evaluated against Gram-positive strains were MICx2 (double the MIC value) and MIC values and against Gram-negative strains 1 and 0.5 mg/mL.

The effect of vincadifformine on the inhibition of *S. aureus* biofilm formation was significant ($p < 0.001$; $p < 0.05$), and a similarly significant effect was seen for the eradication of pre-formed biofilm at MICx2 and MIC values ($p < 0.01$; $p < 0.05$). At MICx2 and MIC concentrations, γ -linolenic acid dramatically reduced biofilm formation and eradicated biofilm which had already formed, and the effect was deemed significant ($p < 0.001$).

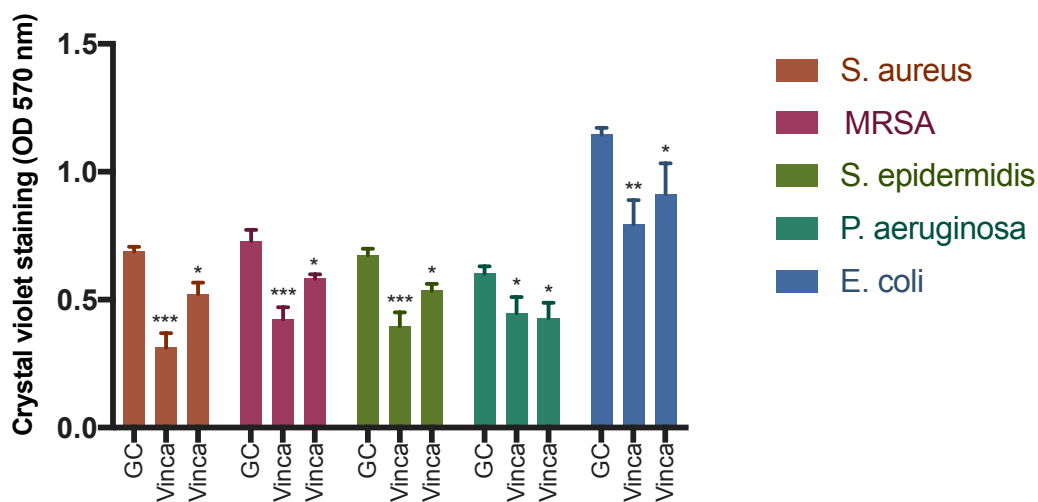
For MRSA, vincadifformine significantly inhibited biofilm formation ($p < 0.001$; $p < 0.05$), and pre-existing biofilm was significantly eradicated ($p < 0.001$). γ -linolenic acid continued to exert a potent inhibiting and eradicating effect on biofilm ($p < 0.001$).

Similar patterns of a significant effect were seen with vincadifformine inhibition of *S. epidermidis* biofilm formation at MICx2 and MIC concentrations ($p < 0.001$; $p < 0.05$), and a comparable effect was seen in the eradication of biofilms ($p < 0.001$; $p < 0.01$). In addition, γ -linolenic acid significantly impacted biofilm inhibition and eradication ($p < 0.001$).

Although vincadifformine showed significant inhibition of *P. aeruginosa* biofilm ($p < 0.05$), it had no impact on pre-formed biofilm ($p > 0.05$) at concentrations 1 and 0.5 mg/mL, on the other hand, the γ -linolenic acid effect on *P. aeruginosa* biofilm was dramatically significant in inhibition and eradication at 1 and 0.5 mg /mL ($p < 0.001$).

For *E. coli*, at the concentration of 1 and 0.5 mg/mL, vincadifformine exhibited a significant effect on biofilm formation ($p < 0.01$; $p < 0.05$) and on the eradication of pre-formed biofilm ($p < 0.001$; $p < 0.05$). Moreover, the inhibition of biofilm was detected at all tested concentrations of γ -linolenic acid ($p < 0.001$), and the same was observed in the eradication of biofilm, which was deemed significant comparing the control ($p < 0.001$; $p < 0.01$).

A)



B)

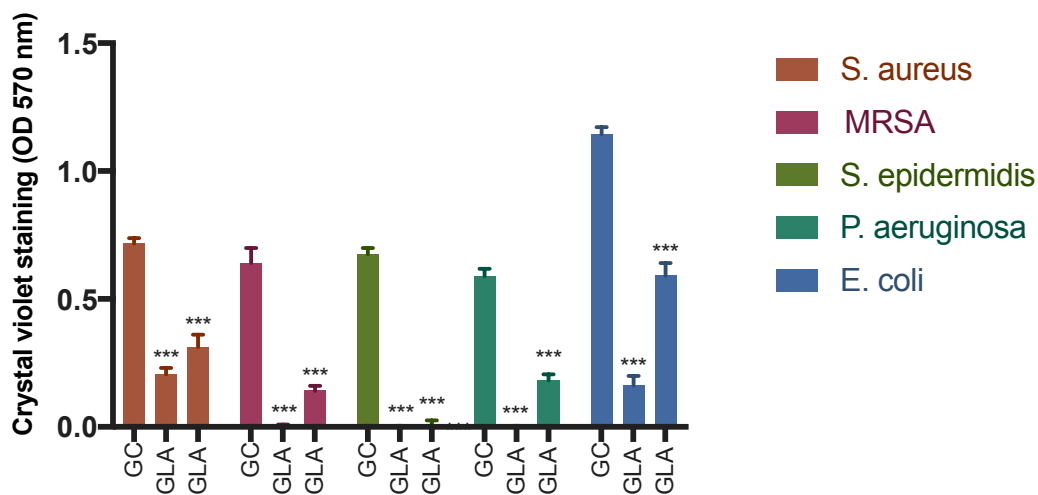
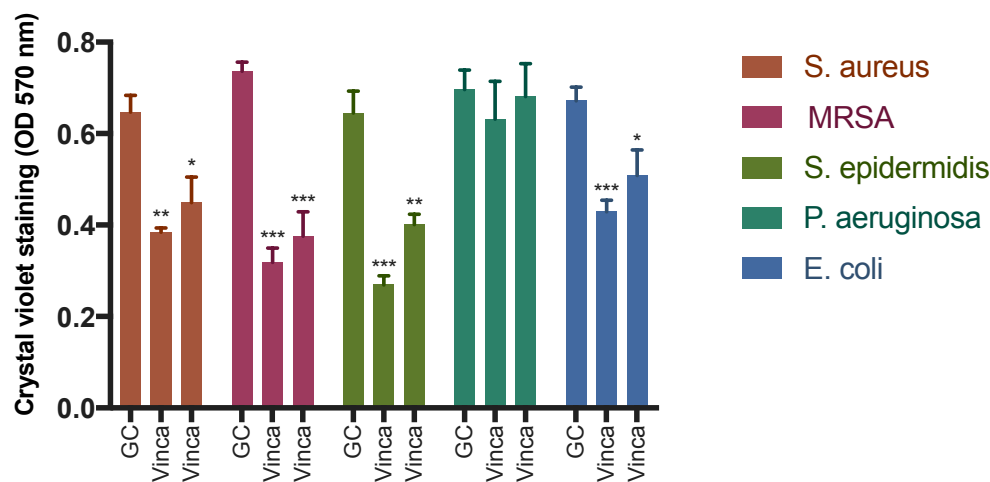


Figure 65 Comparison of the ability of isolated compounds to inhibit biofilm formation for (A) vincadifformine at MICx2 and MIC values for Gram-positive strains and 1 mg/mL and 0.5 mg/mL for Gram-negative strains (B) γ -linolenic acid at MICx2 and MIC values for Gram-positive strains and 1 mg/mL and 0.5 mg/mL for Gram-negative strains, against selected microorganisms in MH broth, following 24 h incubation in 96-well plate using the crystal violet staining method. Data were reported as the mean \pm SE. Three separate experiments were conducted to acquire findings. Analysis of statistically significant differences between treatments and controls via Dunnett post-test (* $p < 0.05$, ** $p < 0.01$, * $p < 0.001$)**

A)



B)

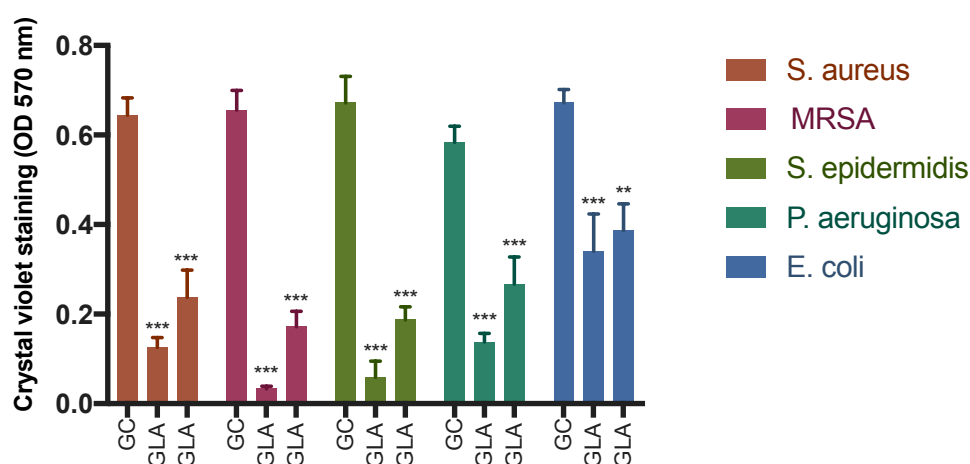


Figure 66 Comparison of the ability of isolated compounds to eradicate pre-formed biofilm for (A) vincadifformine at MICx2 and MIC values for Gram-positive strains and 1 mg/mL and 0.5 mg/mL for Gram-negative strains (B) γ -linolenic acid at MICx2 and MIC values for Gram-positive strains and 1 mg/mL and 0.5 mg/mL for Gram-negative strains, against selected microorganisms in MH broth, following 24 h incubation in 96-well plate using the crystal violet staining method. Data were reported as the mean \pm SE. Three separate experiments were conducted to acquire findings. Analysis of statistically significant differences between treatments and controls via Dunnett post-test (* $p < 0.05$, ** $p < 0.01$, * $p < 0.001$)**

Kenny et al. (2009) reported that unsaturated fatty acids inhibit biofilm formation by disturbing the cell membrane. In one study, their findings were in accordance with ours, in which six

unsaturated fatty acids displayed antibiofilm action, but three saturated fatty acids did not (Lee et al., 2017). This may indicate that the double bonds contribute to the overall antibiofilm activity. Another study reported that combining tobramycin and linolenic acid interfered with quorum sensing and prevented *P. aeruginosa* biofilm formation at higher concentrations. Linolenic acid enhanced the efficacy of tobramycin and inhibited biofilm formation synergistically (Chanda et al., 2017).

Antimicrobial agents used to treat biofilms are often chosen based on their selectivity toward bacteria and ability to effectively permeate the biofilm extracellular polymeric substances matrix (EPS) (Wu et al., 2015). Both compounds demonstrated the capacity to penetrate Gram-positive and, to a lesser extent, negative pre-formed biofilm solid EPS.

In this study, Gram-negative biofilm formation was found to be more resistant to vincadifformine and γ -linolenic acid than Gram-positive biofilm formation. The biofilm formation of *P. aeruginosa* and *E. coli* could only be decreased at a concentration of 1 and 0.5 mg/ mL of vincadifformine and γ -linolenic acid. Due to the presence of a peptidoglycan layer and an extra outer membrane, resistance against Gram-negative pathogens is expected (Vadillo-Rodriguez et al., 2008). Future studies are necessary to evaluate the capacity of isolated compounds to inhibit and remove biofilm of different bacterial strains and investigate the possibility of combining these compounds with antibiotics. For example, a recent study explored the feasibility of combining unsaturated fatty acids with several known antibiotics. They detected lower MIC values with the combination compared to antibiotics against multidrug-resistant *P. aeruginosa* (Selvadoss et al., 2018).

6.5.3 Evaluation of Biofilm Eradication by Live/Dead Bacterial Viability Assay

BacLight Live/Dead Bacterial Viability Kit was used to investigate the structure of *S. aureus*, and MRSA formed biofilm and to evaluate the ability of vincadifformine and γ -linolenic acid to eradicate the biofilm at different concentrations for vincadifformine (MIC, MICx2) and γ -linolenic acid (62.5 $\mu\text{g}/\text{mL}$). CLSM images of the control biofilm revealed a thick and compact structure stained green with SYTO 9, suggesting the presence of viable cells. Using ImageJ and COMSTAT2.1 image analysis software, the acquired Z-stack images data were analysed to get further information on the biofilm structure, such as biofilm mass, mean thickness of biofilm, dead live ratio, and roughness coefficient (Heydorn et al., 2000). The CLSM images were displayed with ImageJ software.

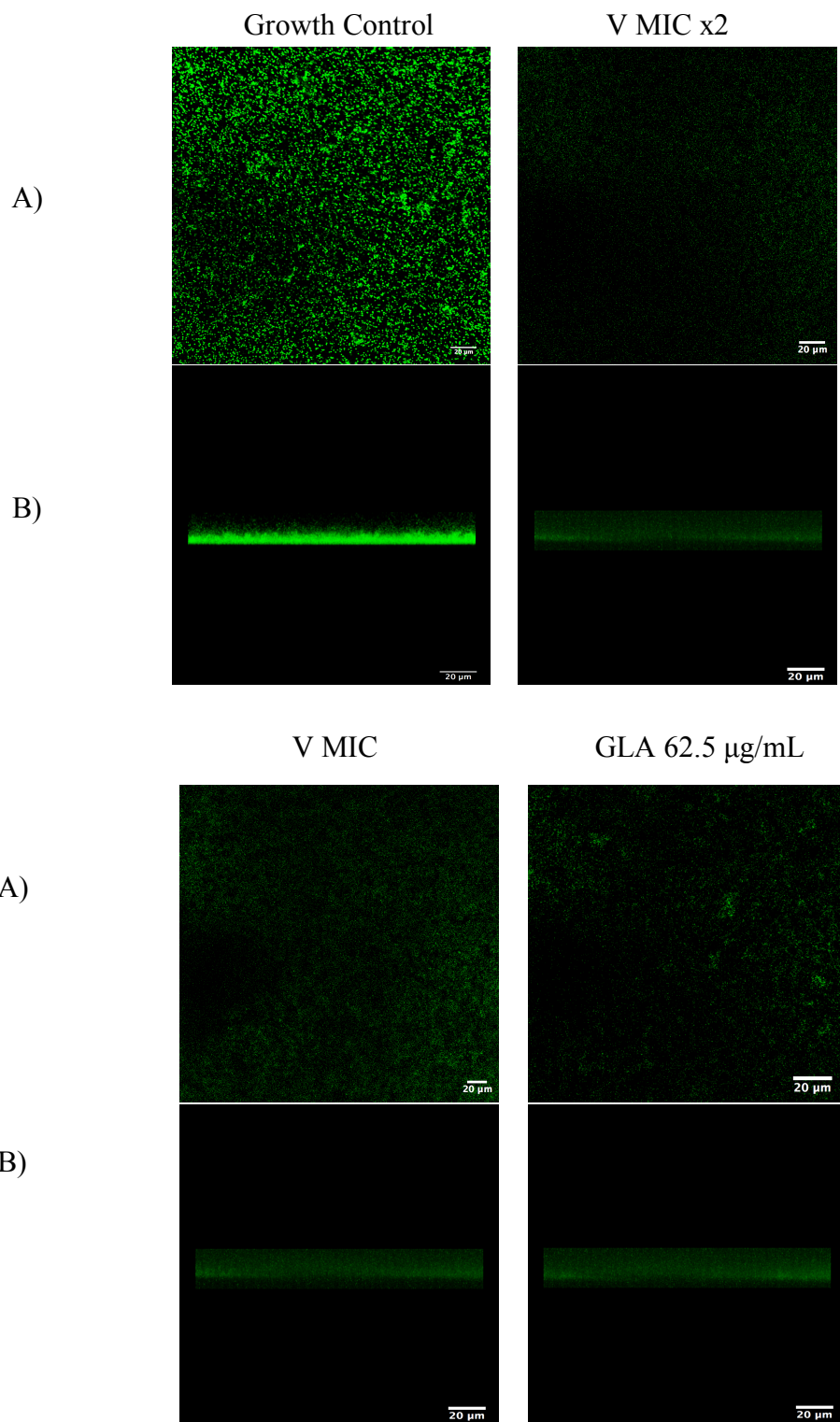
The effect on *S. aureus* validated the previous biofilm eradication crystal violet method (Section 6.5.2), as the addition of vincadifformine and γ -linolenic acid to *S. aureus* biofilm resulted in a significant reduction in biofilm biomass after 24 h incubation, compared to untreated controls ($p < 0.001$, Figure 67). At the same time, a significant increase in the roughness coefficient of biofilm was observed ($p < 0.001$; $p < 0.01$; $p < 0.05$), which indicates the heterogeneity of the formed biofilm. Moreover, all treatments significantly reduced the average biofilm thickness ($p < 0.001$; $p < 0.01$), as presented by the images provided (Figure 67). Both treatments significantly increased the dead-to-live ratio compared to the untreated control at all tested concentrations ($p < 0.001$).

MRSA strain demonstrated resistance toward tested compounds, as vincadifformine showed a significant reduction of biofilm mass at MICx2 value only ($p < 0.05$, Figure 68), without any observed effect on the biomass at MIC value ($p > 0.05$). γ -linolenic acid significantly decreased

the biomass of MRSA at MIC value ($p < 0.05$). A significant increase in the roughness coefficient of the biofilm was only observed with vincadifformine at double the minimum inhibitory concentration ($p < 0.05$), the rest of the treatments had no effect ($p > 0.05$). This variation in the efficacy may be explained by the characteristics of the biofilm, which allow bacteria to be more resistant to antimicrobial agents at MIC value. Thus, higher antimicrobial concentrations will be required to eradicate it. Although vincadifformine at MICx2 concentration decreased the average biofilm thickness, this effect was deemed non-significant, and the same was observed with the rest ($p > 0.05$). The dead-to-live bacteria ratio increased significantly across all tested treatments ($p < 0.001$; $p < 0.05$). These findings confirm the ability of compounds to penetrate biofilm EPS and neutralise the bacterial cells (Cochran et al., 2000).

Due to their low toxicity and broad-spectrum antimicrobial activity, unsaturated fatty acids have emerged as a possible alternative to existing antimicrobials (Yoon et al., 2018). However, unsaturated fatty acids can produce unstable molecules by binding non-specifically to proteins and have an unpleasant flavour, which has limited their general use as antimicrobial agents. Both issues can be solved by administering the unsaturated fatty acids as lipids in combination with a lipolytic enzyme (Refsgaard et al., 2000; Guil-Guerrero et al., 2001; Dierick et al., 2002). Several studies have examined the ability of fatty acids to inhibit the biofilm formation of *S. aureus* (Davies and Marques, 2009), *Candida albicans* (Prasath et al., 2019), and *P. aeruginosa* (Inoue et al., 2008). The antimicrobial activity of unsaturated fatty acids can be influenced by various factors, including the length of the carbon chain, the molecular structure, and the positions and number of double bonds (Desbois and Smith, 2010). This study investigated vincadifformine and γ -linolenic acid anti-biofilm activity against *S. aureus* and MRSA. Both compounds exhibited antibiofilm activity, with MRSA biofilm showing more

resistance. These isolated compounds could be responsible for *A. canariense* and *R. stricta* antimicrobial and antibiofilm action.



C)

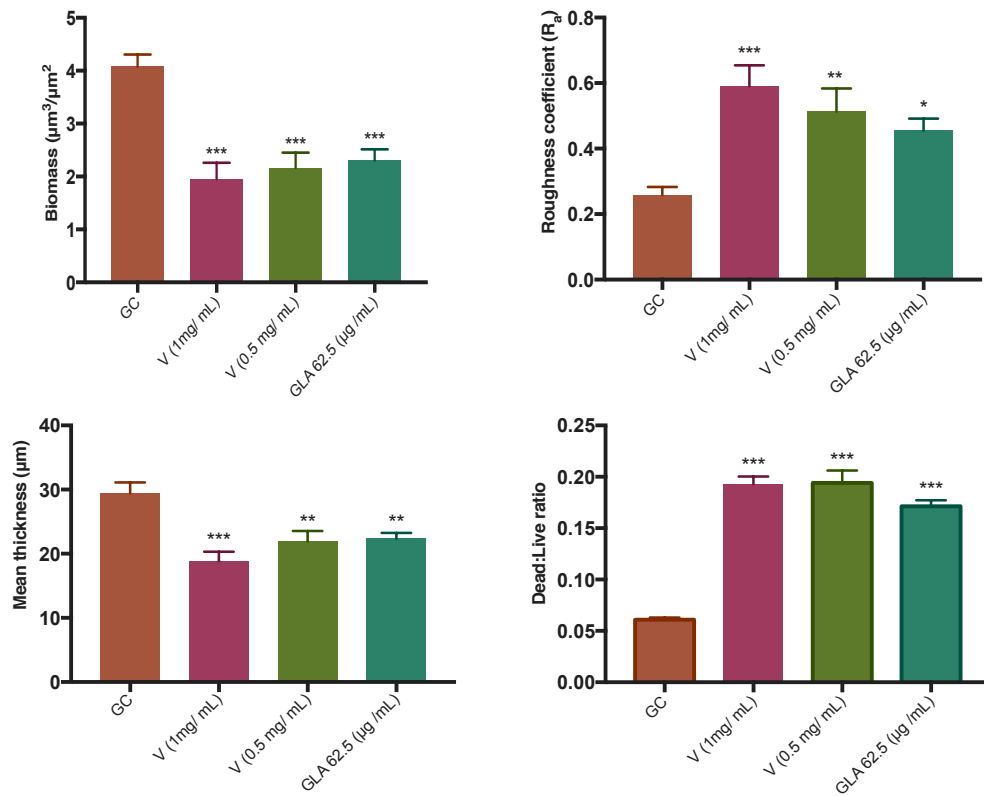
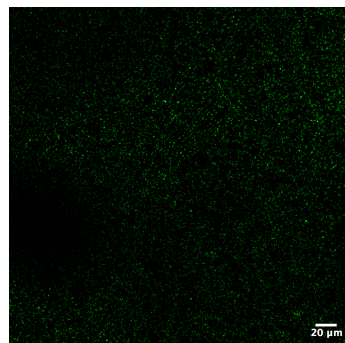
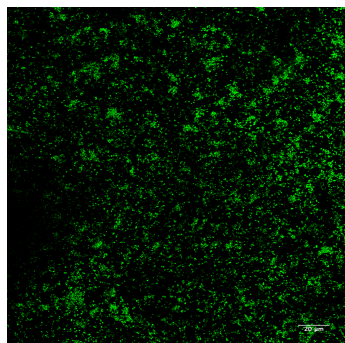


Figure 67 Effects of vincadifformine and γ -linolenic acid on the biofilm eradication of *S. aureus* using a live/dead bacterial viability assay (A and B) showing CLSM images of *S. aureus* 24 h biofilms treated vincadifformine (1 and 0.5 mg/mL), γ -linolenic acid (62.5 $\mu\text{g/mL}$), compared to untreated controls. (C) Biofilm parameters were obtained with the quantitative analysis of CLSM Z stack images via COMSTAT 2.1. Data were reported as the mean \pm SE. Three separate experiments were conducted to acquire findings in triplicate. Analysis of statistically significant differences between treatments and controls via Dunnett post-test (* $p < 0.05$, ** $p < 0.01$, *** $p < 0.001$)

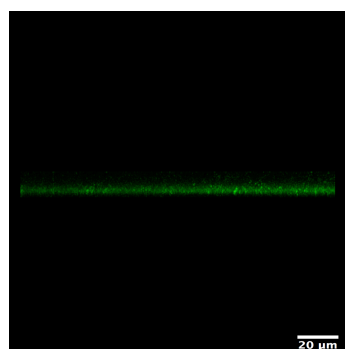
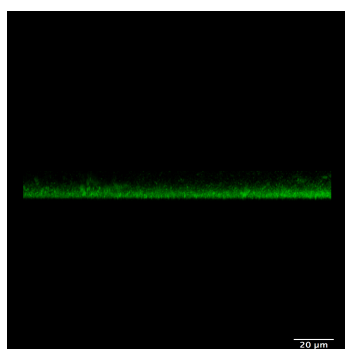
Growth Control

V MIC x2

A)



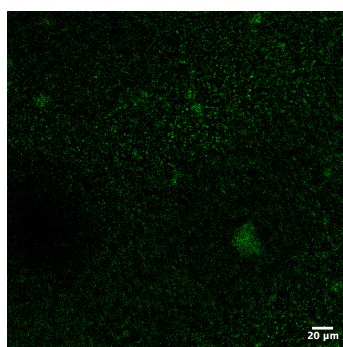
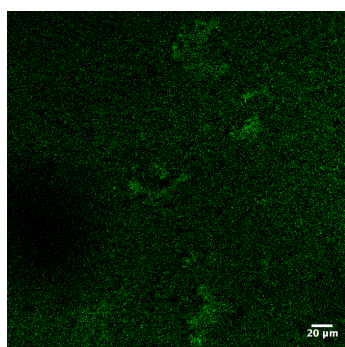
B)



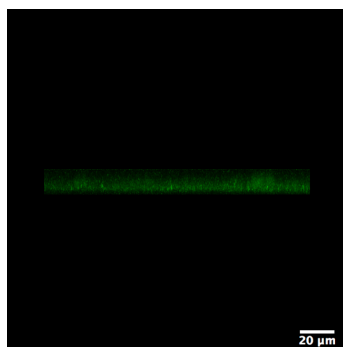
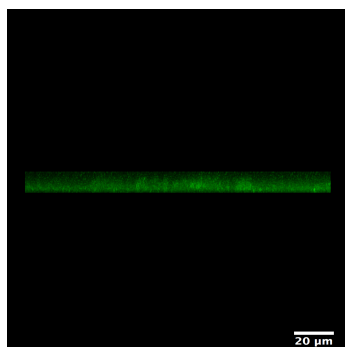
V MIC

GLA 62.5 µg/mL

A)



B)



C)

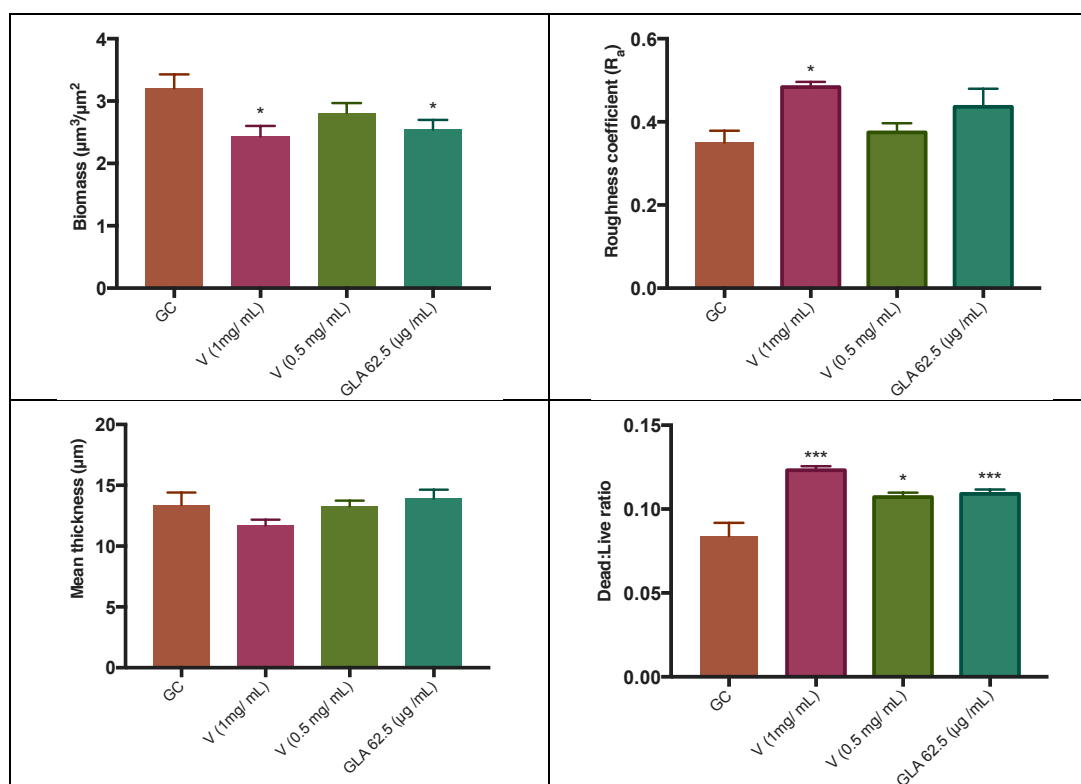


Figure 68 Effects of vincadifformine and γ -linolenic acid on the biofilm eradication of MRSA using a live/dead bacterial viability assay (A and B) showing CLSM images of MRSA 24 h biofilms treated vincadifformine (1 and 0.5 mg/mL), γ -linolenic acid (62.5 μ g/mL), compared to untreated controls. (C) Biofilm parameters were obtained with the quantitative analysis of CLSM Z stack images via COMSTAT 2.1. Data were reported as the mean \pm SE. Three separate experiments were conducted to acquire findings in triplicate. Analysis of statistically significant differences between treatments and controls via Dunnett post-test (* $p < 0.05$, ** $p < 0.01$, *** $p < 0.001$).

6.6 Conclusion

Vincadifformine and γ -linolenic acid demonstrated antibacterial effect against Gram-positive strains, with GLA exhibiting a superior activity. However, against Gram-negative strains, they showed a mild antimicrobial activity, which could be explained by the presence of a peptidoglycan layer and an extra outer membrane. Both compounds exhibited antibiofilm activity against *S. aureus* and MRSA strains. CLSM images and COMSTAT 2.1 quantitative analysis of bacterial biofilm provided qualitative and quantitative confirmation. Both were effective against *S. aureus*, but the MRSA strain was more resistant to isolated compounds. In

general, vincadifformine showed a lower antimicrobial and antibiofilm activity compared to *R. stricta*. These findings suggest that antimicrobial and antibiofilm activity may result from many phytoconstituents' synergistic interactions or multifactorial effects. Thus, the fractionating process may result in loss or decrease such an activity.

Future research is needed to identify the molecular mechanism of action behind antimicrobial and antibiofilm activities and study the feasibility of combining these molecules with antibiotics. In addition, more research is necessary to investigate the antibiofilm actions against mixed-species biofilms.

Chapter 7: Anti-inflammatory Properties of Plant Extracts

7.1 Introduction

Globally, skin wounds have a devastating effect on healthcare systems and economies. Recent reports indicate that almost one billion individuals worldwide suffer from acute or chronic wounds (Garraud et al., 2017). This vast number results in substantial financial costs (Nussbaum et al., 2018). It was predicted that chronic wound treatment costs contributed to up to 3% of overall healthcare expenses in developed countries (Olsson et al., 2019).

Wound healing is a multicellular process that requires the precise coordination of numerous cell types and molecular signalling molecules at the site of the wound. Four distinct, but overlapping steps comprise this process: hemostasis, inflammation, proliferation, and remodeling phase. In brief, hemostasis is the initial phase of wound healing, during which a blood clot develops to stop additional blood loss. Next, neutrophils and macrophages are recruited to clear debris from the wound site to prevent infection during the inflammatory phase. Subsequently, the proliferation stage arrives, in which keratinocytes, endothelial cells, and stem cells are recruited to re-epithelialize and granulate the wound. Angiogenesis, or the formation of new blood vessels from existing vessels, is essential throughout the inflammatory and proliferative phases of wound healing. During the remodelling phase, the granulation tissue is substituted by scar tissue and the quantity of immune cells diminishes, marking the final stage of acute wound healing (Tonnesen et al., 2000; Zahedi et al., 2010; Pereira et al., 2013).

Skin wounds are either acute or chronic, based on their pathogenesis and outcomes. A cascade of molecular processes leads to the regeneration of structural integrity in acute wounds. On the other hand, pathologic processes such as persistent inflammation and infection define chronic wounds that do not heal (Tottoli et al., 2020).

Immune cells' functions in epithelialization are regulated by proinflammatory cytokines, which are released as one of the first mediators in response to skin wounds. Pro-inflammatory cytokines including tumour necrosis factor- α (TNF- α), interleukin (IL)-1, IL-6, and IL-17, all play a role in the inflammation phase of wound healing by activating downstream pathways (Kanji and Das, 2017). Moreover, they promote cell proliferation and differentiation during the re-epithelialization process (Larouche et al., 2018, Xiao et al., 2020). Normal levels of pro-inflammatory cytokines are necessary to prevent infection and promote routine wound healing. On the other hand, excessive production of pro-inflammatory cytokines is problematic, as seen in chronic wounds (Akita, 2019).

In recent years, the importance of keratinocytes in skin wound healing is increasingly being understood. Many different immune genes are expressed by keratinocytes, some of which are induced by skin injury and others by foreign pathogens (Roupé et al., 2010). Interactions between keratinocytes and immune cells are mediated by cytokines, chemokines, antimicrobial peptides (AMPs), and extracellular vesicles released from keratinocytes. This interaction is necessary for wound healing (Brazil et al., 2019). Keratinocytes initiate the inflammatory cascade by sensing pathogen-associated molecular patterns (PAMPs). PAMPs are small molecules found on bacteria and other pathogens, including bacterial endotoxins, lipopolysaccharides (LPS), and viral-derived nucleic acids. In keratinocytes, pattern-recognition receptors (PRRs) such as Toll-like receptors (TLRs), nucleotide-binding oligomerization domain-like receptors, and C-type lectin receptors are expressed and are responsible for recognising PAMPs (Lebre et al., 2007; Chen et al., 2018). As a consequence of the detection by PRRs, several signalling pathways are activated, leading to the release of antimicrobial peptides, cyclooxygenase-2 (COX-2), and pro-inflammatory cytokines, such as

IL-1 β , TNF- α , IL-6, IL-8, CCL2, and CCL20, amongst others (Lebre et al., 2007; Piktel et al., 2019; Jiang et al., 2020).

IL-1 is a critical inflammatory cytokine that may alert the body to a potential threat, trigger gene expression, and induce the skin to release inflammatory mediators. During acute or chronic inflammatory conditions, members of the IL-1 cytokine family stimulate the inflammatory cascade in the skin. Among the 11 known members of the IL-1 family, IL-1 α and IL-1 β play a critical role in inflammation, acting on nearly every cell type and organ system to stimulate the release of additional cytokines, chemokines, adhesion molecules, and mediators in general (Sims et al., 2005; Hu et al., 2010). The pro-inflammatory cytokine IL-6 contributes to innate immune function. It is also necessary for antibody production by B cells. Keratinocytes, fibroblasts, T-lymphocytes, and endothelial cells release IL-6. In addition, it stimulates the transition of M1 pro-inflammatory macrophages to the M2 reparative type. In atopic dermatitis, the secretion of IL-6 by keratinocytes in response to skin injury may play an essential role in developing adaptive immunity (Oyoshi et al., 2009; Kumar et al., 2018; Yang et al., 2019). Keratinocytes and fibroblasts release IL-8 in response to pro-inflammatory cytokines, such as IL-1 α , IL-1 β , interferon- γ , and TNF- α . IL-8 is a potent promoter of polymorphonuclear leukocyte activities, including superoxide production, neutrophil recruitment, chemotaxis, and enzyme release (Futosi et al., 2013; Bernhard et al., 2021). Finally, TNF- α is a crucial mediator that promotes the production of cutaneous and endothelial adhesion molecules. TNF- α plays an important function in cellular regulation by activating a signal transduction pathway involving a mitogen-activated protein kinase. By indirectly inducing inflammation and boosting macrophage-produced growth factors, TNF- α at low levels can enhance wound healing. However, TNF- α has a deleterious influence on healing at

high levels, especially over extended periods (Kupper and Fuhlbrigge, 2004; Barrientos et al., 2008).

Chronic wounds are challenging to manage due to persistent inflammation, and the formation of bacterial biofilms on the surface and within chronic wounds is one cause of this. The interaction between biofilms and the human immune system will activate neutrophils and macrophages, ultimately leading to the accumulation of keratinocytes released pro-inflammatory cytokines such as IL-1 β , TNF- α , and IL-6 (Omar et al., 2017; Wu et al., 2019). Moreover, activated macrophages and neutrophils also release pro-inflammatory cytokines, such as TNF- α and IL-1, and IL-1 β , increasing matrix metalloproteinases (MMP) secretion and decreasing tissue inhibitors of MMPs, and reducing granulation tissue production. This disparity enhances the degradation of the extracellular matrix (ECM), inhibits cell migration, and decreases collagen synthesis and fibroblast proliferation (Mast and Schultz, 1996; Gill and Parks, 2008; Weinstein and Kirsner, 2010). Accumulation of IL-6 is commonly observed in chronic wounds, where it promotes hyper-proliferation of keratinocytes without altering their ability to migrate, corresponding with delayed wound healing. Increased expression of IL-6 at the wound site in diabetic wounds contributes to persistent inflammation. In addition to increasing the likelihood of chronic non-healing wounds, chronic inflammation also increases the risk of visceral fibrotic diseases, such as cardiovascular, renal, and hepatic sclerosis (Ban and Twigg, 2008; Zhu et al., 2008; Lee et al., 2019). IL-8 (CXCL-8) is one of a family of neutrophil chemokines that also includes CXCL1, 2, 3, 5, and 6. Through its potent neutrophil chemoattractant properties, the elevation of IL-8 may contribute to the prolonged inflammatory process observed in chronic wounds (Su and Richmond, 2015; MacLeod and Mansbridge, 2016).

Chronic wounds are commonly thought to be the outcome of a wound healing process that is not working correctly. In the inflammatory phase, wound healing is delayed by the upregulation of inflammatory cytokines, formation of bacterial biofilms, elevated levels of proteolytic enzymes and reactive oxygen species (ROS), as well as decreased mitogenic activity (Caley et al., 2015).

Skin and soft tissue infections (SSTIs) are a disease with complicated pathophysiology; thus, one advantage of employing herbal medicine over isolated compounds is that the same herbal medicine has constituents with antibacterial and others with antioxidant or anti-inflammatory properties and can still have a wound healing activity. Herbal medicines can simultaneously address many elements of SSTIs. Furthermore, several synthetic anti-inflammatory drugs have been demonstrated to cause significant side effects, such as gastrointestinal bleeding and ulceration (Liang et al., 2020). Thus, there is an increasing need for safer alternative therapies to treat inflammation-related diseases. Among the most effective stimulators of pro-inflammatory cytokine production is Gram-negative bacterial lipopolysaccharides (LPS), commonly used in research settings to stimulate the release of pro-inflammatory cytokines from cells (Zhao et al., 2018).

After investigating the antimicrobial, antibiofilm, antioxidant, and wound-healing potential by utilising scratch migration and proliferation assays, the treatment of LPS-stimulated keratinocytes with *A. canariense*, *C. colocynthis*, *M. crassifolia*, *R. stricta*, and *T. macropterus* methanol extracts was carried out to investigate the anti-inflammatory effect by measuring the expression of inflammatory mediators COX-2, TNF- α , IL-1 β , IL-6, and IL-8, linked to the delayed wound healing observed in chronic wounds using enzyme-linked immunosorbent assay (ELISA). In addition, Gram-negative bacterial LPS has been utilised by

many studies (Xie et al., 2012; Cho et al., 2020; Moses et al., 2020), to stimulate the expression of several inflammatory cytokines in different cells, including immortalized keratinocyte cells (Wedler et al., 2014; Kim et al., 2021; Takuathung et al., 2021).

7.2 Chapter Aim and Objectives

This chapter aims to determine the anti-inflammatory effects of five plant extracts by employing enzyme-linked immunosorbent assays (ELISAs) in LPS-stimulated human keratinocyte (HaCaT) cell lines, considering the following objectives:

- To optimize and develop an assay to investigate the capacity of plant extracts to reduce the expression COX-2 through enzyme-linked immunosorbent assays.
- To optimize and develop an assay to study the capacity of plant extracts to reduce the expression of TNF- α , through enzyme-linked immunosorbent assays.
- To optimize and develop an assay to study the capacity of plant extracts to reduce the expression of IL-1 β through enzyme-linked immunosorbent assays.
- To optimize and develop an assay to study the capacity of plant extracts to reduce the expression of IL-6 through enzyme-linked immunosorbent assays.
- To optimize and develop an assay to study the capacity of plant extracts to reduce the expression of IL-8 through enzyme-linked immunosorbent assays.

7.3 Materials

Unless otherwise specified, all materials were purchased from ThermoFisher Scientific (Loughborough, UK). In addition, a solution of phosphate-buffered saline (PBS) was made by adding one tablet of PBS to 200 mL of deionized water. In this study, Dulbecco's Modified

Eagle Medium (Gibco DMEM 1X) contains 4.5 g/L glucose and 0.11 g/L sodium pyruvate stored at 4 °C was utilised, and the antibiotic employed was composed of 100 µg/ mL streptomycin sulphate, 0.25 µg/mL amphotericin B, and 100 U/mL penicillin G sodium. Microplates (24-wells) (flat bottom, transparent, sterile, tissue culture-treated surface, polystyrene plate), and trypan blue stain were all purchased from Sarstedt (Leicester, UK). Human TNF- α (cat 900-M25, lot 1017025-M), IL-1 β (cat 900-M95, lot 0816095-M), IL-6 (cat 900-M16, lot 0618016-M) and IL-8 (cat 900-M18, lot 0119018-M), ABTS Mini ELISA kits and ABTS ELISA Buffer Kits were purchased from PeptoTech Ltd (London, UK). Lipopolysaccharides from *E. coli* purified by phenol extraction was purchased from Merck Life Science (Darmstadt, Germany). Hydrocortisone was purchased from Scientific Laboratory Supplies (Nottingham, UK). All plastic components, including tips and reagent reservoirs, were sterilised by autoclaving at 123 °C for 15 min. The tissue culture laboratory maintained and stored all equipment necessary for the experiments to avoid contamination. Absorbance was measured with a microtiter plate reader (Infinite 200 Pro, Tecan Trading, Männedorf, Switzerland).

7.4 Methods

7.4.1 Preparation of the Stock Solution of Extracts

In preparation for anti-inflammatory assay evaluation, stock solutions of 5 mg/mL plant extracts were prepared by dissolving 50 mg of plant extracts in 100 µL of 90% methanol, followed by the addition of 9.9 mL of DMEM to reach a final volume of 10 mL. The final concentration of methanol was 1%, and stock solutions were filtered, sterilised, and kept at 4 °C. The final stock concentration of plant extracts was 5 mg/mL.

7.4.2 Cell Culture and Stimulation of Inflammatory Mediators by LPS

Stimulation of HaCaT cells was carried out according to Moses et al. (2020) with slight modifications. After trypsinization, cells were seeded at a density of 1.5×10^5 cells per mL, and 1 mL was added to a 24-well plate. The plate was then incubated for 48 h at 37 °C, with 5% CO₂ and 95% relative humidity. After the incubation period, the supernatant was carefully aspirated, and different concentrations of treatments were applied; each experiment included wells for negative and positive controls. After incubating the plates for 4 h, 10 µg/mL LPS from *E. coli* (055:B5) was added to each well. After 48 h incubation, the supernatant was collected and frozen at -70 °C.

7.4.3 Enzyme-Linked Immunosorbent Assays (ELISAs)

7.4.3.1 Modulation of TNF- α , IL-1 β , IL-6, and IL-8 in HaCaT Cells

Modulation in the expression of cytokine levels in HaCaT following the treatment with a range of *A. canariense*, *M. crassifolia*, and *T. macropterus* (200, 150, 100, 50 µg/mL), *C. colocynthis* (10 µg/ mL), and *R. stricta* (100, 75, 50, 25, 12.5 µg/mL) were investigated, following LPS stimulation by ELISAs. Inflammatory mediators' expression levels were compared to untreated HaCaT control. Using Human TNF- α Immunoassay, Human IL-1 β Immunoassay, Human IL-6 Immunoassay, and Human IL-8 Immunoassay (PeproTech Ltd, London, UK), the protein levels of TNF- α , IL-1 β , IL-6, and IL-8 were measured. Experiments were carried out according to manufacture instructions.

Capture antibody (CA) was centrifuged for 20 s, then reconstituted with 110 µL (IL-1 β , IL-6, and IL-8) or 210 µL (TNF- α) sterilised water to the concentration of 100 µg/mL and incubated

at room temperature for 10 minutes. The vial was centrifuged for 3 min at 1000 xg. CA was diluted with PBS to the concentrations of 0.5 µg/mL (IL-1β, IL-6, and IL-8) and 1 µg/mL (TNF-α) by adding 100 µL CA to 19,900 µL PBS then gently vortexed to prevent air bubbles forming. 100 µL of diluted CA was added to each ELISA plate, then sealed firmly and incubated at room temperature overnight.

The next day, the liquid was carefully removed from each well and then rinsed four times with 300 µL washing buffer. After the last wash plates were turned and blotted against clean paper towels to verify the elimination of the wash buffer, 300 µL of block buffer was added to each well, covered, and incubated for at least 1 hour at room temperature. During the incubation time, the standard was centrifuged for 20 s and then reconstituted with 1 mL sterilised water to make up the concentration of 1 µg/ mL, then allowed to stand for 10 min. The vial was subsequently centrifuged for 3 min at 1000 xg. Following the incubation time, blocking buffer was aspirated from each well. Then the previous washing step was repeated four times. To produce a calibration curve, a stock standard was utilized to produce a serial dilution with freshly prepared diluent across the plate from 1000 pg/mL to zero (IL-1β and IL-8), 2000 pg/mL to zero (IL-6), and from 3000 pg/mL to zero (TNF- α); and 100 µL of samples at different concentrations were added to each well. Finally, plates were sealed and incubated for at least 2 h at room temperature.

The detection antibody (DA) was centrifuged for 20 s and then reconstituted with 110 µL PBS (IL-1β and IL-8), 210 µL PBS (IL-6), or 110 µL sterilised water (TNF- α) to a concentration of 100 µg/mL, then allowed to stand for 10 min. Afterward, the vials were centrifuged for 3 min at 1000 xg. DA was diluted with diluent to 0.5 µg/mL (TNF- α, IL-1β, and IL-8), or to 1 µg/mL (IL-6). After incubation, the liquid was aspirated from each well; the previous washing

step was repeated four times. Next, 100 μL DA was added to each well; afterward, plates were covered with film and incubated for 2 h at room temperature.

The avidin-HRP conjugate was thawed and centrifuged for 20 s, diluted by adding 10 μL avidin to 19,990 μL diluent, then gently vortexed. DA was removed from each well and washed four times with washing buffer before adding 100 μL avidin to each well. Then, plates were covered and incubated for 30 min at room temperature. During the incubation period, to ensure that 2,2'-azino-bis (3-ethylbenz-thiazoline-6-sulfonic acid) (ABTS) liquid substrate reached room temperature, it was removed from the fridge, then filtered, sterilised, and kept at 25 $^{\circ}\text{C}$. Plates were washed 4 times with washing buffer, before adding 100 μL liquid substrate to each well then incubated at room temperature for color development.

Color development was monitored at 5 min intervals, by measuring the absorbance with a plate reader at a wavelength of 405 nm with a correction set at 650 nm. Three different sets of samples were used for this ELISA assay. Averages and standard errors were calculated using the corrected values.

7.4.3.2 Modulation of COX-2 in HaCaT Cells

ELISAs were performed to evaluate changes in expression levels of COX-2 in HaCaT cells following the treatment with a range of *A. canariense*, *M. crassifolia*, and *T. macropterus* (200, 150, 100, 50 $\mu\text{g}/\text{mL}$), *C. colocynthis* (10 $\mu\text{g}/\text{mL}$), and *R. stricta* (100, 75, 50, 25, 12.5 $\mu\text{g}/\text{mL}$) concentrations. A human COX-2 ELISA Assay Kit (ThermoFisher Scientific) was utilised to measure the level of COX-2, and the results were compared to untreated HaCaT controls. Experiments were carried out according to manufacturer instructions. Standard was centrifuged

and then reconstituted with 400 μL diluent to prepare 300 ng/mL afterward, gently vortexed, and allowed to stand for 10 min.

The stock standard solution was diluted with diluent to produce the following dilution series: 120, 48, 19.2, 7.68, 3, 1.2, and 0 ng/mL. Then, 100 μL was added to the appropriate well to produce a standard curve. Next, 100 μL of treatments at various concentrations were applied to each well, and the plates were covered and incubated at 25 °C with careful shaking for 2.5 h. Next, each well was aspirated and rinsed four times with 300 μL of washing buffer. After the last wash, plates were turned and blotted on clean paper towels to ensure thorough removal of the wash buffer. Next, 100 μL of prepared biotin conjugate was applied to each well, and the plate was covered and incubated at 25 °C for 1 h with careful shaking. After 1 h, the solution was removed, and the washing process was repeated.

After adding 100 μL of the prepared streptavidin-HRP solution to each well, the plate was covered and kept at 25 °C with careful shaking for 45 min. After the incubation period, the solution was removed, and the previous washing procedure was repeated. Following this, 100 μL of 3,3',5,5'-Tetramethylbenzidine (TMB) substrate was added to each well, the plate was covered, and it was incubated for 30 min at 25 °C in the dark with careful shaking. Lastly, 50 μL of stop solution was added to each well while gently tapping on the side of the plate, and the absorbance was determined at 450 nm within 30 min.

7.4.4 Statistical Analysis

The obtained data were statistically analysed using GraphPad Prism 7.0a (GraphPad Software Inc., San Diego, USA); all data is reported as the mean \pm standard error (SE), and all experiments were conducted on 3 separate occasions. The means and standard errors were

calculated using Excel (Microsoft) software. The statistical analysis was performed using a one-way analysis of variance (ANOVA) with Dunnett post-test, to assess the significance of the difference between the means of the control and experimental groups.

7.5 Results and Discussion

7.5.1 Measuring the Cytokine Levels

ELISAs were performed to measure HaCaT expression of TNF- α , IL-1 β , IL-6, and IL-8 treated with *A. canariense*, *M. crassifolia*, and *T. macropterus* (200, 150, 100, 50 $\mu\text{g/mL}$), *C. colocynthis* (10 $\mu\text{g/mL}$), and *R. stricta* (100, 75, 50, 25, 12.5 $\mu\text{g/mL}$) concentrations. Positive control of hydrocortisone (200 $\mu\text{g/mL}$) was included in each experiment. *A. canariense* showed no effect on the levels of TNF- α ($p>0.05$; Figure 69). The ELISA assay showed a dose-dependent decrease in the levels of TNF- α when treated with *M. crassifolia* (200 and 150 $\mu\text{g/mL}$) and *R. stricta*. The decrease was significant for 200 and 150 $\mu\text{g/mL}$ *M. crassifolia* ($p<0.001$; $p<0.05$) and for 100, 75, 50, and 25 $\mu\text{g/mL}$ *R. stricta* ($p<0.001$; $p<0.05$). A significant decrease in protein levels were similarly observed with 10 $\mu\text{g/mL}$ of *C. colocynthis* ($p<0.001$). Only at 150 and 50 $\mu\text{g/mL}$ did *T. macropterus* demonstrate a significant decrease ($p<0.001$).

For IL-1 β , *A. canariense* (200 and 150 $\mu\text{g/mL}$) demonstrated a significant decrease in the expression of IL-1 β ($p<0.01$; $p<0.05$). Moreover, *R. stricta* (100 and 75 $\mu\text{g/mL}$) exhibited a similar pattern with a significant decrease in the levels of the inflammatory mediator ($p<0.01$; Figure 70). The rest of the treatments showed no effect on the levels of IL-1 β ($p>0.05$).

R. stricta exhibited a dose-dependent decrease in the expression of IL-6 that was deemed significant ($p < 0.001$) at concentrations 100, 75, 50, and 25 $\mu\text{g/mL}$. At the same time, no effect was observed at the lower concentration of 12.5 $\mu\text{g/mL}$ ($p > 0.05$). Another significant decrease in the levels was observed with 10 $\mu\text{g/mL}$ of *C. colocynthis* ($p < 0.001$). *A. canariense*, *M. crassifolia*, and *T. macropterus* all did not affect IL-6 at all tested concentrations ($p > 0.05$; Figure 71).

A. canariense did not influence the levels of the cytokine IL-8 at any of the examined connections ($p > 0.05$). *R. stricta* showed a dose-dependent decrease in the protein level at 100, 75, 50, and 25 $\mu\text{g/mL}$ ($p < 0.001$). At 200 and 150 $\mu\text{g/mL}$, *M. crassifolia* and 200, 150, and 100 $\mu\text{g/mL}$ *T. macropterus* produced a profound decrease in IL-8 ($p < 0.001$). Furthermore, *C. colocynthis* demonstrated a significant reduction in the protein level ($p < 0.001$; Figure 72).

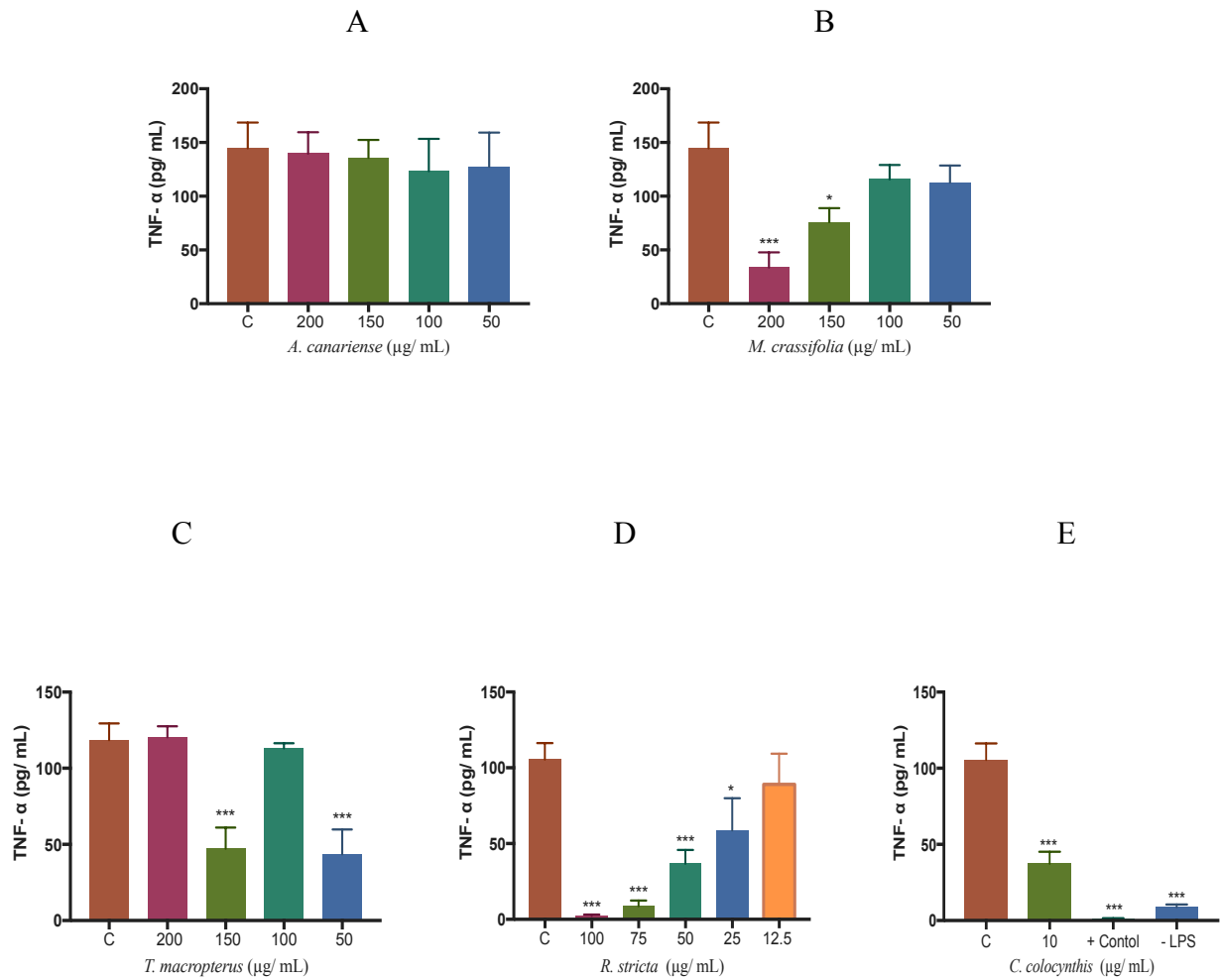


Figure 69 TNF- α levels in HaCaTs, cultured in the presence of (A) *A. canariense* (200, 150, 100, and 50 $\mu\text{g/mL}$), (B) *M. crassifolia* (200, 150, 100, and 50 $\mu\text{g/mL}$), (C) *T. macropteris* (200, 150, 100, and 50 $\mu\text{g/mL}$), (D) *R. stricta* (100, 75, 50, 25, and 12.5 $\mu\text{g/mL}$), (E) *C. colocynthis* (10 $\mu\text{g/mL}$), compared to untreated controls at 48 h. Hydrocortisone (200 $\mu\text{g/mL}$) was included in each experiment to serve as a positive control. Data were presented as mean \pm standard error (SE). Three separate experiments were conducted to acquire findings. Analysis of statistically significant differences between treated cells and untreated controls via Dunnett post-test (* $p < 0.05$, ** $p < 0.01$, *** $p < 0.001$)

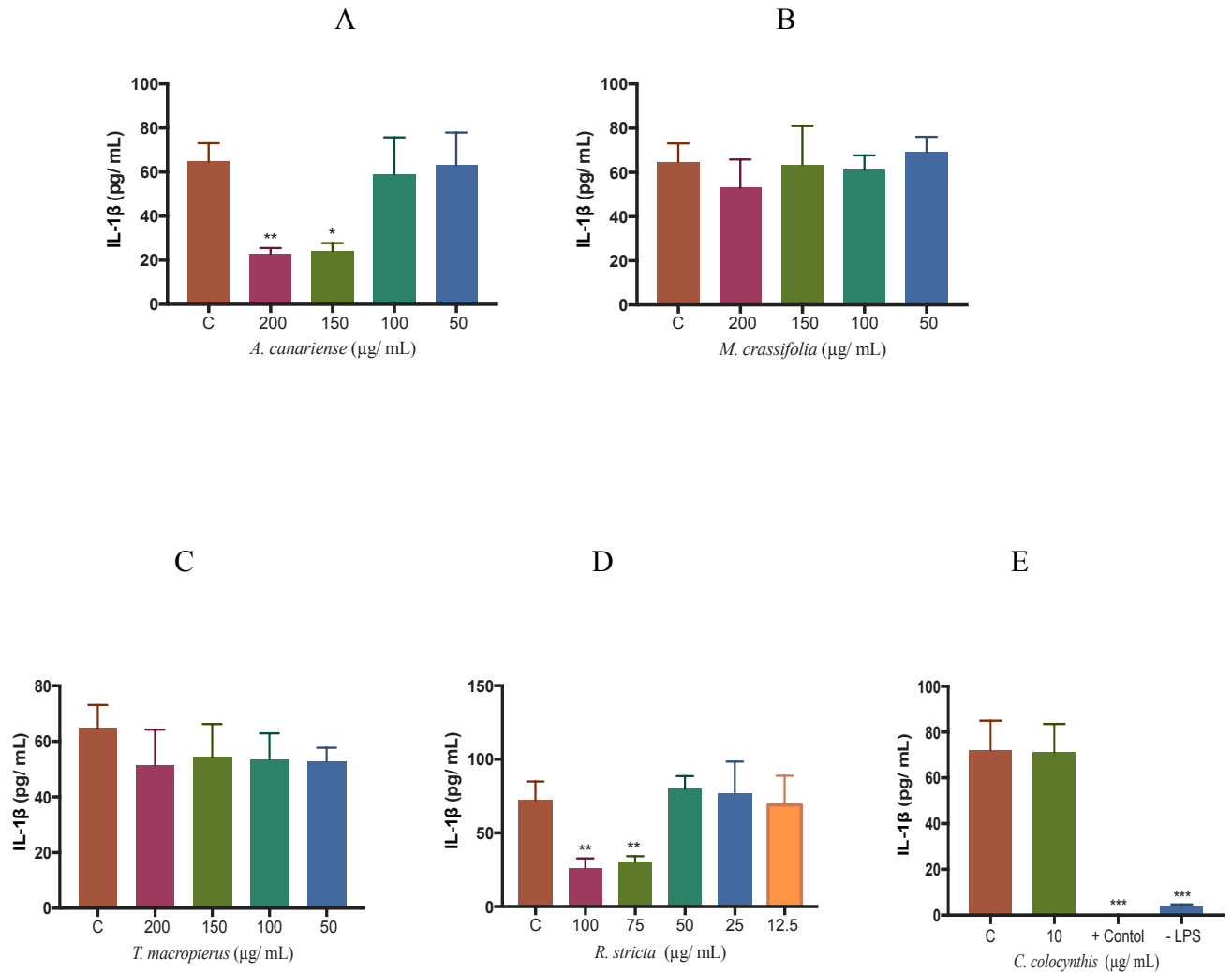


Figure 70 IL-1 β levels in HaCaTs, cultured in the presence of (A) *A. canariense* (200, 150, 100, and 50 $\mu\text{g/mL}$), (B) *M. crassifolia* (200, 150, 100, and 50 $\mu\text{g/mL}$), (C) *T. macropterus* (200, 150, 100, and 50 $\mu\text{g/mL}$), (D) *R. stricta* (100, 75, 50, 25, and 12.5 $\mu\text{g/mL}$), (E) *C. colocynthis* (10 $\mu\text{g/mL}$), compared to untreated controls at 48 h. Hydrocortisone (200 $\mu\text{g/mL}$) was included in each experiment to serve as a positive control. Data were presented as mean \pm standard error (SE). Three separate experiments were conducted to acquire findings. Analysis of statistically significant differences between treated cells and untreated controls via Dunnett post-test (* $p < 0.05$, ** $p < 0.01$, *** $p < 0.001$)

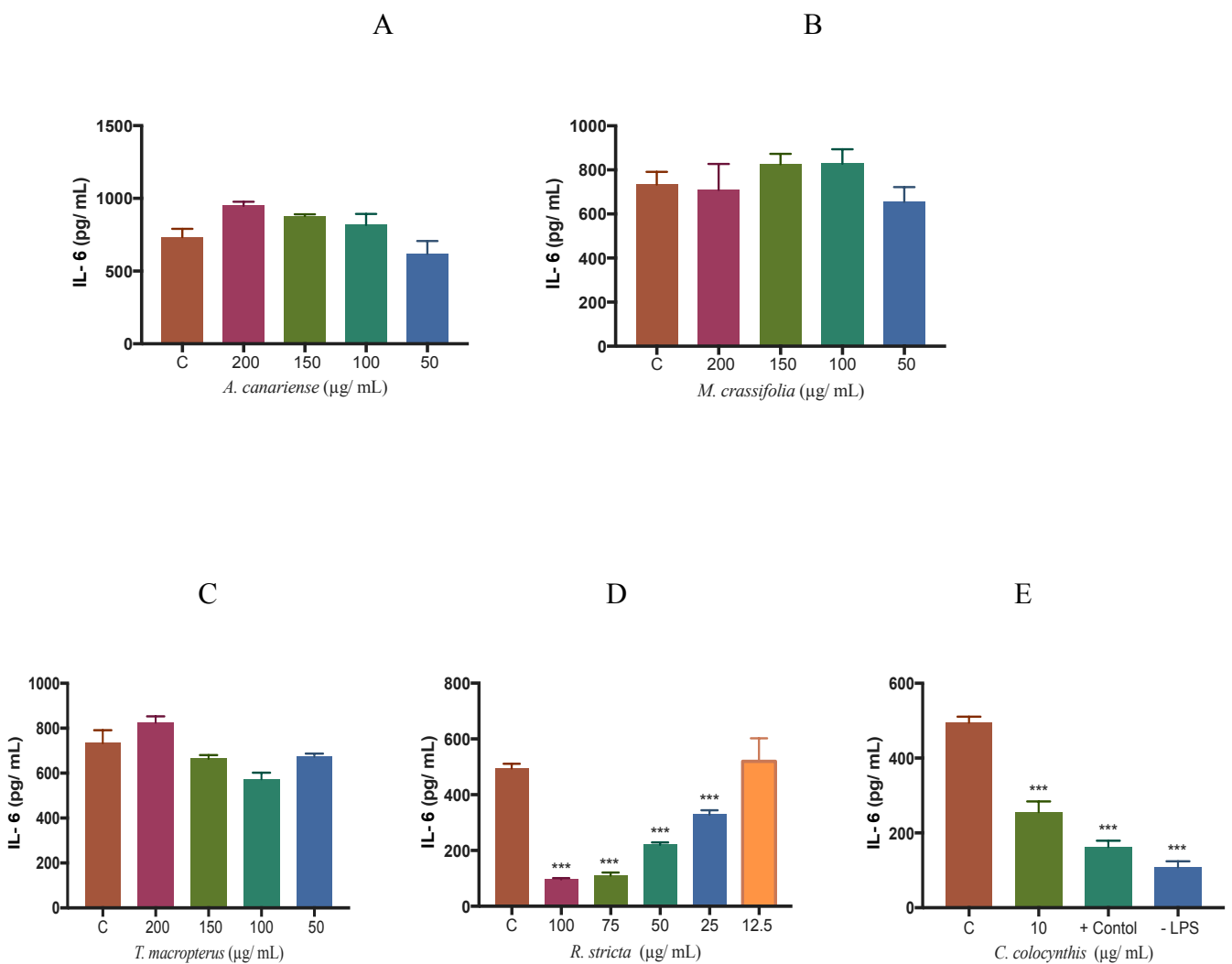


Figure 71 IL-6 levels in HaCaTs, cultured in the presence of (A) *A. canariense* (200, 150, 100, and 50 µg/mL), (B) *M. crassifolia* (200, 150, 100, and 50 µg/mL), (C) *T. macropterus* (200, 150, 100, and 50 µg/mL), (D) *R. stricta* (100, 75, 50, 25, and 12.5 µg/mL), (E) *C. colocynthis* (10 µg/mL), compared to untreated controls at 48 h. Hydrocortisone (200 µg/mL) was included in each experiment to serve as a positive control. Data were presented as mean ± standard error (SE). Three separate experiments were conducted to acquire findings. Analysis of statistically significant differences between treated cells and untreated controls via Dunnett post-test (*p < 0.05, **p < 0.01, ***p < 0.001)

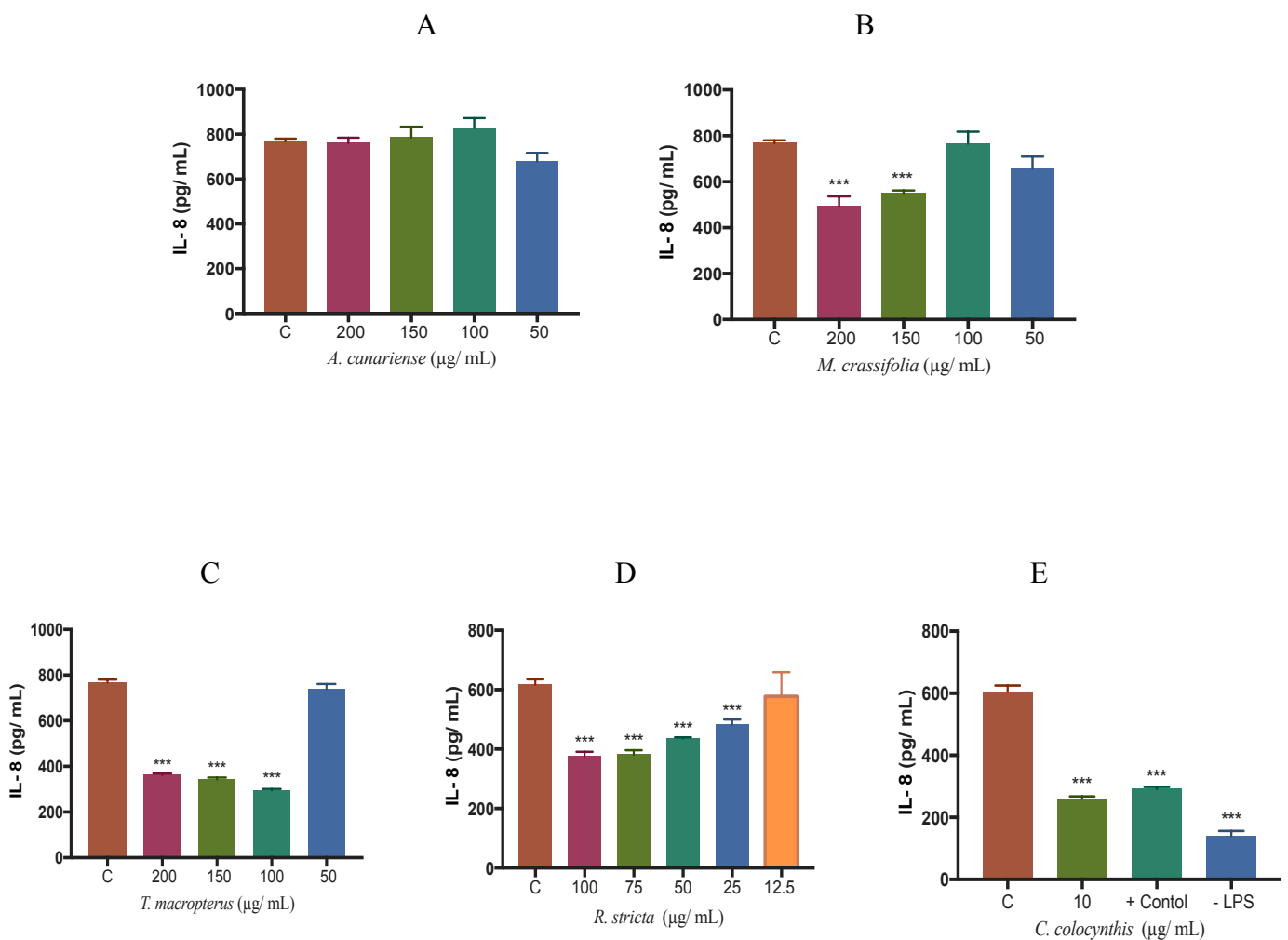


Figure 72 IL-8 levels in HaCaTs, cultured in the presence of (A) *A. canariense* (200, 150, 100, and 50 µg/mL), (B) *M. crassifolia* (200, 150, 100, and 50 µg/mL), (C) *T. macropterus* (200, 150, 100, and 50 µg/mL), (D) *R. stricta* (100, 75, 50, 25, and 12.5 µg/mL), (E) *C. colocynthis* (10 µg/mL), compared to untreated controls at 48 h. Hydrocortisone (200 µg/mL) was included in each experiment to serve as a positive control. Data were presented as mean ± standard error (SE). Three separate experiments were conducted to acquire findings. Analysis of statistically significant differences between treated cells and untreated controls via Dunnett post-test (*p < 0.05, **p < 0.01, ***p < 0.001)

The proliferation of keratinocytes and the production of antimicrobial peptides are two critical functions of pro-inflammatory cytokines during acute wound healing. However, excess production of pro-inflammatory cytokines may result in persistent inflammation and impaired wound healing. As a result, inhibiting the release of pro-inflammatory cytokines has therapeutic value in treating chronic wounds.

In the present study, to further understand the effects of selected medicinal plants on skin cells, we conducted an analysis of keratinocytes stimulated with the pro-inflammatory agent, LPS. In addition to their role as structural cells, keratinocytes play a crucial part in wound healing through their critical immunological functions, including the release of several inflammatory cytokines (Lebre et al., 2007; Brazil et al., 2019). Furthermore, LPS is a well-known HaCaT stimulant that induces the production and secretion of pro-inflammatory mediators (Sikandan et al., 2018; Takuathung et al., 2021).

The data showed that several medicinal plants significantly reduced the release of the pro-inflammatory TNF- α , IL-1 β , IL-6, and IL-8 from keratinocytes. *C. colocynthis* suppressed the pro-inflammatory cytokines TNF- α , IL-6, and IL-8; our findings aligned with a study that used a rat module to demonstrate the topical application of *C. colocynthis* cream will reduce the level of TNF- α and IL-6 (Pashmforosh et al., 2018).

A. canariense significantly decreased IL-1 β level; the anti-inflammatory effect of *A. canariense* might be linked to its active constituent, γ -linolenic acid (GLA), which has been previously identified and isolated in our work. In addition, several studies have reported *in vivo* and *in vitro* inhibition of IL-1 β by GLA (Furse et al., 2002; Chang et al., 2010). A study by Al Shamsi reported the anti-inflammatory effect of *R. stricta* through the inhibition of TNF-

α at concentrations of 120 and 90 $\mu\text{g}/\text{mL}$. However, no effect was observed at 30 and 60 $\mu\text{g}/\text{mL}$ concentrations. This could be attributed to the methodological variations of different extraction methods and cell types and the amounts of active constituents within the extract (Al Shamsi, 2002).

To the best of our knowledge, this is the first study to explore the anti-inflammatory effect of *A. canariense*, *M. crassifolia*, and *T. macropterus*, even for *R. stricta* effect on the expression of IL-1 β , IL-6, and IL-8. Although the anti-inflammatory effect of *T. macropterus* has not been reported, *Tribulus terrestris* plant that belongs to the same family and genus (*zygophyllaceae, tribulus*), inhibited the expression of pro-inflammatory cytokines, such as TNF- α and IL-4, in a macrophage cell line (Oh et al., 2012).

In the inflammatory phase of the wound healing process, TNF- α , for example, is involved in recruiting neutrophils and macrophages to the wound site (Ritsu et al., 2017). TNF- α levels are elevated in patients with chronic wounds, both systemically and at the site of the wound. In one study, topical administration of anti-TNF- α neutralising antibodies inhibits leukocyte migration and NF-B activation, leading to an increase in matrix production and subsequent acceleration of the wound healing process in an aged mouse model (Ashcroft et al., 2012). Furthermore, in macrophages from diabetic patients or a mouse model, inhibiting IL-1 β activity with a neutralising antibody reduces the pro-inflammatory factors, TNF- α , IL-1 β , and IL-6. In addition, it increases the healing-associated marker, CD206, insulin-like growth factor-1, and IL-10 (Mirza et al., 2013). The administration of an IL-1R antagonist to diabetic mice upregulated the pro-wound healing phenotype of macrophages, instead of the pro-inflammatory phenotype, hence promoting wound healing (Perrault et al., 2018).

7.5.2 COX-2 Modulation

HaCaT cell production of the inflammatory mediator cyclooxygenase-2 (COX-2), following LPS stimulation was measured using ELISA after treatment with *A. canariense*, *M. crassifolia*, and *T. macropterus* (200, 150, 100, 50 µg/mL), *C. colocynthis* (10 µg/mL), and *R. stricta* (100, 75, 50, 25, 12.5 µg/mL) concentrations. Positive control of diclofenac (200 µg/mL) was included in each experiment.

A. canariense and *M. crassifolia* had no effect on the release of COX-2 at all of the concentrations evaluated ($p > 0.05$; Figure 73). *T. macropterus* inhibited COX-2 significantly at 200, 150, and 100 µg/mL ($p < 0.01$; $p < 0.05$). *R. stricta* demonstrated a dose-dependent inhibition of COX-2 that was statistically significant at 100, 75, and 50 µg/mL ($p < 0.01$). Moreover, 10 µg/mL *C. colocynthis* inhibited the release of COX-2 significantly ($p < 0.01$).

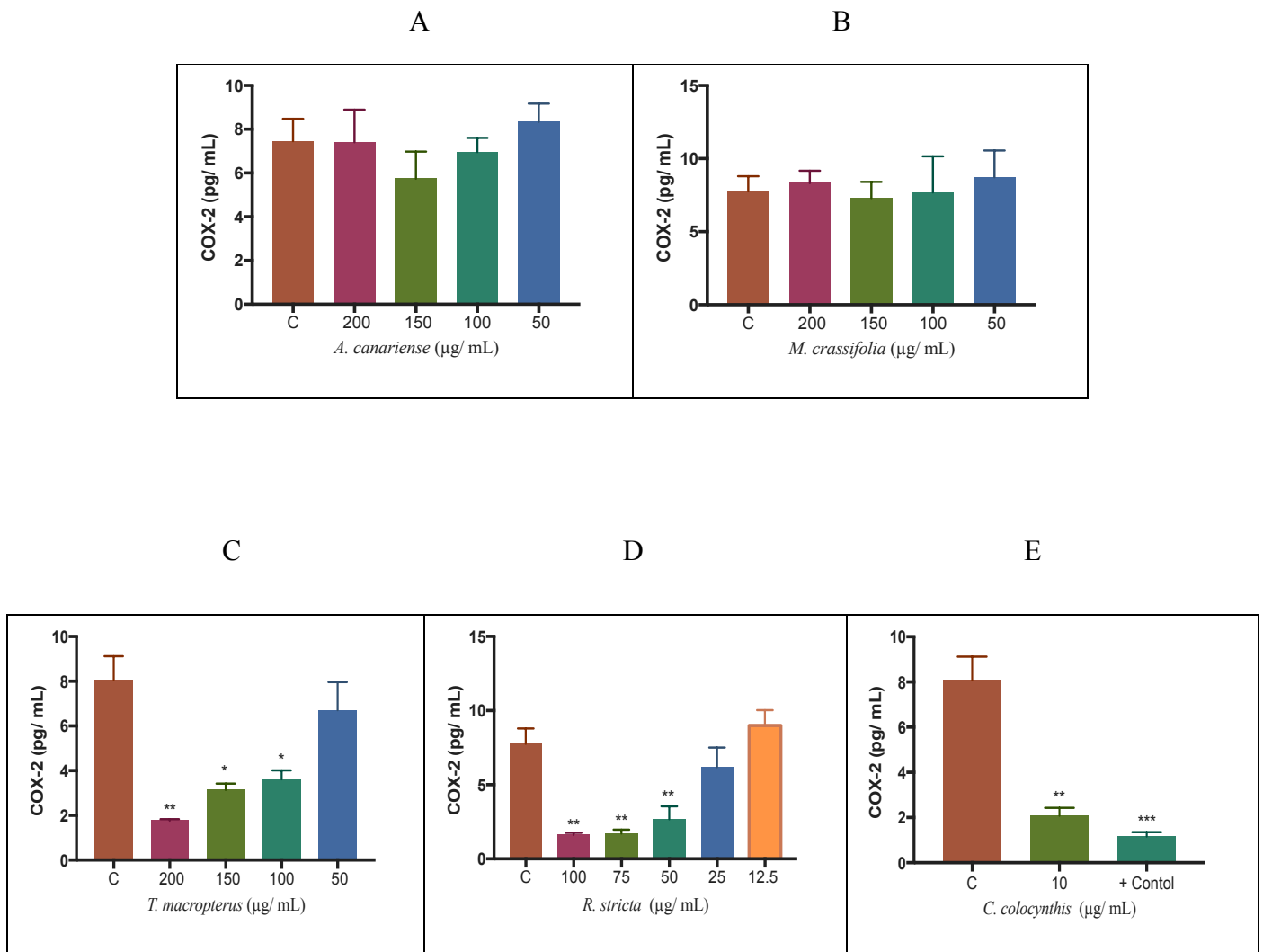


Figure 73 COX-2 levels in HaCaTs, cultured in the presence of (A) *A. canariense* (200, 150, 100, and 50 µg/mL), (B) *M. crassifolia* (200, 150, 100, and 50 µg/mL), (C) *T. macropterus* (200, 150, 100, and 50 µg/mL), (D) *R. stricta* (100, 75, 50, 25, and 12.5 µg/mL), (E) *C. colocythis* (10 µg/mL), compared to untreated controls at 48 h. Diclofenac (200 µg/mL) was included in each experiment to serve as positive control. Data were presented as mean ± standard error (SE). Three separate experiments were conducted to acquire findings. Analysis of statistically significant differences between treated cells and untreated controls via Dunnett post-test (*p < 0.05, **p < 0.01, ***p < 0.001)

COX-1, COX-2, and COX-3 are the three forms of COX. Platelet thromboxane A2 synthesis is among the many essential roles of COX-1, which is routinely produced in the body. Studies indicate that cyclooxygenase-3 (COX-3) plays a crucial role in the mechanisms of fever and

pain in the human cortex. The constitutive COX-2 enzyme induces the synthesis of prostaglandins, eg E2 (PGE₂), from arachidonic acid (Nakanishi and Rosenberg, 2013). PGE₂, is typically produced in most cells, and is the principal mediator of inflammation in epithelial tissues, is produced by the inducible cyclooxygenase-2 (COX-2) in response to injury. Prostaglandin E₂ (PGE₂) stimulates neutrophil, macrophage, and mast cell entrance into the tissue during the first phase of the inflammatory response, resulting in swelling and edema at the site of infection or wound (Wallace, 2001). Moreover, vascular permeability, cellular proliferation, and angiogenesis are all regulated by tissue prostaglandins, which are critical for wound healing (Chandrasekharan et al., 2002; Futagami et al., 2002; Lee et al., 2003; Menter et al., 2010; Ricciotti and FitzGerald, 2011). Determining the modulation of the short-lived COX-2 is a useful indicator of pro- or anti-inflammatory responses to applied substances (Heard, 2020).

Excessive COX-2 expression and elevated PGE₂ levels on the wound bed contribute to the persistent inflammation seen in chronic wounds. Therefore, the failure of chronic wounds to heal could be attributable to the ongoing infiltration of inflammatory cells, which is linked to an increase in ROS production and prostaglandins (Abd-El-Aleem et al., 2001). Several studies reported that the administration of COX-2 inhibitors decreases wound inflammation and stimulates dermal reconstruction and scar formation, by inhibiting the production of inducible nitric oxide synthase (iNOS) and COX-2, hence enhancing the healing of the chronic wound (Wilgus et al., 2003; Romana-Souza et al., 2016).

R. stricta anti-inflammatory activity could be attributed to its previously reported ability to inhibit nuclear factor- κ B (NF- κ B) signalling, influencing the expression of inflammatory cytokines and the COX-2 enzyme (Elkady et al., 2016). One mechanism for inhibiting NF- κ B

activation is to prevent the incoming stimulating signal from having any effect by blocking the binding of the ligand to its binding site; another mechanism is to prevent the cytoplasmic step in the NF- κ B activation pathway by blocking a specific component of the cascade; and a third mechanism is to inhibit NF- κ B nuclear activity, including its translocation to the nucleus and DNA binding (Gilmore and Herscovitch, 2006). Furthermore, Tanira et al. (1996) has shown in an *in vivo* rat model that *R. stricta* (1 or 2 g/kg) decreased rectal temperatures in rats, accelerated the reactions to temperature, and alleviated the paw edema caused by carrageenan induction. They concluded that these findings are suggestive of an aspirin-like action from the plant extract, and inhibition of cyclooxygenase (COX) is likely involved in this process.

Tribulus terrestris, a plant belonging to the same family and genus of *T. macropterus* (*zygophyllaceae, tribulus*), has been shown to have an anti-inflammatory effect. Oh et al. (2012) reported that the ethanolic extract of *T. terrestris* reduced the expression of COX-2 and inducible nitric oxide synthase (iNOS) in stimulated RAW264.7 cells. Hong et al. (2002) reported similar findings that examined the methanol extract of more than 170 medicinal plants, including *T. terrestris*, for the suppression of COX-2 and nitric oxide generation in LPS-induced murine macrophage RAW264.7 cells and obtained similar results. At a concentration of 10 μ g/ml, *T. terrestris* was capable of inhibiting 86% of COX-2 activity. These findings indicate that *T. macropterus* could share the same phytoconstituents responsible for the COX-2 suppression in *T. terrestris*.

Akhzari et al. (2015) found that 70 μ g/ml of *C. colocynthis* inhibits the expression of COX-2 enzyme and other inflammatory cytokines in macrophages stimulated with LPS. The downregulation of COX-2 by these plant extract's constituents will also reduce the local level of pro-inflammatory PGE₂. Any observed downregulation of COX-2 may result from active

site blockade or negative feedback. Moreover, the reduction of COX-2 protein level by *C. colocynthis* could be related to its previously established cytotoxic activity on HaCaTs (Section 3.5.2).

7.6 Conclusion

The anti-inflammatory properties of *A. canariense*, *M. crassifolia*, *T. macropterus*, *C. colocynthis*, and *R. stricta* were evaluated by keratinocytes infected with LPS, following 48 h incubation. Protein levels of COX-2 and inflammatory cytokines, TNF- α , IL-1 β , IL-6, and IL-8, were compared to untreated controls. Compared to the untreated controls, LPS significantly raised the protein levels of COX-2 and inflammatory cytokines. The dose-dependent suppression of COX-2 and several inflammatory cytokines by *R. stricta* could suggest that it inhibits nuclear factor- κ B signalling. *A. canariense* showed a significant reduction in the protein level of IL-1 β and *C. colocynthis* at low concentration revealed a significant reduction in the protein levels of COX-2, TNF- α , IL-6 and IL-8. *T. macropterus* significantly suppressed COX-2, TNF- α , and IL-8 at the protein level. *M. crassifolia* showed significant inhibition of pro-inflammatory cytokines TNF- α and IL-8. These findings support topical formulation development with these promising medicinal plants, especially *M. crassifolia* and *R. stricta*, to be investigated *in vivo* animal models for their anti-inflammatory activity. To validate our findings, future studies are required to look at the gene expression of COX-2 and the inflammatory cytokines, TNF- α , IL-1 β , IL-6, and IL-8.

Chapter 8: General Discussion

8.1 Overview

The objective of this PhD study was to investigate the medicinal properties of five plants traditionally used in Saudi Arabia, focusing on treating skin and soft tissue infections (SSTIs) and chronic wounds. SSTIs typically present with different causes, manifestations, and severity that feature microbial invasion of the skin and subcutaneous soft tissues, ranging from mild to life-threatening infections (Esposito et al., 2011). Recently there has been a rise in the incidence of SSTIs, due to the increase in the number of critically ill patients, the growing of the geriatric population, an increase in the number of immunocompromised patients, and the emergence of multidrug-resistant microorganisms (Esposito et al., 2009).

The causative pathogens leading to SSTIs tend to arise from skin resident and transient microflora. The predominant species is the Gram-positive bacteria *S. aureus* which accounts for 40% of the cases, followed by Gram-negative bacteria *P. aeruginosa* or *E. coli*. *S. aureus* has become increasingly resistant to methicillin in recent decades (MRSA) and has spread worldwide, both in hospital and community settings (Ferry and Etienne, 2007; Ki and Rotstein, 2008; May, 2009).

Antimicrobial resistance (AMR) is regarded as a severe risk to the public health systems in underdeveloped countries and around the world (Founou et al., 2017). According to a recent report, AMR will be responsible for 10 million deaths annually by 2050, overtaking cancer as the leading cause of mortality (O'Neill, 2016). Plant natural products could be a source of antiseptic antimicrobial lead compounds to combat the rising trend of antibiotic resistance. A significant advantage of natural products is that they have a diverse range of chemical diversity, are widely available worldwide, and are shown clinical efficacy. Importantly, their use does

not need the enormous development costs associated with new, synthetic drugs; hence, they are far cheaper (Rates, 2001; Harvey et al., 2015). In addition, natural products are reported to be the source of between 30 and 40% of the most current antimicrobial agents on the market today. Nevertheless, these resources have still been poorly explored to develop further antimicrobial agents from plants (Chattopadhyay et al., 2009).

8.2 Ethnobotanical Fieldwork

Fieldwork to collect medicinal plants was conducted in Saudi Arabia, due to accessibility following the establishment of collaborative work between the Cardiff University School of Pharmacy and Pharmaceutical Sciences in the UK and the Natural Products Department of King Abdulaziz University in Saudi Arabia, and its botanical diversity. The natural flora provides an abundant, largely untapped source of plant-based drugs with more than 2,250 species in 142 families. Additionally, the majority of medicinal plants have not been thoroughly investigated for their pharmacological activities (Saadabi, 2006; Yusuf et al., 2014).

Ethnobotanical and chemotaxonomic approaches were followed to select and collect plant materials. One approach utilizes information about the traditional usage of plants to treat certain diseases, and the second approach employs the study of plants belonging to the same family or genus as those from which demonstrated activity and active compounds have previously been identified (Almeida et al., 2012). Five plants, *A. canariense*, *M. crassifolia*, *T. macropterus*, *C. colocynthis*, and *R. stricta*, were successfully collected. However, an observed limitation we experienced during the fieldwork is that two of the selected plants could not be identified in assigned locations, since they generally grow in 3-4 weeks following the wet

season. All plant materials were extracted with methanol according to a method proposed by Mitscher et al. (1972) and later modified by Ieven et al. (1979). This method is regarded as a practical standard because it provides a low-cost, convenient, and high-performance starting method, in which most compounds are extracted together without regard to polarity range. Moreover, it was impracticable to conduct experimentation with fresh plant material (Cos et al., 2006).

In the preceding chapters, all 5 test plants were investigated together regarding their medicinal properties. This was a sensible approach, as it enabled us to compare the plants in terms of, for example, anti-inflammatory, antimicrobial, and antibiofilm activity, and the relevant discussion sections provide this comparison. However, for this General Discussion, I will examine each plant individually, discussing its efficacy in the tests conducted to demonstrate the plant's potency and, where appropriate determine to what extent the findings support its traditional, folklore use.

8.3 *Aizoon canariense*

This plant is indigenous to Saudi Arabia, Bahrain, and South and North Africa. This plant has been traditionally used to treat hepatitis, jaundice, hypertension, flatulence, and its leaves were applied topically to heal wounds (Hassan-Abdallah et al., 2013; Al-laih et al., 2015). The preliminary screening of *A. canariense* methanolic extract with the agar diffusion method revealed antimicrobial activity against both Gram-positive and negative strains. However, only partial inhibition was observed, which may indicate that the antimicrobial compounds in the plant extract are present in low concentrations or due to the presence of bacteriostatic

compounds in the extract. Additional extract fractionation might boost the activity and isolate the pure compound responsible for this activity.

Elkhalfi et al. (2013) has reported a MIC and MBC value of 4 mg/mL and a clear inhibitory zone against *Pseudomonas syringae*. However, MIC and MBC values could not be obtained in our study using the broth microdilution method at concentrations as high as 20 mg/mL. This may be due to the sensitivity of the tested bacterial strain to the extract and the variations in the methodology used, as the tested concentration for the agar diffusion method was five times higher (100 mg/mL). Moreover, the incubation temperature after inoculation was 28 °C, and the tube dilution method was chosen for determining the MIC and MBC values. In addition to evaluating the activity of *A. canariense* against the planktonic phase of bacteria, antibiofilm activities were investigated. The formation of biofilm facilitates bacterial resistance to antibiotics. In addition, it affects the host's immune response through the development of chronic infections, which are marked by tissue damage and persistent inflammation. Furthermore, this leads to significant challenges in treating SSTIs, such as chronic wounds, consequently limiting therapeutic options (Costerton et al., 2003; López et al., 2010). *A. canariense* effectively inhibited the biofilm formation of *S. aureus* and MRSA and eradicated the preformed biofilm of *S. aureus*.

The burden of treating chronic wounds on healthcare systems is rising rapidly. The rise in the cases of conditions and disorders like diabetes and obesity and the aging population will contribute to the ongoing growth in the incidence and prevalence of chronic wounds. Managing chronic wounds is believed to cost between £2.3 and £3.1 billion a year in the UK (Posnett and Franks, 2008; Green et al., 2014). Assessing the wound healing potential, determining the extracts' safety, and confirming their selectivity were achieved by utilizing immortalized

keratinocytes (HaCaT) as a normal skin cell line. In this study, *A. canariense* demonstrated no effect on the proliferation and migration abilities of HaCaT and showed no cytotoxic activity. Recently, AlQathama et al. (2022) reported a GI₅₀ (50% growth inhibition) of 22 µg/mL with Alamar blue assay against the A375 melanoma cell line. This might be attributed to the sensitivity of A375 to the extract and the different extraction methods utilised in each study. AlQathama's et al. used chloroform to extract plant materials, an organic solvent that tends to extract a selected range of compounds with medium polarities.

Persistent inflammation is another characteristic that makes chronic wounds particularly difficult to treat. Inflammation is an essential process in wound healing since it supports the elimination of potentially harmful pathogenic microbes. However, inflammation may persist for longer if disinfection is insufficient and microbes are not eliminated. Interleukin-1 (IL-1) and tumour necrosis factor- α (TNF- α) are two examples of pro-inflammatory cytokines that can be elevated for an extended period in response to bacterial or endotoxin infection, hence resulting in chronic wounds (Menke et al., 2007). The anti-inflammatory activity of *A. canariense* was investigated for the first time by utilising an LPS-stimulated HaCaT cells, and it exhibited significant inhibition of IL-1 β .

Overproduction of reactive oxygen species (ROS) is another feature of chronic wounds; at low levels, ROS aid the healing process by fighting invading pathogens, but at higher levels, ROS cause oxidative damage to cells and prevents wounds from healing (Sanchez et al., 2018). Thus, the ability of *A. canariense* to scavenge reactive oxygen species was investigated, and it exhibited the lowest antioxidant activity, compared to other selected plants with an IC₅₀ of 822 µg/mL by DPPH assay; our reported findings were in alignment with the published report (El-Amier et al., 2020). This could be due to the low total phenolic content of *A. canariense* with

7.85 mg GAE/g dry extract. Phenolic compounds are secondary plant metabolites and feature an aromatic ring with at least one hydroxyl group. Moreover, the hydroxyl groups of phenolic compounds directly contribute to their antioxidant action, making them suitable electron donors (Bendary et al., 2013; Tungmunnithum et al., 2018).

The bio-guided fractionation approach was followed with liquid-liquid partitioning and column chromatography to identify and isolate active compounds. Active hexane and chloroform fractions were investigated by direct bio-autographic assay, which revealed the presence of several antimicrobial compounds active only against Gram-positive strains. To isolate the antimicrobial compound, *A. canariense* chloroform fraction was subjected to a preparative TLC with a mobile phase: 50% ethyl acetate: 25% hexane: and 25% methanol. The compound molecular formula was investigated with HR ESI-MS, and the chemical structure was validated with NMR; the compound was identified as γ -linolenic acid (GLA), which was aligned with what had been reported in the published literature (Park et al., 2013). The antimicrobial activity of GLA was investigated in both planktonic and biofilm cultures.

The MIC₉₀ of GLA against *S. aureus* was 31.2 μ g/mL. In contrast, the MIC₉₀ against MRSA and *S. epidermidis* was 62.5 μ g/ mL, with MIC₉₀ of 2 mg/mL and 1 mg/mL against *P. aeruginosa* and *E. coli*, respectively, in which Gram-negative bacteria showed a lower degree of susceptibility. GLA showed significant inhibition of both Gram-positive and negative strains biofilm formation, and similar activity was observed in eradicating the preformed one.

A. canariense demonstrated anti-inflammatory, anti-biofilm, and antimicrobial efficacy against Gram-positive microorganisms, with GLA identified as a potential contributor to this antimicrobial activity. In addition, toxicity studies demonstrated that topical application of this

plant should be safe. Therefore, these findings support some of the documented ethnobotanical uses of this species to treat wounds and demonstrate its potential in the pharmaceutical industry.

8.4 *Citrullus colocynthis*

This plant is widely distributed across the Middle East, North Africa, and Western Asia. It has traditionally been used for various ailments, including eye redness, cough, asthma, analgesic, diabetes, jaundice, urinary disorders, ascites, rheumatism, and wound-healing properties (skin infections) (Bnyan et al., 2013; Hussain et al., 2014). Consequently, *C. colocynthis* has been intensively studied using *in vitro* and *in vivo* modules, including antimicrobial activity (Marzouk et al., 2009; Ali et al., 2013; Bnyan et al., 2013; Hameed et al., 2020), antifungal activity (Marzouk et al., 2009; Hameed et al., 2020), antioxidant activity (Kumar et al., 2008; Benariba et al., 2013), anti-inflammatory (Marzouk et al., 2011; Marzouk et al., 2013) cytotoxic activity (Abdulridha et al., 2020; Perveen et al., 2021).

Although we were exploring the medicinal properties of *C. colocynthis*, SSTIs and chronic wounds were our primary emphasis. The antimicrobial activity of the methanolic extract was investigated with agar diffusion and broth microdilution assay against selected bacterial strains; *S. aureus*, MRSA, *S. epidermidis*, *P. aeruginosa*, and *E. coli*, with *C. colocynthis* exhibiting resistance toward all tested microorganisms. One of the main disadvantages of previously selected techniques is that some of the antimicrobial compounds that are not polar will either not diffuse effectively through the agar or precipitate, rendering antimicrobial compounds ineffective. In addition, the turbid and coloured nature of the plant extract solution made it challenging to assess the bacterial growth using the broth microdilution

technique (King et al., 2008; Klančnik et al., 2010). To overcome this challenge, we investigated the antimicrobial activity of *C. colocynthis* using agar incorporation assay and direct bio-autographic assay. Bioautography has several advantages over alternative testing methods, including its simplicity, low cost, and applicability to the assessment of complex lipophilic plant extracts, as well as its ability to reveal the antimicrobial activity of individual compounds within a mixture (Verbitski et al., 2006; Shahverdi et al., 2007).

All microorganisms examined exhibited resistance based on the results of both techniques, which validated the findings of the prior methodology. Although many studies have reported the antimicrobial activity of *C. colocynthis*, we did not observe any antimicrobial activity. This could be due to the significant fluctuation of plant extract active constituents levels depending on the weather and other factors in their geographic region. In addition, different compounds and their mechanisms of action in extracts can be affected by factors, such as growing location, harvest time, methods of processing, and plant parts utilised. In light of this, it may not be easy to draw reliable conclusions from comparing the various data in the literature about the antibacterial activity of plant extracts (Radulovic et al., 2013).

The antioxidant activity of *C. colocynthis* was investigated through cellular and acellular techniques; namely the DPPH assay showed an IC₅₀ of 824 µg/mL aligned with published reports (Kumar et al., 2008; Benariba et al., 2013). In addition, the cellular module was used to determine ROS levels in HaCaT cells. In this approach, adding a menadione compound will produce hydrogen peroxides (H₂O₂) radicals. Our findings showed that cells stimulated with menadione then treated with *C. colocynthis* produced more H₂O₂ than cells treated with menadione only as a positive control, even *C. colocynthis* without cells showed a high level of H₂O₂. This may suggest that this plant directly produces H₂O₂ or contains polyphenolic

chemicals that interact with components of cell culture media to generate H₂O₂ (Ślesak et al., 2007).

Investigation of the effect of *C. colocynthis* on the proliferation and migration of HaCaT using the MTT and scratch wound assays revealed a considerable suppression of both HaCaT important functions. In addition, it had a potent cytotoxic effect as assessed by FACS and CLSM analysis. Numerous studies have examined the cytotoxic effect of this plant, with a recent study identifying cucurbitic acid as the compound responsible for this activity (Abdulridha et al., 2020). Our prior findings showing that *C. colocynthis* may generate H₂O₂ could explain this cytotoxic activity. Since no plant-derived drug has made it to clinical trial despite multiple published studies on its cytotoxicity, *C. colocynthis* may be a valuable source for developing such drugs. Moreover, despite its cytotoxicity, *C. colocynthis* significantly suppressed several inflammatory mediators. A study identified and isolated 11-deoxocucurbitacin as the primary potent anti-inflammatory compound from the seeds of *C. colocynthis* (Marzouk et al., 2013).

Our antimicrobial, antibiofilm, antioxidant and, most importantly, toxicological studies on human skin do not appear to support the documented ethnobotanical uses of *C. colocynthis* for treating SSTIs and wounds. However, it could be a potential source for the development of a new cytotoxic (eg anti-cancer) medication.

8.5 *Maerua crassifolia*

M. crassifolia can be found in the Middle East and Africa. In traditional medicine, it is used to treat skin infections, headaches, fever, gastrointestinal disorders, gastric ulcers, tooth pain, and

wounds healing (Abouri et al., 2012; Volpato et al., 2012; Christian et al., 2014). In addition, several studies have examined *M. crassifolia* for its anti-inflammatory effect (Akuodor, 2016; Christian et al., 2016), antioxidant properties (Chaib et al., 2015; Ckilaka et al., 2015), and antimicrobial effects (Abdel-Sattar et al., 2008; Ckilaka et al., 2015).

Through agar diffusion, broth microdilution, and direct bioautographic assay, we evaluated the antimicrobial activity of the methanolic extract in this study. Our results demonstrated that the whole extract does not possess antimicrobial activity, and the discrepancy with the published reports (Abdel-Sattar et al., 2008; Ckilaka et al., 2015) could be due to the levels of active constituents in the extract, with factors influencing it stated previously in Section 8.1.4. Additionally, the selected microorganisms, the employed methods, the extraction system, and solvents, besides the culture media composition, can all contribute to the activity (Rios et al., 1988; Ross et al., 2001).

Both cellular and acellular methods were used to examine the antioxidant activity of *M. crassifolia*. The high phenolic contents detected by the Folin Ciocalteu assay at 24.89 mg GAE/g dry extract may account for the DPPH assay finding of concentration-dependent antioxidant activity with an IC₅₀ of 448 µg/mL. Moreover, *in vitro* antioxidant activity revealed its ability to scavenge H₂O₂ radicals at low concentrations. Chronic wounds are characterised by inflammation, limited mobility, intense pain, swelling, and immobility (Posnett and Franks, 2008; Green et al., 2014).

A significant finding in this study was that *M. crassifolia* significantly stimulated the proliferative and migratory capacities of HaCaT cells, two of the most critical keratinocyte functions during the wound healing process. These findings provide firm support of

ethnobotanical reports on the traditional use of *M. crassifolia* to promote wound healing (Volpato et al., 2012; Idm'Hand et al., 2020).

Typical characteristics of chronic wounds include higher levels of pro-inflammatory cytokines, proteases, and reactive oxygen species, persistent infection, and decreased migration (Dickinson and Gerecht, 2016). Therefore, the ability of *M. crassifolia* to increase keratinocyte proliferation and migration may be attributed to its capacity to scavenge ROS and suppress inflammatory mediators, making it a potential alternative treatment for chronic wounds. High levels of ROS can cause severe tissue damage and even malignancy transformation by damaging cellular membranes, DNA, lipids, and proteins, slowing the healing process (Jorge et al., 2008). Furthermore, *M. crassifolia* exhibited a substantial reduction in the expression of inflammatory cytokines, TNF- α and IL-8.

Current therapies for skin wounds include dressings, tissue-engineered substitutes, and surgical reconstructive methods employing autografts or allografts to encourage wound re-epithelialization. However, despite their potential clinical benefits, these methods have many severe limitations. These include high cost of production, poor wound bed adhesion, inadequate vascularization, and the inability to replicate skin appendages (Rousselle et al., 2019).

M. crassifolia demonstrated promising free radical scavenging abilities in both cellular and acellular assays, in addition to the suppression of inflammatory cytokines expression and a significant wound healing properties. Consequently, these findings support some of the documented ethnobotanical uses of this species in wounds. In summary, it could be a promising

candidate for topical application to wounds in a suitable pharmaceutical form such as wound dressings.

8.6 *Rhazya stricta*

This plant, rich in alkaloids, is considered a significant medicinal plant throughout the Middle East and South Asia. Traditional uses include treating microbiological infections, sore throat, diabetes mellitus, and some inflammatory diseases, including rheumatism and allergies (Gamal et al., 2010; Baeshen et al., 2016; Bukhari et al., 2017). Many studies have investigated the antimicrobial activity of *R. stricta* against several species, including *S. aureus*, MRSA, *P. aeruginosa*, *N. meningitides*, *E. coli*, *B. subtilis*, *S. typhi*, *S. pyogenes*, and *P. acnes* (Sultana and Khalid, 2010; Abadi et al., 2011; Khan et al., 2016; Alnabati et al., 2021).

Due to its well-documented ethnobotanical uses and previous antimicrobial studies, *R. stricta* is a potential candidate for discovering new antimicrobial compounds to combat the rising trend of antibiotic resistance. In this Thesis, preliminary screening of *R. stricta* methanolic extract with the agar diffusion method revealed a potent antimicrobial activity compared to all studied plant extracts and against all tested Gram-positive and negative strains. Broth microdilution method was utilized to determine the MIC values against selected microorganisms, *S. aureus* and MRSA (312.5 µg/mL), *S. epidermidis* (625 µg/mL), *P. aeruginosa* (1.25 mg/mL), and *E. coli* (5 mg/mL), with MBC values ranging from 0.3 to 10 mg/ mL. Khan et al. (2016) reported that *R. stricta* organic alkaloid extract demonstrated the most significant antimicrobial activity and cell membrane rupture was evident using transmission electron microscopy, suggesting that the antimicrobial action of *R. stricta* may be related to its alkaloid content.

One of the main challenges in the treatment of SSTIs and chronic wounds is the formation of biofilm. Some study suggests that the biofilm matrix contributes to bacterial resistance to antibiotics. Therefore, removing antibiotics from cells via efflux pumps and the complexity of the formed biofilms can render antibiotics ineffective in some cases (Stewart and Franklin, 2008). To determine the antibiofilm potential of *R. stricta*, selected bacteria biofilm were investigated to the best of our knowledge for the first time through a crystal violet technique and validated by CLSM live/dead bacterial viability assay, which revealed potent antibiofilm properties demonstrated by the inhibition of biofilm formation and the eradication of preformed one at the minimum inhibitory concentration (MIC) or lower (MIC/2), likely owing to a direct antimicrobial effect or by inhibiting bacterial attachment to the surface and so preventing colonisation and biofilm formation. In addition, it could also play a role in inhibiting bacterial quorum sensing (QS), which regulates biofilm formation and the secretion of virulence factors. Moreover, biofilm extracellular polymeric substance (EPS) is a physical and chemical barrier against antibiotic penetration. Thus, *R. stricta* could inhibit the formation of EPS facilitating the penetration of other antimicrobial compounds into the biofilm (Del Pozo and Patel, 2007).

Given the limited penetration of existing antibiotics into established biofilms, high dosages of antibiotics are often necessary to remove and debride biofilms (Høiby et al., 2015). This will increase the observed toxicity of antibiotics and will raise the chances of developing resistance. Using the synergistic action of several antibiotics to treat biofilms is one option (Mihailescu et al., 2014). However, as bacterial resistance to antibiotics has risen, the effectiveness of antibiotics has progressively declined. Therefore, antibiotics could be more effective with other therapies, such as antibiofilm agents (Ricciardelli et al., 2018; Lu et al., 2019). *In vitro*, *R.*

stricta exhibits antimicrobial and antibiofilm properties. Despite the need for more research into the mechanisms of these activities, this can be regarded as a milestone in developing novel antibiofilm therapies. In combination with antibiotics, they can serve a secondary and alternative role. Their inhibiting impact on biofilms may assist antibiotics in treating infections and address the problem of bacterial resistance.

R. stricta free radical scavenging activities were investigated through DPPH assay, and results showed that it exhibited the highest capacity for scavenging the DPPH radical with an IC₅₀ of 335 µg/mL. Following the DPPH assay, H₂O₂ scavenging activities of plant extracts in cell culture (HaCaT) were examined, and findings indicated promising *R. stricta* antioxidant activity in both chemical-based and cell-based systems. *R. stricta* had no measurable effect on the wound healing abilities of HaCaT at the tested concentrations. Moreover, it exhibited a delayed but significant reduction of HaCaT proliferation at 120 h and 168 h, with IC₅₀ values of 175 µg/mL and 105.3 µg/mL, respectively. Cytotoxicity results obtained through FACS PI/FD double staining approach demonstrated significant toxicity to HaCaT cells at the highest concentration of 200 µg/mL after 24 h, validated with images obtained from CSLM. Finally, *R. stricta* demonstrated no effect on the migration of HaCaT upon evaluation with scratch wound assay.

Chronic wounds are difficult to treat because bacteria tend to form biofilms on their surface and inside wound beds, contributing to the persistent inflammation that makes them so challenging to treat. Biofilms and the human immune system will interact to activate neutrophils and macrophages, and this causes elevated levels of pro-inflammatory cytokines such as IL-1β, TNF- α, IL-6, and ROS, with an increase in matrix metalloproteinases (MMPs), which damage the extracellular matrix (ECM) and inhibit the epithelialization and proliferation

of keratinocytes (Wu et al., 2019). The anti-inflammatory effect of *R. stricta* was investigated, and a significant dose-dependent reduction in the expressions of several inflammatory cytokines and COX-2 was observed. Elkady et al. (2016) reported that *R. stricta* inhibits nuclear factor- κ B (NF- κ B) signalling by blocking the p65 subunit DNA binding activity. NF- κ B is a transcription factor protein that controls many genes involved in various immunological and inflammatory response pathways. NF- κ B is a crucial modulator of the stimulation of pro-inflammatory genes in both innate and adaptive immune cells. NF- κ B has been involved in the pathogenesis of several inflammatory disorders. Hence, targeting the NF- κ B signalling pathway is a promising strategy for anti-inflammatory therapy (Pai and Thomas, 2008; Oeckinghaus and Ghosh, 2009).

We employed a bioguided fractionation approach, including liquid-liquid partitioning and column chromatography, to identify and isolate the active compounds of interest from *R. stricta*. Direct bio-autographic analysis of the active hexane and chloroform fractions showed the presence of several antimicrobial compounds that were effective against Gram-positive and Gram-negative strains. To isolate the antibacterial compounds, a preparative TLC with a mobile phase of 50% ethyl acetate: 50% hexane was performed on the hexane fraction 6 of *R. stricta*. HR ESI-MS was used to determine the molecular formula and weight, and NMR was used to validate the chemical structure, leading to the compound's identification as vincadifformine, which aligned with previous reports in the published literature (Kumara, 2010). Vincadifformine antimicrobial effects in both planktonic and biofilm conditions were investigated. The MIC₉₀ of the isolated compound against *S. aureus*, MRSA, and *S. epidermidis* were 500 μ g/mL, and the MIC₉₀ for *P. aeruginosa* and *E. coli* was higher than 2 mg/mL. Therefore, Gram-negative bacteria displayed a decreased susceptibility. In addition,

vincadifformine was shown to significantly inhibit biofilm formation of both Gram-positive and negative bacteria and have similar action when it came to eradicating an already established biofilm, with the exception of *P. aeruginosa* preformed biofilm. However, the bioguided fractionation approach was unsuccessful in identifying all antimicrobial compounds that showed efficacy by direct bio-autographic investigation of *R. stricta*.

Since the antimicrobial and antibiofilm activity of the isolated compound is lower than that of the whole *R. stricta* extract, it could be due to compounds losses during fractionating, or it could indicate that synergistic interaction or multifactorial effects between constituents of *R. stricta* phytochemicals are crucial. This is not an uncommon observation regarding plant extracts, highlighting plant extracts' enormous variability and complexity (Gilbert and Alves, 2003). Due to the complexity of plant extract composition, synergism or antagonism effects are one of the limitations to developing antimicrobials derived from medicinal plants (Arima et al., 2002). Nevertheless, there is strong evidence, based on reviews of synergism within and across plant extracts, indicating that the whole extract's effect is superior to the effect of its individual constituent (van Vuuren and Viljoen, 2011; Rather et al., 2013; Kellogg et al., 2016).

R. stricta demonstrated a promising anti-inflammatory, antioxidant, antibiofilm, and antimicrobial efficacy against Gram-positive and Gram-negative microorganisms. Therefore, these findings support some of the documented ethnobotanical uses and suggest a wide range of clinical applications to treat conditions with complex pathophysiologies, such as skin and soft tissue infections, by the multi-target action of the extract.

8.7 *Tribulus macropterus*

Widespread throughout the Middle East and North Africa (Jongbloed et al., 2003), this plant is traditionally used to treat cardiovascular diseases and sexual dysfunction. Although few studies have investigated the medicinal properties of *T. macropterus*, including antioxidant (Ksiksi et al., 2017) and cytotoxic activity (Abdel-Hameed et al., 2007), *Tribulus terrestris* from the same genus and family has been extensively studied for its antimicrobial (Baburao et al., 2009; Hakemi-Vala et al., 2014; Algarni et al., 2022), cardioprotective (Zhang et al., 2010) and wound healing potential (Wesley et al., 2009). Currently, *T. terrestris* is marketed in tablet form under the brand name Tribestan (Zheleva-Dimitrova et al., 2012).

Antimicrobial activities against *S. aureus*, MRSA, *S. epidermidis*, and *E. coli*, were observed in a preliminary screening of *T. macropterus* methanolic extract using the agar diffusion method. However, it exerted a weak activity as only partial inhibition was observed, indicating the presence of bacteriostatic compounds in the extract. Further fractionation of the extract might enhance the activity and isolate the pure compound responsible for this activity. The broth microdilution method revealed that MIC and MBC values were greater than 20 mg/mL. In addition to examining *T. macropterus* efficacy against the planktonic phase of bacteria, antibiofilm activities were also explored. Although *T. macropterus* demonstrated significant inhibition of *S. aureus* biofilm formation and eradication of the preformed one, it did not affect the biofilm of the other tested strains.

In the wound healing work, *T. macropterus* had no observable influence on the proliferation or migration of HaCaT cells at the concentrations used, and no cytotoxic activity was observed. Abdel-Hameed et al. (2007) reported that *T. macropterus* methanolic extract IC₅₀ against

HepG2 tumour cell line was 2.90 $\mu\text{g/mL}$. This may be due to variations in the extract sensitivity towards the cell line. Antioxidant activity of *T. macropterus* examined via DPPH assay showed an IC_{50} of 787 $\mu\text{g/mL}$, with a total phenolic content of 21 mg GAE/g dry extract.

As previously stated, excess production of pro-inflammatory cytokines is seen in chronic wounds (Tottoli et al., 2020). Lipopolysaccharide (LPS) significantly induced the release of inflammatory mediators in the *in vitro* model utilizing HaCaT cells. LPS from *E. coli* is often employed in studies to induce pro-inflammatory cytokine and chemokine production (Zhao et al., 2018). *T. macropterus* exhibited significant inhibition of inflammatory cytokines, $\text{TNF-}\alpha$ and IL-8 levels. Moreover, it showed significant downregulation of COX-2 levels; the latter observation is interesting as it suggests potential as a natural NSAID. Even though the anti-inflammatory effects of *T. macropterus* have not been reported, a related plant, *Tribulus terrestris*, also from the *zygophyllaceae* genus, suppressed the production of inflammatory cytokines, like $\text{TNF-}\alpha$ and IL-4, in a macrophage cell line (Oh et al., 2012).

To discover and isolate active compounds, liquid-liquid partitioning and column chromatography were utilised in a bioguided fractionation approach. Although, the investigation of active hexane and chloroform fractions using a direct bio-autographic assay revealed the presence of several antimicrobial compounds that are exclusively effective against Gram-positive bacteria. The bioassay-guided fractionating failed to identify and isolate the antimicrobial compounds detected via direct bio-autographic assay due to the limiting supply of plant extract and complexity. Reaching the step of pure antimicrobial compounds from plant extracts is complicated due to the involvement of many steps, from extraction to elucidation of a chemical structure and the noticeable plant's complexity and variety. Identifying the specific compounds in plant extracts that have a desired biological effect may be a significant challenge

because there may be hundreds or even thousands of them. Thus, synergism or antagonism effects are also possible (Tian et al., 2009; Wagner and Ulrich-Merzenich, 2009; Efferth and Koch, 2011; Enke and Nagels, 2011; van Vuuren and Viljoen, 2011).

8.8 Future Prospects

This study successfully established the promising activities of several medicinal plants, with one or more of the following properties: antimicrobial, antibiofilm, antioxidant, anti-inflammatory, cytotoxic, and wound healing potential. Several pure compounds responsible for antimicrobial activity were identified and isolated. Other compounds responsible for the rest of the activities were not identified. The bio-guided fractionation of sufficient quantities of these plants would disclose their bioactive constituents, particularly those without published phytochemistry data, such as *A. canariense*, *M. crassifolia*, and *T. macropterus*.

Since the chemical constituents of medicinal plants vary, it is challenging to describe their activity comprehensively. Antimicrobial screening procedures, such as agar diffusion, broth dilution, and TLC bioautography, have been modified to increase their sensitivity. Nonetheless, there may still be too diluted components to detect. In addition, different factors, such as climate conditions, growing locations, harvest time, processing methods, and plant parts used, can influence the chemical constituents of medicinal plants. Consequently, it would be intriguing to investigate the impact of these factors on the constituents and activities of the selected medicinal plants.

The antimicrobial properties of active plant extracts could be further evaluated regarding the precise mechanism of action behind the activity. In the process of developing new

antimicrobial agents, a precise assessment of the mechanism of action is typically the critical factor of the process. Discovering all the potential targets for antimicrobials can help accelerate the optimization process, uncover off-target reactions, and allow for early toxicity studies, all of which can reduce the probability of undesirable side effects (Schenone et al., 2013).

The clinical significance of such agents may be established by *in vivo* comprehensive studies in animal models with targeted skin and soft tissue infections. This could establish a reliable link between *in vivo* and *in vitro* findings. Additionally, future studies could investigate synergistic interactions between compounds within medical plant extracts and between two active medicinal plant extracts, such as combining *R. stricta* for its antibiofilm and antimicrobial properties with *M. crassifolia*, for its wound healing properties to achieve multiple actions against complex conditions. Moreover, the possibility of combining medicinal plant extracts with antibiotics. This can be achieved by investigating the combinations with microdilution assays for MIC values, followed by the checkerboard technique. Moreover, synergy-directed fractionation could be adapted to test the antimicrobial activity of fractions in combinations with antibiotics at fixed concentrations, which may reveal the presence of compounds that potentiate the activity of antibiotics by different mechanisms without exhibiting a direct antimicrobial activity (Junio et al., 2011). Finally, developing topical formulations of these promising medicinal plants with a standardized extraction method could be explored.

The wound healing potential of selected medicinal plants revealed that *M. crassifolia* showed superior wound healing responses with significant induction of HaCaT proliferation and migration. However, further studies could investigate the mechanism behind this effect and evaluate the effect on the migration in the presence of antiproliferative agents, such as mitomycin C (Sadeghi et al., 1998; Grazia et al., 2014), to subsidize the previously established

proliferative effect of *M. crassifolia*. Moreover, the effect on the proliferation and migration of dermal fibroblast cells can be evaluated.

Investigation into medicinal plants' antibiofilm properties and isolated compounds have shown promising results. However, the molecular mechanism of action behind the antibiofilm activity has to be investigated further. Since bacterial biofilms can be formed from a single or mixed species, testing the selected medicinal plant and isolated compounds against a mixed species may be a more accurate reflection of their efficacy in treating chronic wound biofilms. Biofilms formed from multiple microbial species, such as those observed in chronic wound infections, might be evaluated in several proposed modules (Sun et al., 2008; Ganesh et al., 2015).

9. References

- Aati, H., El-Gamal, A., Shaheen, H. and Kayser, O. 2019. Traditional use of ethnomedicinal native plants in the Kingdom of Saudi Arabia. *Journal of Ethnobiology and Ethnomedicine* 15(1), pp. 1–9.
- Abadi, F.J.R., Abdulaziz, A.M., Hadhoud, A.A., Baeshin, N.A., Qari, S.H. and Alhejin, A.M. 2011. An epidemiological Survey and Evaluation of the Antimicrobial Growth Effect of *Rhazya stricta* (Decne) Leaves Extract on Different Genotypes of *Neisseria Meningitidis*. *Egyptian Journal of Medical Microbiology* 20(2), pp. 77–86.
- Abd-El-Aleem, S.A., Ferguson, M.W.J., Appleton, I., Bhowmick, A., McCollum, C.N. and Ireland, G.W. 2001. Expression of cyclooxygenase isoforms in normal human skin and chronic venous ulcers. *The Journal of Pathology: A Journal of the Pathological Society of Great Britain and Ireland* 195(5), pp. 616–623.
- Abdel-Hameed, E.S., El-Nahas, H.A., El-Wakil, E.A. and Ahmed, W.S. 2007. Cytotoxic Cholestane and Pregnane Glycosides from *Tribulus macropterus*. *Zeitschrift fur Naturforschung - Section C Journal of Biosciences* 62(5–6), pp. 319–325.
- Abdel-Hassan, I.A., Abdel-Barry, J.A. and Tariq Mohammed, S. 2000. The hypoglycemic and antihyperglycaemic effect of *Citrullus colocynthis* fruit aqueous extract in normal and alloxan diabetic rabbits. *Journal of Ethnopharmacology* 71(1–2), pp. 325–330.
- Abdel-Sattar, E., Harraz, F.M. and El-Gayed, S.H. 2008. Antimicrobial activity of extracts of some plants collected from the Kingdom of Saudi Arabia. *Medical Science* 15(1), pp. 25-33.
- Abdel-Zaher, A.O., Salim, S.Y., Assaf, M.H. and Abdel-Hady, R.H. 2005. Antidiabetic activity and toxicity of *Zizyphus spina-christi* leaves. *Journal of ethnopharmacology* 101(1–3), pp. 129–138.
- Abdulridha, M.K., Al-Marzoqi, A.-H. and Ghasemian, A. 2020. The anticancer efficiency of *Citrullus colocynthis* toward the colorectal cancer therapy. *Journal of Gastrointestinal Cancer* 51(2), pp. 439–444.
- Abouri, M., El Mousadik, A., Msanda, F., Boubaker, H., Saadi, B. and Cherifi, K. 2012. An ethnobotanical survey of medicinal plants used in the Tata Province, Morocco. *International Journal of Medicinal Plant Research* 1(7), pp. 99–123.
- Abraham, J. and Mathew, S. 2019. Merkel cells: a collective review of current concepts. *International Journal of Applied and Basic Medical Research* 9(1), p. 9.
- Abreu, A.C., McBain, A.J. and Simoes, M. 2012. Plants as sources of new antimicrobials and resistance-modifying agents. *Natural product reports* 29(9), pp. 1007–1021.
- Adan, A., Kiraz, Y., & Baran, Y. 2016. Cell Proliferation and Cytotoxicity Assays. *Current pharmaceutical biotechnology*, 17 14, pp. 1213-1221.
- Ads, E.N., Rajendrasozhan, S., Hassan, S.I., Sharawy, S.M.S. and Humaidi, J.R. 2017. Phytochemical, antimicrobial and cytotoxic evaluation of *Zizyphus spina-christi* (L.) stem bark. *Biomedical Research* 28(15), pp. 6646–6653.

- Agyare, C., Akindede, A.J. and Steenkamp, V. 2019. Natural products and/or isolated compounds on wound healing. *Evidence-Based Complementary and Alternative Medicine* 2019(1), pp. 1-3.
- Ahmad, H., Bhatti, G.R. and Latif, A. 2004. Medicinal Flora of the Thar Desert : an Overview of Problems and Their Feasible Solutions. *Zonas Áridas* , pp. 73–83.
- Akbik, D., Ghadiri, M., Chrzanowski, W. and Rohanizadeh, R. 2014. Curcumin as a wound healing agent. *Life sciences* 116(1), pp. 1–7.
- Akhgari, A., Laakso, I., Seppänen-Laakso, T., Yrjönen, T., Vuorela, H., Oksman-Caldentey, K.-M. and Rischer, H. 2015. Analysis of indole alkaloids from *Rhazya stricta* hairy roots by ultra-performance liquid chromatography-mass spectrometry. *Molecules* 20(12), pp. 22621–22634.
- Akhzari, M., Mirghiasi, S.M., Vassaf, M., Bidgoli, M. and Tari, Z. 2015. The effect of *Citrullus colocynthis* on the reduction of inflammatory agents in osteoarthritis. *Molecular Biology* 4(04), pp 1-6.
- Akita, S. 2019. Wound repair and regeneration: mechanisms, signaling. *International Journal of Molecular Sciences* 20(24), p. 6328.
- Akuodor, G.C., Essien, A.D., Akpan, J.L., Chilaka, K.C., Uwaezuoke, N.J.I., Nwadike, K.I., Nwobodo, N.N. and Ezeokpo, B.C. 2016. Analgesic, antiinflammatory and antipyretic activities of methanolic leaf extract of *Maerua crassifolia*. *Journal of Coastal Life Medicine* 4(3), pp. 225–230.
- Akuodor, G.C., Ibrahim, J.A., Akpan, J.L., Okorie, A.U. and Ezeokpo, B.C. 2014. Phytochemical and anti-diarrhoeal properties of methanolic leaf extract of *Maerua crassifolia* Forssk. *European journal of medicinal plants* 4(10), p. 1223.
- Al Shamsi, A., 2002. Adipocyte Specific Release of Tumor Necrosis Factor in Response to Medicinal Plants and Synthetic Nucleosides In Vitro. MSc. United Arab Emirates University.
- Al-Abbas, N. and Shaer, N. 2021. Apoptotic and Anti-Proliferative Effects of *Rhazya Stricta* Nanoparticles against Hepatocellular Carcinoma (Hep G-2 And Huh-7) Cell Lines. *Mansoura Medical Journal* 50(2), pp. 27–35.
- Al-Dabbagh, B., Elhaty, I.A., Al Hrouf, A., Al Sakkaf, R., El-Awady, R., Ashraf, S.S. and Amin, A. 2018. Antioxidant and anticancer activities of *Trigonella foenum-graecum*, *Cassia acutifolia* and *Rhazya stricta*. *BMC complementary and alternative medicine* 18(1), pp. 1–12.
- Al-Ghaithi, F., El-Ridi, M.R., Adeghate, E. and Amiri, M.H. 2004. Biochemical effects of *Citrullus colocynthis* in normal and diabetic rats. *Molecular and Cellular Biochemistry* 261(1), pp. 143–149.
- Al-Ghamdi, M.S. 2001. The anti-inflammatory, analgesic and antipyretic activity of *Nigella sativa*. *Journal of ethnopharmacology* 76(1), pp. 45–48.
- Al-Laith, A.A., Alkhuzai, J. and Freije, A. 2015. Assessment of antioxidant activities of three wild medicinal plants from Bahrain. *Arabian Journal of Chemistry* 8, pp. 1–7.
- Al-Rawi, S. and Fetters, M.D. 2012. Traditional Arabic & Islamic medicine: a conceptual model for clinicians and researchers. *Global Journal of Health Science* 4(3), p. 164.
- Al-Yahya, M.A., 1984. Kuwait: Proc. III Int. Conf. Islamic. *Medicine*, 349.
- Al-Zharani, M., Nasr, F.A., Abutaha, N., Alqahtani, A.S., Noman, O.M., Mubarak, M. and Wadaan, M.A. 2019. Apoptotic induction and anti-migratory effects of *Rhazya stricta* fruit extracts on a human breast cancer cell line. *Molecules* 24(21), p. 3968.

- Alanzi, A., Assiri, A., Aldayel, F., Allam, A., Bin-Bakheet, O., Alanzi, F., Alhaydhal, A. and Alrasheed, L. 2016. Herbal medicine among saudis: awareness, uses, reasons and common herbs. *International Journal of Research in Medical Sciences* 1(2), pp. 13–19.
- Ali, A.A., Alian, A. and Elmahi, H.A. 2013. Phytochemical Analysis of Some Chemical Metabolites of Colocynth Plant (*Citrullus colocynthis* L) and its Activities as Antimicrobial and Antiplasmodial. *Journal of Basic and Applied Scientific Research* 3(5), pp. 228–236.
- Ali, B.H., Bashir, A.K., Tanira, M.O.M., Medvedev, A.E., Jarrett, N., Sandler, M. and Glover, V. 1998. Effect of Extract of *Rhazya stricta*, a Traditional Medicinal Plant, on Rat Brain Tribulin. *Pharmacology Biochemistry and Behavior* 59(3), pp. 671–675.
- Ali, M.A., Abul Farah, M., Al-Hemaid, F.M. and Abou-Tarboush, F.M. 2014. In vitro cytotoxicity screening of wild plant extracts from Saudi Arabia on human breast adenocarcinoma cells. *Genetics and Molecular Research* 13(2), pp. 3981–3990.
- Almehdar, H., Abdallah, H.M., Osman, A.M.M. and Abdel-Sattar, E.A. 2012. In vitro cytotoxic screening of selected Saudi medicinal plants. *Journal of Natural Medicines* 66(2), pp. 406–412.
- Alnabati, N.A., Al-Hejin, A.M., Noor, S.O., Ahmed, M.M.M., Abu-Zeid, M. and Mleeh, N.T., 2021. The antibacterial activity of four Saudi medicinal plants against clinical isolates of *Propionibacterium acnes*. *Biotechnology & Biotechnological Equipment*, 35(1), pp.415-424.
- AlQathama, A., Bader, A., Al-Rehaily, A., Gibbons, S. and Prieto, J.M. 2022. In vitro cytotoxic activities of selected Saudi medicinal plants against human malignant melanoma cells (A375) and the isolation of their active principles. *European Journal of Integrative Medicine* 49, p. 102083.
- Alshehri, M.A., Alanazi, N.A., Panneerselvam, C., Trivedi, S., Maggi, F., Sut, S. and Dall'Acqua, S. 2020. Phytochemical analysis of *Rhazya stricta* extract and its use in fabrication of silver nanoparticles effective against mosquito vectors and microbial pathogens. *Science of the Total Environment* 700, p. 134443.
- Alsterholm, M., FLYTSTRÖM, I., Bergbrant, I.-M. and Faergemann, J. 2010. Fusidic acid-resistant *Staphylococcus aureus* in impetigo contagiosa and secondarily infected atopic dermatitis. *Acta dermato-venereologica* 90(1), pp. 52-57.
- Altok, E., Bayçın, D., Bayraktar, O. and Ülkü, S. 2008. Isolation of polyphenols from the extracts of olive leaves (*Olea europaea* L.) by adsorption on silk fibroin. *Separation and Purification Technology* 62(2), pp. 342–348.
- Altoparlak, U., Erol, S., Akcay, M.N., Celebi, F. and Kadanali, A. 2004. The time-related changes of antimicrobial resistance patterns and predominant bacterial profiles of burn wounds and body flora of burned patients. *Burns* 30(7), pp. 660–664.
- Amarante-Mendes, G.P., Adjemian, S., Branco, L.M., Zanetti, L.C., Weinlich, R. and Bortoluci, K.R. 2018. Pattern recognition receptors and the host cell death molecular machinery. *Frontiers in immunology* 9, p. 2379.
- Andreassi, M., Forleo, P., Dilohjo, A., Masci, S., Arate, G. and Amerio, P. 1997. Efficacy of γ -linolenic acid in the treatment of patients with atopic dermatitis. *Journal of International Medical Research* 25(5), pp. 266–274.
- Andriessen, M.P., Van Bergen, B.H., Spruijt, K.I., Go, I.H., Schalkwijk, J. and Van De Kerkhof, P.C. 1995. Epidermal proliferation is not impaired in chronic venous ulcers. *Acta dermato-venereologica* 75(6), pp. 459–462.

- Archer, N.K., Mazaitis, M.J., Costerton, J.W., Leid, J.G., Powers, M.E. and Shirtliff, M.E. 2011. Staphylococcus aureus biofilms: properties, regulation, and roles in human disease. *Virulence* 2(5), pp. 445–459.
- Arima, H., Ashida, H. and Danno, G. 2002. Rutin-enhanced Antibacterial Activities of Flavonoids against Bacillus cereus and Salmonella enteritidis. *Bioscience, Biotechnology, and Biochemistry* 66(5), pp. 1009–1014.
- Arm, J.P., Boyce, J.A., Wang, L., Chhay, H., Zahid, M., Patil, V., Govindarajulu, U., Ivester, P., Weaver, K.L., Sergeant, S., Israel, E. and Chilton, F.H. 2013. Impact of botanical oils on polyunsaturated fatty acid metabolism and leukotriene generation in mild asthmatics. *Lipids in Health and Disease* 12(1), p. 141.
- Aryal, S., Baniya, M.K., Danekhu, K., Kunwar, P., Gurung, R. and Koirala, N. 2019. Total phenolic content, flavonoid content and antioxidant potential of wild vegetables from Western Nepal. *Plants* 8(4), p. 96.
- Asadi-Samani, M., Bahmani, M. and Rafieian-Kopaei, M. 2014. The chemical composition, botanical characteristic and biological activities of Borago officinalis: A review. *Asian Pacific Journal of Tropical Medicine* 7(S1), pp. S22–S28.
- Ashcroft, G.S., Jeong, M., Ashworth, J.J., Hardman, M., Jin, W., Moutsopoulos, N., Wild, T., McCartney-Francis, N., Sim, D. and McGrady, G. 2012. Tumor necrosis factor-alpha (TNF- α) is a therapeutic target for impaired cutaneous wound healing. *Wound Repair and Regeneration* 20(1), pp. 38–49.
- Atanasov, A.G., Waltenberger, B., Pferschy-Wenzig, E.-M., Linder, T., Wawrosch, C., Uhrin, P., Temml, V., Wang, L., Schwaiger, S. and Heiss, E.H. 2015. Discovery and resupply of pharmacologically active plant-derived natural products: A review. *Biotechnology advances* 33(8), pp. 1582–1614.
- B.J.R. Nicolaus, C. Coronelli, A. Binaghi. 1961. Microbiological determination of antibiotics by thin layer chromatograms, *Farmaco. Ed. Prat.*, 16 pp. 349-370.
- Baburao, B., Rajyalakshmi, G., Venkatesham, A., Kiran, G., Shyamsunder, A. and Gangarao, B. 2009. Anti-inflammatory and antimicrobial activities of methanolic extract of Tribulus terrestris Linn plant. *International Journal of Chemical Science* 7(3), pp. 1867–1872.
- Baeshen, M.N., Al-Attas, S.G., Ahmed, M.M., Hanafy, A.A.E.M. El, Anwar, Y., Alotibi, I.A. and Baeshen, N.A. 2016. The effect of Rhazya stricta aqueous leaves extract on MRSA genotypes in Jeddah province. *Biotechnology and Biotechnological Equipment* 30(2), pp. 368–374.
- Bagge, N., Ciofu, O., Skovgaard, L.T. and HØlby, N. 2000. Rapid development in vitro and in vivo of resistance to ceftazidime in biofilm-growing Pseudomonas aeruginosa due to chromosomal β -lactamase. *Apmis* 108(9), pp. 589–600.
- Bagheri, M., Mostafavinia, A., Abdollahifar, M.-A., Amini, A., Ghoreishi, S.K., Chien, S., Hamblin, M.R., Bayat, S. and Bayat, M. 2020. Combined effects of metformin and photobiomodulation improve the proliferation phase of wound healing in type 2 diabetic rats. *Biomedicine & Pharmacotherapy* 123, p. 109776.
- Bahri-Sahloul, R., Fredj, R. Ben, Boughalleb, N., Shriaa, J., Saguem, S., Hilbert, J.-L., Trotin, F., Ammar, S., Bouzid, S. and Harzallah-Skhiri, F. 2014. Phenolic composition and antioxidant and antimicrobial activities of extracts obtained from Crataegus azarolus L. var. aronia (Willd.) Batt. ovaries calli. *Journal of Botany* 2014(1), pp. 1-11.

- Bak, R.O. and Mikkelsen, J.G. 2010. Regulation of cytokines by small RNAs during skin inflammation. *Journal of biomedical science* 17(1), pp. 1–19.
- Bakr, R.O., El-Behairy, M.F., Elissawy, A.M., Elimam, H. and Fayed, M.A.A. 2021. New Adenosine Derivatives from *Aizoon canariense* L.: In Vitro Anticholinesterase, Antimicrobial, and Cytotoxic Evaluation of Its Extracts. *Molecules* 26(5), p. 1198.
- Balasundram, N., Sundram, K. and Samman, S. 2006. Phenolic compounds in plants and agri-industrial by-products: Antioxidant activity, occurrence, and potential uses. *Food Chemistry* 99(1), pp. 191–203.
- Ban, C.R. and Twigg, S.M. 2008. Fibrosis in diabetes complications: pathogenic mechanisms and circulating and urinary markers. *Vascular health and risk management* 4(3), p. 575.
- Bandyopadhyay, D. 2021. Topical antibacterials in dermatology. *Indian Journal of Dermatology* 66(2), p. 117.
- Banerjee, S. and Argáez, C. 2018. Topical Antibiotics for Infection Prevention: A Review of the Clinical Effectiveness and Guidelines. *Canadian Agency for Drugs and Technologies in Health*.
- Barbieri, R., Coppo, E., Marchese, A., Daglia, M., Sobarzo-Sánchez, E., Nabavi, S.F. and Nabavi, S.M. 2017. Phytochemicals for human disease: An update on plant-derived compounds antibacterial activity. *Microbiological research* 196, pp. 44–68.
- Barrientos, S., Stojadinovic, O., Golinko, M.S., Brem, H. and Tomic-Canic, M. 2008. Growth factors and cytokines in wound healing. *Wound repair and regeneration* 16(5), pp. 585–601.
- Bartlett, J.G., Gilbert, D.N. and Spellberg, B. 2013. Seven ways to preserve the miracle of antibiotics. *Clinical Infectious Diseases* 56(10), pp. 1445–1450.
- Bashir, A.K., Abdalla, A.A., Hassan, E.S., Wasfi, I.A., Amiri, M.A. and Crabb, T.A. 1994. Alkaloids with antimicrobial activity from the root of *Rhzyza stricta* Decn. growing in United Arab Emirates. *Arab Gulf Journal of Scientific Research* 12(1), pp. 119–131.
- Bavington, C. and Page, C. 2005. Stopping bacterial adhesion: a novel approach to treating infections. *Respiration* 72(4), pp. 335–344.
- Beauclerk, A.A.D. and Cundliffe, E. 1987. Sites of action of two ribosomal RNA methylases responsible for resistance to aminoglycosides. *Journal of molecular biology* 193(4), pp. 661–671.
- Begue, W.J. and Kline, R.M. 1972. The use of tetrazolium salts in bioauthographic procedures. *Journal of Chromatography A* 64(1), pp. 182–184.
- Benariba, N., Djaziri, R., Bellakhdar, W., Belkacem, N., Kadiata, M., Malaisse, W.J. and Sener, A. 2013. Phytochemical screening and free radical scavenging activity of *Citrullus colocynthis* seeds extracts. *Asian Pacific journal of tropical biomedicine* 3(1), pp. 35–40.
- Bendary, E., Francis, R.R., Ali, H.M.G., Sarwat, M.I. and El Hady, S. 2013. Antioxidant and structure–activity relationships (SARs) of some phenolic and anilines compounds. *Annals of Agricultural Sciences* 58(2), pp. 173–181.
- Berglund, D.L., Taffs, R.E. and Robertson, N.P. 1987. A rapid analytical technique for flow cytometric analysis of cell viability using calcofluor white M2R. *Cytometry* 8(4), pp. 421–426.
- Bernard, J.J. and Gallo, R.L. 2011. Protecting the boundary: the sentinel role of host defense peptides in the skin. *Cellular and Molecular Life Sciences* 68(13), pp. 2189–2199.

Bernhard, S., Hug, S., Stratmann, A.E.P., Erber, M., Vidoni, L., Knapp, C.L., Thomaß, B.D., Fauler, M., Nilsson, B. and Ekdahl, K.N. 2021. Interleukin 8 elicits rapid physiological changes in neutrophils that are altered by inflammatory conditions. *Journal of innate immunity* 13(4), pp. 225–241.

Bessen, H.A. 1986. Therapeutic and toxic effects of digitalis: William Withering, 1785. *Journal of Emergency Medicine* 4(3), pp. 243–248.

Beutler, B. 2002. LPS in microbial pathogenesis: promise and fulfilment. *Journal of Endotoxin Research* 8(5), pp. 329–335.

Bhadane, B.S., Patil, M.P., Maheshwari, V.L. and Patil, R.H., 2018. Ethnopharmacology, phytochemistry, and biotechnological advances of family Apocynaceae: A review. *Phytotherapy research*, 32(7), pp.1181-1210.

Bjarnsholt, T., Kirketerp-Møller, K., Jensen, P., Madsen, K., Phipps, R., Kroghfelt, K., Høiby, N. and Givskov, M., 2008. Why chronic wounds will not heal: a novel hypothesis. *Wound Repair and Regeneration*, 16(1), pp.2-10.

Blondeau, J.M. 2009. New concepts in antimicrobial susceptibility testing: the mutant prevention concentration and mutant selection window approach. *Veterinary dermatology* 20(5-6), pp. 383–396.

Bnyan, I., Hasan, H. and Ewadh, M. 2013. Antibacterial activity of *Citrullus colocynthis* against different types of bacteria. *Advances in Life Science and Technology* 7, pp. 48–51.

Boateng, J. and Catanzano, O. 2015. Advanced therapeutic dressings for effective wound healing—a review. *Journal of pharmaceutical sciences* 104(11), pp. 3653–3680.

Borges, A., José, H., Homem, V. and Simões, M. 2020. Comparison of Techniques and Solvents on the Antimicrobial and Antioxidant Potential of Extracts from *Acacia dealbata* and *Olea europaea*. *Antibiotics* 9(2), p. 48.

Borlinghaus, J., Albrecht, F., Gruhlke, M.C.H., Nwachukwu, I.D. and Slusarenko, A.J. 2014. Allicin: chemistry and biological properties. *Molecules* 19(8), pp. 12591–12618.

Boukamp, P. 1988. Normal Keratinization in a Spontaneously Immortalized. *Journal of Cell Biology* 106, pp. 761–771.

Bowler, P.G., Duerden, B.I. and Armstrong, D.G. 2001. Wound microbiology and associated approaches to wound management. *Clinical microbiology reviews* 14(2), pp. 244–269.

Braga, L.C., Shupp, J.W., Cummings, C., Jett, M., Takahashi, J.A., Carmo, L.S., Chartone-Souza, E. and Nascimento, A.M.A. 2005. Pomegranate extract inhibits *Staphylococcus aureus* growth and subsequent enterotoxin production. *Journal of Ethnopharmacology* 96(1–2), pp. 335–339.

Brancato, S.K. and Albina, J.E. 2011. Wound macrophages as key regulators of repair: origin, phenotype, and function. *The American journal of pathology* 178(1), pp. 19–25.

Brazil, J.C., Quiros, M., Nusrat, A. and Parkos, C.A. 2019. Innate immune cell–epithelial crosstalk during wound repair. *The Journal of clinical investigation* 129(8), pp. 2983–2993.

Breijyeh, Z., Jubeh, B. and Karaman, R. 2020. Resistance of gram-negative bacteria to current antibacterial agents and approaches to resolve it. *Molecules* 25(6), p. 1340.

Brem, H., Tomic-Canic, M., Tarnovskaya, A., Ehrlich, H.P., Baskin-Bey, E., Gill, K., Carasa, M., Weinberger, S., Entero, H. and Vladeck, B. 2001. Healing of elderly patients with diabetic foot ulcers, venous stasis ulcers, and pressure ulcers. *Surgical technology international* 11, pp. 161–167.

- Brown, N.M., Goodman, A.L., Horner, C., Jenkins, A. and Brown, E.M. 2021. Treatment of methicillin-resistant *Staphylococcus aureus* (MRSA): updated guidelines from the UK. *JAC-antimicrobial resistance* 3(1), p. dlaa114.
- Bukhari, N.A., Al-Otaibi, R.A. and Ibbrahim, M.M. 2017. Phytochemical and taxonomic evaluation of *Rhazya stricta* in Saudi Arabia. *Saudi Journal of Biological Sciences* 24(7), pp. 1513–1521.
- Caesar, L.K. and Cech, N.B. 2019. Synergy and antagonism in natural product extracts: when 1+ 1 does not equal 2. *Natural product reports* 36(6), pp. 869–888.
- Caley, M.P., Martins, V.L.C. and O'Toole, E.A. 2015. Metalloproteinases and wound healing. *Advances in wound care* 4(4), pp. 225–234.
- Cameron, M., Gagnier, J.J. and Chrubasik, S. 2011. Herbal therapy for treating rheumatoid arthritis. *Cochrane Database of Systematic Reviews* (2).
- Cañedo-Dorantes, L. and Cañedo-Ayala, M. 2019. Skin acute wound healing: a comprehensive review. *International journal of inflammation* 2019, pp. 1-15.
- Carson, C.F., Hammer, K.A. and Riley, T. V 2006. *Melaleuca alternifolia* (tea tree) oil: a review of antimicrobial and other medicinal properties. *Clinical microbiology reviews* 19(1), pp. 50–62.
- Castelo Branco Rangel de Almeida, C. de F., de Vasconcelos Cabral, D.L., Rangel de Almeida, C.C.B., Cavalcanti de Amorim, E.L., de Araújo, J.M. and de Albuquerque, U.P. 2012. Comparative study of the antimicrobial activity of native and exotic plants from the Caatinga and Atlantic Forest selected through an ethnobotanical survey. *Pharmaceutical Biology* 50(2), pp. 201–207.
- Cegelski, L., Marshall, G.R., Eldridge, G.R. and Hultgren, S.J. 2008. The biology and future prospects of antivirulence therapies. *Nature Reviews Microbiology* 6(1), pp. 17–27.
- Celik, T.A. 2012. Potential genotoxic and cytotoxic effects of plant extracts. *A compendium of essays on alternative therapy*, pp. 233–250.
- Celiksoy, V., Moses, R.L., Sloan, A.J., Moseley, R. and Heard, C.M. 2021. Synergistic in vitro antimicrobial activity of pomegranate rind extract and zinc (II) against *Micrococcus luteus* under planktonic and biofilm conditions. *Pharmaceutics* 13(6), p. 851.
- Chaib, F., Sahki, R., Sabaou, N., Rached, W. and Bennaceur, M. 2015. Phytochemical investigation and biological activities of some Saharan plants from Hoggar. *Journal of Agricultural Science* 7(7), p. 163.
- Chaieb, K., Kouidhi, B., Jrah, H., Mahdouani, K. and Bakhrouf, A. 2011. Antibacterial activity of Thymoquinone, an active principle of *Nigella sativa* and its potency to prevent bacterial biofilm formation. *BMC complementary and alternative medicine* 11(1), pp. 1–6.
- Chambers, E.S. and Vukmanovic-Stejic, M. 2020. Skin barrier immunity and ageing. *Immunology* 160(2), pp. 116–125.
- Chambers, H.F. and DeLeo, F.R. 2009. Waves of resistance: *Staphylococcus aureus* in the antibiotic era. *Nature Reviews Microbiology* 7(9), pp. 629–641.
- Chanda, W. et al. 2017. Combined effect of linolenic acid and tobramycin on *Pseudomonas aeruginosa* biofilm formation and quorum sensing. *Experimental and Therapeutic Medicine* 14(5), pp. 4328–4338.
- Chandrasekharan, N. V, Dai, H., Roos, K.L.T., Evanson, N.K., Tomsik, J., Elton, T.S. and Simmons, D.L. 2002. COX-3, a cyclooxygenase-1 variant inhibited by acetaminophen and other

analgesic/antipyretic drugs: cloning, structure, and expression. *Proceedings of the National Academy of Sciences* 99(21), pp. 13926–13931.

Chang, C.-S., Sun, H.-L., Lii, C.-K., Chen, H.-W., Chen, P.-Y. and Liu, K.-L. 2010. Gamma-linolenic acid inhibits inflammatory responses by regulating NF- κ B and AP-1 activation in lipopolysaccharide-induced RAW 264.7 macrophages. *Inflammation* 33(1), pp. 46–57.

Chattopadhyay, D., Chawla-Sarkar, M., Chatterjee, T., Dey, R.S., Bag, P., Chakraborti, S. and Khan, M.T.H., 2009. Recent advancements for the evaluation of anti-viral activities of natural products. *New Biotechnology*, 25(5), pp.347-368.

Chaturvedi, P., Singh, A.K., Shukla, S. and Agarwal, L. 2014. Prevalence of mupirocin resistant *Staphylococcus aureus* isolates among patients admitted to a tertiary care hospital. *North American journal of medical sciences* 6(8), p. 403.

Chawech, R., Jarraya, R., Girardi, C., Vansteelandt, M., Marti, G., Nasri, I., Racaud-Sultan, C. and Fabre, N. 2015. Cucurbitacins from the leaves of *Citrullus colocynthis* (L.) Schrad. *Molecules* 20(10), pp. 18001–18015.

Cheenpracha, S., Raksat, A., Ritthiwigrom, T. and Laphookhieo, S. 2014. Monoterpene indole alkaloids from the twigs of *Kopsia arborea*. *Natural Product Communications* 9(10), p. 1934578X1400901010.

Chen, S.X., Zhang, L.-J. and Gallo, R.L. 2019. Dermal white adipose tissue: a newly recognized layer of skin innate defense. *Journal of Investigative Dermatology* 139(5), pp. 1002–1009.

Chen, Y.E., Fischbach, M.A. and Belkaid, Y. 2018. Skin microbiota–host interactions. *Nature* 553(7689), pp. 427–436.

Cho, B.O., Che, D.N., Kim, J.-S., Kim, J.H., Shin, J.Y., Kang, H.J. and Jang, S. Il 2020. In vitro anti-inflammatory and anti-oxidative stress activities of kushenol C isolated from the roots of *Sophora flavescens*. *Molecules* 25(8), p. 1768.

Christenhusz, M.J.M. and Byng, J.W. 2016. The number of known plants species in the world and its annual increase. *Phytotaxa* 261(3), pp. 201–217.

Christian, A.G., Akanimo, E.G., Ahunna, A.G., Nwakaego, E.M. and Chimsorom, C.K. 2014. Antimalarial potency of the methanol leaf extract of *Maerua crassifolia* Forssk (Capparaceae). *Asian Pacific Journal of Tropical Disease* 4(1), pp. 35–39.

Christian, A.G., Uwaezuoke, N.J. and Nwadike, K.I. 2016. Analgesic, anti-inflammatory and antipyretic activities of methanolic leaf extract of *Maerua crassifolia* Journal of Coastal Life Medicine. *Journal of Coastal Life Medicine* 4(3), pp. 225–230.

Chung, H.Y., Lee, E.K., Choi, Y.J., Kim, J.M., Kim, D.H., Zou, Y., Kim, C.H., Lee, J., Kim, H.S. and Kim, N.D. 2011. Molecular inflammation as an underlying mechanism of the aging process and age-related diseases. *Journal of dental research* 90(7), pp. 830–840.

Ckilaka, K.C., Akuodor, G.C., Akpan, J.L., Ogiji, E.D., Eze, C.O. and Ezeokpo, B.C. 2015. Antibacterial and antioxidant activities of methanolic leaf extract of *Maerua crassifolia*. *Journal of Applied Pharmaceutical Science* 5(10), pp. 147–150.

Cochran, W.L., McFeters, G.A. and Stewart, P.S. 2000. Reduced susceptibility of thin *Pseudomonas aeruginosa* biofilms to hydrogen peroxide and monochloramine. *Journal of applied microbiology* 88(1), pp. 22–30.

Coffey, B.M. and Anderson, G.G. 2014. Biofilm formation in the 96-well microtiter plate. In: *Pseudomonas Methods and Protocols*. Springer, pp. 631–641.

- Colegate, S.M. and Molyneux, R.J. 2008. Bioactive Natural Products: Detection, Isolation, and Structural Determination. 2nd Edition, *CRC Press, Boca Raton*, xiii, pp 605.
- Collenette, S. 1998. A checklist of botanical species in Saudi Arabia. *International Asclepiad Society*, pp 80.
- Cos, P., Vlietinck, A.J., Berghe, D. Vanden and Maes, L. 2006. Anti-infective potential of natural products: How to develop a stronger in vitro ‘proof-of-concept’. *Journal of Ethnopharmacology* 106(3), pp. 290–302.
- Coșarcă, S.-L., Moacă, E.-A., Tanase, C., Muntean, D.L., Pavel, I.Z. and Dehelean, C.A. 2019. Spruce and beech bark aqueous extracts: Source of polyphenols, tannins and antioxidants correlated to in vitro antitumor potential on two different cell lines. *Wood Science and Technology* 53(2), pp. 313–333.
- Costerton, W., Veeh, R., Shirtliff, M., Pasmore, M., Post, C. and Ehrlich, G. 2003. The application of biofilm science to the study and control of chronic bacterial infections. *The Journal of clinical investigation* 112(10), pp. 1466–1477.
- Coulombe, P.A. 1997. Towards a molecular definition of keratinocyte activation after acute injury to stratified epithelia. *Biochemical and biophysical research communications* 236(2), pp. 231–238.
- Cracowski, J.-L. and Roustit, M. 2020. Human skin microcirculation. *Comprehensive Physiology* 10(3), pp. 1105–1154.
- Cragg, G.M. and Newman, D.J. 2013. Natural products: A continuing source of novel drug leads. *Biochimica et Biophysica Acta - General Subjects* 1830(6), pp. 3670–3695.
- Crone, S., Vives-Flórez, M., Kvich, L., Saunders, A.M., Malone, M., Nicolaisen, M.H., Martínez-García, E., Rojas-Acosta, C., Catalina Gomez-Puerto, M. and Calum, H. 2020. The environmental occurrence of *Pseudomonas aeruginosa*. *Apmis* 128(3), pp. 220–231.
- Dadgostar, P. 2019. Antimicrobial resistance: implications and costs. *Infection and Drug Resistance* 12, pp. 3903–3910.
- Dai, C., Shih, S. and Khachemoune, A. 2020. Skin substitutes for acute and chronic wound healing: an updated review. *Journal of Dermatological Treatment* 31(6), pp. 639–648.
- Das, J.R., Bhakoo, M., Jones, M. V and Gilbert, P. 1998. Changes in the biocide susceptibility of *Staphylococcus epidermidis* and *Escherichia coli* cells associated with rapid attachment to plastic surfaces. *Journal of applied microbiology* 84(5), pp. 852–858.
- Daur, I. 2012. Plant flora in the rangeland of western Saudi Arabia. *Pakistan Journal of Botany* 44, pp. 23–26.
- Davies, D. 2003. Understanding biofilm resistance to antibacterial agents. *Nature reviews Drug discovery* 2(2), pp. 114–122.
- Davies, D.G. and Marques, C.N.H. 2009. A fatty acid messenger is responsible for inducing dispersion in microbial biofilms. *Journal of bacteriology* 191(5), pp. 1393–1403.
- De Kievit, T.R., Parkins, M.D., Gillis, R.J., Srikumar, R., Ceri, H., Poole, K., Iglewski, B.H. and Storey, D.G. 2001. Multidrug efflux pumps: expression patterns and contribution to antibiotic resistance in *Pseudomonas aeruginosa* biofilms. *Antimicrobial agents and chemotherapy* 45(6), pp. 1761–1770.
- Deckers, J., Hammad, H. and Hoste, E. 2018. Langerhans cells: sensing the environment in health and disease. *Frontiers in immunology* 9, p. 93.

- Del Pozo, J.L. and Patel, R., 2007. The challenge of treating biofilm-associated bacterial infections. *Clinical Pharmacology & Therapeutics*, 82(2), pp.204-209.
- Delazar, A., Gibbons, S., Kosari, A.R., Nazemiyeh, H., Modarresi, M., Nahar, L. and Sarker, S.D. 2006. Flavone C-glycosides and cucurbitacin glycosides from *Citrullus colocynthis*. *DARU Journal of Pharmaceutical Sciences* 14(3), pp. 109–114.
- Demidova-Rice, T.N., Durham, J.T. and Herman, I.M. 2012. Wound healing angiogenesis: innovations and challenges in acute and chronic wound healing. *Advances in wound care* 1(1), pp. 17–22.
- Desbois, A.P. and Lawlor, K.C. 2013. Antibacterial activity of long-chain polyunsaturated fatty acids against *Propionibacterium acnes* and *Staphylococcus aureus*. *Marine Drugs* 11(11), pp. 4544–4557.
- Desbois, A.P. and Smith, V.J. 2010. Antibacterial free fatty acids: activities, mechanisms of action and biotechnological potential. *Applied microbiology and biotechnology* 85(6), pp. 1629–1642.
- Desmarchelier, C. 2010. Neotropics and natural ingredients for pharmaceuticals: why isn't South American biodiversity on the crest of the wave? *Phytotherapy Research* 24(6), pp. 791–799.
- Di Grazia, A., Luca, V., Segev-Zarko, L.A.T., Shai, Y. and Mangoni, M.L., 2014. Temporins A and B stimulate migration of HaCaT keratinocytes and kill intracellular *Staphylococcus aureus*. *Antimicrobial agents and chemotherapy*, 58(5), pp.2520-2527.
- Dias, D.A., Urban, S. and Roessner, U. 2012. A Historical overview of natural products in drug discovery. *Metabolites* 2(2), pp. 303–336.
- Dickinson, L.E. and Gerecht, S. 2016. Engineered biopolymeric scaffolds for chronic wound healing. *Frontiers in physiology* 7, p. 341.
- Dierick, N.A., Decuypere, J.A., Molly, K., Van Beek, E. and Vanderbeke, E. 2002. The combined use of triacylglycerols (TAGs) containing medium chain fatty acids (MCFAs) and exogenous lipolytic enzymes as an alternative to nutritional antibiotics in piglet nutrition: II. In vivo release of MCFAs in gastric cannulated and slaughtered piglets by endogenous and exogenous lipases; effects on the luminal gut flora and growth performance. *Livestock Production Science* 76(1–2), pp. 1–16.
- Dissemond, J., Augustin, M., Dietlein, M., Faust, U., Keuthage, W., Lobmann, R., Münter, K.-C., Strohal, R., Stücker, M. and Traber, J. 2020. Efficacy of MMP-inhibiting wound dressings in the treatment of chronic wounds: a systematic review. *Journal of Wound Care* 29(2), pp. 102–118.
- Dolan, S.K. 2020. Current knowledge and future directions in developing strategies to combat *Pseudomonas aeruginosa* infection. *Journal of molecular biology* 432(20), pp. 5509–5528.
- Dryden, M.S. 2010. Complicated skin and soft tissue infection. *Journal of antimicrobial chemotherapy* 65(suppl_3), pp. iii35–iii44.
- Dulmovits, B.M. and Herman, I.M. 2012. Microvascular remodeling and wound healing: a role for pericytes. *The international journal of biochemistry & cell biology* 44(11), pp. 1800–1812.
- Duscher, D., Maan, Z.N., Whittam, A.J., Sorkin, M., Hu, M.S., Walmsley, G.G., Baker, H., Fischer, L.H., Januszyk, M. and Wong, V.W. 2015. Fibroblast-specific deletion of hypoxia inducible factor-1 critically impairs murine cutaneous neovascularization and wound healing. *Plastic and reconstructive surgery* 136(5), p. 1004.
- Edwards, R. and Harding, K., 2004. Bacteria and wound healing. *Current Opinion in Infectious Diseases*, 17(2), pp.91-96.

- Efferth, T. and Koch, E. 2011. Complex interactions between phytochemicals. The multi-target therapeutic concept of phytotherapy. *Current drug targets* 12(1), pp. 122–132.
- Efthymiopoulos, I., Hellier, P., Ladommatos, N., Russo-Profilo, A., Eveleigh, A., Aliev, A., Kay, A. and Mills-Lamprey, B. 2018. Influence of solvent selection and extraction temperature on yield and composition of lipids extracted from spent coffee grounds. *Industrial Crops and Products* 119, pp. 49–56.
- Egbuniwe, I.U., Karagiannis, S.N., Nestle, F.O. and Lacy, K.E. 2015. Revisiting the role of B cells in skin immune surveillance. *Trends in immunology* 36(2), pp. 102–111.
- El-Amier, Y.A. and Al-hadithy, O.N. 2020. Phytochemical constituents, antioxidant and allelopathic activities of *Aizoon canariense* L. On *Zea mays* (L.) and associated weeds. *Plant Archives* 20(1), pp. 303–310.
- El-Amier, Y.A., Haroun, S.A., El-Shehaby, O.A. and Al-hadithy, O.N. 2016. Antioxidant and antimicrobial properties of some wild Aizoaceae species growing in Egyptian desert. *Journal of Environmental Sciences* 45, pp. 1–10.
- El-Ashram, S., El-Samad, L.M., Basha, A.A. and El Wakil, A. 2021. Naturally-derived targeted therapy for wound healing: Beyond classical strategies. *Pharmacological Research* 170, p. 105749.
- Elias, S.T., Borges, G.A., Amorim, D.A., Rêgo, D.F., Simeoni, L.A., Silveira, D., Fonseca-Bazzo, Y.M., Paula, J.E., Fagg, C.W. and Barros, I. 2015. Radiation induced a supra-additive cytotoxic effect in head and neck carcinoma cell lines when combined with plant extracts from Brazilian Cerrado biome. *Clinical oral investigations* 19(3), pp. 637–646.
- Elkady, A.I., Hussein, R.A. and El-Assouli, S.M. 2016. Harmal Extract Induces Apoptosis of HCT116 Human Colon Cancer Cells, Mediated by Inhibition of Nuclear Factor- κ B and Activator Protein-1 Signaling Pathways and Induction of Cytoprotective Genes. *Asian Pacific Journal of Cancer Prevention* 17(4), pp. 1947–1959.
- Elkhalfi, B., Essari, A., Serrano Delgado, A. and Soukri, A. 2013. Antibacterial activity of plant methanolic extracts on a field isolate of *Pseudomonas syringae* pv tomato from the Casablanca region (Morocco). *Advances in Bioscience and Biotechnology*, 4, 1-9.
- Eloff, J.N., Katerere, D.R. and McGaw, L.J. 2008. The biological activity and chemistry of the southern African Combretaceae. *Journal of Ethnopharmacology* 119(3), pp. 686–699.
- Elyashberg, M. 2015. Identification and structure elucidation by NMR spectroscopy. *TrAC Trends in Analytical Chemistry* 69, pp. 88–97.
- Enke, C.G. and Nagels, L.J. 2011. Undetected components in natural mixtures: how many? What concentrations? Do they account for chemical noise? What is needed to detect them? *Analytical chemistry* 83(7), pp. 2539–2546.
- Enoch, S. and Leaper, D., 2008. Basic science of wound healing. *Surgery (Oxford)*, 26(2), pp.31-37.
- Esposito, S. et al. 2017. Diagnosis and management of skin and soft-tissue infections (SSTI). A literature review and consensus statement: an update. *Journal of Chemotherapy* 29(4), pp. 197–214.
- Esposito, S., Bassetti, M., Borre, S., Bouza, E., Dryden, M., Fantoni, M., Gould, I.M., Leoncini, F., Leone, S. and Milkovich, G. 2011. Diagnosis and management of skin and soft-tissue infections (SSTI): a literature review and consensus statement on behalf of the Italian Society of Infectious Diseases and International Society of Chemotherapy. *Journal of Chemotherapy* 23(5), pp. 251–262.
- Esposito, S., Leone, S., Petta, E., Noviello, S. and Iori, I. 2009. Skin and soft tissue infections: classification and epidemiology. *Le Infezioni in Medicina* 17, pp. 6–17.

- Ettenson, D.S. and Gotlieb, A.I. 1994. Endothelial wounds with disruption in cell migration repair primarily by cell proliferation. *Microvascular research* 48(3), pp. 328–337.
- Evans, J.L., Goldfine, I.D., Maddux, B.A. and Grodsky, G.M. 2002. Oxidative stress and stress-activated signaling pathways: a unifying hypothesis of type 2 diabetes. *Endocrine reviews* 23(5), pp. 599–622.
- Ezzat, S.M., Abdel-Sattar, E., Harraz, F.M. and Ghareib, S.A. 2014. Antihyperglycemic and antihyperlipidemic effects of the methanol extracts of *Cleome ramosissima* Parl., *Barleria bispinosa* (Forssk.) Vahl. and *Tribulus macropterus* Boiss. *Bulletin of Faculty of Pharmacy, Cairo University* 52(1), pp. 1–7.
- Fan, Y.-Y. and Chapkin, R.S. 1998. Importance of Dietary γ -Linolenic Acid in Human Health and Nutrition. *The Journal of Nutrition* 128(9), pp. 1411–1414.
- Felgueiras, H.P. 2021. An insight into biomolecules for the treatment of skin infectious diseases. *Pharmaceutics* 13(7), p. 1012.
- Ferreira-Machado, S.C., Rodrigues, M.P., Nunes, A.P.M., Dantas, F.J.S., De Mattos, J.C.P., Silva, C.R., Moura, E.G., Bezerra, R. and Caldeira-de-Araujo, A. 2004. Genotoxic potentiality of aqueous extract prepared from *Chrysobalanus icaco* L. leaves. *Toxicology Letters* 151(3), pp. 481–487.
- Ferry, T. and Etienne, J. 2007. Community acquired MRSA in Europe. *BMJ* 335(7627), pp. 947–948.
- Fisher, T.K., Wolcott, R., Wolk, D.M., Bharara, M., Kimbriel, H.R. and Armstrong, D.G. 2010. Diabetic foot infections: a need for innovative assessments. *The international journal of lower extremity wounds* 9(1), pp. 31–36.
- Fitz-Gibbon, S., Tomida, S., Chiu, B.-H., Nguyen, L., Du, C., Liu, M., Elashoff, D., Erfe, M.C., Loncaric, A. and Kim, J. 2013. Propionibacterium acnes strain populations in the human skin microbiome associated with acne. *Journal of investigative dermatology* 133(9), pp. 2152–2160.
- Fjell, C.D., Hiss, J.A., Hancock, R.E.W. and Schneider, G. 2012. Designing antimicrobial peptides: form follows function. *Nature reviews Drug discovery* 11(1), pp. 37–51.
- Flattery-O'Brien, J.A. and Dawes, I.W. 1998. Hydrogen Peroxide Causes RAD9 -dependent Cell Cycle Arrest in G_2 in *Saccharomyces cerevisiae* whereas Menadione Causes G_1 Arrest Independent of RAD9 Function. *Journal of Biological Chemistry* 273(15), pp. 8564–8571.
- Fleming, A. 1929. On the antibacterial action of cultures of a penicillium, with special reference to their use in the isolation of *B. influenzae*. *International Journal of Experimental Pathology*, 10, 226-236.
- Florey, Me., Adelaide, M.B. and Florey, H.W. 1943. General and local administration of penicillin. *The Lancet* 241(6239), pp. 387–397.
- Fonder, M., Mamelak, A., Lazarus, G. and Chanmugam, A., 2007. Occlusive Wound Dressings in Emergency Medicine and Acute Care. *Emergency Medicine Clinics of North America*, 25(1), pp.235-242.
- Foolad, N., Brezinski, E.A., Chase, E.P. and Armstrong, A.W. 2013. Effect of Nutrient Supplementation on Atopic Dermatitis in Children: A Systematic Review of Probiotics, Prebiotics, Formula, and Fatty Acids. *JAMA Dermatology* 149(3), pp. 350–355.
- Fouché, M., Willers, C., Hamman, S., Malherbe, C. and Steenekamp, J., 2020. Wound healing effects of Aloe muth-muth: In vitro investigations using immortalized human keratinocytes (HaCaT). *Biology*, 9(11), p.350.

- Founou, R.C., Founou, L.L. and Essack, S.Y. 2017. Clinical and economic impact of antibiotic resistance in developing countries: a systematic review and meta-analysis. *PloS one* 12(12), p. e0189621.
- Frank, S., Kampfer, H., Podda, M., Kaufmann, R. and Pfeilschifter, J. 2000. Identification of copper/zinc superoxide dismutase as a nitric oxide-regulated gene in human (HaCaT) keratinocytes: implications for keratinocyte proliferation. *Biochemical Journal* 346(3), p. 719.
- Frazer, B.W., Lynn, J., Charlebois, E.D., Lambert, L., Lowery, D. and Perdreau-Remington, F. 2005. High prevalence of methicillin-resistant *Staphylococcus aureus* in emergency department skin and soft tissue infections. *Annals of emergency medicine* 45(3), pp. 311–320.
- Fredricks, D.N. 2001. Microbial ecology of human skin in health and disease. In: *Journal of Investigative Dermatology Symposium Proceedings*. Elsevier, pp. 167–169.
- Freije, A., Alkhuzai, J. and Al-Laith, A.A. 2013. Fatty acid composition of three medicinal plants from Bahrain: New potential sources of γ -linolenic acid and dihomo- γ -linolenic. *Industrial Crops and Products* 43, pp. 218–224.
- Freire-Moran, L., Aronsson, B., Manz, C., Gyssens, I.C., So, A.D., Monnet, D.L., Cars, O. and group, E.-E. working 2011. Critical shortage of new antibiotics in development against multidrug-resistant bacteria—Time to react is now. *Drug resistance updates* 14(2), pp. 118–124.
- Frykberg, R.G. and Banks, J. 2015. Challenges in the Treatment of Chronic Wounds. *Advances in Wound Care* 4(9), pp. 560–582.
- Furse, R.K., Rossetti, R.G., Seiler, C.M. and Zurier, R.B. 2002. Oral administration of gamma-linolenic acid, an unsaturated fatty acid with anti-inflammatory properties, modulates interleukin-1 β production by human monocytes. *Journal of clinical immunology* 22(2), pp. 83–91.
- Futagami, A., Ishizaki, M., Fukuda, Y., Kawana, S. and Yamanaka, N. 2002. Wound healing involves induction of cyclooxygenase-2 expression in rat skin. *Laboratory investigation* 82(11), pp. 1503–1513.
- Futosi, K., Fodor, S. and Mócsai, A. 2013. Reprint of Neutrophil cell surface receptors and their intracellular signal transduction pathways. *International immunopharmacology* 17(4), pp. 1185–1197.
- Galli, S.J., Borregaard, N. and Wynn, T.A. 2011. Phenotypic and functional plasticity of cells of innate immunity: macrophages, mast cells and neutrophils. *Nature immunology* 12(11), pp. 1035–1044.
- Gamal, E.E.G., Khalifa, S.A.K., Gameel, A.S. and Emad, M.A. 2010. Traditional medicinal plants indigenous to Al-Rass province, Saudi Arabia. *Journal of Medicinal Plants Research* 4(24), pp. 2680–2683.
- Ganesh, K., Sinha, M., Mathew-Steiner, S.S., Das, A., Roy, S. and Sen, C.K., 2015. Chronic wound biofilm model. *Advances in wound care*, 4(7), pp.382-388.
- Gardner, S.E., Hillis, S.L., Heilmann, K., Segre, J.A. and Grice, E.A. 2013. The neuropathic diabetic foot ulcer microbiome is associated with clinical factors. *Diabetes* 62(3), pp. 923–930.
- Garlanda, C., Dinarello, C.A. and Mantovani, A. 2013. The interleukin-1 family: back to the future. *Immunity* 39(6), pp. 1003–1018.
- Garraud, O., Hozzein, W.N. and Badr, G. 2017. Wound healing: time to look for intelligent, ‘natural’ immunological approaches? *BMC immunology* 18(1), pp. 1–8.
- Giamarellos-Bourboulis, E.J., Grecka, P., Dionyssiou-Asteriou, A. and Giamarellou, H. 1995. In-vitro inhibitory activity of gamma-linolenic acid on *Escherichia coli* strains and its influence on their susceptibilities to various antimicrobial agents. *Journal of Antimicrobial Chemotherapy* 36(2), pp. 327–334.

- Gilani, S.A., Kikuchi, A., Shinwari, Z.K., Khattak, Z.I. and Watanabe, K.N. 2007. Phytochemical, pharmacological and ethnobotanical studies of *Rhazya stricta* Decne. *Phytotherapy Research: An International Journal Devoted to Pharmacological and Toxicological Evaluation of Natural Product Derivatives* 21(4), pp. 301–307.
- Gilbert, B. and Alves, L. 2003. Synergy in plant medicines. *Current medicinal chemistry* 10(1), pp. 13–20.
- Gill, S.E. and Parks, W.C. 2008. Metalloproteinases and their inhibitors: regulators of wound healing. *The international journal of biochemistry & cell biology* 40(6–7), pp. 1334–1347.
- Gilmore, T.D. and Herscovitch, M. 2006. Inhibitors of NF- κ B signaling: 785 and counting. *Oncogene* 25(51), pp. 6887–6899.
- Gniadecki, R. 1998. Regulation of keratinocyte proliferation. *General Pharmacology: The Vascular System* 30(5), pp. 619–622.
- Godowski, K.C. 1989. Antimicrobial action of sanguinarine. *The Journal of clinical dentistry* 1(4), pp. 96–101.
- Gokhale, N. 2008. Medical management approach to infectious keratitis. *Indian Journal of Ophthalmology*, 56(3), p.215.
- Goldberg, S.R. and Diegelmann, R.F. 2020. What makes wounds chronic. *Surgical Clinics* 100(4), pp. 681–693.
- Goodall, R.R. and Levi, A.A. 1946. A microchromatographic method for the detection and approximate determination of the different penicillins in a mixture. *Nature* 158(4019), pp. 675–676.
- Gordon, R.J. and Lowy, F.D. 2008. Pathogenesis of methicillin-resistant *Staphylococcus aureus* infection. *Clinical infectious diseases* 46(Supplement_5), pp. S350–S359.
- Gorlenko, C.L., Kiselev, H.Y., Budanova, E. V, Zamyatnin Jr, A.A. and Ikryannikova, L.N. 2020. Plant secondary metabolites in the battle of drugs and drug-resistant bacteria: new heroes or worse clones of antibiotics? *Antibiotics* 9(4), p. 170.
- Greaves, N.S., Ashcroft, K.J., Baguneid, M. and Bayat, A. 2013. Current understanding of molecular and cellular mechanisms in fibroplasia and angiogenesis during acute wound healing. *Journal of dermatological science* 72(3), pp. 206–217.
- Green, J., Jester, R., McKinley, R. and Pooler, A. 2014. The impact of chronic venous leg ulcers: a systematic review. *Journal of wound care* 23(12), pp. 601–612.
- Grice, E.A. and Segre, J.A. 2011. The skin microbiome. *Nature reviews microbiology* 9(4), pp. 244–253.
- Grice, E.A. and Segre, J.A. 2012. Interaction of the microbiome with the innate immune response in chronic wounds. *Current topics in innate immunity* II, pp. 55–68.
- Grice, E.A., Snitkin, E.S., Yockey, L.J., Bermudez, D.M., Program, N.C.S., Liechty, K.W., Segre, J.A., Mullikin, J., Blakesley, R. and Young, A. 2010. Longitudinal shift in diabetic wound microbiota correlates with prolonged skin defense response. *Proceedings of the National Academy of Sciences* 107(33), pp. 14799–14804.

Grinnell, F. and Petroll, W.M. 2010. Cell motility and mechanics in three-dimensional collagen matrices. *Annual review of cell and developmental biology* 26, pp. 335–361.

Grove, G.L. and Kligman, A.M. 1983. Age-associated changes in human epidermal cell renewal. *Journal of Gerontology* 38(2), pp. 137–142.

Guil-Guerrero, J.L., García Maroto, F.F. and Giménez Giménez, A. 2001. Fatty acid profiles from forty-nine plant species that are potential new sources of γ -linolenic acid. *JAOCS, Journal of the American Oil Chemists' Society* 78(7), pp. 677–684.

Guil-Guerrero, J.L., Giménez-Giménez, A., Robles-Medina, A., del Mar Reboloso-Fuentes, M., Belarbi, E., Esteban-Cerdán, L. and Molina-Grima, E. 2001. Hexane reduces peroxidation of fatty acids during storage. *European journal of lipid science and technology* 103(5), pp. 271–278.

Guo, S. and DiPietro, L.A. 2010. Critical review in oral biology & medicine: Factors affecting wound healing. *Journal of Dental Research* 89(3), pp. 219–229.

Gupta, N. and Jain, U. 2010. Prominent wound healing properties of indigenous medicines. *Journal of Natural Pharmaceuticals* 1(1), p. 2.

Gurib-Fakim, A. 2006. Medicinal plants: traditions of yesterday and drugs of tomorrow. *Molecular aspects of Medicine* 27(1), pp. 1–93.

Gwynn, M.N., Portnoy, A., Rittenhouse, S.F. and Payne, D.J. 2010. Challenges of antibacterial discovery revisited. *Annals of the New York Academy of Sciences* 1213(1), pp. 5–19.

Hakemi-Vala, M., Makhmor, M., Kobarfar, F., Kamalinejad, M., Heidary, M. and Khoshnood, S., 2014. Investigation of antimicrobial effect of *Tribulus terrestris* L. against some gram positive and negative bacteria and candida spp. *Novelty Biomed*, 2(3), pp.85-90.

Hameed, B., Ali, Q., Hafeez, M.M. and Malik, A. 2020. Antibacterial and antifungal activity of fruit, seed and root extracts of *Citrullus colocynthis* plant. *Biological and Clinical Sciences Research Journal* 2020(1), pp 1-6.

Hamilton, G.R. and Baskett, T.F. 2000. In the arms of Morpheus: the development of morphine for postoperative pain relief. *Canadian Journal Of Anesthesia* 47: 4, pp. 367–374.

Harding, K.G., Morris, H.L. and Patel, G.K. 2002. Clinical review Healing chronic wounds. *British medical journal* 324, pp. 160–163.

Härle-Bachor, C. and Boukamp, P. 1996. Telomerase activity in the regenerative basal layer of the epidermis in human skin and in immortal and carcinoma-derived skin keratinocytes. *Proceedings of the National Academy of Sciences of the United States of America* 93(13), pp. 6476–6481.

Harmand, P.-O., Duval, R., Liagre, B., Jayat-Vignoles, C., Beneytout, J.-L., Delage, C. and Simon, A. 2003. Ursolic acid induces apoptosis through caspase-3 activation and cell cycle arrest in HaCat cells. *International Journal of Oncology* 23(1), pp. 105–112.

Harvey, A.L., Edrada-Ebel, R. and Quinn, R.J. 2015. The re-emergence of natural products for drug discovery in the genomics era. *Nature reviews drug discovery* 14(2), pp. 111–129.

Hassan-Abdallah, A., Merito, A., Hassan, S., Aboubaker, D., Djama, M., Asfaw, Z. and Kelbessa, E. 2013. Medicinal plants and their uses by the people in the Region of Randa, Djibouti. *Journal of Ethnopharmacology* 148(2), pp. 701–713.

Hassan, H.M.A. 2015. A Short History of the Use of Plants as Medicines from Ancient Times. *CHIMIA International Journal for Chemistry* 69(10), pp. 622–623.

- Hayeri, M.R., Ziai, P., Shehata, M.L., Teytelboym, O.M. and Huang, B.K. 2016. Soft-tissue infections and their imaging mimics: from cellulitis to necrotizing fasciitis. *Radiographics* 36(6), pp. 1888–1910.
- Heard, C.M. 2020. An ex vivo skin model to probe modulation of local cutaneous arachidonic acid inflammation pathway. *Journal of Biological Methods* 7(4), p. e138.
- Henderson, C. and Goldbach-Mansky, R. 2010. Monogenic IL-1 mediated autoinflammatory and immunodeficiency syndromes: finding the right balance in response to danger signals. *Clinical immunology* 135(2), pp. 210–222.
- Hengzhuang, W., Wu, H., Ciofu, O., Song, Z. and Høiby, N. 2012. In vivo pharmacokinetics/pharmacodynamics of colistin and imipenem in *Pseudomonas aeruginosa* biofilm infection. *Antimicrobial agents and chemotherapy* 56(5), pp. 2683–2690.
- Hesketh, M., Sahin, K.B., West, Z.E. and Murray, R.Z. 2017. Macrophage phenotypes regulate scar formation and chronic wound healing. *International journal of molecular sciences* 18(7), p. 1545.
- Heydorn, A., Nielsen, A.T., Hentzer, M., Sternberg, C., Givskov, M., Ersbøll, B.K. and Molin, S. 2000. Quantification of biofilm structures by the novel computer program COMSTAT. *Microbiology* 146(10), pp. 2395–2407.
- Hoffman, P.S. 2020. Antibacterial discovery: 21st century challenges. *Antibiotics* 9(5), pp 213.
- Høiby, N., Bjarnsholt, T., Moser, C., Bassi, G.L., Coenye, T., Donelli, G., Hall-Stoodley, L., Holá, V., Imbert, C., Kirketerp-Møller, K. and Lebeaux, D., 2015. ESCMID guideline for the diagnosis and treatment of biofilm infections 2014. *Clinical microbiology and infection*, 21, pp.S1-S25.
- Hong, C.H., Hur, S.K., Oh, O.-J., Kim, S.S., Nam, K.A. and Lee, S.K. 2002. Evaluation of natural products on inhibition of inducible cyclooxygenase (COX-2) and nitric oxide synthase (iNOS) in cultured mouse macrophage cells. *Journal of Ethnopharmacology* 83(1–2), pp. 153–159.
- Hopkins, A.L. 2008. Network pharmacology: the next paradigm in drug discovery. *Nature chemical biology* 4(11), pp. 682–690.
- Hostettmann, K., Marston, A. and Hostettmann, M. 1998. Sample preparation and purification. In: *Preparative Chromatography Techniques*. Springer, pp. 3–14.
- Houston, D.M.J., Bugert, J.J., Denyer, S.P. and Heard, C.M. 2017. Potentiated virucidal activity of pomegranate rind extract (PRE) and punicalagin against Herpes simplex virus (HSV) when co-administered with zinc (II) ions, and antiviral activity of PRE against HSV and aciclovir-resistant HSV. *PloS one* 12(6), p. e0179291.
- Howes, M.R., Quave, C.L., Collemare, J., Tatsis, E.C., Twilley, D., Lulekal, E., Farlow, A., Li, L., Cazar, M. and Leaman, D.J. 2020. Molecules from nature: Reconciling biodiversity conservation and global healthcare imperatives for sustainable use of medicinal plants and fungi. *Plants, People, Planet* 2(5), pp. 463–481.
- Hu, Y., Liang, D., Li, X., Liu, H.-H., Zhang, X., Zheng, M., Dill, D., Shi, X., Qiao, Y. and Yeomans, D. 2010. The role of interleukin-1 in wound biology. Part II: In vivo and human translational studies. *Anesthesia & Analgesia* 111(6), pp. 1534–1542.
- Huang, Y.-Z., Gou, M., Da, L.-C., Zhang, W.-Q. and Xie, H.-Q. 2020. Mesenchymal stem cells for chronic wound healing: current status of preclinical and clinical studies. *Tissue Engineering Part B: Reviews* 26(6), pp. 555–570.
- Huseini, H., Darvishzadeh, F., Heshmat, R., Jafariazar, Z., Raza, M. and Larijani, B. 2009. The clinical investigation of *Citrullus colocynthis*(L.) schrad fruit in treatment of Type II diabetic patients: a randomized, double blind, placebo-controlled clinical trial. *Phytotherapy Research*, 23(8), pp.1186-1189.

- Hussain, A.I., Rathore, H.A., Sattar, M.Z.A., Chatha, S.A.S., Sarker, S.D. and Gilani, A.H. 2014. *Citrullus colocynthis* (L.) Schrad (bitter apple fruit): A review of its phytochemistry, pharmacology, traditional uses and nutritional potential. *Journal of Ethnopharmacology* 155(1), pp. 54–66.
- Hussain, A.I., Rathore, H.A., Sattar, M.Z.A., Chatha, S.A.S., ud din Ahmad, F., Ahmad, A. and Johns, E.J. 2013. Phenolic profile and antioxidant activity of various extracts from *Citrullus colocynthis* (L.) from the Pakistani flora. *Industrial crops and products* 45, pp. 416–422.
- Hussin, A.H. 2001. Adverse effects of herbs and drug-herbal interactions. *Malaysian Journal of Pharmacy* 1(2), pp. 39–44.
- Idm'Hand, E., Msanda, F. and Cherifi, K. 2020. Ethnobotanical study and biodiversity of medicinal plants used in the Tarfaya Province, Morocco. *Acta Ecologica Sinica* 40(2), pp. 134–144.
- Inoue, T., Shingaki, R. and Fukui, K. 2008. Inhibition of swarming motility of *Pseudomonas aeruginosa* by branched-chain fatty acids. *FEMS Microbiology Letters* 281(1), pp. 81–86.
- Iqbal, S., Bhangar, M.I., Akhtar, M., Anwar, F., Ahmed, K.R. and Anwer, T. 2006. Antioxidant properties of methanolic extracts from leaves of *Rhazya stricta*. *Journal of medicinal food* 9(2), pp. 270–275.
- James, G.A., Swogger, E., Wolcott, R., Pulcini, E. deLancey, Secor, P., Sestrich, J., Costerton, J.W. and Stewart, P.S. 2008. Biofilms in chronic wounds. *Wound Repair and regeneration* 16(1), pp. 37–44.
- James, W.D., Elston, D. and Berger, T. 2011. Andrew's diseases of the skin E-book: clinical dermatology. *Elsevier Health Sciences*.
- Järbrink, K., Ni, G., Sönnergren, H., Schmidtchen, A., Pang, C., Bajpai, R. and Car, J. 2016. Prevalence and incidence of chronic wounds and related complications: a protocol for a systematic review. *Systematic reviews* 5(1), pp. 1–6.
- Jiang, T., Ghosh, R. and Charcosset, C. 2021. Extraction, purification and applications of curcumin from plant materials-A comprehensive review. *Trends in Food Science & Technology* 112, pp. 419–430.
- Jiang, Y., Tsoi, L.C., Billi, A.C., Ward, N.L., Harms, P.W., Zeng, C., Maverakis, E., Kahlenberg, J.M. and Gudjonsson, J.E. 2020. Cytokinocytes: the diverse contribution of keratinocytes to immune responses in skin. *JCI insight* 5(20).
- Joa-Sub Oh, S.H.B., Ahn, E.-K., Jeong, W. and Hong, S.S. 2012. Anti-inflammatory activity of *Tribulus terrestris* in RAW264. 7 Cells (54.2). *Journal of Immunology* 188(1), pp. 52–54.
- Jones, K.H., Senft, J.A. 1985. An improved method to determine cell viability by simultaneous staining with fluorescein diacetate-propidium iodide. *Journal of Histochemistry and Cytochemistry* 33(1), pp. 77–79.
- Jongbloed, M., Feulner, G., Böer, B. and Western, A.R. 2003. The Comprehensive Guide to the Wild Flowers of the United Arab Emirates. Abu Dhabi, UAE: *Environmental Research and Wildlife Development Agency*.
- Jorge, M.P., Madjarof, C., Ruiz, A.L.T.G., Fernandes, A.T., Rodrigues, R.A.F., de Oliveira Sousa, I.M., Foglio, M.A. and de Carvalho, J.E. 2008. Evaluation of wound healing properties of *Arrabidaea chica* Verlot extract. *Journal of Ethnopharmacology* 118(3), pp. 361–366.

- Joshi, N., Pohlmeier, L., Ben-Yehuda Greenwald, M., Haertel, E., Hiebert, P., Kopf, M. and Werner, S. 2020. Comprehensive characterization of myeloid cells during wound healing in healthy and healing-impaired diabetic mice. *European journal of immunology* 50(9), pp. 1335–1349.
- Junio, H.A., Sy-Cordero, A.A., Etefagh, K.A., Burns, J.T., Micko, K.T., Graf, T.N., Richter, S.J., Cannon, R.E., Oberlies, N.H. and Cech, N.B. 2011. Synergy-directed fractionation of botanical medicines: a case study with goldenseal (*Hydrastis canadensis*). *Journal of natural products* 74(7), pp. 1621–1629.
- Kachur, K. and Suntres, Z. 2020. The antibacterial properties of phenolic isomers, carvacrol and thymol. *Critical Reviews in Food Science and Nutrition* 60(18), pp. 3042–3053.
- Kaltalioglu, K. and Coskun-Cevher, S. 2015. A bioactive molecule in a complex wound healing process: platelet-derived growth factor. *International journal of dermatology* 54(8), pp. 972–977.
- Kanitakis, J. 2002. Anatomy, histology and immunohistochemistry of normal human skin. *European Journal of Dermatology* 12(4), pp. 390–400.
- Kanji, S. and Das, H. 2017. Advances of stem cell therapeutics in cutaneous wound healing and regeneration. *Mediators of inflammation* 2017, pp. 1-14.
- Karakaya, S., El, S.N., Karagözlü, N. and Şahin, S. 2011. Antioxidant and antimicrobial activities of essential oils obtained from oregano (*Origanum vulgare* ssp. *hirtum*) by using different extraction methods. *Journal of medicinal food* 14(6), pp. 645–652.
- Karbasizade, V., Dehghan, P., Sichani, M.M., Shahanipoor, K., Sepahvand, S., Jafari, R. and Yousefian, R. 2017. Evaluation of three plant extracts against biofilm formation and expression of quorum sensing regulated virulence factors in *Pseudomonas aeruginosa*. *Pakistan Journal of pharmaceutical sciences* 30, pp. 585-589.
- Karimi, K., Odhav, A., Kollipara, R., Fike, J., Stanford, C. and Hall, J.C. 2017. Acute cutaneous necrosis: a guide to early diagnosis and treatment. *Journal of cutaneous medicine and surgery* 21(5), pp. 425–437.
- Kaye, K.S., Petty, L.A., Shorr, A.F. and Zilberberg, M.D. 2019. Current epidemiology, etiology, and burden of acute skin infections in the United States. *Clinical Infectious Diseases* 68(Suppl 3), pp. S193–S199.
- Kellogg, J.J., Todd, D.A., Egan, J.M., Raja, H.A., Oberlies, N.H., Kvalheim, O.M. and Cech, N.B. 2016. Biochemometrics for Natural Products Research: Comparison of Data Analysis Approaches and Application to Identification of Bioactive Compounds. *Journal of Natural Products* 79(2), pp. 376–386.
- Kenny, J.G., Ward, D., Josefsson, E., Jonsson, I.-M., Hinds, J., Rees, H.H., Lindsay, J.A., Tarkowski, A. and Horsburgh, M.J. 2009. The *Staphylococcus aureus* response to unsaturated long chain free fatty acids: survival mechanisms and virulence implications. *PLoS One* 4(2), p. e4344.
- Khaksari, M., Rezvani, M.E., SOLEYMANI, A. and SAJADI, M.A. 2000. The effect of topically applied water extract of *Rhazya stricta* on cutaneous wound healing in rats. *Semnan University of Medical Sciences* (1), pp. 1–10.
- Khalid, A., Algarni, A.S., Homeida, H.E., Sultana, S., Javed, S.A., Abdalla, H., Alhazmi, H.A., Albratty, M. and Abdalla, A.N. 2022. Phytochemical, Cytotoxic, and Antimicrobial Evaluation of *Tribulus terrestris* L., *Typha domingensis* Pers., and *Ricinus communis* L.: Scientific Evidences for Folkloric Uses. *Evidence-Based Complementary and Alternative Medicine* 2022, pp. 1-11.

- Khalifa, S.A.M., Shedid, E.S., Saied, E.M., Jassbi, A.R., Jamebozorgi, F.H., Rateb, M.E., Du, M., Abdel-Daim, M.M., Kai, G.-Y. and Al-Hammady, M.A.M. 2021. Cyanobacteria—From the oceans to the potential biotechnological and biomedical applications. *Marine Drugs* 19(5), p. 241.
- Khan, H. 2014. Medicinal Plants in Light of History: Recognized Therapeutic Modality. *Journal of Evidence-Based Complementary and Alternative Medicine* 19(3), pp. 216–219.
- Khan, R., Baeshen, M.N., Saini, K.S., Bora, R.S., Al-Hejin, A.M. and Baeshen, N.A. 2016. Antibacterial activities of *Rhazya stricta* leaf extracts against multidrug-resistant human pathogens. *Biotechnology & Biotechnological Equipment* 30(5), pp. 1016–1025.
- Khan, R., Baeshen, M.N., Saini, K.S., Bora, R.S., Al-Hejin, A.M., El-Hamidy, S.M. and Baeshen, N.A. 2016. Antibacterial activity of *Rhazya stricta* non-alkaloid extract against methicillin-resistant *Staphylococcus aureus*. *Biological Systems Open Access* 5(157), p. 2.
- Khan, S. and Khan, G.M. 2007. In vitro antifungal activity of *Rhazya stricta*. *Pakistan Journal of Pharmaceutical Sciences* 20(4), pp. 279–284.
- Khanna, S., Biswas, S., Shang, Y., Collard, E., Azad, A., Kauh, C., Bhasker, V., Gordillo, G.M., Sen, C.K. and Roy, S., 2010. Macrophage dysfunction impairs resolution of inflammation in the wounds of diabetic mice. *PloS one*, 5(3), p.e9539.
- Ki, V. and Rotstein, C. 2008. Bacterial skin and soft tissue infections in adults: a review of their epidemiology, pathogenesis, diagnosis, treatment and site of care. *Canadian Journal of Infectious Diseases and Medical Microbiology* 19(2), pp. 173–184.
- Kim, B.E., Howell, M.D., Guttman, E., Gilleaudeau, P.M., Cardinale, I.R., Boguniewicz, M., Krueger, J.G. and Leung, D.Y.M. 2011. TNF- α downregulates filaggrin and loricerin through c-Jun N-terminal kinase: role for TNF- α antagonists to improve skin barrier. *Journal of Investigative Dermatology* 131(6), pp. 1272–1279.
- Kim, H.K. 2016. *Adenophora remotiflora* protects human skin keratinocytes against UVB-induced photo-damage by regulating antioxidative activity and MMP-1 expression. *Nutrition Research and Practice* 10(4), pp. 371–376.
- Kim, M.-J., Hyun, J.-N., Kim, J.-A., Park, J.-C., Kim, M.-Y., Kim, J.-G., Lee, S.-J., Chun, S.-C. and Chung, I.-M. 2007. Relationship between phenolic compounds, anthocyanins content and antioxidant activity in colored barley germplasm. *Journal of Agricultural and Food Chemistry* 55(12), pp. 4802–4809.
- Kim, S.-Y., Hong, M., Kim, T.-H., Lee, K.Y., Park, S.J., Hong, S.H., Sowndhararajan, K. and Kim, S. 2021. Anti-Inflammatory Effect of Liverwort (*Marchantia polymorpha* L.) and *Racomitrium* Moss (*Racomitrium canescens* (Hedw.) Brid.) Growing in Korea. *Plants* 10(10), p. 2075.
- King, T., Dykes, G. and Kristianti, R. 2008. Comparative evaluation of methods commonly used to determine antimicrobial susceptibility to plant extracts and phenolic compounds. *Journal of AOAC International* 91(6), pp. 1423–1429.
- Kinghorn, A.D. 1998. Cancer chemopreventive agents discovered by activity-guided fractionation. *Current Organic Chemistry* 2(6), pp. 597–612.
- Kite, P., Eastwood, K., Sugden, S. and Percival, S.L. 2004. Use of in vivo-generated biofilms from hemodialysis catheters to test the efficacy of a novel antimicrobial catheter lock for biofilm eradication in vitro. *Journal of clinical microbiology* 42(7), pp. 3073–3076.
- Klančnik, A., Piskernik, S., Jeršek, B. and Možina, S.S. 2010. Evaluation of diffusion and dilution methods to determine the antibacterial activity of plant extracts. *Journal of microbiological methods* 81(2), pp. 121–126.

- Koh, T.J. and DiPietro, L.A. 2011. Inflammation and wound healing: the role of the macrophage. *Expert reviews in molecular medicine* 13, pp. 1-12.
- Kokabi, M., Sirousazar, M. and Hassan, Z.M. 2007. PVA–clay nanocomposite hydrogels for wound dressing. *European polymer journal* 43(3), pp. 773–781.
- Kolarsick, P., Kolarsick, M. and Goodwin, C. 2011. Anatomy and Physiology of the Skin. *Journal of the Dermatology Nurses' Association* 3, pp. 203–213.
- Kościuczuk, E.M., Lisowski, P., Jarczak, J., Strzałkowska, N., Jóźwik, A., Horbańczuk, J., Krzyżewski, J., Zwierzchowski, L. and Bagnicka, E. 2012. Cathelicidins: family of antimicrobial peptides. *A review. Molecular biology reports* 39(12), pp. 10957–10970.
- Krishna, S. and Miller, L.S. 2012. Host–pathogen interactions between the skin and *Staphylococcus aureus*. *Current opinion in microbiology* 15(1), pp. 28–35.
- Krishna, S., and Miller, L. S. 2012. Innate and adaptive immune responses against *Staphylococcus aureus* skin infections. *Seminars in immunopathology*, 34(2), pp. 261–280.
- Krithika, R., Mohankumar, R., Verma, R.J., Shrivastav, P.S., Mohamad, I.L., Gunasekaran, P. and Narasimhan, S. 2009. Isolation, characterization and antioxidative effect of phyllanthin against CCl₄-induced toxicity in HepG2 cell line. *Chemico-biological interactions* 181(3), pp. 351–358.
- Ksikisi, T., Palakkott, A.R. and Ppoyil, S.B.T. 2017. *Tribulus arabicus* and *Tribulus macropterus* are Comparable to *Tribulus terrestris*: An Antioxidant Assessment Taoufik. *Current Bioactive Compounds* 13, pp. 82–87.
- Kuete, V., Fankam, A.G., Wiench, B. and Efferth, T. 2013. Cytotoxicity and Modes of Action of the Methanol Extracts of Six Cameroonian Medicinal Plants against Multidrug-Resistant Tumor Cells. Anant, S. ed. *Evidence-Based Complementary and Alternative Medicine* 2013, pp. 285903.
- Kujath, P. and Michelsen, A. 2008. Wounds – From Physiology to Wound Dressing. *Deutsches Aerzteblatt Online* 105(13), pp. 239-248.
- Kumar, B., Sharma, D., Sharma, P., Katoch, V.M., Venkatesan, K. and Bisht, D. 2013. Proteomic analysis of *Mycobacterium tuberculosis* isolates resistant to kanamycin and amikacin. *Journal of proteomics* 94, pp. 68–77.
- Kumar, S., Kumar, D., Jusha, M., Saroha, K., Singh, N. and Vashishta, B. 2008. Antioxidant and free radical scavenging potential of *Citrullus colocynthis* (L.) Schrad. methanolic fruit extract. *Acta Pharmaceutica* 58(2), pp. 215–221.
- Kumara C, P., 2010. Studies Towards the Total Syntheses of *Aspidosperma* and *Nitraria* class of Alkaloids: Syntheses of Vincadifformine, Isonitramine and Sibirine. PhD. *university of Pune*.
- Kupper, T.S. and Fuhlbrigge, R.C. 2004. Immune surveillance in the skin: mechanisms and clinical consequences. *Nature Reviews Immunology* 4(3), pp. 211–222.
- Kwan, E.E. and Huang, S.G. 2008. Structural elucidation with NMR spectroscopy: practical strategies for organic chemists. *European journal of organic chemistry* 2008(16), pp. 2671–2688.
- Landén, N.X., Li, D. and Stähle, M. 2016. Transition from inflammation to proliferation: a critical step during wound healing. *Cellular and Molecular Life Sciences* 73(20), pp. 3861–3885.
- Langfield, R.D., Scarano, F.J., Heitzman, M.E., Kondo, M., Hammond, G.B. and Neto, C.C. 2004. Use of a modified microplate bioassay method to investigate antibacterial activity in the Peruvian medicinal plant *Peperomia galioides*. *Journal of Ethnopharmacology* 94(2), pp. 279–281.

- Lansky, E., Shubert, S. and Neeman, I. 2000. Pharmacological and therapeutic properties of pomegranate. Production, processing and marketing of pomegranate in the Mediterranean region: *Advances in research and technology* 42, pp. 231–235.
- Larouche, J., Sheoran, S., Maruyama, K. and Martino, M.M. 2018. Immune regulation of skin wound healing: mechanisms and novel therapeutic targets. *Advances in wound care* 7(7), pp. 209–231.
- Larson, E.L., Cronquist, A.B., Whittier, S., Lai, L., Lyle, C.T. and Della Latta, P. 2000. Differences in skin flora between inpatients and chronically ill outpatients. *Heart & Lung* 29(4), pp. 298–305.
- Lata, M., Sharma, D., Deo, N., Tiwari, P.K., Bisht, D. and Venkatesan, K. 2015. Proteomic analysis of ofloxacin-mono resistant Mycobacterium tuberculosis isolates. *Journal of proteomics* 127, pp. 114–121.
- Lau, W. M 2008. Improved Topical Therapeutic Systems Based on Co-Drugs. PhD thesis, *Cardiff University, Cardiff*.
- Łazarski, G. 2021. Asperugo Procumbens: a Review of Botany, Traditional Uses, Phytochemistry and Pharmacology. *Pakistan Journal of Medical and Health Sciences* 15(10), pp. 3092–3095.
- Lazarus, G.S., Cooper, D.M., Knighton, D.R., Margolis, D.J., Percoraro, R.E., Rodeheaver, G. and Robson, M.C. 1994. Definitions and guidelines for assessment of wounds and evaluation of healing. *Wound repair and regeneration* 2(3), pp. 165–170.
- Leaper, D., Assadian, O. and Edmiston, C.E. 2015. Approach to chronic wound infections. *British Journal of Dermatology* 173(2), pp. 351–358.
- Lebre, M.C., van der Aar, A.M.G., van Baarsen, L., van Capel, T.M.M., Schuitemaker, J.H.N., Kapsenberg, M.L. and de Jong, E.C. 2007. Human keratinocytes express functional Toll-like receptor 3, 4, 5, and 9. *Journal of Investigative Dermatology* 127(2), pp. 331–341.
- Lee, E.G., Luckett-Chastain, L.R., Calhoun, K.N., Frempah, B., Bastian, A. and Gallucci, R.M. 2019. Interleukin 6 function in the skin and isolated keratinocytes is modulated by hyperglycemia. *Journal of immunology research* 2019, pp. 1-9.
- Lee, J.-H., Kim, Y.-G., Park, J.G. and Lee, J. 2017. Supercritical fluid extracts of Moringa oleifera and their unsaturated fatty acid components inhibit biofilm formation by Staphylococcus aureus. *Food Control* 80, pp. 74–82.
- Lee, J.L., Mukhtar, H., Bickers, D.R., Kopelovich, L. and Athar, M. 2003. Cyclooxygenases in the skin: pharmacological and toxicological implications. *Toxicology and applied pharmacology* 192(3), pp. 294–306.
- Lee, S.H., Jeong, S.K. and Ahn, S.K. 2006. An update of the defensive barrier function of skin. *Yonsei medical journal* 47(3), pp. 293–306.
- Legerská, B., Chmelová, D. and Ondrejovič, M. 2020. TLC-Bioautography as a fast and cheap screening method for the detection of α -chymotrypsin inhibitors in crude plant extracts. *Journal of Biotechnology* 313(December 2019), pp. 11–17.
- Levac, D., Cázares, P., Yu, F. and De Luca, V. 2016. A picrinine N-methyltransferase belongs to a new family of γ -tocopherol-like methyltransferases found in medicinal plants that make biologically active monoterpenoid indole alkaloids. *Plant Physiology* 170(4), pp. 1935–1944.
- Li, B. and Wang, J.H.-C. 2011. Fibroblasts and myofibroblasts in wound healing: force generation and measurement. *Journal of tissue viability* 20(4), pp. 108–120.

- Li, D., Peng, H., Qu, L.E., Sommar, P., Wang, A., Chu, T., Li, X., Bi, X., Liu, Q. and Sérézal, I.G. 2021. miR-19a/b and miR-20a promote wound healing by regulating the inflammatory response of keratinocytes. *Journal of Investigative Dermatology* 141(3), pp. 659–671.
- Li, H.-B., Wong, C.-C., Cheng, K.-W. and Chen, F. 2008. Antioxidant properties in vitro and total phenolic contents in methanol extracts from medicinal plants. *LWT-Food Science and Technology* 41(3), pp. 385–390.
- Li, J.W.-H. and Vederas, J.C. 2009. Drug discovery and natural products: end of an era or an endless frontier? *Science* 325(5937), pp. 161–165.
- Li, Y.-H. and Tian, X. 2012. Quorum sensing and bacterial social interactions in biofilms. *Sensors* 12(3), pp. 2519–2538.
- Liang, Q., Chalamaiah, M., Liao, W., Ren, X., Ma, H. and Wu, J. 2020. Zein hydrolysate and its peptides exert anti-inflammatory activity on endothelial cells by preventing TNF- α -induced NF- κ B activation. *Journal of Functional Foods* 64, p. 103598.
- Lim, J.S., Park, H.S., Cho, S. and Yoon, H.S. 2018. Antibiotic susceptibility and treatment response in bacterial skin infection. *Annals of Dermatology* 30(2), pp. 186–191.
- Lim, J.Z.M., Ng, N.S.L. and Thomas, C. 2017. Prevention and treatment of diabetic foot ulcers. *Journal of the Royal Society of Medicine* 110(3), pp. 104–109.
- Liu, Y., Peterson, D.A., Kimura, H. and Schubert, D. 2002. Mechanism of Cellular 3-(4,5-Dimethylthiazol-2-yl)-2,5-Diphenyltetrazolium Bromide (MTT) Reduction. *Journal of Neurochemistry* 69(2), pp. 581–593.
- Loh, J., Soh, K.Y. and Proft, T. 2020. Generation of Bioluminescent Group A Streptococcus for Biophotonic Imaging. In: Group A Streptococcus. *Springer*, pp. 71–77.
- Long, L.H., Hoi, A. and Halliwell, B. 2010. Instability of, and generation of hydrogen peroxide by, phenolic compounds in cell culture media. *Archives of Biochemistry and Biophysics* 501(1), pp. 162–169.
- Loor, G., Kondapalli, J., Schriewer, J., Chandel, N., Vanden Hoek, T. and Schumacker, P. 2010. Menadione triggers cell death through ROS-dependent mechanisms involving PARP activation without requiring apoptosis. *Free Radical Biology and Medicine*, 49(12), pp.1925-1936.
- López-Alarcón, C. and Denicola, A. 2013. Evaluating the antioxidant capacity of natural products: A review on chemical and cellular-based assays. *Analytica Chimica Acta* 763, pp. 1–10.
- López, D., Vlamakis, H. and Kolter, R. 2010. Biofilms. *Cold Spring Harbor perspectives in biology* 2(7), p. a000398.
- Lü, J., Lin, P.H., Yao, Q. and Chen, C. 2010. Chemical and molecular mechanisms of antioxidants: experimental approaches and model systems. *Journal of cellular and molecular medicine* 14(4), pp. 840–860.
- Lu, L., Hu, W., Tian, Z., Yuan, D., Yi, G., Zhou, Y., Cheng, Q., Zhu, J. and Li, M. 2019. Developing natural products as potential anti-biofilm agents. *Chinese Medicine* 14(1), pp. 1–17.
- Lucas, T., Waisman, A., Ranjan, R., Roes, J., Krieg, T., Müller, W., Roers, A. and Eming, S.A. 2010. Differential roles of macrophages in diverse phases of skin repair. *The Journal of Immunology* 184(7), pp. 3964–3977.

- Luna, J.M., Rufino, R.D., Sarubbo, L.A., Rodrigues, L.R.M., Teixeira, J.A.C. and de Campos-Takaki, G.M. 2011. Evaluation antimicrobial and antiadhesive properties of the biosurfactant Lunasan produced by *Candida sphaerica* UCP 0995. *Current Microbiology* 62(5), pp. 1527–1534.
- Lyddiard, D., Jones, G.L. and Greatrex, B.W. 2016. Keeping it simple: Lessons from the golden era of antibiotic discovery. *FEMS Microbiology Letters* 363(8), pp. 2016–2018.
- Macfarlane, G.J., El-Metwally, A., De Silva, V., Ernst, E., Dowds, G.L., Moots, R.J. and Medicines, on behalf of the A.R.U.K.W.G. on C. and A. 2011. Evidence for the efficacy of complementary and alternative medicines in the management of rheumatoid arthritis: a systematic review. *Rheumatology* 50(9), pp. 1672–1683.
- Mackowiak, P.A. 1982. The normal microbial flora. *New England Journal of Medicine* 307(2), pp. 83–93.
- MacLeod, A.S. and Mansbridge, J.N. 2016. The innate immune system in acute and chronic wounds. *Advances in wound care* 5(2), pp. 65–78.
- Magnet, S., Courvalin, P. and Lambert, T. 2001. Resistance-nodulation-cell division-type efflux pump involved in aminoglycoside resistance in *Acinetobacter baumannii* strain BM4454. *Antimicrobial agents and chemotherapy* 45(12), pp. 3375–3380.
- Mah, T.-F. 2012. Biofilm-specific antibiotic resistance. *Future microbiology* 7(9), pp. 1061–1072.
- Mah, T.-F.C. and O’Toole, G.A. 2001. Mechanisms of biofilm resistance to antimicrobial agents. *Trends in microbiology* 9(1), pp. 34–39.
- Mahlpuu, M., Håkansson, J., Ringstad, L. and Björn, C. 2016. Antimicrobial peptides: an emerging category of therapeutic agents. *Frontiers in cellular and infection microbiology* 6, pp. 194.
- Mahmood, R., Malik, F., Shamas, S., Ahmed, T., Kausar, M., Rubnawaz, S., Ashfaq, M., Hussain, S., Green, B.D. and Mirza, B. 2020. Pharmacological evaluation of *Rhazya stricta* root extract. *Boletín Latinoamericano y del Caribe de Plantas Medicinales y Aromáticas* 19(2), pp. 188-206.
- Mancini, E., Senatore, F., Del Monte, D., De Martino, L., Grulova, D., Scognamiglio, M., Snoussi, M. and De Feo, V. 2015. Studies on chemical composition, antimicrobial and antioxidant activities of five *Thymus vulgaris* L. essential oils. *Molecules* 20(7), pp. 12016–12028.
- Marchese, A., Orhan, I.E., Daglia, M., Barbieri, R., Di Lorenzo, A., Nabavi, S.F., Gortzi, O., Izadi, M. and Nabavi, S.M. 2016. Antibacterial and antifungal activities of thymol: A brief review of the literature. *Food chemistry* 210, pp. 402–414.
- Marikovsky, M., Vogt, P., Eriksson, E., Rubin, J.S., Taylor, W.G., Sasse, J. and Klagsbrun, M. 1996. Wound fluid-derived heparin-binding EGF-like growth factor (HB-EGF) is synergistic with insulin-like growth factor-I for Balb/MK keratinocyte proliferation. *Journal of investigative dermatology* 106(4), pp. 616–621.
- Marino, M., Bersani, C. and Comi, G. 1999. Antimicrobial activity of the essential oils of *Thymus vulgaris* L. measured using a bioimpedometric method. *Journal of food protection* 62(9), pp. 1017–1023.
- Marwat, S.K., Rehman, F., Usman, K., Shah, S.S., Anwar, N. and Ullah, I. 2012. A review of phytochemistry, bioactivities and ethno medicinal uses of *Rhazya stricta* Decsne (Apocynaceae). *African Journal of Microbiology Research* 6(8), pp. 1629–1641.

- Marzouk, B., Mahjoub, M.A., Bouraoui, A., Fenina, N., Aouni, M. and Marzouk, Z. 2013. Anti-inflammatory and analgesic activities of a new cucurbitacin isolated from *Citrullus colocynthis* seeds. *Medicinal Chemistry Research* 22(8), pp. 3984–3990.
- Marzouk, B., Marzouk, Z., Décor, R., Edziri, H., Haloui, E., Fenina, N. and Aouni, M. 2009. Antibacterial and anticandidal screening of Tunisian *Citrullus colocynthis* Schrad. from Medenine. *Journal of ethnopharmacology* 125(2), pp. 344–349.
- Marzouk, B., Marzouk, Z., Fenina, N., Bouraoui, A. and Aouni, M. 2011. Anti-inflammatory and analgesic activities of Tunisian *Citrullus colocynthis* Schrad. immature fruit and seed organic extracts. *European Review for Medical and Pharmacological Sciences* 15(6), pp. 665–672.
- Masoko, P. and Eloff, J.N. 2005. The diversity of antifungal compounds of six South African *Terminalia* species (Combretaceae) determined by bioautography. *African Journal of Biotechnology* 4(12), pp. 1425-1431.
- Mast, B.A. and Schultz, G.S. 1996. Interactions of cytokines, growth factors, and proteases in acute and chronic wounds. *Wound Repair and Regeneration* 4(4), pp. 411–420.
- Matsuura, H.N. and Fett-Neto, A.G. 2015. Plant alkaloids: main features, toxicity, and mechanisms of action. *Plant toxins* 2(7), pp. 1–5.
- May, A.K. 2009. Skin and soft tissue infections. *Surgical Clinics of North America* 89(2), pp. 403–420.
- McCaig, L.F., McDonald, L.C., Mandal, S. and Jernigan, D.B. 2006. Staphylococcus aureus–associated skin and soft tissue infections in ambulatory care. *Emerging infectious diseases* 12(11), p. 1715.
- McGaw, L.J., Jäger, A.K. and Van Staden, J. 2002. Antibacterial effects of fatty acids and related compounds from plants. *South African Journal of Botany* 68(4), pp. 417–423.
- MChir, S., Burton, M. 2013. Microbial keratitis. *FOCUS, The Royal College of Ophthalmologists*, pp. 1–5.
- McNeil, J.C., Hulten, K.G., Kaplan, S.L. and Mason, E.O., 2014. Decreased susceptibilities to retapamulin, mupirocin, and chlorhexidine among *Staphylococcus aureus* isolates causing skin and soft tissue infections in otherwise healthy children. *Antimicrobial agents and chemotherapy*, 58(5), pp.2878-2883.
- Meena, M.C. and Patni, V. 2008. Isolation and identification of flavonoid “quercetin” from *Citrullus colocynthis* (Linn.) Schrad. *Asian J Exp Sci* 22(1), pp. 137–142.
- Mekkes, J., Loots, M.A.M., Van Der Wal, A.C. and Bos, J.D. 2003. Causes, investigation and treatment of leg ulceration. *British Journal of dermatology* 148(3), pp. 388–401.
- Menke, N.B., Ward, K.R., Witten, T.M., Bonchev, D.G. and Diegelmann, R.F. 2007. Impaired wound healing. *Clinics in dermatology* 25(1), pp. 19–25.
- Mensor, L.L., Menezes, F.S., Leitão, G.G., Reis, A.S., Santos, T.C. dos, Coube, C.S. and Leitão, S.G. 2001. Screening of Brazilian plant extracts for antioxidant activity by the use of DPPH free radical method. *Phytotherapy research* 15(2), pp. 127–130.
- Menter, D.G., Schilsky, R.L. and DuBois, R.N. 2010. Cyclooxygenase-2 and Cancer Treatment: Understanding the Risk Should Be Worth the Reward Cyclooxygenase-2-Based Cancer Targeting. *Clinical cancer research* 16(5), pp. 1384–1390.
- Micallef, L., Belaubre, F., Pinon, A., Jayat-Vignoles, C., Delage, C., Charveron, M. and Simon, A. 2009. Effects of extracellular calcium on the growth-differentiation switch in immortalized keratinocyte

HaCaT cells compared with normal human keratinocytes. *Experimental dermatology* 18(2), pp. 143–151.

Mihailescu, R., Furustrand Tabin, U., Corvec, S., Oliva, A., Betrisey, B., Borens, O. and Trampuz, A. 2014. High activity of fosfomycin and rifampin against methicillin-resistant *Staphylococcus aureus* biofilm in vitro and in an experimental foreign-body infection model. *Antimicrobial agents and chemotherapy* 58(5), pp. 2547–2553.

Miles, B.Y.A.A. and Misra, S.S. 1931. The Estimation of the Bactericidal Power of the Blood. *The Journal of hygiene* 38(6), pp. 732–749.

Miller, M.B. and Bassler, B.L. 2001. Quorum sensing in bacteria. *Annual review of microbiology* 55(1), pp. 165–199.

Mirsaleh-Kohan, N., Robertson, W.D. and Compton, R.N. 2008. Electron ionization time-of-flight mass spectrometry: Historical review and current applications. *Mass spectrometry reviews* 27(3), pp. 237–285.

Mirski, T., Niemcewicz, M., Bartoszcze, M., Gryko, R. and Michalski, A. 2018. Utilisation of peptides against microbial infections—a review. *Annals of Agricultural and Environmental Medicine* 25(2), pp. 205–210.

Mirza, R.E., Fang, M.M., Ennis, W.J. and Koh, T.J. 2013. Blocking interleukin-1 β induces a healing-associated wound macrophage phenotype and improves healing in type 2 diabetes. *Diabetes* 62(7), pp. 2579–2587.

Misic, A.M., Gardner, S.E. and Grice, E.A. 2014. The wound microbiome: modern approaches to examining the role of microorganisms in impaired chronic wound healing. *Advances in wound care* 3(7), pp. 502–510.

Mitscher, L.A., Leu R.P., Bathala M.S., Wu W.N., Beal J.L. 1972. Antimicrobial agents from higher plants—1. Introduction, rationale, and methodology. *Lloydia* 35, 157–176.

Moellering Jr, R.C. 2010. The problem of complicated skin and skin structure infections: the need for new agents. *Journal of antimicrobial chemotherapy* 65(suppl_4), pp. iv3–iv8.

Moffarah, A.S., Mohajer, M. Al, Hurwitz, B.L. and Armstrong, D.G. 2016. Skin and soft tissue infections. *Diagnostic Microbiology of the Immunocompromised Host*, pp. 691–708.

Mohan, S., Syam, S., Abdelwahab, S.I. and Thangavel, N. 2018. An anti-inflammatory molecular mechanism of action of α -mangostin, the major xanthone from the pericarp of *Garcinia mangostana*: an in silico, in vitro and in vivo approach. *Food & function* 9(7), pp. 3860–3871.

Moldovan, Z., Buleandră, M., Oprea, E. and Mnea, Z. 2017. Studies on Chemical Composition and Antioxidant Activity of *Rudbeckia triloba*. *Journal of Analytical Methods in Chemistry* 2017, pp. 1–8.

Moloney, M.G. 2016. Natural Products as a Source for Novel Antibiotics. *Trends in Pharmacological Sciences* 37(8), pp. 689–701.

Monnier, L., Mas, E., Ginet, C., Michel, F., Villon, L., Cristol, J.-P. and Colette, C. 2006. Activation of oxidative stress by acute glucose fluctuations compared with sustained chronic hyperglycemia in patients with type 2 diabetes. *Jama* 295(14), pp. 1681–1687.

Moses, R.L., Boyle, G.M., Howard-Jones, R.A., Errington, R.J., Johns, J.P., Gordon, V., Reddell, P., Steadman, R. and Moseley, R. 2020. Novel epoxy-tiglianes stimulate skin keratinocyte wound healing responses and re-epithelialization via protein kinase C activation. *Biochemical Pharmacology* 178, p. 114048..

Moses, R.L., Dally, J., Lundy, F.T., Langat, M., Kiapranis, R., Tsolaki, A.G., Moseley, R. and Prescott, T.A.K. 2020. Lepiniopsis ternatensis sap stimulates fibroblast proliferation and down regulates macrophage TNF- α secretion. *Fitoterapia* 141, p. 104478.

Mosmann, T.R., 1983. Rapid colorimetric assay for cellular growth and survival: application to proliferation and cytotoxicity assays. *Journal of Immunological Methods* 65, 55–63.

Mosser, D.M. and Edwards, J.P. 2008. Exploring the full spectrum of macrophage activation. *Nature reviews immunology* 8(12), pp. 958–969.

Mothana, R.A.A. and Lindequist, U. 2005. Antimicrobial activity of some medicinal plants of the island Soqotra. *Journal of ethnopharmacology* 96(1–2), pp. 177–181.

Mounanga, M.B., Mewono, L. and Angone, S.A. 2015. Toxicity studies of medicinal plants used in sub-Saharan Africa. *Journal of Ethnopharmacology* 174, pp. 618–627.

Mukherjee, A. and Patil, S.D. 2012. Effects of Alkaloid Rich Extract of Citrullus colocynthis Fruits on Artemia Salina and Human Cancerous (MCF-7 AND HEPG-2) Cells. *Journal of PharmaSciTech* 1(2), pp. 15–19.

Munita, J.M., Arias, C.A., Unit, A.R. and Santiago, A. De 2016. Mechanisms of Antibiotic Resistance Jose. *Microbiol Spectr* 4(2), pp. 1–37.

Murthy, K., & Mishra, S. 2008. TLC Determination of Betulinic Acid from Nymphodies macrospermum: A New Botanical Source for Tagara. *Chromatographia*, 68(9-10), pp. 877–880.

Mustofa, M., Valentin, A. and Lewin, G. 2006. In vitro Antiplasmodial Activity and Cytotoxicity of Vincadifformine and Its Semisynthetic Derivatives. *Indonesian Journal of Biotechnology* 11(1), pp. 878–883.

Nakanishi, M. and Rosenberg, D.W. 2013. Multifaceted roles of PGE2 in inflammation and cancer. In: *Seminars in immunopathology*. Springer, pp. 123–137. Wallace, J.L. 2001. Prostaglandian biology in inflammatory bowel disease. *Gastroenterology Clinics* 30(4), pp. 971–980.

Natnoo, S. 2014. Flora: A Source Of Traditional Medicine In Jammu And Kashmir With Special Reference To Chenab Valley. *International Journal of Recent Scientific Research* Vol. 5, Issue, 12, pp. 2286-2288.

Naves, P., del Prado, G., Huelves, L., Gracia, M., Ruiz, V., Blanco, J., Dahbi, G., Blanco, M., del Carmen Ponte, M. and Soriano, F. 2008. Correlation between virulence factors and in vitro biofilm formation by Escherichia coli strains. *Microbial pathogenesis* 45(2), pp. 86–91.

Ncube, N.S., Afolayan, A.J. and Okoh, A.I. 2008. Assessment techniques of antimicrobial properties of natural compounds of plant origin: current methods and future trends. *African journal of biotechnology* 7(12), pp. 1797-1806.

Ndlovu, B., De Kock, M., Klaasen, J. and Rahiman, F. 2021. In vitro comparison of the anti-proliferative effects of Galenia africana on human skin cell lines. *Scientia Pharmaceutica* 89(1), p. 12.

Nehdi, I.A., Sbihi, H., Tan, C.P. and Al-Resayes, S.I. 2013. Evaluation and characterisation of Citrullus colocynthis (L.) Schrad seed oil: Comparison with Helianthus annuus (sunflower) seed oil. *Food Chemistry* 136(2), pp. 348–353.

Newman, D.J. and Cragg, G.M. 2020. Natural products as sources of new drugs over the nearly four decades from 01/1981 to 09/2019. *Journal of natural products* 83(3), pp. 770–803.

NG Heatley 1944. A method for the assay of penicillin. *Biochemical Journal* 38(1), p. 61.

- Nikaido, H. 2003. Molecular basis of bacterial outer membrane permeability revisited. *Microbiology and molecular biology reviews* 67(4), pp. 593–656.
- Nizet, V., Ohtake, T., Lauth, X., Trowbridge, J., Rudisill, J., Dorschner, R.A., Pestonjamas, V., Piraino, J., Huttner, K. and Gallo, R.L. 2001. Innate antimicrobial peptide protects the skin from invasive bacterial infection. *Nature* 414(6862), pp. 454–457.
- Noble, R.L. 1990. The discovery of the vinca alkaloids—chemotherapeutic agents against cancer. *Biochemistry and cell biology* 68(12), pp. 1344–1351.
- Noipa, T., Srijaranai, S., Tuntulani, T. and Ngeontae, W. 2011. New approach for evaluation of the antioxidant capacity based on scavenging DPPH free radical in micelle systems. *Food Research International* 44(3), pp. 798–806.
- Novak, M.L. and Koh, T.J. 2013. Macrophage phenotypes during tissue repair. *Journal of leukocyte biology* 93(6), pp. 875–881.
- Nussbaum, S.R., Carter, M.J., Fife, C.E., DaVanzo, J., Haught, R., Nusgart, M. and Cartwright, D. 2018. An economic evaluation of the impact, cost, and medicare policy implications of chronic nonhealing wounds. *Value in Health* 21(1), pp. 27–32.
- Nwachukwu, I.D., Sarteshnizi, R.A., Udenigwe, C.C. and Aluko, R.E. 2021. A Concise Review of Current In Vitro Chemical and Cell-Based Antioxidant Assay Methods. *Molecules* 26(16), p. 4865.
- O’Neill, J. 2016. Tackling drug-resistant infections globally: final report and recommendations.
- O’Sullivan, J.N., Rea, M.C., O’Connor, P.M., Hill, C. and Ross, R.P. 2019. Human skin microbiota is a rich source of bacteriocin-producing staphylococci that kill human pathogens. *FEMS Microbiology Ecology* 95(2), p. fyy241.
- Obaid, A.Y., Voleti, S., Bora, R.S., Hajrah, N.H., Omer, A.M.S., Sabir, J.S.M. and Saini, K.S. 2017. Cheminformatics studies to analyze the therapeutic potential of phytochemicals from *Rhazya stricta*. *Chemistry Central Journal* 11(1), pp. 1–21.
- Oberlies, N.H. and Kroll, D.J. 2004. Camptothecin and taxol: historic achievements in natural products research. *Journal of natural products* 67(2), pp. 129–135.
- Oeckinghaus, A. and Ghosh, S., 2009. The NF- κ B family of transcription factors and its regulation. *Cold Spring Harbor perspectives in biology*, 1(4), p.a000034.
- Ohlendorf, C., W.W., Tomford, H.J., Mankin. 1996. Chondrocyte survival in cryopreserved osteochondral articular cartilage. *Journal of Orthopaedic Research* 14(3), pp. 413–416.
- Olaru, F. and Jensen, L.E. 2010. Chemokine expression by human keratinocyte cell lines after activation of Toll-like receptors. *Experimental dermatology* 19(8), pp. e314–e316.
- Olsson, M., Järbrink, K., Divakar, U., Bajpai, R., Upton, Z., Schmidtchen, A. and Car, J. 2019. The humanistic and economic burden of chronic wounds: A systematic review. *Wound Repair and Regeneration* 27(1), pp. 114–125.
- Oluyemisi, F., Henry, O. and Peter, O. 2012. Standardization of herbal medicines-A review. *International Journal of Biodiversity and Conservation* 4(3), pp. 101–112.
- Omar, A., Wright, J.B., Schultz, G., Burrell, R. and Nadworny, P. 2017. Microbial biofilms and chronic wounds. *Microorganisms* 5(1), p. 9.
- Otto, M. 2014. Staphylococcus aureus toxins. *Current opinion in microbiology* 17, pp. 32–37.

- Owen, L., White, A.W. and Laird, K. 2019. Characterisation and screening of antimicrobial essential oil components against clinically important antibiotic-resistant bacteria using thin layer chromatography-direct bioautography hyphenated with GC-MS, LC-MS and NMR. *Phytochemical analysis* 30(2), pp. 121–131.
- Oyama, Y. and Masuda, T. 2001. Flow cytometric estimation on cytotoxic activity of leaf extracts from seashore plants in subtropical Japan. *Japanese Journal of Pharmacology* 85(Supplement 1), p. 135P.
- Oyoshi, M.K., He, R., Kumar, L., Yoon, J. and Geha, R.S. 2009. Cellular and molecular mechanisms in atopic dermatitis. *Advances in immunology* 102, pp. 135–226.
- Pai, S. and Thomas, R., 2008. Immune deficiency or hyperactivity-Nf-kb illuminates autoimmunity. *Journal of autoimmunity*, 31(3), pp.245-251.
- Parasuraman, S. 2018. Herbal drug discovery: challenges and perspectives. *Current Pharmacogenomics and Personalized Medicine (Formerly Current Pharmacogenomics)* 16(1), pp. 63–68.
- Park, N.-H., Choi, J.-S., Hwang, S.-Y., Kim, Y.-C., Hong, Y.-K., Cho, K.K. and Choi, I.S. 2013. Antimicrobial activities of stearidonic and gamma-linolenic acids from the green seaweed *Enteromorpha linza* against several oral pathogenic bacteria. *Botanical studies* 54(1), pp. 1–9.
- Pashmforosh, Marzieh, Rajabi Vardanjani, Hossein, Rajabi Vardanjani, Hassan, Pashmforosh, Mahdi and Khodayar, M.J. 2018. Topical Anti-Inflammatory and Analgesic Activities of *Citrullus colocynthis* Extract Cream in Rats. *Medicina* 54(4), pp. 1-11.
- Pastar, I., Stojadinovic, O. and Tomic-Canic, M. 2008. Role of keratinocytes in healing of chronic wounds. *Surgical technology international* 17, pp. 105–112.
- Pastar, I., Stojadinovic, O., Yin, N.C., Ramirez, H., Nusbaum, A.G., Sawaya, A., Patel, S.B., Khalid, L., Isseroff, R.R. and Tomic-Canic, M. 2014. Epithelialization in wound healing: a comprehensive review. *Advances in wound care* 3(7), pp. 445–464.
- Pastar, I., Wong, L.L., Egger, A.N. and Tomic-Canic, M., 2018. Descriptive vs mechanistic scientific approach to study wound healing and its inhibition: Is there a value of translational research involving human subjects?. *Experimental dermatology*, 27(5), pp.551-562.
- Paterson, G.K., Harrison, E.M. and Holmes, M.A. 2014. The emergence of mecC methicillin-resistant *Staphylococcus aureus*. *Trends in microbiology* 22(1), pp. 42–47.
- Patra, J.K., Das, G., Fraceto, L.F., Campos, E.V.R., Rodriguez-Torres, M. del P., Acosta-Torres, L.S., Diaz-Torres, L.A., Grillo, R., Swamy, M.K. and Sharma, S. 2018. Nano based drug delivery systems: recent developments and future prospects. *Journal of nanobiotechnology* 16(1), pp. 1–33.
- Percival, S.L. 2005. Assessing the effectiveness of tetrasodium ethylenediaminetetraacetic acid as a novel central venous catheter (CVC) lock solution against biofilms using a laboratory model system. *Infection Control & Hospital Epidemiology* 26, pp. 515–519.
- Percival, S.L., Emanuel, C., Cutting, K.F. and Williams, D.W. 2012. Microbiology of the skin and the role of biofilms in infection. *International wound journal* 9(1), pp. 14–32.
- Percival, S.L., Hill, K.E., Williams, D.W., Hooper, S.J., Thomas, D.W. and Costerton, J.W. 2012. A review of the scientific evidence for biofilms in wounds. *Wound repair and regeneration* 20(5), pp. 647–657.
- Percival, S.L., Thomas, J.G. and Williams, D. 2010. An introduction to the world of microbiology and biofilmology. *Microbiology of wounds* 1, pp. 1–58.

- Pereira, R.F., Barrias, C.C., Granja, P.L. and Bartolo, P.J. 2013. Advanced biofabrication strategies for skin regeneration and repair. *Nanomedicine* 8(4), pp. 603–621.
- Perrault, D.P., Bramos, A., Xu, X., Shi, S. and Wong, A.K. 2018. Local administration of interleukin-1 receptor antagonist improves diabetic wound healing. *Annals of plastic surgery* 80(5), p. S317.
- Perveen, S., Ashfaq, H., Ambreen, S., Ashfaq, I., Kanwal, Z. and Tayyeb, A. 2021. Methanolic extract of *Citrullus colocynthis* suppresses growth and proliferation of breast cancer cells through regulation of cell cycle. *Saudi Journal of Biological Sciences* 28(1), pp. 879–886.
- Petrovska, B.B. 2012. Historical review of medicinal plants' usage. *Pharmacognosy reviews* 6(11), p. 1.
- Phoboo, S., Shetty, K. and ElObeid, T. 2015. In vitro assays of anti-diabetic and anti-hypertensive potential of some traditional edible plants of Qatar. *Journal of Medicinally Active Plants* 4(3), pp. 22–29.
- Phondani, P.C., Bhatt, A., Elsarrag, E. and Horr, Y.A. 2016. Ethnobotanical magnitude towards sustainable utilization of wild foliage in Arabian Desert. *Journal of traditional and complementary medicine* 6(3), pp. 209–218.
- Piktel, E., Wnorowska, U., Cieśluk, M., Deptula, P., Pogoda, K., Misztalewska-Turkowicz, I., Paprocka, P., Niemirowicz-Laskowska, K., Wilczewska, A.Z. and Janmey, P.A. 2019. Inhibition of inflammatory response in human keratinocytes by magnetic nanoparticles functionalized with PBP10 peptide derived from the PIP2-binding site of human plasma gelsolin. *Journal of nanobiotechnology* 17(1), pp. 1–19.
- Piluzza, G. and Bullitta, S. 2011. Correlations between phenolic content and antioxidant properties in twenty-four plant species of traditional ethnoveterinary use in the Mediterranean area. *Pharmaceutical biology* 49(3), pp. 240–247.
- Pimm, S.L., Jenkins, C.N., Abell, R., Brooks, T.M., Gittleman, J.L., Joppa, L.N., Raven, P.H., Roberts, C.M. and Sexton, J.O. 2014. The biodiversity of species and their rates of extinction, distribution, and protection. *science* 344(6187), p. 1246752.
- Pitt, J.J. 2009. Principles and applications of liquid chromatography-mass spectrometry in clinical biochemistry. *The Clinical Biochemist Reviews* 30(1), p. 19.
- Plonka, P.M., Passeron, T., Brenner, M., Tobin, D.J., Shibahara, S., Thomas, A., Slominski, A., Kadekaro, A.L., Hershkovitz, D. and Peters, E. 2009. What are melanocytes really doing all day long...? *Experimental dermatology* 18(9), pp. 799–819.
- Posadzki, P., Watson, L. and Ernst, E. 2013. Contamination and adulteration of herbal medicinal products (HMPs): an overview of systematic reviews. *European journal of clinical pharmacology* 69(3), pp. 295–307.
- Posnett, J. and Franks, P.J. 2008. The burden of chronic wounds in the UK. *Nursing times* 104(3), pp. 44–45.
- Pozzi, C., Waters, E.M., Rudkin, J.K., Schaeffer, C.R., Lohan, A.J., Tong, P., Loftus, B.J., Pier, G.B., Fey, P.D. and Massey, R.C. 2012. Methicillin resistance alters the biofilm phenotype and attenuates virulence in *Staphylococcus aureus* device-associated infections. *PLoS pathogens* 8(4), pp. e1002626.
- Pradhan, L., Nabzdyk, C., Andersen, N. D., LoGerfo, F. W., & Veves, A. 2009. Inflammation and neuropeptides: the connection in diabetic wound healing. *Expert reviews in molecular medicine*, 11, pp. e2.

- Prame Kumar, K., Nicholls, A.J. and Wong, C.H.Y. 2018. Partners in crime: neutrophils and monocytes/macrophages in inflammation and disease. *Cell and tissue research* 371(3), pp. 551–565.
- Prasath, K.G., Sethupathy, S. and Pandian, S.K. 2019. Proteomic analysis uncovers the modulation of ergosterol, sphingolipid and oxidative stress pathway by myristic acid impeding biofilm and virulence in *Candida albicans*. *Journal of proteomics* 208, p. 103503.
- Purkait, S., Bhattacharya, A., Bag, A. and Chattopadhyay, R.R. 2021. TLC bioautography-guided isolation of essential oil components of cinnamon and clove and assessment of their antimicrobial and antioxidant potential in combination. *Environmental Science and Pollution Research* 28(1), pp. 1131–1140.
- Pushparaj Selvadoss, P., Nellore, J., Balaraman Ravindran, M., Sekar, U. and Tippabathani, J. 2018. Enhancement of antimicrobial activity by liposomal oleic acid-loaded antibiotics for the treatment of multidrug-resistant *Pseudomonas aeruginosa*. *Artificial Cells, Nanomedicine, and Biotechnology* 46(2), pp. 268–273.
- Radulovic, N.S., Blagojevic, P.D., Stojanovic-Radic, Z.Z. and Stojanovic, N.M. 2013. Antimicrobial plant metabolites: structural diversity and mechanism of action. *Current medicinal chemistry* 20(7), pp. 932–952.
- Raff, A.B. and Kroshinsky, D. 2016. Cellulitis a review. *JAMA - Journal of the American Medical Association* 316(3), pp. 325–337.
- Rafieian-Kopaei, M. 2012. Medicinal plants and the human needs. *Journal of HerbMed Pharmacology* 1(1), pp. 1-2.
- Rahbar, A. and Nabipour, I. 2010. The Hypolipidemic Effect of *Citrullus colocynthis* on Patients with Hyperlipidemia. *Pakistan Journal of Biological Sciences*, 13(24), pp.1202-1207.
- Raja, K.S., Garcia, M.S. and Isseroff, R.R. 2007. Wound re-epithelialization: modulating keratinocyte migration in wound healing. *Frontiers in Bioscience-Landmark* 12(8), pp. 2849–2868.
- Ramakrishnan, K., Salinas, R.C. and Higuera, N.I.A. 2015. Skin and soft tissue infections. *American family physician* 92(6), pp. 474–483.
- Rates, S.M.K. 2001. Plants as source of drugs. *Toxicon* 39(5), pp. 603–613.
- Rather, M.A., Bhat, B.A. and Qurishi, M.A. 2013. Multicomponent phytotherapeutic approach gaining momentum: Is the “one drug to fit all” model breaking down? *Phytomedicine* 21(1), pp. 1–14.
- Rathinakumar, R., Walkenhorst, W.F. and Wimley, W.C. 2009. Broad-spectrum antimicrobial peptides by rational combinatorial design and high-throughput screening: the importance of interfacial activity. *Journal of the American Chemical Society* 131(22), pp. 7609–7617.
- Raziyeva, K., Kim, Y., Zharkinbekov, Z., Kassymbek, K., Jimi, S. and Saparov, A. 2021. Immunology of acute and chronic wound healing. *Biomolecules* 11(5), p. 700.
- Refsgaard, H.H.F., Brockhoff, P.M.B. and Jensen, B. 2000. Free polyunsaturated fatty acids cause taste deterioration of salmon during frozen storage. *Journal of Agricultural and Food Chemistry* 48(8), pp. 3280–3285.
- Reynolds, W.F. and Mazzola, E.P. 2015. Nuclear magnetic resonance in the structural elucidation of natural products. *Progress in the Chemistry of Organic Natural Products* 100, pp. 223–309.
- Rezai, M., Davoodi, A., Asori, M. and Azadbakht, M. 2017. Cytotoxic activity of *Citrullus colocynthis* (L.) schrad fruit extract on gastric adenocarcinoma and breast cancer cell lines. *International Journal of Pharmaceutical Sciences Review and Research* 45(1), pp. 175–178.

- Rezk, A., Al-Hashimi, A., John, W., Schepker, H., Ullrich, M.S. and Brix, K. 2015. Assessment of cytotoxicity exerted by leaf extracts from plants of the genus *Rhododendron* towards epidermal keratinocytes and intestine epithelial cells. *BMC Complementary and Alternative Medicine* 15(1), pp. 1–18.
- Rezvani Ghomi, E., Khalili, S., Nouri Khorasani, S., Esmaeely Neisiany, R. and Ramakrishna, S. 2019. Wound dressings: Current advances and future directions. *Journal of Applied Polymer Science* 136(27), p. 47738.
- Ricciardelli, A., Casillo, A., Papa, R., Monti, D.M., Imbimbo, P., Vrenna, G., Artini, M., Selan, L., Corsaro, M.M. and Tutino, M.L. 2018. Pentadecanal inspired molecules as new anti-biofilm agents against *Staphylococcus epidermidis*. *Biofouling* 34(10), pp. 1110–1120.
- Ricciotti, E. and FitzGerald, G.A. 2011. Prostaglandins and inflammation. *Arteriosclerosis, thrombosis, and vascular biology* 31(5), pp. 986–1000.
- Rios, J.-L., Recio, M.C. and Villar, A. 1988. Screening methods for natural products with antimicrobial activity: a review of the literature. *Journal of ethnopharmacology* 23(2–3), pp. 127–149.
- Ritsu, M., Kawakami, K., Kanno, E., Tanno, H., Ishii, K., Imai, Y., Maruyama, R. and Tachi, M. 2017. Critical role of tumor necrosis factor- α in the early process of wound healing in skin. *Journal of Dermatology & Dermatologic Surgery* 21(1), pp. 14–19.
- Roche, E.D., Renick, P.J., Tetens, S.P., Ramsay, S.J., Daniels, E.Q. and Carson, D.L. 2012. Increasing the presence of biofilm and healing delay in a porcine model of MRSA-infected wounds. *Wound Repair and Regeneration* 20(4), pp. 537–543.
- Rogers, N.M., Seeger, F., Garcin, E.D., Roberts, D.D. and Isenberg, J.S. 2014. Regulation of soluble guanylate cyclase by matricellular thrombospondins: implications for blood flow. *Frontiers in physiology* 5, p. 134.
- Romana-Souza, B., Dos Santos, J.S., Bandeira, L.G. and Monte-Alto-Costa, A. 2016. Selective inhibition of COX-2 improves cutaneous wound healing of pressure ulcers in mice through reduction of iNOS expression. *Life sciences* 153, pp. 82–92.
- Ross, Z.M., O’Gara, E.A., Hill, D.J., Sleightholme, H. V and Maslin, D.J. 2001. Antimicrobial properties of garlic oil against human enteric bacteria: evaluation of methodologies and comparisons with garlic oil sulfides and garlic powder. *Applied and environmental microbiology* 67(1), pp. 475–480.
- Roupé, K.M., Nybo, M., Sjöbring, U., Alberius, P., Schmidtchen, A. and Sørensen, O.E. 2010. Injury is a major inducer of epidermal innate immune responses during wound healing. *Journal of Investigative Dermatology* 130(4), pp. 1167–1177.
- Rousselle, P., Braye, F. and Dayan, G. 2019. Re-epithelialization of adult skin wounds: Cellular mechanisms and therapeutic strategies. *Advanced Drug Delivery Reviews* 146, pp. 344–365.
- Rousselle, P., Montmasson, M. and Garnier, C. 2019. Extracellular matrix contribution to skin wound re-epithelialization. *Matrix Biology* 75, pp. 12–26.
- Rozario, T. and DeSimone, D.W. 2010. The extracellular matrix in development and morphogenesis: a dynamic view. *Developmental biology* 341(1), pp. 126–140.
- Ryu, S., Han, H.M., Song, P.I., Armstrong, C.A. and Park, Y. 2015. Suppression of propionibacterium acnes infection and the associated inflammatory response by the antimicrobial peptide P5 in Mice. *PLoS ONE* 10(7), pp. 1–18.

- Saad, B., Azaizeh, H. and Said, O. 2005. Tradition and perspectives of Arab herbal medicine: a review. *Evidence-Based Complementary and Alternative Medicine* 2(4), pp. 475–479.
- Saadabi, A.M.A. 2006. Antifungal Activity of Some Saudi Plants Used in Traditional Medicine. *Asian Journal of Plant Sciences* 5(5), pp. 907–909.
- Sadeghi, H.M., Seitz, B., Hayashi, S., LaBree, L. and McDonnell, P.J., 1998. In vitro effects of mitomycin-C on human keratocytes. *Journal of Refractive Surgery*, 14(5), pp.534-540.
- Saeed, M.E.M., Boulos, J.C., Elhaboub, G., Rigano, D., Saab, A., Loizzo, M.R., Hassan, L.E.A., Sugimoto, Y., Piacente, S. and Tundis, R. 2019. Cytotoxicity of cucurbitacin E from *Citrullus colocynthis* against multidrug-resistant cancer cells. *Phytomedicine* 62, p. 152945.
- Sanchez, M.C., Lancel, S., Boulanger, E. and Nevier, R. 2018. Targeting oxidative stress and mitochondrial dysfunction in the treatment of impaired wound healing: A systematic review. *Antioxidants* 7(8), pp. 1–14.
- Sanford, J.A. and Gallo, R.L. 2013. Functions of the skin microbiota in health and disease. In: *Seminars in immunology*. Elsevier, pp. 370–377.
- Santoni, G., Cardinali, C., Morelli, M.B., Santoni, M., Nabissi, M. and Amantini, C. 2015. Danger-and pathogen-associated molecular patterns recognition by pattern-recognition receptors and ion channels of the transient receptor potential family triggers the inflammasome activation in immune cells and sensory neurons. *Journal of neuroinflammation* 12(1), pp. 1–10.
- Santoro, M.M. and Gaudino, G. 2005. Cellular and molecular facets of keratinocyte reepithelization during wound healing. *Experimental cell research* 304(1), pp. 274–286.
- Sasidharan, S., Chen, Y., Saravanan, D., Sundram, K.M. and Latha, L.Y. 2011. Extraction, isolation and characterization of bioactive compounds from plants' extracts. *African journal of traditional, complementary and alternative medicines* 8(1), pp. 1-10.
- Schäfer, M. and Werner, S. 2008. Oxidative stress in normal and impaired wound repair. *Pharmacological research* 58(2), pp. 165–171.
- Schenone, M., Dančik, V., Wagner, B.K. and Clemons, P.A. 2013. Target identification and mechanism of action in chemical biology and drug discovery. *Nature chemical biology*. 9(4), pp. 232–240.
- Schilrreff, P. and Alexiev, U., 2022. Chronic Inflammation in Non-Healing Skin Wounds and Promising Natural Bioactive Compounds Treatment. *International Journal of Molecular Sciences*, 23(9), p.4928.
- Schröder, J.M. and Harder, J. 2006. Antimicrobial skin peptides and proteins. *Cellular and Molecular Life Sciences CMLS* 63(4), pp. 469–486.
- Schürer, N., Köhne, A., Schliep, V., Barlag, K. and Goerz, G., 1993. Lipid composition and synthesis of HaCaT cells, an immortalized human keratinocyte line, in comparison with normal human adult keratinocytes. *Experimental dermatology*, 2(4), pp.179-185.
- Seeram, N., Schulman, R. and Heber, D. 2006. Pomegranates. *Boca Raton: CRC Taylor & Francis 1st Edition*, pp. 262.
- Shaer, N.A. 2019. Can crude alkaloids extract of *Rhazya stricta* induce apoptosis in pancreatic cancer: In vitro study? *Pathophysiology* 26(1), pp. 97–101.

- Shahverdi, A.R., Abdolpour, F., Monsef-Esfahani, H.R. and Farsam, H. 2007. A TLC bioautographic assay for the detection of nitrofurantoin resistance reversal compound. *Journal of Chromatography B* 850(1–2), pp. 528–530.
- Shalchi, Z., Gurbaxani, A., Baker, M. and Nash, J. 2011. Antibiotic resistance in microbial keratitis: Ten-year experience of corneal scrapes in the United Kingdom. *Ophthalmology* 118(11), pp. 2161–2165.
- Sharma, D., Lata, M., Singh, R., Deo, N., Venkatesan, K. and Bisht, D. 2016. Cytosolic proteome profiling of aminoglycosides resistant Mycobacterium tuberculosis clinical isolates using MALDI-TOF/MS. *Frontiers in microbiology* 7, p. 1816.
- Sharma, N.K., Ahirwar, D., Jhade, D. and Gupta, S. 2009. Medicinal and pharmacological potential of nigella sativa: a review. *Ethnobotanical Leaflets* 2009(7), p. 11.
- Shaw, T.J. and Martin, P. 2009. Wound repair at a glance. *Journal of cell science* 122(18), pp. 3209–3213.
- Shehzad, A., Qureshi, M., Jabeen, S., Ahmad, R., Alabdall, A.H., Aljafary, M.A. and Al-Suhaimi, E. 2018. Synthesis, characterization and antibacterial activity of silver nanoparticles using Rhazya stricta. *PeerJ* 6, pp. e6086.
- Shen, B. 2015. A new golden age of natural products drug discovery. *Cell* 163(6), pp. 1297–1300.
- Shetty, S., Udupa, S. and Udupa, L. 2008. Evaluation of antioxidant and wound healing effects of alcoholic and aqueous extract of Ocimum sanctum Linn in rats. *Evidence-Based Complementary and Alternative Medicine* 5(1), pp. 95–101.
- Shewiyo, D.H., Kaale, E., Risha, P.G., Dejaegher, B., Smeyers-Verbeke, J. and Vander Heyden, Y. 2012. Optimization of a reversed-phase-high-performance thin-layer chromatography method for the separation of isoniazid, ethambutol, rifampicin and pyrazinamide in fixed-dose combination antituberculosis tablets. *Journal of Chromatography A* 1260, pp. 232–238.
- Shofler, D., Rai, V., Mansager, S., Cramer, K. and Agrawal, D.K. 2021. Impact of resolvin mediators in the immunopathology of diabetes and wound healing. *Expert Review of Clinical Immunology* 17(6), pp. 681–690.
- Sikandan, A., Shinomiya, T. and Nagahara, Y. 2018. Ashwagandha root extract exerts anti-inflammatory effects in HaCaT cells by inhibiting the MAPK/NF- κ B pathways and by regulating cytokines. *International journal of molecular medicine* 42(1), pp. 425–434.
- Silman, M.R. 2007. Plant species diversity in Amazonian forests. In: Tropical rainforest responses to climatic change. *Springer*, pp. 269–294.
- Silver, L.L. 2011. Challenges of antibacterial discovery. *Clinical microbiology reviews* 24(1), pp. 71–109.
- Simonsen, S.M.E., Van Orman, E.R., Hatch, B.E., Jones, S.S., Gren, L.H., Hegmann, K.T. and Lyon, J.L. 2006. Cellulitis incidence in a defined population. *Epidemiology & Infection* 134(2), pp. 293–299.
- Simor, A.E., Stuart, T.L., Louie, L., Watt, C., Ofner-Agostini, M., Gravel, D., Mulvey, M., Loeb, M., McGeer, A. and Bryce, E. 2007. Mupirocin-resistant, methicillin-resistant Staphylococcus aureus strains in Canadian hospitals. *Antimicrobial agents and chemotherapy* 51(11), pp. 3880–3886.
- Sims, J., Towne, J. and Blumberg, H. 2005. IL-1 family members in inflammatory skin disease. *Cytokines as Potential Therapeutic Targets for Inflammatory Skin Diseases*, pp. 187–191.

- Sindrilaru, A. and Scharffetter-Kochanek, K. 2013. Disclosure of the culprits: macrophages—versatile regulators of wound healing. *Advances in wound care* 2(7), pp. 357–368.
- Singh, S.B. and Barrett, J.F. 2006. Empirical antibacterial drug discovery - Foundation in natural products. *Biochemical Pharmacology* 71(7), pp. 1006–1015.
- Skiryecz, A., Kierszniowska, S., Méret, M., Willmitzer, L. and Tzotzos, G. 2016. Medicinal bioprospecting of the Amazon rainforest: a modern Eldorado? *Trends in biotechnology* 34(10), pp. 781–790.
- Skuli, N., Majmundar, A.J., Krock, B.L., Mesquita, R.C., Mathew, L.K., Quinn, Z.L., Runge, A., Liu, L., Kim, M.N. and Liang, J. 2012. Endothelial HIF-2 α regulates murine pathological angiogenesis and revascularization processes. *The Journal of clinical investigation* 122(4), pp. 1427–1443.
- Ślesak, I., Libik, M., Karpinska, B., Karpinski, S. and Miszalski, Z. 2007. The role of hydrogen peroxide in regulation of plant metabolism and cellular signalling in response to environmental stresses. *Acta Biochimica Polonica* 54(1), pp. 39–50.
- Spellberg, B. 2018. The maturing antibiotic mantra: “shorter is still better”. *Journal of hospital medicine* 13(5), pp. 361–362.
- Starr, C.G., Maderdrut, J.L., He, J., Coy, D.H. and Wimley, W.C. 2018. Pituitary adenylate cyclase-activating polypeptide is a potent broad-spectrum antimicrobial peptide: Structure-activity relationships. *Peptides* 104, pp. 35–40.
- Stermitz, F.R., Scriven, L.N., Tegos, G. and Lewis, K. 2002. Two flavonols from *Artemisa annua* which potentiate the activity of berberine and norfloxacin against a resistant strain of *Staphylococcus aureus*. *Planta medica* 68(12), pp. 1140–1141.
- Stewart, P.S. 1998. A review of experimental measurements of effective diffusive permeabilities and effective diffusion coefficients in biofilms. *Biotechnology and bioengineering* 59(3), pp. 261–272.
- Stewart, P.S. and Franklin, M.J. 2008. Physiological heterogeneity in biofilms. *Nature Reviews Microbiology* 6(3), pp. 199–210.
- Sticher, O. 2008. Natural product isolation. *Natural Product Reports* 25(3), pp. 517–554.
- Stockert, J.C., Blázquez-Castro, A., Cañete, M., Horobin, R.W. and Villanueva, Á. 2012. MTT assay for cell viability: Intracellular localization of the formazan product is in lipid droplets. *Acta Histochemica* 114(8), pp. 785–796.
- Stojadinovic, O., Brem, H., Vouthounis, C., Lee, B., Fallon, J., Stallcup, M., Merchant, A., Galiano, R.D. and Tomic-Canic, M. 2005. Molecular pathogenesis of chronic wounds: the role of β -catenin and c-myc in the inhibition of epithelialization and wound healing. *The American journal of pathology* 167(1), pp. 59–69.
- Stojadinovic, O., Pastar, I., Vukelic, S., Mahoney, M.G., Brennan, D., Krzyzanowska, A., Golinko, M., Brem, H. and Tomic-Canic, M. 2008. Deregulation of keratinocyte differentiation and activation: a hallmark of venous ulcers. *Journal of cellular and molecular medicine* 12(6b), pp. 2675–2690.
- Stover, E. and Mercure, E.W. 2007. The pomegranate: A new look at the fruit of paradise. *HortScience* 42(5), pp. 1088–1092.
- Su, Y. and Richmond, A. 2015. Chemokine regulation of neutrophil infiltration of skin wounds. *Advances in wound care* 4(11), pp. 631–640.

- Suaya, J.A., Eisenberg, D.F., Fang, C. and Miller, L.G. 2013. Skin and soft tissue infections and associated complications among commercially insured patients aged 0–64 years with and without diabetes in the US. *PLoS One* 8(4), pp. e60057.
- Subramani, R., Narayanasamy, M. and Feussner, K.-D. 2017. Plant-derived antimicrobials to fight against multi-drug-resistant human pathogens. *3 Biotech* 7(3), pp. 1–15.
- Sultana, N. and Khalid, A. 2010. Phytochemical and enzyme inhibitory studies on indigenous medicinal plant *Rhazya stricta*. *Natural product research* 24(4), pp. 305–314.
- Sumner, J. 2000. The natural history of medicinal plants. London: Timber Press.
- Sun, B.K., Sibrashvili, Z. and Khavari, P.A., 2014. Advances in skin grafting and treatment of cutaneous wounds. *Science*, 346(6212), pp.941-945.
- Sun, Y., Dowd, S.E., Smith, E., Rhoads, D.D. and Wolcott, R.D., 2008. In vitro multispecies Lubbock chronic wound biofilm model. *Wound repair and regeneration*, 16(6), pp.805-813.
- Tagliabue, A. and Rappuoli, R. 2018. Changing priorities in vaccinology: antibiotic resistance moving to the top. *Frontiers in immunology* 9, p. 1068.
- Takeuchi, O. and Akira, S. 2010. Pattern Recognition Receptors and Inflammation. *Cell* 140(6), pp. 805–820.
- Takuathung, M.N., Potikanond, S., Sookkhee, S., Mungkornasawakul, P., Jearanaikulvanich, T., Chinda, K., Wikan, N. and Nimlamool, W., 2021. Anti-psoriatic and anti-inflammatory effects of *Kaempferia parviflora* in keratinocytes and macrophage cells. *Biomedicine & Pharmacotherapy*, 143, pp.112229.
- Tanira, M.O.M., Ali, B.H., Bashir, A.K. and Chandranath, I. 1996. Some pharmacologic and toxicologic studies on *Rhazya stricta* Decne in rats, mice and rabbits. *General Pharmacology* 27(7), pp. 1261–1267.
- Tanira, M.O.M., Ali, B.H., Bashir, A.K., Stephen, S. and Lukic, M. 1998. *Rhazya stricta* enhances IL-1 and TNF α production by macrophages in mice. *FASEB Journal* 12(5), pp. A764.
- Tawaha, K.A. 2006. Cytotoxicity Evaluation of Jordanian Wild Plants using Brine Shrimp Lethality Test. *Journal of Applied Sciences* 8(1), pp. 12–17.
- Tawfika, K., Al-Barazib, M., Bashirb, M., Al-Marzouq, W., AlSoufif, R. and Kharsab, H. 2015. A comparative study of antioxidant activities of ziziphus and colocynth from Saudi Arabia deserts and proposed pharmaceutical products. *IRJPAS* 5(3), pp. 8–13.
- Taylor, G., Lehrer, M.S., Jensen, P.J., Sun, T.-T. and Lavker, R.M. 2000. Involvement of follicular stem cells in forming not only the follicle but also the epidermis. *Cell* 102(4), pp. 451–461.
- Tegos, G.P., Masago, K., Aziz, F., Higginbotham, A., Stermitz, F.R. and Hamblin, M.R. 2008. Inhibitors of bacterial multidrug efflux pumps potentiate antimicrobial photoinactivation. *Antimicrobial agents and chemotherapy* 52(9), pp. 3202–3209.
- Theuretzbacher, U. and Piddock, L.J. V 2019. Non-traditional antibacterial therapeutic options and challenges. *Cell host & microbe* 26(1), pp. 61–72.
- Thi, M.T.T., Wibowo, D. and Rehm, B.H.A. 2020. *Pseudomonas aeruginosa* biofilms. *International journal of molecular sciences* 21(22), p. 8671.

- Thomson, C.H. 2011. Biofilms: do they affect wound healing? *International Wound Journal* 8(1), pp. 63–67.
- Tian, F., Li, B., Ji, B., Zhang, G. and Luo, Y. 2009. Identification and structure–activity relationship of gallotannins separated from *Galla chinensis*. *LWT-Food Science and Technology* 42(7), pp. 1289–1295.
- Timoszuk, M., Bielawska, K. and Skrzydlewska, E. 2018. Evening primrose (*Oenothera biennis*) biological activity dependent on chemical composition. *Antioxidants* 7(8), pp. 1–11.
- Tobin, D.J. and Paus, R. 2001. Graying: gerontobiology of the hair follicle pigmentary unit. *Experimental gerontology* 36(1), pp. 29–54.
- Tognetti, L., Martinelli, C., Berti, S., Hercogova, J., Lotti, T., Leoncini, F. and Moretti, S. 2012. Bacterial skin and soft tissue infections: Review of the epidemiology, microbiology, aetiopathogenesis and treatment: A collaboration between dermatologists and infectivologists. *Journal of the European Academy of Dermatology and Venereology* 26(8), pp. 931–941.
- Tomasek, J.J., Gabbiani, G., Hinz, B., Chaponnier, C. and Brown, R.A. 2002. 532 Myofibroblasts and mechano-regulation of connective tissue remodelling. *Nat Rev Mol Cell Biol* 3(349–363), p. 534.
- Tomic-Canic, M., Burgess, J.L., O’Neill, K.E., Strbo, N. and Pastar, I. 2020. Skin microbiota and its interplay with wound healing. *American journal of clinical dermatology* 21(1), pp. 36–43.
- Tomic-Canic, M., Komine, M., Freedberg, I.M. and Blumenberg, M. 1998. Epidermal signal transduction and transcription factor activation in activated keratinocytes. *Journal of dermatological science* 17(3), pp. 167–181.
- Tong, S.Y.C., Davis, J.S., Eichenberger, E., Holland, T.L. and Fowler Jr, V.G. 2015. *Staphylococcus aureus* infections: epidemiology, pathophysiology, clinical manifestations, and management. *Clinical microbiology reviews* 28(3), pp. 603–661.
- Tonnesen, M.G., Feng, X. and Clark, R.A.F. 2000. Angiogenesis in wound healing. In: *Journal of investigative dermatology symposium proceedings*. Elsevier, pp. 40–46.
- Tottoli, E.M., Dorati, R., Genta, I., Chiesa, E., Pisani, S. and Conti, B. 2020. Skin wound healing process and new emerging technologies for skin wound care and regeneration. *Pharmaceutics* 12(8), pp. 735.
- Tounekti, T., Mahdhi, M. and Khemira, H. 2019. Ethnobotanical study of indigenous medicinal plants of Jazan region, Saudi Arabia. *Evidence-based complementary and alternative medicine* 2019(1), pp. 1–45.
- Toy, L.W. and Macera, L. 2011. Evidence-based review of silver dressing use on chronic wounds. *Journal of the American Academy of Nurse Practitioners* 23(4), pp. 183–192.
- Trenam, C.W., Blake, D.R. and Morris, C.J. 1992. Skin inflammation: reactive oxygen species and the role of iron. *Journal of investigative dermatology* 99(6), pp. 675–682.
- Tse, B.N., Adalja, A.A., Houchens, C., Larsen, J., Inglesby, T. V and Hatchett, R. 2017. Challenges and opportunities of nontraditional approaches to treating bacterial infections. *Clinical Infectious Diseases* 65(3), pp. 495–500.
- Tse, W.P., Che, C.T., Liu, K. and Lin, Z.X. 2006. Evaluation of the anti-proliferative properties of selected psoriasis-treating Chinese medicines on cultured HaCaT cells. *Journal of Ethnopharmacology* 108(1), pp. 133–141.

- Tseng, B.S., Zhang, W., Harrison, J.J., Quach, T.P., Song, J.L., Penterman, J., Singh, P.K., Chopp, D.L., Packman, A.I. and Parsek, M.R. 2013. The extracellular matrix protects *Pseudomonas aeruginosa* biofilms by limiting the penetration of tobramycin. *Environmental microbiology* 15(10), pp. 2865–2878.
- Tu, Y. 2011. The discovery of artemisinin (qinghaosu) and gifts from Chinese medicine. *Nature medicine* 17(10), pp. 1217–1220.
- Tungmunnithum, D., Thongboonyou, A., Pholboon, A. and Yangsabai, A. 2018. Flavonoids and other phenolic compounds from medicinal plants for pharmaceutical and medical aspects: An overview. *Medicines* 5(3), p. 93.
- Vadillo-Rodriguez, V., Beveridge, T.J. and Dutcher, J.R. 2008. Surface viscoelasticity of individual gram-negative bacterial cells measured using atomic force microscopy. *Journal of bacteriology* 190(12), pp. 4225–4232.
- van Vuuren, S. and Viljoen, A., 2011. Plant-based antimicrobial studies—methods and approaches to study the interaction between natural products. *Planta medica*, 77(11), pp.1168-1182.
- Velnar, T., Bailey, T. and Smrkolj, V. 2009. The wound healing process: An overview of the cellular and molecular mechanisms. *Journal of International Medical Research* 37(5), pp. 1528–1542.
- Verbitski, S.M., Gourdin, G.T., Ikenouye, L.M. and McChesney, J.D. 2006. Rapid screening of complex mixtures by thin layer chromatography-bioluminescence. *American Biotechnology Laboratory* 24(9), p. 40.
- Vinh, D.C. and Embil, J.M. 2005. Rapidly progressive soft tissue infections. *The Lancet infectious diseases* 5(8), pp. 501–513.
- Volk, S.W. and Bohling, M.W. 2013. Comparative wound healing—are the small animal veterinarian’s clinical patients an improved translational model for human wound healing research? *Wound Repair and Regeneration* 21(3), pp. 372–381.
- Volpato, G., Kourková, P. and Zelený, V. 2012. Healing war wounds and perfuming exile: the use of vegetal, animal, and mineral products for perfumes, cosmetics, and skin healing among Sahrawi refugees of Western Sahara. *Journal of Ethnobiology and Ethnomedicine* 8(1), pp. 1–20.
- Wagner, H. and Ulrich-Merzenich, G. 2009. Synergy research: approaching a new generation of phytopharmaceuticals. *Phytomedicine* 16(2–3), pp. 97–110.
- Walker, J.T., Verran, J., Boyd, R.D. and Percival, S. 2001. Microscopy methods to investigate structure of potable water biofilms. In: *Methods in enzymology*. Elsevier, pp. 243–255.
- Wall, M.E. and Wani, M.C. 1996. Camptothecin and taxol: from discovery to clinic. *Journal of ethnopharmacology* 51(1–3), pp. 239–254.
- Wallace, J.L. 2001. Prostaglandin biology in inflammatory bowel disease. *Gastroenterology Clinics* 30(4), pp. 971–980.
- Walsh, C. 2000. Molecular mechanisms that confer antibacterial drug resistance. *Nature* 406(6797), pp. 775–781.
- Wang, C.-Z., Mehendale, S.R. and Yuan, C.-S. 2007. Commonly used antioxidant botanicals: active constituents and their potential role in cardiovascular illness. *The American journal of Chinese medicine* 35(04), pp. 543–558.
- Watkins, R., Wu, L., Zhang, C., Davis, R.M. and Xu, B. 2015. Natural product-based nanomedicine: recent advances and issues. *International journal of nanomedicine* 10, p. 6055.

- Webb, E., Neeman, T., Bowden, F.J., Gaida, J., Mumford, V. and Bissett, B. 2020. Compression therapy to prevent recurrent cellulitis of the leg. *New England Journal of Medicine* 383(7), pp. 630–639.
- Wedler, J., Daubitz, T., Schlotterbeck, G. and Butterweck, V. 2014. In vitro anti-inflammatory and wound-healing potential of a *Phyllostachys edulis* leaf extract—identification of isoorientin as an active compound. *Planta Medica* 80(18), pp. 1678–1684.
- Weinstein, D.A. and Kirsner, R.S. 2010. Refractory ulcers: The role of tumor necrosis factor- α . *Journal of the American Academy of Dermatology* 63(1), pp. 146–154.
- Weller, M.G., 2012. A unifying review of bioassay-guided fractionation, effect-directed analysis and related techniques. *Sensors*, 12(7), pp.9181-9209.
- Werner, S. and Grose, R. 2003. Regulation of wound healing by growth factors and cytokines. *Physiological reviews* 83(3), pp. 835–870.
- Wesley, J.J., Christina, A.J.M., Chidambaranathan, N. and Ravikumar, K. 2009. Wound healing activity of the leaves of *Tribulus terrestris* (Linn) aqueous extract in rats. *Journal of Pharmacy Research* 2(5), pp. 841–843.
- Wi, T., Lahra, M.M., Ndowa, F., Bala, M., Dillon, J.A.R., Ramon-Pardo, P., Eremin, S.R., Bolan, G. and Unemo, M. 2017. Antimicrobial resistance in *Neisseria gonorrhoeae*: Global surveillance and a call for international collaborative action. *PLoS Medicine* 14(7), pp. 1–16.
- Wilburg, J., Kasprowicz, A. and Heczko, P.B. 1984. Composition of normal bacterial flora of human skin in relation to the age and sex of examined persons. *Przegląd dermatologiczny* 71(6), pp. 551–557.
- Wilgus, T.A., Vodovotz, Y., Vittadini, E., Clubbs, E.A. and Oberyszyn, T.M. 2003. Reduction of scar formation in full-thickness wounds with topical celecoxib treatment. *Wound Repair and Regeneration* 11(1), pp. 25–34.
- Wilkins, M.R., Kendall, M.J. and Wade, O.L. 1985. William Withering and digitalis. *British Medical Journal* (Clinical research ed.) 290, pp. 7–8.
- Willenborg, S., Lucas, T., Van Loo, G., Knipper, J.A., Krieg, T., Haase, I., Brachvogel, B., Hammerschmidt, M., Nagy, A. and Ferrara, N. 2012. CCR2 recruits an inflammatory macrophage subpopulation critical for angiogenesis in tissue repair. *Blood, The Journal of the American Society of Hematology* 120(3), pp. 613–625.
- Williamson, D., Ritchie, S.R., Best, E., Upton, A., Leversha, A., Smith, A. and Thomas, M.G. 2015. A bug in the ointment: topical antimicrobial usage and resistance in New Zealand. *New Zealand Medical Journal* 128(1426), pp. 103–109.
- Williamson, D.A., Monecke, S., Heffernan, H., Ritchie, S.R., Roberts, S.A., Upton, A., Thomas, M.G. and Fraser, J.D., 2014. High usage of topical fusidic acid and rapid clonal expansion of fusidic Acid-Resistant *Staphylococcus aureus*: a cautionary tale. *Clinical infectious diseases*, 59(10), pp.1451-1454.
- Williamson, E.M. 2001. Synergy and other interactions in phytomedicines. *Phytomedicine* 8(5), pp. 401–409.
- Wink, M. and Twardowski, T. 1992. Allelochemical properties of alkaloids. Effects on plants, bacteria and protein biosynthesis. In: *Allelopathy*. Springer, pp. 129–150.
- Wu, H., Moser, C., Wang, H.-Z., Høiby, N. and Song, Z.-J. 2015. Strategies for combating bacterial biofilm infections. *International journal of oral science* 7(1), pp. 1–7.
- Wu, Y.-K., Cheng, N.-C. and Cheng, C.-M. 2019. Biofilms in chronic wounds: pathogenesis and diagnosis. *Trends in biotechnology* 37(5), pp. 505–517.

- Wynn, T.A. and Barron, L. 2010. Macrophages: master regulators of inflammation and fibrosis. In: Seminars in liver disease. *Thieme Medical Publishers*, pp. 245–257.
- Wynn, T.A. and Ramalingam, T.R. 2012. Mechanisms of fibrosis: therapeutic translation for fibrotic disease. *Nature medicine* 18(7), pp. 1028–1040.
- Xiao, T., Yan, Z., Xiao, S. and Xia, Y. 2020. Proinflammatory cytokines regulate epidermal stem cells in wound epithelialization. *Stem cell research & therapy* 11(1), pp. 1–9.
- Xie, C., Kang, J., Li, Z., Schauss, A.G., Badger, T.M., Nagarajan, S., Wu, T. and Wu, X. 2012. The açai flavonoid velutin is a potent anti-inflammatory agent: blockade of LPS-mediated TNF- α and IL-6 production through inhibiting NF- κ B activation and MAPK pathway. *The Journal of nutritional biochemistry* 23(9), pp. 1184–1191.
- Xu, J., Lamouille, S. and Derynck, R. 2009. TGF- β -induced epithelial to mesenchymal transition. *Cell research* 19(2), pp. 156–172.
- Xu, K.D., McFeters, G.A. and Stewart, P.S. 2000. Biofilm resistance to antimicrobial agents. *Microbiology* 146(3), pp. 547–549.
- Y. M. Al-Sodany, A. B. Salih, H.A.M. 2013. Medicinal plants in Saudi Arabia: I. Sarrwat Mountains at Taif. *Academic Journal of Plant Sciences* 6(6 (4)), pp. 134–145.
- Yang, L. and Stöckigt, J. 2010. Trends for diverse production strategies of plant medicinal alkaloids. *Natural product reports* 27(10), pp. 1469–1479.
- Yang, W., Tao, Y., Wu, Y., Zhao, X., Ye, W., Zhao, D., Fu, L., Tian, C., Yang, J. and He, F. 2019. Neutrophils promote the development of reparative macrophages mediated by ROS to orchestrate liver repair. *Nature communications* 10(1), pp. 1–14.
- Yin, D., Wakimoto, N., Xing, H., Lu, D., Huynh, T., Wang, X., Black, K.L. and Koeffler, H.P. 2008. Cucurbitacin B markedly inhibits growth and rapidly affects the cytoskeleton in glioblastoma multiforme. *International Journal of Cancer* 123(6), pp. 1364–1375.
- Yoon, B.K., Jackman, J.A., Valle-González, E.R. and Cho, N.-J. 2018. Antibacterial free fatty acids and monoglycerides: biological activities, experimental testing, and therapeutic applications. *International journal of molecular sciences* 19(4), p. 1114.
- Youn, S.H., Choi, C.W., Choi, J.W. and Youn, S.W. 2013. The skin surface pH and its different influence on the development of acne lesion according to gender and age. *Skin research and technology* 19(2), pp. 131–136.
- Yusuf, M., Al-Oqail, M., Al-Sheddr, E., Al-Rehaily, A. and Rahman, M. 2014. Diversity of Medicinal Plants in the Flora of Saudi Arabia 3: An inventory of 15 Plant Families and their Conservation Management. *International Journal of Environment*, 3(3), pp. 312-320.
- Yuyama, K.T., Rohde, M., Molinari, G., Stadler, M. and Abraham, W.R. 2020. Unsaturated fatty acids control biofilm formation of staphylococcus aureus and other gram-positive bacteria. *Antibiotics* 9(11), pp. 1–11.
- Zahedi, P., Rezaeian, I., Ranaei-Siadat, S., Jafari, S. and Supaphol, P. 2010. A review on wound dressings with an emphasis on electrospun nanofibrous polymeric bandages. *Polymers for Advanced Technologies* 21(2), pp. 77–95.

- Zaman, K. 1990. Studies on the chemical constituents of roots of *Rhazya stricta* Decne. *Institute/University/Department details University of Karachi/HEJ Research Institute of Chemistry*, pp. 1–250.
- Zaman, S. Bin, Hussain, M.A., Nye, R., Mehta, V., Mamun, K.T. and Hossain, N. 2017. A review on antibiotic resistance: alarm bells are ringing. *Cureus* 9(6), pp. e1403.
- Zapata, R.O., Bramante, C.M., de Moraes, I.G., Bernardineli, N., Gasparoto, T.H., Graeff, M.S.Z., Campanelli, A.P. and Garcia, R.B. 2008. Confocal Laser Scanning Microscopy Is Appropriate to Detect Viability of *Enterococcus faecalis* in Infected Dentin. *Journal of Endodontics* 34(10), pp. 1198–1201.
- Zaynab, M., Fatima, M., Abbas, S., Sharif, Y., Umair, M., Zafar, M.H. and Bahadar, K. 2018. Role of secondary metabolites in plant defense against pathogens. *Microbial pathogenesis* 124, pp. 198–202.
- Zhang, G.Y., Langan, E.A., Meier, N.T., Funk, W., Siemers, F. and Paus, R., 2019. Thyroxine (T4) may promote re-epithelialisation and angiogenesis in wounded human skin ex vivo. *PLoS One*, 14(3), pp.e0212659.
- Zhang, H., Zhang, L., Peng, L., Dong, X., Wu, D., Wu, V.C.-H. and Feng, F. 2012. Quantitative structure-activity relationships of antimicrobial fatty acids and derivatives against *Staphylococcus aureus*. *Journal of Zhejiang University Science B* 13(2), pp. 83–93.
- Zhang, L., Ma, Y., Pan, X., Chen, S., Zhuang, H. and Wang, S. 2018. A composite hydrogel of chitosan/heparin/poly (γ -glutamic acid) loaded with superoxide dismutase for wound healing. *Carbohydrate polymers* 180, pp. 168–174.
- Zhang, Q., Lyu, Y., Huang, J., Zhang, X., Yu, N., Wen, Z. and Chen, S. 2020. Antibacterial activity and mechanism of sanguinarine against *Providencia rettgeri* in vitro. *PeerJ* 8, p. e9543.
- Zhang, S., Li, H. and Yang, S.J., 2010. Tribulosin protects rat hearts from ischemia/reperfusion injury. *Acta Pharmacologica Sinica*, 31(6), pp.671-678.
- Zhang, T.C. and Bishop, P.L. 1996. Evaluation of substrate and pH effects in a nitrifying biofilm. *Water environment research* 68(7), pp. 1107–1115.
- Zhao, B., Li, R., Yang, F., Yu, F., Xu, N., Zhang, F., Ge, X. and Du, J. 2018. LPS-induced vitamin D receptor decrease in oral keratinocytes is associated with oral lichen planus. *Scientific reports* 8(1), pp. 1–9.
- Zhao, G., Usui, M.L., Lippman, S.I., James, G.A., Stewart, P.S., Fleckman, P. and Olerud, J.E. 2013. Biofilms and inflammation in chronic wounds. *Advances in wound care* 2(7), pp. 389–399.
- Zheleva-Dimitrova, D., Obreshkova, D. and Nedialkov, P. 2012. Antioxidant activity of *tribulus terrestris*—a natural product in infertility therapy. *International Journal of Pharmacy and Pharmaceutical Sciences* 4(4), pp. 508–511.
- Zheng, C.J., Yoo, J.-S., Lee, T.-G., Cho, H.-Y., Kim, Y.-H. and Kim, W.-G. 2005. Fatty acid synthesis is a target for antibacterial activity of unsaturated fatty acids. *FEBS letters* 579(23), pp. 5157–5162.
- Zhu, B.-M., Ishida, Y., Robinson, G.W., Pacher-Zavisin, M., Yoshimura, A., Murphy, P.M. and Hennighausen, L. 2008. SOCS3 negatively regulates the gp130–STAT3 pathway in mouse skin wound healing. *Journal of investigative dermatology* 128(7), pp. 1821–1829.
- Zuo, L., Zhou, T., Pannell, B.K., Ziegler, A.C. and Best, T.M. 2015. Biological and physiological role of reactive oxygen species—the good, the bad and the ugly. *Acta physiologica* 214(3), pp. 329–348.